

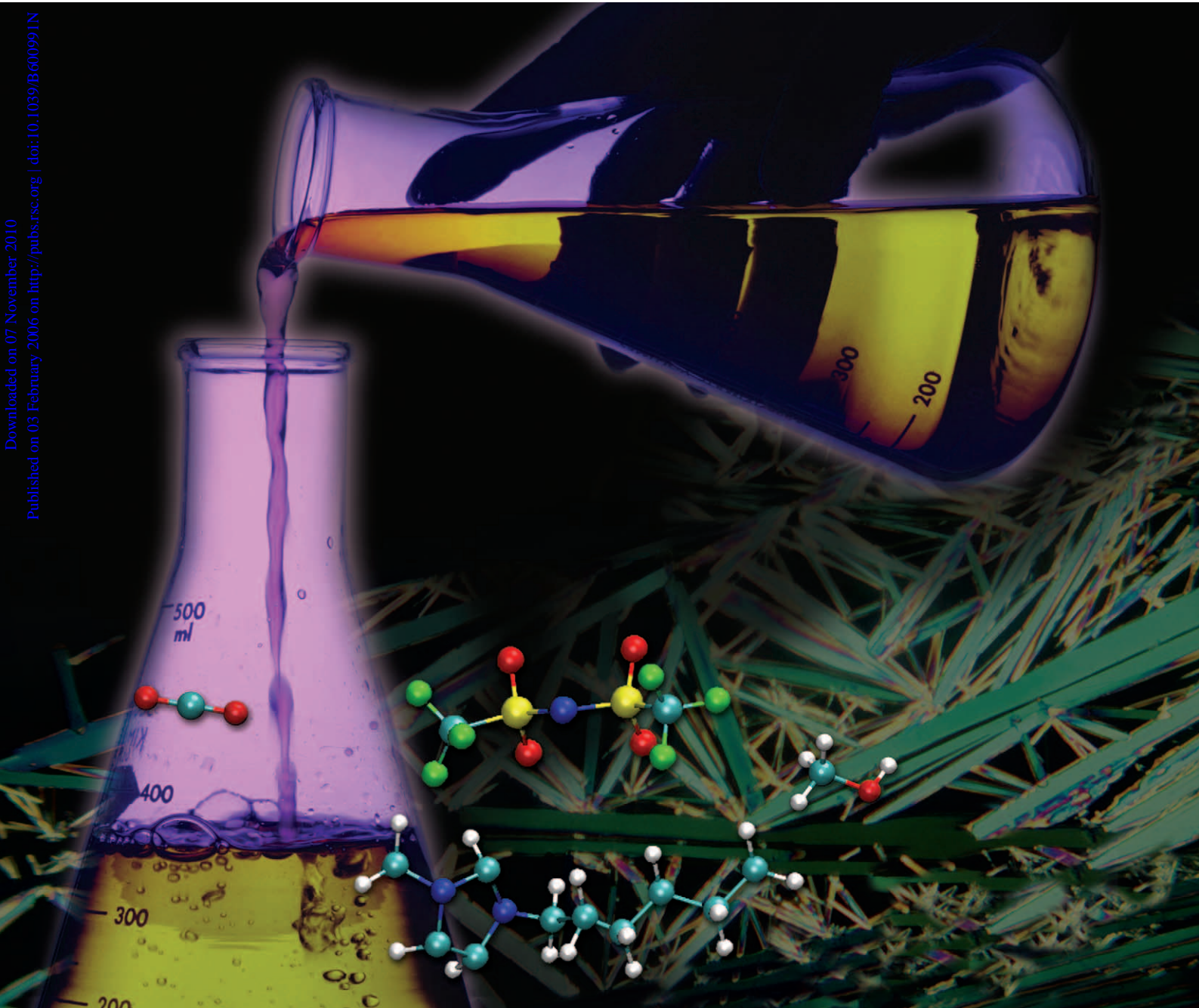
Green Chemistry

Cutting-edge research for a greener sustainable future

www.rsc.org/greenchem

Volume 8 | Number 2 | February 2006 | Pages 113–224

Downloaded on 07 November 2010
Published on 03 February 2006 on <http://pubs.rsc.org> | doi:10.1039/B600991N



ISSN 1463-9262

RSC Publishing

Sjöström
Models for green chemistry
Endo *et al.*
Gas–solid phase fixation of CO₂

Brennecke *et al.*
Removal of solids using CO₂
Dubey *et al.*
Mesoporous polymer–silica catalysts



1463-9262 (2006) 8:2;1-C



Image reproduced by permission of Tom Schweich, *J. Environ. Monit.* 2005, 1

03030516

JEM

Journal of Environmental Monitoring

Comprehensive, high quality coverage of multidisciplinary, international research relating to the measurement, pathways, impact and management of contaminants in all environments.

- Dedicated to the analytical measurement of environmental pollution
- Assessing exposure and associated health risks
- Fast times to publication
- Impact factor: 1.366
- High visibility - cited in MEDLINE



RSC Publishing

www.rsc.org/jem

Green Chemistry

Cutting-edge research for a greener sustainable future

www.rsc.org/greenchem

RSC Publishing is a not-for-profit publisher and a division of the Royal Society of Chemistry. Any surplus made is used to support charitable activities aimed at advancing the chemical sciences. Full details are available from www.rsc.org

IN THIS ISSUE

ISSN 1463-9262 CODEN GRCHFJ 8(2) 113–224 (2006)



Cover

Carbon dioxide can be used as an antisolvent to precipitate solid crystals from mixtures of ionic liquids and organics, even at relatively low pressures. Image reproduced by permission of Joan Brennecke from *Green Chem.*, 2006, 8(2), 141.

CHEMICAL TECHNOLOGY

T5

Chemical Technology highlights the latest applications and technological aspects of research across the chemical sciences.

Chemical Technology

February 2006/Volume 3/Issue 2

www.rsc.org/chemicaltechnology

EDITORIAL

125

Reflections on “green chemistry” in 2005

Walter Leitner reflects on the development of *Green Chemistry* and the field of green chemistry in 2005.



EDITORIAL STAFF

Editor

Sarah Ruthven

News writer

Markus Hölscher

Publishing assistant

Emma Hacking

Team leader, serials production

Stephen Wilkes

Administration coordinator

Sonya Spring

Editorial secretaries

Lynne Braybrook, Jill Segev, Julie Thompson

Publisher

Adrian Kybett

Green Chemistry (print: ISSN 1463-9262; electronic: ISSN 1463-9270) is published 12 times a year by the Royal Society of Chemistry, Thomas Graham House, Science Park, Milton Road, Cambridge, UK CB4 0WF.

All orders, with cheques made payable to the Royal Society of Chemistry, should be sent to RSC Distribution Services, c/o Portland Customer Services, Commerce Way, Colchester, Essex, UK CO2 8HP. Tel +44 (0) 1206 226050; E-mail sales@rscdistribution.org

2006 Annual (print + electronic) subscription price: £859; US\$1571. 2006 Annual (electronic) subscription price: £773; US\$1414. Customers in Canada will be subject to a surcharge to cover GST. Customers in the EU subscribing to the electronic version only will be charged VAT.

If you take an institutional subscription to any RSC journal you are entitled to free, site-wide web access to that journal. You can arrange access via Internet Protocol (IP) address at www.rsc.org/ip. Customers should make payments by cheque in sterling payable on a UK clearing bank or in US dollars payable on a US clearing bank. Periodicals postage paid at Rahway, NJ, USA and at additional mailing offices. Airfreight and mailing in the USA by Mercury Airfreight International Ltd., 365 Blair Road, Avenel, NJ 07001, USA.

US Postmaster: send address changes to Green Chemistry, c/o Mercury Airfreight International Ltd., 365 Blair Road, Avenel, NJ 07001. All despatches outside the UK by Consolidated Airfreight.

PRINTED IN THE UK

Advertisement sales: Tel +44 (0) 1223 432246; Fax +44 (0) 1223 426017; E-mail advertising@rsc.org

Green Chemistry

Cutting-edge research for a greener sustainable future

www.rsc.org/greenchem

Green Chemistry focuses on cutting-edge research that attempts to reduce the environmental impact of the chemical enterprise by developing a technology base that is inherently non-toxic to living things and the environment.

EDITORIAL BOARD

Chair

Professor Colin Raston,
Department of Chemistry
University of Western Australia
Perth, Australia
E-mail clration@chem.uwa.edu.au

Dr Janet Scott, Centre for Green
Chemistry, Monash University,
Australia

Professor Buxing Han, Chinese
Academy of Sciences
E-mail hanbx@iccas.ac.cn

Dr A Michael Warhurst,
University of Massachusetts,
USA
E-mail michael-warhurst@uml.edu

Associate editors

Professor C. J. Li, McGill
University, Canada
E-mail cj.li@mcgill.ca

Scientific editor

Professor Walter Leitner,
RWTH-Aachen, Germany
E-mail leitner@itmc.rwth-aachen.de

Professor Tom Welton,
Imperial College, UK
E-mail t.welton@ic.ac.uk

Professor Kyoko Nozaki
Kyoto University, Japan
E-mail nozaki@chembio.tu-tokyo.ac.jp

Professor Roshan Jachuck,
Clarkson University, USA
E-mail rjachuck@clarkson.edu

Members

Professor Joan Brennecke,
University of Notre Dame, USA
Professor Steve Howdle, University
of Nottingham, UK

Dr Paul Anastas, Green Chemistry
Institute, USA
E-mail p_anastas@acs.org

INTERNATIONAL ADVISORY EDITORIAL BOARD

James Clark, York, UK
Avelino Corma, Universidad
Politécnica de Valencia, Spain
Mark Harmer, DuPont Central
R&D, USA
Herbert Hugel, Lanxess Fine
Chemicals, Germany
Makoto Misono, Kogakuin
University, Japan
Robin D. Rogers, Centre for Green
Manufacturing, USA

Kenneth Seddon, Queen's
University, Belfast, UK
Roger Sheldon, Delft University of
Technology, The Netherlands
Gary Sheldrake, Queen's
University, Belfast, UK
Pietro Tundo, Università ca
Foscari di Venezia, Italy
Tracy Williamson, Environmental
Protection Agency, USA

INFORMATION FOR AUTHORS

Full details of how to submit material for publication in Green Chemistry are given in the Instructions for Authors (available from <http://www.rsc.org/authors>). Submissions should be sent via ReSource: <http://www.rsc.org/resource>.

Authors may reproduce/republish portions of their published contribution without seeking permission from the RSC, provided that any such republication is accompanied by an acknowledgement in the form: (Original citation) – Reproduced by permission of the Royal Society of Chemistry.

© The Royal Society of Chemistry 2006. Apart from fair dealing for the purposes of research or private study for non-commercial purposes, or criticism or review, as permitted under the Copyright, Designs and Patents Act 1988 and the Copyright and Related Rights Regulations 2003, this publication may only be reproduced, stored or transmitted, in any form or by any means, with the prior permission in writing of the Publishers or in the case of reprographic reproduction in accordance with the terms of

licences issued by the Copyright Licensing Agency in the UK. US copyright law is applicable to users in the USA.

The Royal Society of Chemistry takes reasonable care in the preparation of this publication but does not accept liability for the consequences of any errors or omissions.

Ⓢ The paper used in this publication meets the requirements of ANSI/NISO Z39.48-1992 (Permanence of Paper).

Royal Society of Chemistry: Registered Charity No. 207890

NEWS

126

First China–USA Green Chemistry Workshop

Robin D. Rogers

The First China–USA Green Chemistry Workshop was held in Beijing, China, May 27–June 1, 2005.

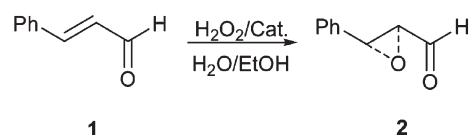


HIGHLIGHT

128

Highlights

Markus Hölscher reviews some of the recent literature in green chemistry.



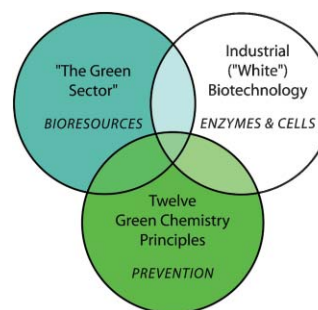
PERSPECTIVE

130

Green chemistry in perspective—models for GC activities and GC policy and knowledge areas

Jesper Sjöström

This article presents two new models that give a perspective on green chemistry (GC). The first model is a classification model of GC activities. The second model, shown in the illustration opposite, concerns GC policy and knowledge areas.



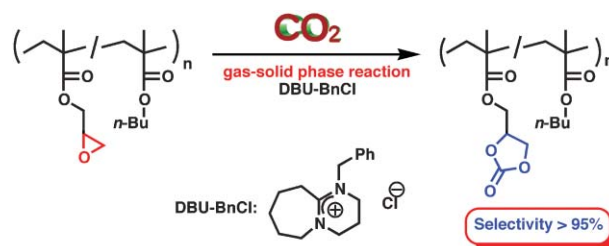
COMMUNICATIONS

138

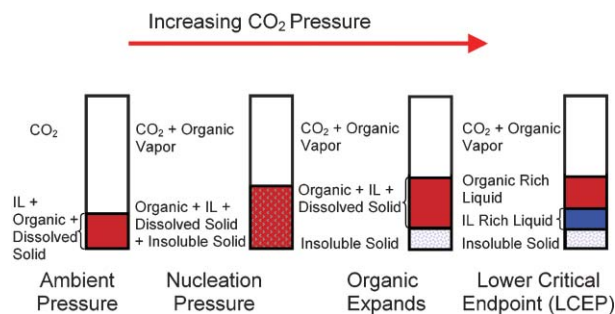
Selective gas–solid phase fixation of carbon dioxide into oxirane-containing polymers: synthesis of polymer bearing cyclic carbonate group

Bungo Ochiai, Tokinori Iwamoto and Takeshi Endo*

Gas–solid phase fixation of carbon dioxide into oxirane-containing polymers proceeds selectively without concomitant crosslinking reactions, which have previously been unavoidable due to the dense arrangement of oxirane groups.



141

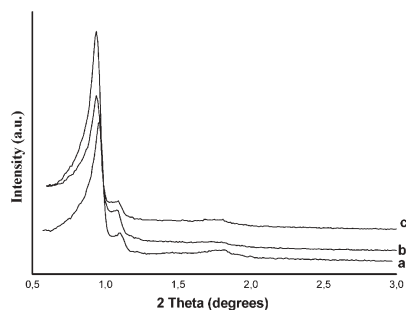


Removal of ammonium bromide, ammonium chloride, and zinc acetate from ionic liquid/organic mixtures using carbon dioxide

Eric M. Saurer, Sudhir N. V. K. Aki and Joan F. Brennecke*

CO₂ can be used to precipitate solids from ionic liquid solutions.

144

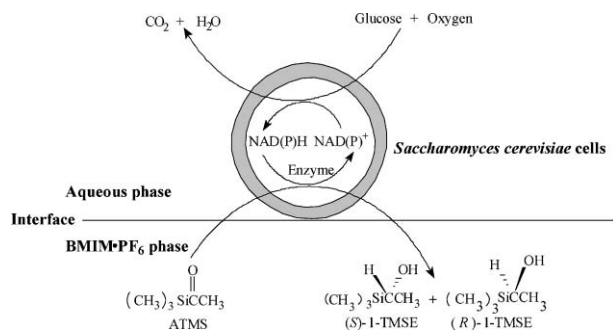


Mesoporous polymer–silica catalysts for selective hydroxylation of phenol

Amit Dubey, Minkee Choi and Ryong Ryoo

Mesoporous polymer–silica nanocomposite materials with redox functional groups such as ferrocene were synthesized and exhibited very high activity and selectivity towards catalytic hydroxylation of phenol.

147

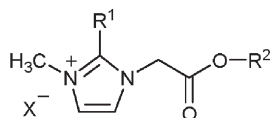


Use of ionic liquids to improve whole-cell biocatalytic asymmetric reduction of acetyltrimethylsilane for efficient synthesis of enantiopure (*S*)-1-trimethylsilylethanol

Wen-Yong Lou, Min-Hua Zong* and Thomas J. Smith

Compared with *n*-hexane, BMIM·PF₆ and BMIM·BF₄ boost the activity, stereoselectivity and stability of immobilized *Saccharomyces cerevisiae* cells, and exhibit greater biocompatibility.

156



Biodegradable ionic liquids

Part III. The first readily biodegradable ionic liquids

Nicholas Gathergood, Peter J. Scammells* and M. Teresa Garcia*

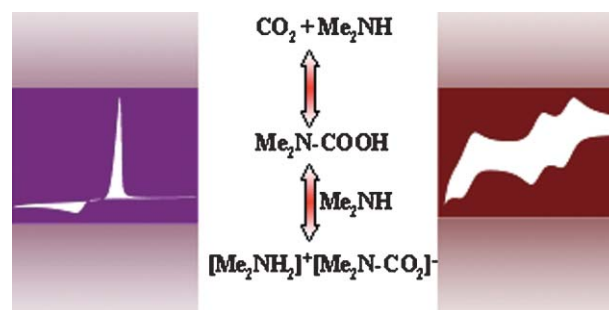
Further research toward the discovery of biodegradable ionic liquids (ILs) is described. The biodegradability of the target ILs was evaluated using the 'Closed Bottle' and 'CO₂ Headspace' tests. This research has identified the first ILs which can be classified as 'readily biodegradable' under aerobic conditions.

161

A critical assessment of electrochemistry in a distillable room temperature ionic liquid, DIMCARB

Anand I. Bhatt, Alan M. Bond,* Douglas R. MacFarlane, Jie Zhang, Janet L. Scott, Christopher R. Strauss, Philip I. Iotov and Sasha V. Kalcheva

The electrochemical behaviour of a 'distillable' room temperature ionic liquid, DIMCARB, formed from gaseous CO_2 and Me_2NH is reported. Overall the results show that DIMCARB is highly suitable for electrochemical studies.

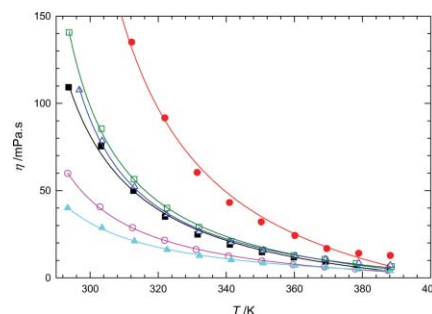


172

Density and viscosity of several pure and water-saturated ionic liquids

J. Jacquemin, P. Husson, A. A. H. Padua and V. Majer

The aim of this paper is to provide practical conclusions on the density and viscosity of ionic liquids, pure and water-saturated, *via* the collection of original experimental data and the comparison of these data with those presented in the literature.

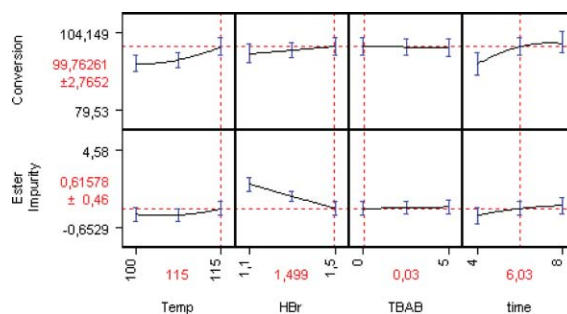


181

An organic solvent free process for the demethylation of 4-(4-methoxyphenyl)butanoic acid

Laurent Delhaye, Khalid Diker, Thomas Donck and Alain Merschaert*

A mild and efficient organic solvent free process has been developed for the synthesis of 4-(4-hydroxyphenyl)butanoic acid, a key intermediate in the synthesis of LY518674.

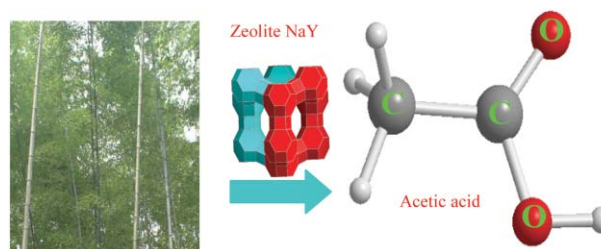


183

Catalytic pyrolysis of several kinds of bamboos over zeolite NaY

W. Y. Qi, C. W. Hu,* G. Y. Li, L. H. Guo, Y. Yang, J. Luo, X. Miao and Y. Du

The renewable bamboo samples are converted to simple monomeric compounds *via* catalytic pyrolysis processes. This provides a sustainable approach for the production of chemicals.



191

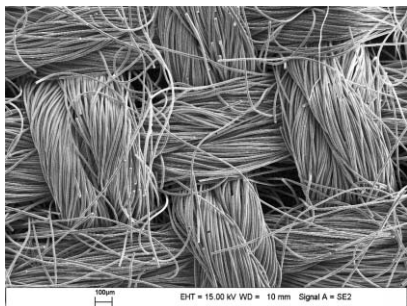


In(OTf)₃-catalyzed thiolysis of 1,2-epoxides by arylthiols under SFC. A new approach for the synthesis of thiazolopyridinium ionic liquids

Francesco Fringuelli, Ferdinando Pizzo,*
Simone Tortoioli, Cristiano Zuccaccia and Luigi Vaccaro*

In(OTf)₃ (2 mol%) is an efficient catalyst for the C-β-regioselective thiolysis of 1,2-epoxides by arylthiols under solvent-free condition. Two [1,3]thiazolo[3,2-*a*]pyridin-4-ium-based ionic liquids have been prepared *via* In(OTf)₃-catalyzed thiolysis of 1,2-epoxyhexane by 2-mercaptopyridine.

197

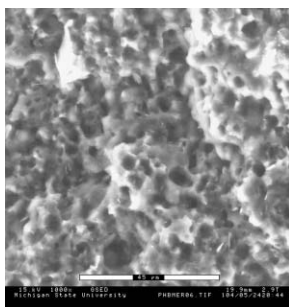


Supported ionic liquids catalysts for fine chemicals: citral hydrogenation

Jyri-Pekka Mikkola,* Pasi Virtanen, Hannu Karhu,
Tapio Salmi and Dmitry Yu. Murzin

The quest for new concepts in catalysis involving fine chemicals production is discussed.

206

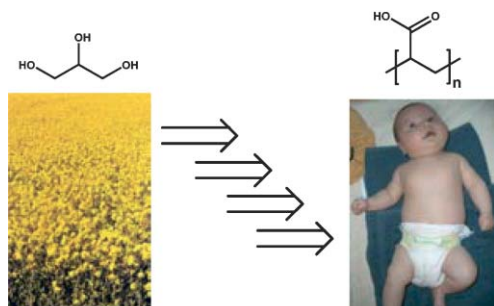


Biodegradable toughened polymers from renewable resources: blends of polyhydroxybutyrate with epoxidized natural rubber and maleated polybutadiene

Yashodhan Parulekar and Amar K. Mohanty*

Novel toughened polyhydroxybutyrate (PHB) based materials were successfully developed through reactive extrusion of PHB and epoxidized natural rubber (ENR) using maleated rubber (MR) as compatibilizer. (Image: PHB/ENR/MR (scale bar: 45 μm).)

214



Catalytic dehydration of glycerol in sub- and supercritical water: a new chemical process for acrolein production

L. Ott, M. Bicker and H. Vogel*

A novel production process for acrolein from biodiesel-derived glycerol is introduced. The usage of a homogeneous catalyst leads to an economical and ecological alternative to the established crude oil based process.

ADDITIONS AND CORRECTIONS

221

An environmentally benign process for the efficient synthesis of cyclohexanone and 2-methylfuran

H.-Y. Zheng, Y.-L. Zhu, Z.-Q. Bai, L. Huang, H.-W. Xiang and Y.-W. Li

AUTHOR INDEX

- | | | | |
|----------------------------|-----------------------------|---------------------------|------------------------------|
| Aki, Sudhir N. V. K., 141 | Gathergood, Nicholas, 156 | Merschaeert, Alain, 181 | Scammells, Peter J., 156 |
| Bhatt, Anand I., 161 | Guo, L. H., 183 | Miao, X., 183 | Scott, Janet L., 161 |
| Bicker, M., 214 | Hu, C. W., 183 | Mikkola, Jyri-Pekka, 197 | Sjöström, Jesper, 130 |
| Bond, Alan M., 161 | Husson, P., 172 | Mohanty, Amar K., 206 | Smith, Thomas J., 147 |
| Brennecke, Joan F., 141 | Iotov, Philip I., 161 | Murzin, Dmitry Yu., 197 | Strauss, Christopher R., 161 |
| Choi, Minkee, 144 | Iwamoto, Tokinori, 138 | Ochiai, Bungo, 138 | Tortoioli, Simone, 191 |
| Delhaye, Laurent, 181 | Jacquemin, J., 172 | Ott, L., 214 | Vaccaro, Luigi, 191 |
| Diker, Khalid, 181 | Kalcheva, Sasha V., 161 | Padua, A. A. H., 172 | Virtanen, Pasi, 197 |
| Donck, Thomas, 181 | Karhu, Hannu, 197 | Parulekar, Yashodhan, 206 | Vogel, H., 214 |
| Du, Y., 183 | Li, G. Y., 183 | Pizzo, Ferdinando, 191 | Yang, Y., 183 |
| Dubey, Amit, 144 | Lou, Wen-Yong, 147 | Qi, W. Y., 183 | Zhang, Jie, 161 |
| Endo, Takeshi, 138 | Luo, J., 183 | Ryoo, Ryong, 144 | Zong, Min-Hua, 147 |
| Fringuelli, Francesco, 191 | MacFarlane, Douglas R., 161 | Salmi, Tapio, 197 | Zuccaccia, Cristiano, 191 |
| Garcia, M. Teresa, 156 | Majer, V., 172 | Saurer, Eric M., 141 | |

FREE E-MAIL ALERTS AND RSS FEEDS


Contents lists in advance of publication are available on the web *via* www.rsc.org/greenchem - or take advantage of our free e-mail alerting service (www.rsc.org/ej_alert) to receive notification each time a new list becomes available.

RSS Try our RSS feeds for up-to-the-minute news of the latest research. By setting up RSS feeds, preferably using feed reader software, you can be alerted to the latest Advance Articles published on the RSC web site. Visit www.rsc.org/publishing/technology/rss.asp for details.

ADVANCE ARTICLES AND ELECTRONIC JOURNAL

Free site-wide access to Advance Articles and the electronic form of this journal is provided with a full-rate institutional subscription. See www.rsc.org/ejs for more information.

* Indicates the author for correspondence: see article for details.

 Electronic supplementary information (ESI) is available *via* the online article (see <http://www.rsc.org/esi> for general information about ESI).

Issues in Toxicology

New series from the RSC

Series Editors

Professor Diana Anderson, *University of Bradford, UK*

Dr Michael D Waters, *National Institute of Environmental Health Science, USA*

Dr Timothy C Marrs, *Food Standards Agency, UK*

This series is devoted to coverage of modern toxicology and assessment of risk and is responding to the resurgence in interest in these areas of scientific investigation.

Topics covered include: hair in toxicology; toxicogenomics; reproductive (particularly male mediated) toxicology; biomarkers in toxicology; and possible chemical warfare.

Ideal as a reference and guide to investigations in the biomedical, biochemical and pharmaceutical sciences.

Readership

Academic researchers, graduate students, government institutions

Market

Toxicology, biomedicine, biochemistry, forensics and environmental/pollution sciences

Format

Hardcover

First title in the series

Hair in Toxicology: An Important Bio-Monitor

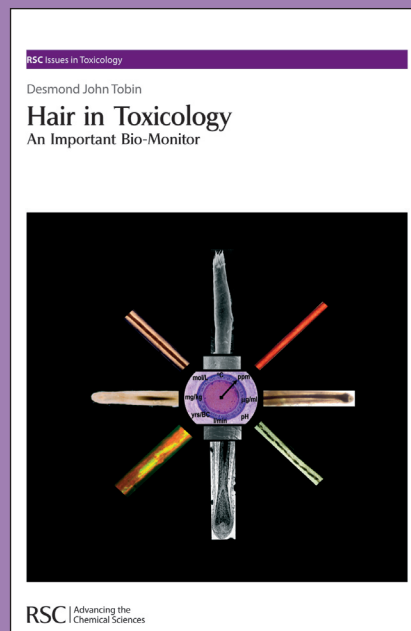
Edited by Desmond John Tobin, *University of Bradford, UK*

The first book of its kind devoted exclusively to in-depth analysis of the hair shaft, as an important tool for a diverse range of scientific investigations.

It covers:

- Information on the exposure of hair to chemicals and pollutants
- Toxicological issues relevant to the use of 'hair care' products
- The ability of hair to capture information on personal identity, chemical exposure, and environmental interactions
- How hair can provide an understanding of human life from archaeological and historical perspectives
- Future direction in the use of hair in toxicology

0 85404 587 2 | 297 pages | £79.95 | 2005



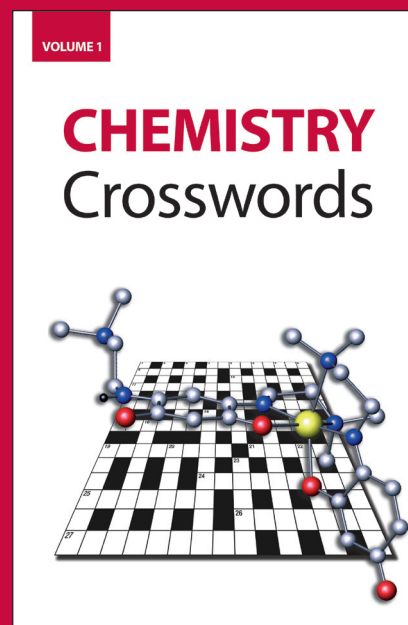
14 across. Alchemy provokes
angry rebuke?(9,10)

Answer: Chemistry Crosswords

- With interesting clues spanning all areas of chemistry
- The perfect gift for a chemist
- Go online buy your copy today!

Try our other puzzle book
Chemistry Su Doku Vol. 1

Softcover | 0 85404 689 5 | 2005 | 106 pages | £7.95



Looking for a stimulating read?

Try Critical Reviews in Chem Soc Rev - they provide:

- accessibility to the general reader via a specially written introduction
- a critical discussion of the existing state of knowledge
- a balanced assessment of the current primary literature
- emphasis on implications for the wider scientific community

See below for recent examples of Critical Reviews:



Cyclam complexes and their applications in medicine

Xiangyang Liang and Peter J Sadler

The syntheses and catalytic applications of unsymmetrical ferrocene ligands

Robert C J Atkinson, Vernon C Gibson and Nicholas J Long

Recent developments in the supramolecular chemistry of terpyridine-metal complexes

Harold Hofmeier and Ulrich S Schubert

Chiral N-heterocyclic carbenes as stereodirecting ligands in asymmetric catalysis

Vincent César, Stéphane Bellemin-Lapponaz and Lutz H Gade

Microwaves in organic synthesis. Thermal and non-thermal microwave effects

Antonio de la Hoz, Ángel Diaz-Hortiz and Andrés Moreno

Stimuli responsive polymers for biomedical applications

Carolina de las Heras Alarcón, Sivanand Pennadam and Cameron Alexander

Anti-inflammatory metabolites from marine sponges

Robert A Keyzers and Michael T Davies-Coleman

Activity of water in aqueous systems: a frequently neglected property

Mike J Blandamer, Jan B F N Engberts, Peter T Gleeson and João Carlos R Reis

Role of sulfur chirality in the chemical processes of biology

Ronald Bentley

The cyclopropene pyrolysis story

Robin Walsh

Dinitroso and polynitroso compounds

Brian G. Gowenlock and George B. Richter-Addo

Reflections on “green chemistry” in 2005

DOI: 10.1039/b600591h

On December 11–13 2005, the Royal Society of Chemistry held an international conference at Robinson College, Cambridge, to discuss the role of catalysis and biocatalysis in green chemistry. Almost at the same time, various sections of PACIFICHEM 2005 were dealing with related topics on the other side of the globe in Hawaii. These events marked a successful final for a large number of highly stimulating symposia featuring green chemistry topics last year all around the world. This prompted me to look back on 2005 and to reflect a little bit on the development of the journal and the field in that year. (The fact that I was co-chairing the meeting in freezing Cambridge and envied my colleagues in sunny Waikiki had of course nothing to do with this!).

From the many things that happened in the context of green chemistry in 2005, two things were most vivid in my recollections. In early summer, the latest impact factors for scientific journals were published and *Green Chemistry* achieved the remarkable value of 3.50. I have to admit that this exceeded even my most optimistic expectations! This index puts *Green Chemistry* among the most widely cited chemistry journals and shows that it covers a highly topical

field at a very high scientific standard. This extraordinary success reflects the enthusiasm and activity of a fast growing scientific community and is a stimulation to further increase our efforts to ensure the best service to our authors and readers.

The second unexpected news came with the announcement of 2005's Nobel Prize. Of course, it was already anticipated for a while within the chemical community that the contributions of Yves Chauvin, Bob Grubbs, and Richard Schrock to the development of olefin metathesis as an inevitable tool in modern synthetic chemistry would be recognized in Stockholm. It was, however, a very positive surprise to see that the potential of their fundamental achievements for application in green chemistry was mentioned explicitly as part of the motivation for the committee's decision (<http://nobelprize.org/chemistry/laureates/2005/press.html>).

So, does this mean we are all set? The field is flourishing, it is recognized as an important part of chemistry, and now the journal just needs to harvest the fruits of the research that is going on all around the world? Well, I guess things are not yet that simple. There are still two extreme positions which I often

encounter in discussion with colleagues and between which the journal has to continuously adjust its position. One would be that all chemical progress is *a priori* “green” because it will somehow improve chemical processes and thus we do not need to worry about green chemistry in the first place. Although it would be nice if this was the case, the past and present environmental disasters arising from chemical production show that we can unfortunately “improve” processes pretty much in the wrong direction. The other argument is that there might be a tendency for more routine chemistry to label itself “green” in order to be recognized as good science. The only answer to such a dangerous trend is to continuously apply the highest possible standards in all areas of green chemistry such as research proposals and projects, teaching exercises, conferences and of course publications.

With these brief reflections, I hope that all *Green Chemistry* staff, board members, authors, reviewers and readers had a terrific start to 2006, and that we will all have fun continuing this scientific success story further!

Walter Leitner
RWTH-Aachen, Germany

First China–USA Green Chemistry Workshop

DOI: 10.1039/b516635g

The First China–USA Green Chemistry Workshop was held in Beijing, China, May 27–June 1, 2005.

In one of the first joint US National Science Foundation/Natural Science Foundation of China workshops, 11 US, one Canadian, and 12 Chinese participants met May 27–June 1, 2005 in Beijing to discuss the ‘Science Drivers and Implementation Challenges of Green Chemistry’. The workshop was co-organized by Professor Robin D. Rogers (Director of the Center for Green Manufacturing at The University of Alabama) and by Professor Shengming Ma (Shanghai Institute of Organic Chemistry and Zhejiang University).

Dr Ken Doxsee (US) and Dr Chen Yong-Jun (China) represented the funding agencies and articulated the goals of defining concrete research objectives (“science drivers”) and identifying potential US–China collaborative efforts. The participants focused on issues of energy, clean solvents, novel catalysis, renewable resources, eco-efficiency, and the like; in short, those elements that are central to the principles of green chemistry and to the principles of sustainable engineering. The group considered such questions as ‘Why is green chemistry necessary?’; ‘What are the global and international challenges that require green chemistry approaches?’; ‘How can a diverse workforce be developed for this field?’; ‘How can new green technologies be implemented?’; ‘How can green chemistry progress be measured?’; and

‘How can environmental advantages of a green technology be assessed?’.

Scientific lectures in areas each country considers to be ‘green chemistry’ were presented against the backdrop of significant discussions of the cultural differences, the relationships between industry and academic institutes, policy implementation, and the role of government and funding agencies in developing a scientific field. The workshop provided an excellent opportunity and starting point for scientists and engineers from both countries to get to know each other, exchange points of view, and begin developing a framework for future collaboration in an area of increasing social importance.

In China, “green” is a very popular and “positive” word. There are a couple of institutes specifically devoted to research in green chemistry in Chinese universities. In the whole country there are also a few research groups focusing their attention exclusively on green chemistry. It is common that the professors in the Chinese Academy of Sciences and universities have a very strong “green” view for their research projects.

The National Natural Science Foundation of China is a very strong supporter for research in the area of green chemistry. Since 2000 more than 300 individual projects in green chemistry, including more than 10 key

programs (18 200 000 RMB) and one major project (8 000 000 RMB) in green chemistry have been funded. The Chinese government encourages research projects closely related to industrial application. Interestingly, however, while some of the Chinese work seems very applied and ready for transition, work in US universities is often clearly less ready, yet more often transitioned.

The problem in China is that the term ‘green chemistry’ has been misused and this has become an obstacle to getting society to believe green chemistry is important. (In some cases it is abused by business people to attract customers to their not-so-green products.) There is also a large gap between academic laboratory work and industrial practice.

China has large state run petroleum chemical companies, most of the processes they are using are relatively clean, and the scientists from the related academic institutes are conducting research seeking more environmentally green technology. However, most of the pollution from the chemical industry is produced in the process of manufacturing fine chemicals and pharmaceuticals. In this territory, although some advanced technologies are being applied, more attention should be paid to the environmental impact since a multitude of small fine chemical companies are actively involved in the fine chemical industry.

Hot Areas of Green Chemistry were identified by the participants and included: Catalysis; New Chemistries; Green Process; Design for Biodegradation; New Sources of Renewable Energy and Feedstocks; Enhanced Energy Efficiency; Utilization of Quantitative Life Cycle Assessment Tools; and Education, Education, Education. The role of education was clearly identified at the Workshop as being crucial if green chemistry, and sustainability in general, are to become primary aspects of the chemistry profession, both in the US



and in China. Interestingly, several educational audiences were identified, each of which requires a unique approach:

- **The Academic Community (Faculty and Students):** Strategies need to be developed for making green chemistry—and, more broadly, Education for Sustainable Development—an integral part of what students are taught, in both the US and China.

- **The Chemical Industry (Leaders and Research Managers):** Awareness of, and interest in, green chemistry must be increased in the chemical industry, in both the US and China.

- **Government Officials, Funding Agencies, and Non-Governmental Organizations:** A specific recommendation emerged for education and training initiatives (short courses, workshops, *etc.*

in the US, with follow-on activities in China) with a US/China focus. The specific target group would be the cadre of Chinese graduate students, postdoctoral research staff, and beginning faculty who are currently enrolled in or training at US universities, and are planning to return to China in the near future to take up academic or industrial positions.

Specific Recommendations arising from the Workshop tended to run the gamut from political to social to developmental. It was a clear sign that the research community has a lot of follow work to do in order to more fully define and articulate the mission of green chemistry, much less how it can be systematically implemented. Nonetheless, it is clear that the US and China are both

dealing with similar sustainability issues: energy needs, greater use of biomass resources, cleaner chemical processing, *etc.* Together, China and the US can determine the role of green chemistry in the economic growth and development of the planet. It is hoped that this meeting has taken at least a small step toward ensuring that our respective research communities work together in educational and research initiatives designed to bring green chemistry ideals and new sustainable technologies to fruition.

Martin Abraham (Toledo), *Jeffrey Steinfeld* (MIT), and *Shengming Ma* (Shanghai) were instrumental in the drafting of this report.

Robin D. Rogers, The University of Alabama, USA

Highlights

DOI: 10.1039/b600296j

Markus Hölscher reviews some of the recent literature in green chemistry

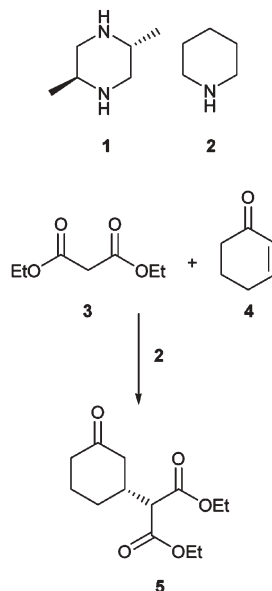
Tetrazole derived catalysts for asymmetric malonate conjugate addition to enones

Organocatalytic approaches to asymmetric transformations combine all the advantages which are valid in general for classical homogeneous catalysis with the charm of not having a metal present in the reaction mixture. Despite the efficiency of properly tuned metal centres (type of metal, ligand, solvent, reaction conditions, *etc.*) there always is the potential danger of contaminating products with the catalyst metal due to leaching processes, which even in the ppb range might be undesired due to the quality requirements of the product (health, safety). Apart from these issues organocatalysts might be easier to obtain, to handle or to deposit than their classical metallic counterparts. One interesting case in which catalytic transformations are possible with classical organometallic catalysts and organocatalysts is the conjugate addition of malonates to enones. Ley *et al.* from the University of Cambridge have recently investigated the performance of bases **1** and **2** as organocatalysts in the addition of various malonates of type **3** to various enones such as **4**.¹

The authors find the performance of piperidine (**2**) results in higher conversions compared to the usage of **1** under otherwise identical reaction conditions, while ee values range between moderate to high. As an example, the addition of malonate **3** to cyclohexenone **4** in the presence of **2** resulted in the formation of **5** with 89% conversion and 92% ee. The substrate width proved to be fairly broad rendering this interesting transformation an alternative to other catalytic varieties.

Exceptionally high carbon dioxide storage in metal organic frameworks

Though chemically harmless it is generally acknowledged that carbon dioxide is



contributing a significant if not alarming extent to the green house effect which leads to a constant increase of the atmosphere's temperature with all the known fatal consequences this may result in. One of the urgent steps that needs to be taken during the next few decades is the serious and drastic enforcement in reducing the amount of CO₂ emitted to the atmosphere. One possibility at hand is the storage of CO₂ in areas in which its formation cannot be prevented. As the treatment of CO₂, *e.g.* from the exhaust gas streams of power plants by passing it through aqueous amine solutions, is costly and inefficient, effective adsorption in porous materials can be an interesting alternative, which was pursued by Millward and Yaghi from the University of Michigan.² The authors compared a variety of metal organic frameworks with structurally defined micropore volume in adsorption experiments with CO₂. The material which proved to show the highest adsorption capacity for CO₂ is synthesized by reacting a mixture of H3BTB (BTB = 1,3,5-benzenetribenzoate) and Zn(NO₃)₂·6H₂O at 100 °C in diethylformamide (DEF) resulting in the formation of crystals of compound

Zn₄O(BTB)₂(DEF)₁₅(H₂O)₃, which was named MOF-177. The pores of this compound have average diameters of *ca.* 11–17 Å and upon adsorption of CO₂ at pressures of *ca.* 35 bar the adsorption capacity was determined to be 33.5 mmol g⁻¹. This clearly outperforms all other materials tested and also the best reported zeolite (zeolite 13X, 7.4 mmol g⁻¹) and the carbon material MAXSORB (25 mmol g⁻¹). Despite this interesting progress it should also be noted that storage is most certainly only one of the required steps to minimize the CO₂ problem as the question of what is happening to the stored CO₂ in the long term also needs to be addressed.

Copper nanoparticles in quasi-homogeneous methanol syntheses

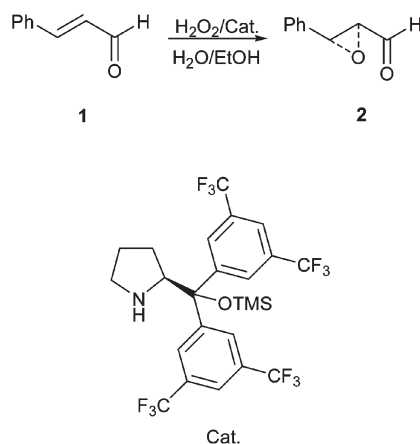
Approximately 28 million tons of methanol are made each year from synthesis gas, demonstrating the importance of industrial methanol syntheses. The technically used catalyst is a heterogeneous Cu/ZnO/Al₂O₃ catalyst, for which the Cu and the Zn centres are said to be active sites. Despite the many reports about copper-based catalysts for this reaction no clear understanding of the nature of the active sites, the role of Cu and ZnO and the reaction mechanism has evolved. Schüth *et al.* from the Max-Planck-Institute for Coal Research, Mülheim, have started to shed light on how methanol might be formed, by following an approach which deviates substantially from the technical procedure, but adds lots of substantial information about this reaction.³ The authors synthesized copper nanoparticles by reducing copper acetylacetonate in THF with different trialkylaluminium compounds, yielding deep red colloidal copper nanoparticles stabilized by the organoaluminium compounds. The nanoparticles were stable over months in the absence of air and their sizes were *ca.* 4.5 nm according to TEM analyses. High-resolution TEM

analyses showed the nanoparticles to be crystalline, and EXAFS experiments showed copper to be present in the oxidation state zero. Furthermore EXAFS analyses proved the absence of oxygen and also showed that the coordination number of the Cu centres was significantly lower (10.9) than for bulk copper (12). THF solutions of freshly prepared samples proved active for the synthesis of methanol from synthesis gas starting at temperatures as low as 130 °C. Catalytic productivity P ($\text{mol}_{\text{MeOH}} \text{kg}_{\text{Cu}}^{-1} \text{h}^{-1}$) ranged between 2.6 and 25.2 mol for temperatures between 130 °C and 170 °C. A comparison between a commercially available ICI catalyst and the Cu nanoparticles at 150 °C showed the nanoparticles to be less productive (4.0) than the ICI catalyst (5.5), however, the nanoparticles do not contain ZnO. Information about the reaction mechanism also was collected. Exchanging H_2 in the $\text{H}_2/\text{CO}/\text{CO}_2$ synthesis gas mixture by D_2 showed deuterium to be incorporated in the methanol molecules confirming the generation of methanol truly stems from the synthesis gas. The formation of methyl formate, which might be interpreted as being a by-product, was found to reach a constant concentration after an induction period, in which the concentration increased. To clarify if methyl formate is a by-product or an intermediate the reaction was carried out with synthesis gas only with no CO_2 present and methanol production was found to be negligible. In the second test experiment only H_2 and CO_2 were used but no CO resulting in initial methanol formation which dropped to zero after 10 h. The third test experiment used again CO/H_2 and a trace of methyl formate yielding fast initial methanol formation. The combined conclusion from these three experiments suggests the reduction of CO_2 to methyl formate to be the initial step for methanol formation with hydrogenolysis of methyl formate generating methanol. These remarkably active Cu nanoparticles might serve as the entrance

to a detailed understanding of the technical process in the future.

Water–alcohol solutions as solvents for organocatalytic asymmetric epoxidation

Water is *the* environmentally friendly solvent, and so it is not surprising that its use in chemical transformation has attracted much interest. Furthermore it is cheap and safe. Catalytic asymmetric epoxidations are important in organic chemistry as they result in the formation of optically active epoxy products. If such reactions could be carried out in water or mixtures of water and other environmentally harmless solvents, major progress would be made for applied asymmetric catalysis. Jørgensen *et al.* from Aarhus University investigated the performance of a pyrrolidine catalyst for the epoxidation of α,β -unsaturated aldehydes in water–alcohol mixtures.⁴



The authors started their study by running the epoxidation of **1** in the presence of aqueous H_2O_2 and dichloromethane, which was a good solvent, as it resulted in a conversion of 99% yielding an enantiomeric excess of 96% with a dr value of 97 : 3. Interestingly, pure water is fairly useless as a solvent as the conversions obtained stayed as low as 28%. However, upon addition of ethanol, which also is an environmentally

acceptable solvent the reaction proceeded with good conversions (97% for a water–ethanol mixture with 1 : 1 ratio). The dr value was 87 : 13 and the ee value amounted to 92%. THF–water mixtures do not perform well and also the variations of the oxidant did not lead to any better results.

Eden Project opens one of the most sustainable buildings in the world

Over 100 years *ca.* 12 trees can remove approximately 9 tons of CO_2 from the atmosphere. This amount is saved annually from now on by the new photovoltaic system built into “the core”, which is at the heart of the Eden Project in Cornwall. The Eden Project was established as one of the landmark Millennium projects in the UK to mark the year 2000 and is structured as an educational charitable trust. The trust’s interests lie in explaining how the natural world works seen through the lens of plants, exploring how people might best organise themselves in the face of this knowledge and thereby reach an understanding of what sustainability might mean and, through best practice of these principles, create an organisation that is sustainable to act as a model for others. The core is the new Education Centre of the Eden Project and London-based leading solar photovoltaics (PV) company Solarcentury has equipped the core with a sustainable PV system which will generate *ca.* 20 000 kW h of electricity each year: enough energy to light an average three-bedroom house for over 33 years.

References

- 1 K. R. Knudsen, C. E. T. Mitchell and S. Ley, *Chem. Commun.*, 2006, 66–68.
- 2 A. R. Millward and O. M. Yaghi, *J. Am. Chem. Soc.*, 2005, in press.
- 3 S. Vukojevic, O. Trapp, J.-D. Grunwaldt, C. Kiener and F. Schüth, *Angew. Chem.*, 2005, **117**, 8192.
- 4 W. Zhuang, M. Marigo and K. A. Jørgensen, *Org. Biomol. Chem.*, 2005, **3**, 3883–3885.

Green chemistry in perspective—models for GC activities and GC policy and knowledge areas

Jesper Sjöström

Received 8th August 2005, Accepted 16th November 2005

First published as an Advance Article on the web 6th December 2005

DOI: 10.1039/b511316d

This article presents two new models that give a perspective on green chemistry (GC). The first model is a classification model of different *green chemistry activities*, while the second model concerns *green chemistry policy and knowledge areas* (green chemistry principles, industrial biotechnology and “the green sector”). A broad view of green chemistry is used, where all activities with the aim of greening of chemistry and chemical practice are included. The classification model consists of three main parts: (1) research activities ((a) basic chemical research; (b) chemical engineering), (2) management activities ((a) laboratory practice; (b) production; (c) consumption) and (3) policy activities. This article refers to over seventy publications, covering a broad area of research and type.

Introduction

Due to global contamination and other environmental and health risks of chemicals¹ there is an urgent need for a “greening² of chemistry” in a broad sense.³ The public image of chemistry has been unfavourable since the 1960s, due to the fact that chemists and the chemical industry until recently to a large extent have ignored the environmental impacts of chemical activities.⁴ As a response to the “green challenge” and as a way to improve the image of chemistry, the so-called green chemistry movement started in the US in the early 1990s.⁵ Since then it has spread all over the world. In addition to the US, both Italy and the UK early launched major programs in green chemistry. Today there are research programmes and centres in green chemistry in America, Europe, Asia, Australia and Africa.⁶ The number of scientific

publications with the key word “green chemistry” has increased substantially during the last five years.⁷

Green chemistry is not a scientific discipline in the normal sense. Instead it is a *meta-discipline* that covers most of chemistry and chemical engineering.⁸ The guiding principle is prevention rather than cure. The founding fathers Paul Anastas and John Warner formulated the widely spread twelve principles of green chemistry in 1998.⁹ Since then these principles have been supplemented with twelve more practically oriented principles for process chemists¹⁰ and, more recently, with twelve general principles of green engineering.¹¹ To summarise, the principles of green chemistry entail: (1) renewables as chemical feedstocks, (2) substitution¹² of hazardous chemicals, and (3) reduced consumption of chemicals and energy.

Some researchers have broadened the picture from just the technological development, and have discussed chemistry in relation to different sustainability perspectives (history, ethics, sociology, economics, *etc.*).¹³ Other researchers have discussed chemical engineering in relation to sustainable development.¹⁴ For example, Jin *et al.* have problematised the ideal of economic growth of the mainstream environmental policy making, and debates.

The purpose of this article is to suggest two models that may systematise our understanding of various green chemistry activities and policy/knowledge areas, respectively. The first model is a classification model of different *green chemistry activities*, while the second model is about *green chemistry policy and knowledge areas*.

In this journal, “green chemistry” is normally associated with the twelve principles of green chemistry and connected research about benign chemical reactions and products. In this article, however, I am using a broader view of green chemistry, where I include all activities and policy/knowledge areas with the aim of greening of chemistry and chemical practice. Such a broader view is useful to get an understanding of societal processes in the direction of greening of chemistry.

Research Policy Institute, Lund University, Ideon Alfa 1, Scheelevägen 15, SE-223 63 Lund, Sweden



Jesper Sjöström

Jesper Sjöström was born in Malmö, Sweden in 1974. In 2002, he received a PhD in the field of surface and colloidal chemistry at Lund University, Sweden. In addition to chemistry, he has studied environmental management and science teaching. Furthermore, he has studied pharmaceuticals and has practical experience of pharmaceutical R&D. Since 2003 he has been undertaking research within the broad field of STS (= Science,

Technology and Society) at the Research Policy Institute at Lund University. One of his projects focuses on the emerging innovation system of green chemistry.

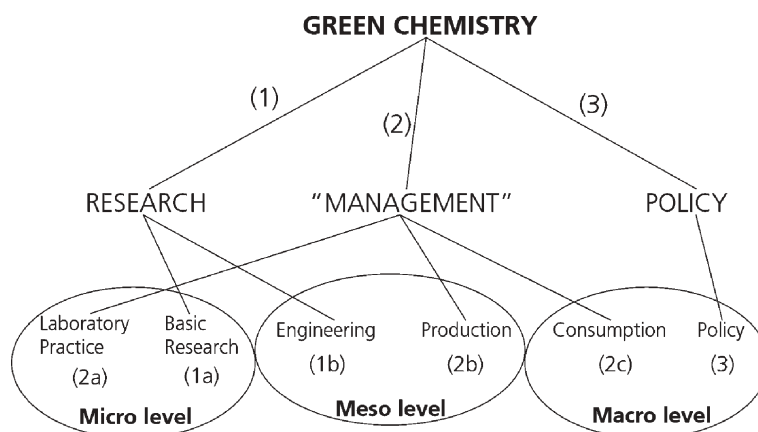


Fig. 1 Classification model of green chemistry activities.

Classification model of GC activities

The classification model (see Fig. 1) consists of the following three main parts: *research activities* (science and technology), *management activities* (organisation) and *policy activities*. The research activities, in turn, are divided into two parts: (1a) basic chemical research, and (1b) chemical engineering. The management activities are divided into three parts: (2a) cleaner laboratory practice, (2b) cleaner production, and (2c) sustainable consumption. Both cleaner laboratory practice and basic chemical research are activities on the *micro* level (molecular and laboratory level). Chemical engineering and cleaner production are activities on the *meso* level (production processes and products), and systems of sustainable consumption¹⁵ and policy activities on a *macro* level (system level).

Thomas Graedel, one of the founders of the field industrial ecology, has earlier presented a four-level system for green chemistry (see Fig. 2).¹⁶

His model focuses on chemical production and consumption on different societal levels. The model suggested here differs in mainly two ways from the model of Graedel: (1) In addition to research, production and consumption, my model includes laboratory practice; and (2), in contrast to Graedel who uses circles within circles, I place the different activities side by side. The reason for this is that I want to emphasise that all the activities are important; the practical “green chemistry” performances are made by individuals on the “micro level”.

A systematic discussion of the parts in the classification model (see Fig. 1) follows below.

(1) Research activities

Two types of research activities can be identified within the meta-discipline of green chemistry. One type (1a) is oriented towards making basic chemical reactions more ecologically friendly, whereas the other type (1b) is oriented towards process development. Type 1a is concentrated on synthesis (*i.e.*, to discover, improve and optimise synthesis pathways), whereas type 1b has a focus on good economisation (of materials, substances and energy). Most of the topics discussed in a recent workshop about green chemistry and engineering in the UK can be classified as either based on basic research (“New Chemical Routes—Solvents and Chemicals”;

“Catalysis, Biocatalysis and Materials”) or as being more oriented toward engineering (“Raw Materials, Agriculture and Chemistry”; “New Process and Process Strategies”). *Via* these topics the whole life cycles of chemicals were covered.¹⁷

(1a) Basic chemical research. The early green chemistry movement had a focus on green molecules and synthesis, that is, basic chemical research. Most of the twelve principles are aimed at improving organic synthesis. It refers to the use of alternative solvents, different catalysts, and improvements of the molecular performance in different ways. Still there are many publications dealing with green chemistry in the small laboratory scale, that is, the first steps in a development process. Two main types of activities can be identified in the area of basic green chemistry research: (1) catalysts development, and (2) alternative solvents (*e.g.* supercritical fluids, ionic liquids and water).

(1b) Chemical engineering. More closely related to the interest of the chemical industry is the improvement of

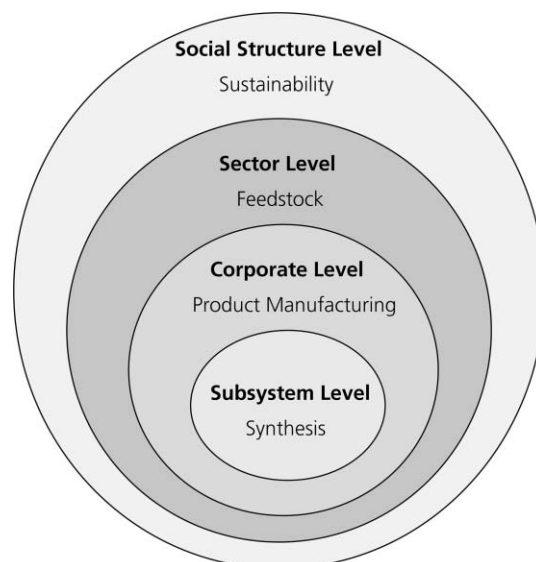


Fig. 2 Graedel's four-level system for a sustainable green chemistry (Fig. 3 in ref. 16).

chemical production processes, including reaction conditions and separations. Research activities in the area of green chemical engineering are, for example, the use of renewable resources as chemical feedstock and efficient material, and energy flows in chemical production processes. Dale has discussed the transformation from crude oil to renewable resources within the chemical industry.¹⁸

(2) Management activities

Green chemistry does not necessarily refer to research activities with the goal of being technologically innovative. The concept also includes different forms of behaviour and management. As was mentioned above, green chemistry management activities can be divided into three types: (2a) cleaner laboratory practice, (2b) cleaner production, and (2c) sustainable consumption. The purpose of all these activities is cleaner chemical practice.

(2a) Cleaner laboratory practice. Cleaner laboratory practice refers to behaviour and education with the purpose of creating more environmentally friendly ways of doing laboratory work. This work can be implemented in R&D laboratories, but also in schools and university education. It has recently been discussed how to effectively minimise hazardous waste in academia using the green chemistry approach.¹⁹

Green chemistry educations can also be classified within this type of activity. Some US universities have degree programs in green chemistry. In Europe, the *European Chemistry Thematic Network* (ECTN)²⁰—an education network consisting of about 90 universities from 24 European countries—has had a working group on “Green and Sustainable Chemistry”. The group suggested a “public display of the twelve principles of green and sustainable chemistry in all chemistry departments”. It also discussed possible changes in laboratory practice, such as reductions of scale, replacement of experiments and increased use of computer simulations. Similarly, Tallmadge *et al.* have discussed the incorporation of the principles of environmental stewardship into the high school chemistry classrooms by using micro-scale chemistry.²¹

(2b) Cleaner production. Cleaner production is the international term for more environmentally friendly product manufacturing in a broad sense.²² The focus is primarily on the corporate level. Important for cleaner production—which is typically regarded as a way to achieve industrial ecology—are environmental technologies. Except for the manufacturing, processing and formulation steps, green chemistry concepts can also be applied to the other stages in product manufacturing (*e.g.*, materials acquisition and input; packaging and distribution; product use; recycling, reuse and disposal). Anastas and Lankey have used the term “life cycle innovation” for this approach.²³ In line with this, Graedel claims that “green chemistry is more than green synthesis”. Consequently, he has tried to place green chemistry in the context of industrial ecology.²⁴ In the area of industrial sustainable development, many different concepts are in use. These can be divided into macro-scale concepts (sustainable development and industrial ecology), firm-wide concepts (cleaner

production and pollution prevention) and operational concepts (*e.g.* waste minimisation, recycling and pollution control).²⁵ Hamner argues that cleaner production is what a good environmental management system is supposed to implement. The concept of pollution prevention is very similar to cleaner production, but more focused on the manufacturing process. The former is a term used in the US, whereas the latter was coined by the United Nations. Since the mid-1980s there has been a change in focus from cleaner production processes over environmental management to cleaner products.²⁶ Recently, Jenck *et al.* reviewed the area of achievements and prospects for a sustainable chemical industry in Europe.²⁷

In the area of cleaner chemical production there are mainly two types of activities. The first type is boundary organisations between industry and academia. Several green chemistry organisations publish textbooks and journals, arrange conferences, and also function as links between academia and industry. The purpose of these organisations is to spread concepts, knowledge and experience in the area of green chemistry. Examples of such organisations are the *Green Chemistry Institute* (GCI)²⁸ in the US, the *Green Chemistry Network* (GCN)²⁹ in the UK and the *Green and Sustainable Chemistry Network*³⁰ in Japan. A network with a special focus on industry implementations and transfer of technology to the industry is the *Crystal Faraday Partnership* in the UK. It was launched as a virtual green chemical technology centre in 2002 by the Royal Chemical Society, the Chemical Industries Association and the Institution of Chemical Engineers. The purpose of the network is to connect academic green chemistry researchers with chemical firms.

The second type is change programmes within companies. Since the late 1980s the chemical industry has had a voluntary program called *Responsible Care*.³¹ It is a self-regulated program (without sanctions) with the purpose to improve environment, health and safety performance beyond state regulations. These improvements should cover both production processes and products. Today it is a commitment of the international chemical industry globally. The basic principles are regulated by the *International Council of Chemical Associations* (ICCA) and every country formulates its own program in line with the local industry culture. The practical work, however, is implemented by the member companies themselves. Today approximately 45 countries have Responsible Care programs.

The American Responsible Care program was until recently based on ten guiding principles and six codes of management practices. These codes address how a firm interacts with the community (community awareness and emergency response code), manages its facilities (pollution prevention, process safety and employee health and safety codes) and interacts with supplier and customers (the distribution and product stewardship codes).³² The ICCA has outlined eight elements of their Responsible Care program, where the ten guiding principles are the first element.

As a response to the criticism of the American Responsible Care program,³³ the *American Chemical Council* (ACC) recently strengthened the program. For example, the program now includes a management system (Responsible Care

Management System) compatible with the ISO 14001 environmental management system. Furthermore, to increase transparency, ACC members must, starting in 2004, publicly report their performance on an annual basis based on a series of environmental and business metrics.³⁴ With the recent changes of Responsible Care there will also be a closer connection between the program and laboratory practice at the member companies.³⁵

During the last years there has been an increasing focus on product performance. The part of the Responsible Care program dealing with products is called *Product Stewardship*. To achieve green chemical products one can use different management and evaluation tools, such as product chain management and LCA. One suggested business model is to sell services instead of products. In this way, the economic interest no longer lies in selling the chemical product, but in providing a chemical service. The concept has, for instance, been called “full chemical management”,³⁶ “servicing”,³⁷ and “chemical leasing”.³⁸

(2c) Sustainable consumption. With the term sustainable consumption³⁹ the role of improved consumption patterns is highlighted. In the context of chemicals the term refers not only to the use of benign chemicals and in lower amounts, but also to the question if the chemicals are needed at all; perhaps we should think of the “zero-alternative” before we try to substitute feedstocks, productions processes and hazardous chemicals.

The European Commission has presented an environmental technologies action plan (ETAP) with the purpose of bridging the objectives of economic growth (and innovation) and cleaner environment.⁴⁰ This environmental research policy is based on *the policy discourse of ecological modernisation*, which is the mainstream discourse among European governments and research funding agencies.⁴¹ It can be described with terms such as “green business” and “multi-sector collaborations”, and is based on a fundamental belief in scientific-technological progress.⁴² However, it has been criticised for only problematising production, but not consumption.⁴³ McNeill points out that the total amount of pollution in the world has increased, although the pollution per production unit has decreased due to cleaner technologies; nevertheless, the total level of consumption is increasing.⁴⁴

An issue of importance for chemical legislation is the substitution of hazardous chemicals. In the Gothenburg region in Sweden there is a practically oriented project called “Project Green Chemistry”. The purpose of this is to apply the concept of “green chemistry” by stimulating the development of more environmentally friendly consumption patterns of chemical products on the micro level. The project has, together with many regional companies, worked with for example lubricants, tyres, bottom colours for boats and car service chemicals.⁴⁵

(3) Policy activities

Within the area of green chemistry there are also policy activities in several different sub-areas. These include (innovative) green chemistry,⁴⁶ industrial (“white”) biotechnology,⁴⁷ renewable resources,⁴⁸ substitution of hazardous

chemicals,⁴⁹ chemical safety⁵⁰ and an eco-transition of the chemical industry.⁵¹ In March 2004, the European Commission arranged a Round Table on White Biotechnology in Brussels. At the meeting were representatives of many different stakeholders, including the industry sector organisations EuropaBio,⁵² Cefic⁵³ and ERRMA.⁵⁴ A year later Cefic and EuropaBio formulated a vision for their technology platform on “sustainable chemistry”.⁵⁵ This technology platform consists of the following four parts: (1) materials technology, (2) reaction and process design, (3) industrial (“white”) biotechnology, and (4) horizontal issues (innovation framework and economic outcomes). As both part (2) and (3) in a broad sense can be classified as “green chemistry,” it is useful to examine how these two knowledge areas are interconnected to each other (see further below).

In the EU a new chemical legislation called *REACH* (= Registration, Evaluation and Authorization of Chemicals) is being developed.⁵⁶ The proposed legislation has resulted in a political battleground and very intense and effective lobbying. For instance, the Bush Administration has “campaigned” against REACH. The leaders of the UK, France and Germany have also tried to delay and weaken it.⁵⁷ Also, certain NGOs, such as WWF and Greenpeace, have been involved in lobbying, but instead for a stronger legislation.⁵⁸

Model of GC policy and knowledge areas

To get a mental image of the connection between different policy/knowledge areas related to green chemistry, I have also developed another model (see Fig. 3). It consists of the following three partly overlapping parts: (1) “*the green sector*” (agriculture and forestry), (2) *industrial biotechnology* (biotechnology) and (3) *green chemistry principles* (chemistry). Below I will briefly try to shed more light upon these three parts, as well as upon the policy context, and the intersections between the policy/knowledge areas.

A knowledge-based bio-economy

In the EU there is currently much focus on the vision of an European knowledge-based bio-economy.⁵⁹ In the supposed “vision society” it is common with renewable feedstocks, bio-based processing in a broad sense and bio-based products, such as food, bioenergy, biomaterials, and “green chemicals”.⁶⁰ The vision has been formulated within the discourse of ecological modernisation.

As an instrument for implementing new technologies in the EU, different stakeholders are brought together in technology platforms. In addition to the already mentioned platform on sustainable chemistry, there are also platforms on, for instance, “Plants for the future” and “Innovative and sustainable use of forest resources”.

(1) “The green sector”. During the last decades there has been an increasing interest in materials and energy made from renewable resources. In such a bio-based economy fats and sugars are the “crude oil”. Both the US⁶¹ and Europe⁶² have produced policy documents about how to increase the relative amount of renewable resources in the chemical feedstock supply.

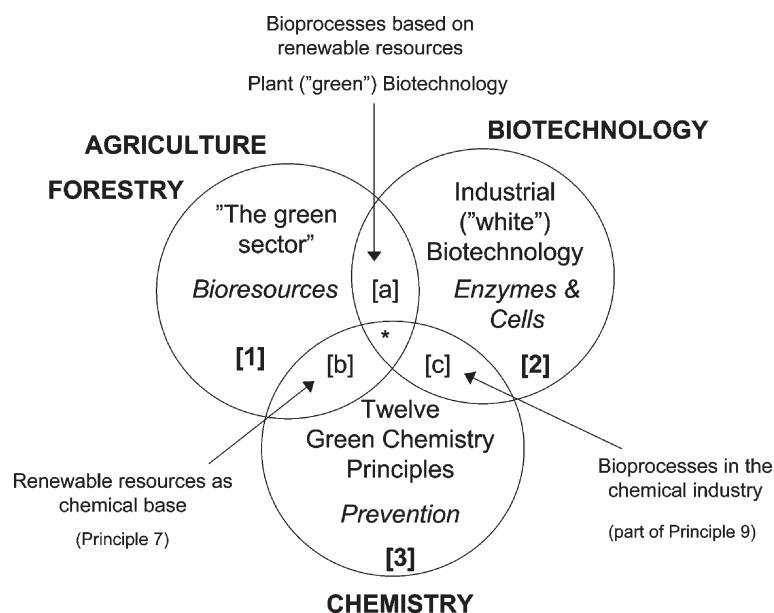


Fig. 3 Model of green chemistry policy and knowledge areas.

(2) Industrial biotechnology. A generally used definition of biotechnology is that it is “any technological application that uses biological systems, living organisms, or derivatives thereof, to make or modify products or processes for specific use”. Much of modern biotechnology is based on the recombinant DNA technology, that was developed in the early 1970s. This technology made it possible to transfer genes from one organism to another and created the base for genetic engineering.⁶³ Modern biotechnology can be divided into the following parts: genetic engineering (genomics), protein engineering (proteomics), bioinformatics, downstream processing (separation technologies) and fermentation technologies.

In recent years, the biotechnology industry in Europe has been divided on the basis of colours:

- *White biotechnology* is the same as industrial biotechnology, that is, industrial use of biological processes (enzymes or organisms) to produce different products.

- *Red biotechnology* is biotechnology related to the biomedicine and/or healthcare sectors, for instance, pharma, gene therapy or genetic testing.

- *Green biotechnology* is biotechnology applied to agricultural processes, such as GM-seeds.

Industrial (“white”) biotechnology is an emerging field within modern biotechnology, that serves the chemical industry among several other industries. Examples of bioprocesses covered by the term are fermentation processes for the production of enzymes, vitamins and antibiotics and enzyme based processes for the production of biofuel, bulk chemicals (e.g. ethanol), (bio)polymers, fine chemicals (e.g. pharmaceutical intermediates) and speciality chemicals.⁶⁴ White biotechnology is seen as having a large potential to contribute to a more sustainable future.⁶⁵ It is seen as giving cleaner production processes with less waste and less impact on the environment and has potential to improve industrial production along all three dimensions of sustainable development

(economy, environment and social development).⁶⁶ However, the concept of white biotechnology is still mainly a policy concept that has not widely penetrated the scientific community working with e.g. industrial biocatalysis.

According to the technology platform on sustainable chemistry the research within the area of industrial biotechnology can be organised in the following nine parts:⁶⁷

- Novel enzymes and micro-organisms
- Fermentation science
- Metabolic engineering and modelling
- Performance proteins and nano-composite materials
- Microbial genomics and bio-informatics
- Biocatalyst function and optimisation
- Bio-catalytic process design
- Innovative down-stream processing
- Integrated bio-refineries

Several of these parts are consistent with the twelve principles of green chemistry.

(3) Green chemistry principles. As was indicated previously the twelve principles of green chemistry can be seen as the knowledge “marriage” between chemical practice and industrial ecology. Much of the activities in the early green chemistry movement were founded on principles for eco-improvements of chemical reactions. However, industrial ecology deals with eco-principles on an industrial level and with management and assessments. Examples of industrial ecology activities are cleaner production, interlinking of material flows and recycling, services instead of products, eco technology (e.g. green engineering⁶⁸), life-cycle assessments,⁶⁹ risk assessments, environmental management and cleaner products.

Intersections

In the intersection of agriculture/forestry and biotechnology (a) in Fig. 3, there are two policy/knowledge areas:

bioprocesses based on renewable resources, and plant (“green”) biotechnology. For both these areas there are high expectations, due to their potential to build up a sustainable bio-based economy, which combines eco-efficient bioprocesses with renewable resources.⁷⁰

In the intersection of agriculture/forestry and chemistry (b) one finds renewable chemical feedstocks (green chemistry principle 7). An example of a chemical product based on renewable resources, but normally produced by conventional chemical processes, is biosurfactants. In the intersection between biotechnology and chemistry (c), on the other hand, one finds bioprocesses in the chemical industry (biocatalysis is part of green chemistry principle 9). An example of a chemical product produced by a bioprocess, but based on petroleum feedstock, is acrylamide.

In the center (*) of Fig. 3 one finds bioproduced chemicals based on renewable resources.

Final notes

In this article, I have presented two new models, which provide social perspectives on different green chemistry activities and policy/knowledge areas, respectively. Together with the over seventy publications that are referred to in the article, the two models have given an overview of the area of green chemistry. Hopefully, this overview will be of use as researchers, practitioners, and companies try to become better oriented in the field, not least as future paths are decided.

I finish the article with a few words about the implementation of green chemistry:

Lancaster has systemised different drivers and barriers for implementation of green chemistry and technology in society.⁷¹ The drivers can be divided into the following four categories: (1) economic drivers, (2) legislation/regulatory pull, (3) market pull/public relations, and (4) science and technology push. Similarly, the barriers can be divided in the following four categories: (1) knowledge/technological barriers, (2) culture/communication barriers, (3) economic barriers, and (4) regulatory/legislation barriers.

Moreover, Eissen *et al.* have similarly discussed the status and implementation of green and sustainable chemistry. They used a five-level model consisting of the following parts:⁷²

- Processes (*e.g.* new technologies, synthesis improvements, more effective unit operations)
- Products (*e.g.* fewer base chemicals, improved molecular performance)
- Innovation environment (*e.g.* management systems, collaboration)
- Political environment (*e.g.* legislation, voluntary programs, education)
- Evaluation (*e.g.* synthesis index, process parameters, LCAs, socio-political analysis)

In January 2004 a workshop on the theme “Sustainable Chemistry—Integrated Management of Chemicals, Products and Processes” was held in Germany.⁷³ The aim of the workshop was to provide representatives from academia, authorities, environmental NGOs and industry from OECD countries with a forum to discuss the development and implementation of green and sustainable chemistry. As a

follow up to the workshop, the journal *Environmental Science and Pollution Research* recently started a paper series covering the following five sustainable chemistry topics: (1) principles and perspectives, (2) sustainable chemicals, (3) sustainable production and processing, (4) sustainable products, and (5) implementation of sustainable chemistry.⁷⁴ It is interesting to note that this paper series covers all the parts of my classification model (Fig. 1)—from cleaner laboratory practice at the micro level, *via* green chemistry innovations at the meso level, to policy and consumption patterns at the macro level.

Acknowledgements

Mikael Klintman and Mats Benner are acknowledged for valuable comments on previous drafts of the manuscript. Financial support from the Foundation for Strategic Environmental Research (MISTRA), *via* the research program GREENCHEM⁷⁵ at Lund University, is gratefully acknowledged.

References

- 1 J. Thornton, Implementing green chemistry. An environmental policy for sustainability, *Pure Appl. Chem.*, 2001, **73**, 8, 1231–1236; J. Houlihan, *BodyBurden—The Pollution in People*, Environmental Working Group, 2003; M. Sotoudeh, Problem areas with respect to eco-efficiency, in *Innovation and Cleaner Technologies as a Key to Sustainable Development: the Case of the Chemical Industry*, ed. P. Eder and M. Sotoudeh, IPTS report, EUR 19055 EN, 2000.
- 2 According to Gladwin “greening” may be “viewed as a process by which human activity is made compatible with biospheric capacity”. T. N. Gladwin, in *Environmental Strategies for Industry—International Perspectives on Research Needs and Policy Implications*, ed. K. Fischer and J. Schot, The Greening of Industry Network, Island Press, Washington, D.C, 1993, p. 38.
- 3 T. Collins, Towards sustainable chemistry, *Science*, 2001, **291**, 48–49.
- 4 E. J. Woodhouse, Change of state? The greening of chemistry, in *Synthetic Planet: Chemical Politics and the Hazards of Modern Life*, ed. M. J. Casper, Routledge, New York, 2003, ch. 9; A. J. Hoffman, Institutional evolution and change: Environmentalism and the US chemical industry, *Acad. Manage. J.*, 1999, **42**, 4, 251–371; C. Russell, Chemistry in society, in *The New Chemistry*, ed. N. Hall, Cambridge University Press, Cambridge, 2000, pp. 465–484; P. H. Spitz, The chemical industry and the environment—meeting the challenge, in *The Chemical Industry at the Millennium—Maturity, Restructuring, and Globalization*, ed. P. H. Spitz, Chemical Heritage Press, Philadelphia, 2003.
- 5 I. Amato, The slow birth of green chemistry, *Science*, 1993, **259**, 1538–1541.
- 6 P. T. Anastas and M. M. Kirchhoff, Origins, current status, and future challenges of green chemistry, *Acc. Chem. Res.*, 2002, **35**, 9, 686–694; P. Tundo, P. Anastas, D. S. Black, J. Breen, T. Collins, S. Memoli, J. Miyamoto, M. Polyakoff and W. Tumas, Synthetic pathways and processes in green chemistry. Introductory overview, *Pure Appl. Chem.*, 2000, **72**, 1207–1228; E. J. Woodhouse and S. Breyman, Green chemistry as social movement? *Science, Technol. Human Values*, 2005, **30**, 199–222; J. C. Warner, A. S. Cannon and K. M. Dye, Green chemistry, *Environ. Impact Assess. Rev.*, 2004, **24**, 775–799.
- 7 S. K. Ritter, Green chemistry progress report, *Chem. Eng. News*, 2002, **80**, November 25, 19–23.
- 8 R. Mestres, A brief structured view of green chemistry issues, *Green Chem.*, 2004, **6**, G10–G12.
- 9 P. T. Anastas and J. Warner, *Green Chemistry: Theory and Practice*, Oxford University Press, Oxford, 1998.
- 10 N. Winterton, Twelve more green chemistry principles, *Green Chem.*, 2001, **3**, G73–G75.

- 11 P. T. Anastas and J. B. Zimmerman, Design through the 12 principles of green engineering, *Environ. Sci. Technol.*, 2003, **37**, 5, 94A–101A.
- 12 In a recent EU report substitution was defined as “the replacement or reduction of hazardous substances in products and processes by less hazardous or non-hazardous, or by achieving an equivalent functionality via technological or organisational measures”, J. Lohse, M. Wirts, A. Ahrens, K. Heitmann, S. Lundie, L. Lißner and A. Wagner, *Substitution of Hazardous Chemicals in Products and Processes*, final report compiled for the Directorate General Environment, Nuclear Safety and Civil Protection of the Commission of the European Communities, Ökopol GmbH & Kooperationsstelle Hamburg, Hamburg, 2003.
- 13 M. Eissen, J. O. Metzger, E. Schmidt and U. Schneidewind, 10 years after Rio—concepts on the contribution of chemistry to a sustainable development, *Angew. Chem., Int. Ed.*, 2002, **41**, 414–436; S. Bösch, D. Lenoir and M. Scheringer, Sustainable chemistry: starting points and prospects, *Naturwissenschaften*, 2003, **90**, 3, 93–102; see also papers about ethics of chemistry, in *HYLE-Int. J. Philos. Chem.*, 2001, **7**(2) and 2002, **8**(1).
- 14 R. J. Batterham, Ten years of sustainability: where do we go from here, *Chem. Eng. Sci.*, 2003, **58**, 2167–2179; Y. Jin, D. Wang and F. Wei, The ecological perspective in chemical engineering, *Chem. Eng. Sci.*, 2004, **59**, 1885–1895.
- 15 Certainly, the private consumers practice is on the micro level, but as a consumption system it is on the macro level.
- 16 T. E. Graedel, Green chemistry as systems science, *Pure Appl. Chem.*, 2001, **73**, 8, 1243–1246.
- 17 Royal Society of Chemistry, *Benign and Sustainable Chemical Technologies*, report from a workshop sponsored by the Royal Society of Chemistry, October 2003. (One topic was “Environmental Biotechnology” that I do not think more generally should be classified as green chemistry. However, biotechnology for the development of environmentally friendly production processes, which the workshop called “new environmental biotechnology”, can be considered as green chemistry).
- 18 B. E. Dale, ‘Greening’ the chemical industry: research and development priorities for biobased industrial products, *J. Chem. Technol. Biotechnol.*, 2003, **78**, 1093–1103.
- 19 D. Mooney, Effectively minimizing hazardous waste in academia: the green chemistry approach, *Chem. Health Saf.*, 2004, **11**, 3, 24–28.
- 20 www.cpe.fr/ectn.
- 21 W. Tallmadge, M. Hohman, C. Ruth and G. Bilek, A local pollution prevention group collaborates with a high school intermediate unit bringing the benefits of microscale chemistry to high school chemistry labs in the Lake Erie watershed, *Chem. Health Saf.*, 2004, **11**, 4, 30–33.
- 22 www.cleanerproduction.com.
- 23 P. T. Anastas and R. L. Lankey, Life cycle assessment and green chemistry: the yin and yang of industrial ecology, *Green Chem.*, 2000, **2**, 289–295.
- 24 T. Graedel, Green chemistry in an industrial ecology context, *Green Chem.*, 1999, **1**, G126–G128.
- 25 B. Hamner, What is the relationship between cleaner production, pollution prevention, waste minimization and ISO 14000?, paper presented at the 1st Asian Conference on Cleaner Production in the Chemical Industry, Taipei, Taiwan, December, 9–10, 1996.
- 26 A. Remmen, Greening of Danish industry—changes in concepts and policies, *Technol. Anal. Strategic Manage.*, 2001, **13**, 1, 53–69.
- 27 J. F. Jenck, F. Agterberg and M. J. Droscher, Products and processes for a sustainable chemical industry: a review of achievements and prospects, *Green Chem.*, 2004, **6**, 544–556.
- 28 www.chemistry.org (search: “Green Chemistry Institute”).
- 29 www.chemsoc.org/networks/gen.
- 30 www.gscn.net.
- 31 P. Coombes, Responsible care—a journey of profound cultural change, *Chemicalweek*, 1991, **148**, 26, 9–14; P. Simmons and B. Wynne, Responsible care: trust, credibility, and environmental management, in *Environmental Strategies for Industry—International Perspectives on Research Needs and Policy Implications*, ed. K. Fischer and J. Schot, The Greening of Industry Network, Island Press, Washington, D.C., 1993.
- 32 A. A. King and M. J. Lenox, Industry self-regulation without sanctions: the chemical industry’s Responsible Care program, *Acad. Manage. J.*, 2000, **43**, 4, 698–716; B. D. Solomon and J. R. Mihelcic, Environmental management codes and continuous environmental improvements: Insights from the chemical industry, *Bus. Strategy Environ.*, 2001, **10**, 215–224.
- 33 A. A. King and M. J. Lenox, Industry self-regulation without sanctions: the chemical industry’s Responsible Care program, *Acad. Manage. J.*, 2000, **43**, 4, 698–716; Chemical Industry Archives, The inside story of ‘responsible care’, 2001-03-25, downloaded 2003-11-21 at www.chemicalindustryarchives.org.
- 34 T. F. Yosie, Responsible care at 15 years, *Environ. Sci. Technol.*, 2003, **37**, 21, 400A–406A.
- 35 R. Mullin, Cracking the sustainability code—chemists move to the front line as public concern shifts to products, *Chem. Eng. News*, 2004, **82**, 1, 17.
- 36 M. Lancaster, *Green chemistry: an introductory text*, Royal Society of Chemistry, Cambridge, 2002, pp. 298–299.
- 37 P. Eder and M. Sotoudeh, *Innovation and cleaner technologies as a key to sustainable development: the case of the chemical industry*, IPTS report, EUR 19055 EN, 2000.
- 38 T. Jakl, R. Joas, R. Nolte, R. Schott and A. Windsperger, *Chemical Leasing—An Intelligent and Integrated Business Model with the View of Sustainable Development in Materials Management*, Springer, 2004.
- 39 Sustainable Consumption was one of the main topics dealt with in the World Summit on Sustainable Development in Johannesburg 2002.
- 40 EU Commission, *Stimulating Technologies for Sustainable Development: An Environmental Technologies Action Plan for the European Union*, COM(2004) 38 final, 2004-01-28; I. Calleja, L. Delgado, P. Eder, A. Kroll, J. Lindblom, C. van Wunnik, O. Wolf, F. Gouarderes and J. Langendorff, *Promoting environmental technologies: sectorial analyses, barriers and measures*, IPTS report, EUR 21002 EN, 2004. (Environmental technologies are seen as an important bridge between sustainable development and the Lisbon Strategy, saying that the EU should become “the most competitive and dynamic knowledge-based economy in the world”).
- 41 For previous analyses of the policy discourse of ecological modernisation, see: A. Mol, *Globalization and Environmental Reform*, MIT press, Cambridge, 2001; M. A. Hajer, *The Politics of Environmental Discourse: Ecological Modernization and the Policy Process*, Clarendon Press, Oxford, 1995.
- 42 N. Carter, *The Politics of the Environment—Ideas, Activism, Policy*, Cambridge University Press, 2001, pp. 211–221; A. Jamison, Science, technology and the quest for sustainable development, *Technol. Anal. Strategic Manage.*, 2001, **13**, 1, 9–22; G. Berger, A. Flynn, F. Hines and R. Johns, Ecological modernization as a basis for environmental policy: Current environmental discourse and policy and the implications on environmental supply chain management, *Innovation: Eur. J. Social Sci. Res.*, 2001, **14**, 1, 55–72; N. A. Ashford, Government and environmental innovation in Europe and North America, *Am. Behav. Sci.*, 2002, **45**, 9, 1417–1434.
- 43 M. S. Carolan, Ecological modernization theory: what about consumption?, *Soc. Nat. Resour.*, 2004, **17**, 3, 247–260.
- 44 J. R. McNeill, *Någonting är nytt under solen—Nittonhundratalets miljöhistoria*, SNS Förlag (translation of *Something New Under the Sun: An Environmental History of the Twentieth-Century World*, 2000), 2003, p. 350.
- 45 Sustainable European Regions Network, Green chemistry—affecting producer and consumer behaviour globally from a regional base, 2004-03-17, the document was found on the Internet 2004-05-07.
- 46 OECD, *Need for Research and Development Programmes in Sustainable Chemistry*, Paris, 2002; A. A. Jensen, *Background for Establishing a EU Green Chemistry Award Scheme in Connection with REACH*, final report to the European Commission, 2004; M. Polliakoff, J. M. Fitzpatrick, T. R. Farren and P. T. Anastas, Green chemistry: science and politics of change, *Science*, 2002, **297**, 807–810.
- 47 OECD, *Biotechnology for Clean Industrial Products and Processes—Towards Industrial Sustainability*, Paris, 1998; OECD, *The Application of Biotechnology to Industrial Sustainability*, Paris, 2001; Council for Chemical Research, *New Biocatalysts: Essential Tools for a Sustainable 21st Century Chemical Industry*,

- Washington, D.C, 2001; *Modern Biotechnology and the Greening of Industry: The Introduction of Process-integrated Biocatalysts in Companies—Effect of Dynamics in Internal and External Networks*, ed. O. Wolf and P. Sørup, IPTS report, EUR 19582 EN, 2000; *The Assessment of Future Environmental and Economic Impacts of Process-Integrated Biocatalysts*, ed. O. Wolf, IPTS report, EUR 20407 EN, 2002; Royal Belgian Academy Council of Applied Science, *Industrial Biotechnology and Sustainable Chemistry*, 2004; EuropaBio and ESAB—Section Applied Biocatalysis, *A Vision for 2025: Industrial or White Biotechnology—A Driver of Sustainable Growth in Europe*, 2005.
- 48 Executive steering group, *The Technology Roadmap for Plant/Crop-based Renewable Resources 2020—Renewables Vision 2020*, 1999; Office of Industrial Technologies and Office of Energy Efficiency and Renewable Energy, *Agriculture—Industry of the Future. Accelerating the Growth of the Emerging Biobased Products Industry*, 2001; *Energetics Industrial Bioproducts: Today and Tomorrow*, prepared for the US Department of Energy, 2003; *Current Situation and Future Prospects of EU Industry Using Renewable Raw Materials*, ed. J. Ehrenberg, working group “Renewable Raw Materials”, ERRMA, Brussels, February 2002.
 - 49 J. Lohse, M. Wirts, A. Ahrens, K. Heitmann, S. Lundie, L. Lißner and A. Wagner, *Substitution of Hazardous Chemicals in Products and Processes*, final report compiled for the Directorate General Environment, Nuclear Safety and Civil Protection of the Commission of the European Communities. Ökopol GmbH & Kooperationsstelle Hamburg, Hamburg, 2003.
 - 50 B.-U. Hildebrandt and U. Schlottmann, Chemical safety—an international challenge, *Angew. Chem., Int. Ed.*, 1998, **37**, 1316–1326.
 - 51 An example is Cefic’s Research Consortia “Chemistry in Transition” under the SUSTECH umbrella.
 - 52 www.europabio.org.
 - 53 www.cefic.be.
 - 54 www.errma.com.
 - 55 SusChem, *A European Technology Platform for SUSTAINABLE CHEMISTRY—The Vision for 2025 and Beyond*, final draft, endorsed at a stakeholder event in Barcelona, 4 March 2005.
 - 56 O. Wolf and L. Delgado, *The Impact of REACH on Innovation in the Chemical Industry*, IPTS report, EUR 20999 EN, 2003.
 - 57 United States House of Representatives, *The Chemical Industry, the Bush Administration, and European Efforts to Regulate Chemicals*, prepared for Rep. Henry A. Waxman, 2004.
 - 58 www.euractiv.com (search LinksDossier: “Chemicals policy review (REACH)”).
 - 59 www.bio-economy.net.
 - 60 M. Lex, Industrial biotechnology takes off in Europe. What happens in Sweden?—Views from the European Commission, Power Point Presentation held in Stockholm, 2005-04-04.
 - 61 Executive steering group, *The technology roadmap for plant/crop-based renewable resources 2020—renewables vision 2020*, 1999.
 - 62 *Current Situation and Future Prospects of EU Industry Using Renewable Raw Materials*, ed. J. Ehrenberg, working group “Renewable Raw Materials”, ERRMA, Brussels, February 2002.
 - 63 R. Bud, Biotechnology in the Twentieth Century, *Social Studies Sci.*, 1991, **21**, 415–457.
 - 64 EuropaBio, *White Biotechnology: Gateway to a More Sustainable Future*, Brussels, 2003.
 - 65 Royal Belgian Academy Council of Applied Science, *Industrial Biotechnology and Sustainable Chemistry*, 2004.
 - 66 G. Frazzetto, Analysis: white biotechnology, *EMBO Rep.*, 2003, **4**, 9, 835–837.
 - 67 SusChem, *A European Technology Platform for SUSTAINABLE CHEMISTRY—The Vision for 2025 and Beyond*, final draft, endorsed at a stakeholder event in Barcelona, 4 March 2005, p. 34.
 - 68 Green engineering is defined by the Green Chemistry Institute as “The design, commercialization, and use of processes and products that are feasible and economical while minimizing the generation of pollution at the source and the risk to human health and the environment”.
 - 69 Life-cycle assessment (LCA) is defined by the Green Chemistry Institute as “An objective process to evaluate the environmental burdens associated with a product, process, or activity by identifying energy and materials used and wastes released to the environment; used to evaluate and implement opportunities for environmental improvements”.
 - 70 W. F. Brown, in *The Biobased Economy of the Twenty-First Century: Agriculture Expanding into Health, Energy, Chemicals, and Materials*, ed. A. Eaglesham, NABC (= National Agricultural Biotechnology Council), Report 12, 2000; ACS Division of Cellulose & Renewable Materials, Abstracts 227th ACS National meeting. Anaheim, California March 28–April 1, Track: Feedstocks for the Future: Renewables for the Production of Chemicals and Materials, 2004.
 - 71 M. Lancaster, *Green Chemistry: An Introductory Text*, Royal Society of Chemistry, Cambridge, 2002, table 10.1.
 - 72 M. Eissen, J. O. Metzger, E. Schmidt and U. Schneidewind, 10 Years after Rio—concepts on the contribution of chemistry to a sustainable development, *Angew. Chem. Int. Ed.*, 2002, **41**, 414–436.
 - 73 *Report on the International Workshop on Sustainable Chemistry—Integrated Management of Chemicals, Products and Processes*, 2004.
 - 74 K. G. Steinhäuser, P. Greiner, S. Richter, J. Penning and M. Angrick, Sustainable chemistry: signal for innovation or only slogan? *Environ. Sci. Pollut. Res.*, 2004, **11**, 5, 281–283.
 - 75 www.greenchem.lu.se.

Selective gas–solid phase fixation of carbon dioxide into oxirane-containing polymers: synthesis of polymer bearing cyclic carbonate group†

Bungo Ochiai, Tokinori Iwamoto and Takeshi Endo*

Received 30th November 2005, Accepted 3rd January 2006

First published as an Advance Article on the web 10th January 2006

DOI: 10.1039/b516881c

Gas–solid phase fixation of carbon dioxide into oxirane-containing polymers proceeds selectively without concomitant crosslinking reactions, which have previously been unavoidable due to the dense arrangement of oxirane groups. The fixation reaction obeys first-order kinetics, supporting the selectivity of the reaction.

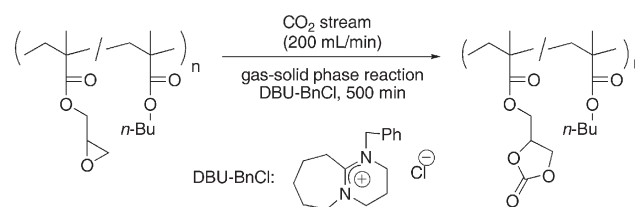
Introduction

Reactions free from volatile organic compounds (VOCs), *e.g.*, the use of ionic liquid¹ and aqueous² or solid phase³ reactions, have been developed to construct environmentally benign processes. Among them, solid phase reactions are advantageous, because they may provide the desired products directly without purification processes, which typically require VOCs. However, the dense arrangement of reactant groups and the heterogeneity in solid phase reactions often make the selective and quantitative reactions difficult. For instance, we have investigated the gas–solid phase fixation of carbon dioxide into oxirane-containing (co)polymers based on glycidyl methacrylate (GMA) that affords the polymers carrying cyclic carbonate structures.^{4–7} This gas–solid phase reaction involves polymerization of the oxirane group that affords crosslinked polymers carrying cyclic carbonate, which are potentially applicable to lithium ion storage materials and enzyme immobilization.^{8,9} This crosslinking reaction takes place *via* an anionic route, whose propagating species are the alkoxide intermediate generated from the oxirane groups and ammonium salts. Namely, the alkoxide should react with carbon dioxide predominantly over the dense arrangement of oxirane groups to avoid crosslinking reactions. If one wishes to obtain soluble polymers as precursors for adhesive, optical, and photo-resist materials,^{9,10} the polymers must have formability. In order to meet the requirement for solubility, the reaction must have been stopped even though the incorporation ratios are insufficient. Although *n*-butyl methacrylate (BMA) was found to be a suitable comonomer to obtain the copolymers carrying cyclic carbonate with a high conversion (80%), the concomitant crosslinking prevents the fabrication of a soluble polymer with quantitative conversion.⁷ We have preliminary found that the Lewis acidity of the

ammonium catalysts is an important factor for the selectivity of the reaction (*e.g.*, benzyl-trialkylammonium salts are more effective than tetraalkylammonium salts to maintain the selectivity of the carbon dioxide incorporation toward the crosslinking, in spite of the weaker activities). Accordingly, we examined 1,8-diazabicyclo[5.4.0]undec-7-ene benzyl chloride salt (DBU-BnCl) as a new catalyst for this gas–solid phase reaction, based on the presumption that a catalyst with a weakly Lewis acidic cation would be more suitable to improve the selectivity.

Results and discussion

Films of poly(GMA₃₁-*co*-BMA₆₉) containing DBU-BnCl (6 mol% relative to GMA unit) were heated at 90–120 °C under a carbon dioxide atmosphere (flow rate: 200 mL min⁻¹) for 500 min, and the carbon dioxide incorporation behavior was traced by gravimetric increase monitored by thermogravimetric analysis (Scheme 1).



Scheme 1 Gas–solid phase fixation of carbon dioxide with poly(GMA-*co*-BMA).

Regardless of the temperature, the carbon dioxide incorporation ratios exceed 94%, which have not been achieved in the previously examined reactions. A decrease of the incorporation ratios was not observed, indicating the absence of decarboxylation reactions that take place at high temperatures using typical catalysts.^{4,7} The rates of the incorporation increased with the temperature (Fig. 1). The first-order kinetic plots for this reaction shows almost linear relationships *versus* the reaction time until the conversions reached 85%, indicating the excellent selectivity of this gas–solid phase reaction and the constant permeability of carbon dioxide into the film regardless of the conversion (see ESI†). The slopes of the lines revealed the apparent rate constants as $k_{90\text{ }^\circ\text{C}} = 9.74 \times 10^{-3}$, $k_{100\text{ }^\circ\text{C}} = 1.76 \times 10^{-2}$, $k_{110\text{ }^\circ\text{C}} = 3.20 \times 10^{-2}$, and $k_{120\text{ }^\circ\text{C}} = 4.55 \times 10^{-2}$ (min⁻¹).† The rate constant at 100 °C is identical to that in the reaction of glycidyl phenyl ether with atmospheric carbon dioxide in *N*-methyl pyrrolidinone catalyzed by benzyl trimethylammonium chloride,¹¹ and it supports the good selectivity of this

Department of Polymer Science and Engineering, Faculty of Engineering, Yamagata University, Jonan 4-3-16, Yonezawa, Yamagata, 992-8510, Japan. E-mail: tendo@yz.yamagata-u.ac.jp; Fax: +81-238-26-3090; Tel: +81-238-26-3090

† Electronic supplementary information (ESI) available: Kinetic results. See DOI: 10.1039/b516881c

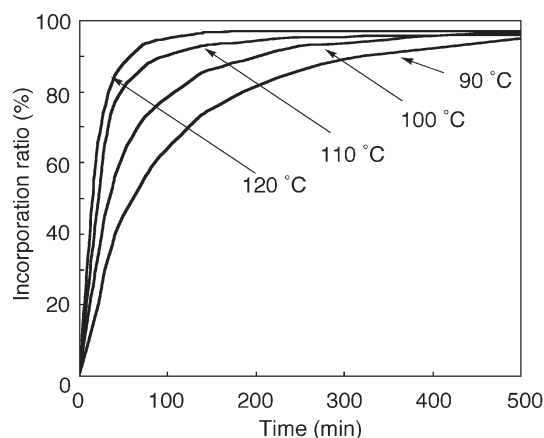


Fig. 1 Time versus carbon dioxide incorporation ratios in the gas–solid phase reaction of carbon dioxide with poly(GMA₃₁-co-BMA₆₉) catalyzed by DBU-BnCl (6 mol%).

gas–solid phase reaction. The logarithms of these rate constants correlate linearly with the reciprocals of the temperatures (see ESI†), indicating that this gas–solid phase reaction obeying Arrhenius's equation involves negligible side reactions (*i.e.*, cross-linking reactions overconsuming the oxirane groups are negligible). The activation energy of this gas–solid phase reaction was calculated from the slope of the line to be 62.2 kJ mol⁻¹, which agrees with the reported activation energies in the reaction of oxiranes and carbon dioxide.¹²

The resulting polymers are soluble in CHCl₃ when the reactions were conducted at 90–110 °C, while the polymer obtained by the reaction at 120 °C was insoluble in any organic solvent in spite of the high incorporation ratio (97%). The resulting soluble polymers were analyzed by ¹H NMR spectroscopy and size exclusion chromatography (SEC). Fig. 2 shows the ¹H NMR spectrum of the polymer obtained by the reaction at 90 °C. The signals assignable to the oxirane group in poly(GMA₃₁-co-BMA₆₉) were very small in the spectrum of the polymer after the reaction, which shows clear signals assignable to the carbonate group instead. The integral ratios of the signals agree well with the copolymer composition (*i.e.*, 91 and 90% by the calculations from ¹H NMR spectroscopy and thermogravimetry, respectively).

The SEC profiles of the original and the resulting polymers are indicated in Fig. 3. An obvious shoulder was not observable in all the SEC profiles, indicating that the polymerization of the oxirane group is almost ignorable. However, the molecular weights are higher than the expected value, probably due to the slight degree of coupling of the polymer chains. The molecular weight distributions of the resulting polymers increase slightly as the reaction temperature increases, suggesting a trace degree of the side reaction that may be controlled by the reaction temperature.

Conclusions

DBU-BnCl quantitatively catalyzes the gas–solid phase reaction of carbon dioxide into an oxirane-containing copolymer by suppressing undesired crosslinking reactions, which had been unavoidable due to the dense arrangement of oxirane groups susceptible to nucleophilic additions and too high an activity of the catalysts.

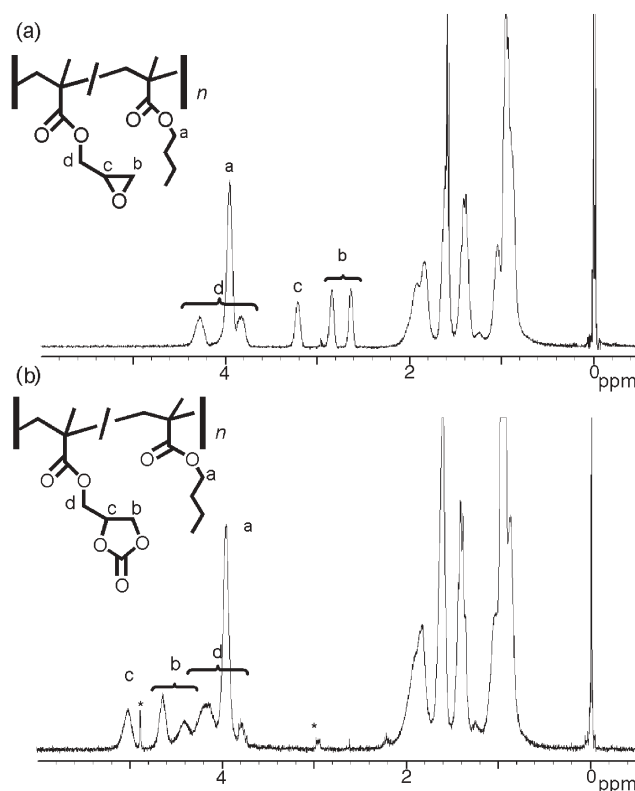


Fig. 2 ¹H NMR spectra of poly(GMA₃₁-co-BMA₆₉) (a) and the polymer after its gas–solid phase reaction with carbon dioxide at 90 °C (b). Asterisks indicate the signals of DBU-BnCl.

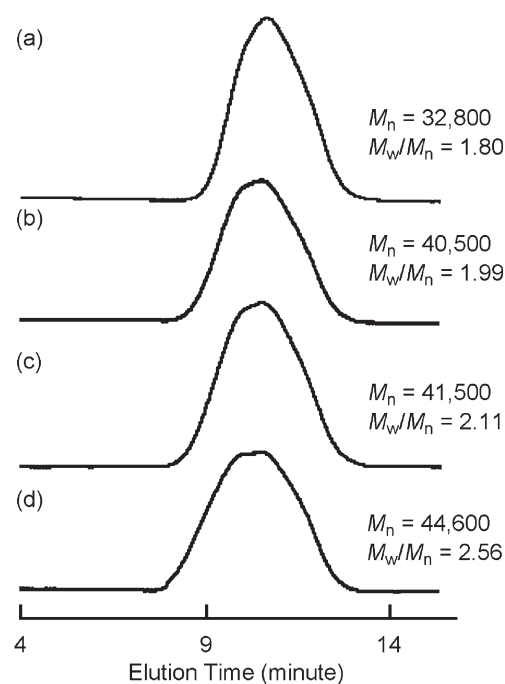


Fig. 3 SEC profiles of poly(GMA₃₁-co-BMA₆₉) (a) and the polymers after its gas–solid phase reaction with carbon dioxide at 90 (b), 100 (c), and 110 (d) °C.

Namely, this gas–solid phase reaction proved the existence of negligible undesired reactions by polymerization of the oxirane groups and decarboxylation of the produced cyclic carbonate groups. The selectivity of this reaction is emphasized by the first-order kinetics, which are consistent with the solution phase reactions. Because this reaction can provide both soluble and insoluble polymers containing cyclic carbonate groups that keep the conversion almost quantitative, this method will be an environmentally benign process for preparing a wide-range of materials carrying the cyclic carbonate structure.

Experimental

Measurement

¹H NMR spectra were measured on a JEOL JNM-LA-270 instrument using tetramethylsilane as an internal standard (270 MHz). Size exclusion chromatography (SEC) measurements were performed on a Tosoh HLC-8120 GPC equipped with Tosoh TSK-gel α -M, α -4000, α -3000, and α -2500 tandem columns and a refractive index detector. *N,N*-dimethyl formamide (DMF) containing 50 mM lithium bromide and 50 mM phosphoric acid was used as an eluent at 40 °C. Polystyrene standards were used for calibration. Thermogravimetric analyses (TGA) were performed on a Seiko TG/DTA6000 (EXSTER6000). Differential scan calorimetry (DSC) measurements were performed on Seiko DSC-220 under a nitrogen atmosphere (scan rate: 10 °C min⁻¹). Density measurement was performed on a Shimadzu Accupic 1300 digital pycnometer.

Materials

BMA (Tokyo Kasei Kogyo) and GMA (Kanto Chemical) were dried over CaH₂ and distilled under reduced pressure. Acetonitrile (Kanto Chemical) for film preparation was dried over CaH₂ and distilled under a nitrogen atmosphere. DBU-BnCl was prepared according to the literature.¹³ The amount of DBU-BnCl was indicated as molar percent toward oxirane groups in the copolymers. The radical copolymerization procedure was described in the previous reports.^{5–7} The copolymers and copolymer films were prepared as reported.^{5–7} Other materials were used as received unless otherwise noted.

Typical procedure for carbon dioxide incorporation into poly(GMA-co-BMA)

A typical procedure is shown as follows: a TGA sample pan containing copolymer film (5 mg) was placed in the TGA instrument under a carbon dioxide atmosphere (gas flow rate: 200 mL min⁻¹). The temperature was raised to the reaction temperature and the incorporation behavior was investigated with gravimetric changes monitored by TGA.

References

‡ The *k* value was defined from the equation $\ln([\text{Ox}]_0/[\text{Ox}]) = kt$; where $[\text{Ox}]_0$ and $[\text{Ox}]_t$ are the temporal and initial concentrations of the oxirane group, respectively, and *t* is the reaction time. The concentration of the initial oxirane group and the sum of the concentration of final carbonate and oxirane groups in the film were calculated to be 2.44–2.48 and 2.68 mol L⁻¹, respectively, from the densities of the films (1.26–1.21 and 1.27 g cm⁻³). The concentration of oxirane group during the reaction was calculated based on the presumption that this concentration correlates linearly with the carbon dioxide incorporation ratio.

- 1 R. D. Makote, H. M. Luo and S. Dai, *Chem. Rev.*, 2002, **102**, 3667; K. Przemyslaw, *Prog. Polym. Sci.*, 2003, **29**, 3.
- 2 S. Kobayashi and K. Makabe, *Acc. Chem. Res.*, 2002, **35**, 209; M. F. Cunningham, *Prog. Polym. Sci.*, 2002, **27**, 1039; B. Ochiai, Y. Satoh and T. Endo, *Green Chem.*, 2005, **7**, 765.
- 3 F. Toda, *Synthesis*, 1993, 303; K. Tanaka, D. Fujimoto, T. Oeser, H. Irgartinger and F. Toda, *Chem. Commun.*, 2000, 413; G. W. V. Cave, C. L. Raston and J. L. Scott, *Chem. Commun.*, 2001, 2159; D. Braga, L. Maini, M. Mazzotti, K. Rubini, A. Masic, R. Gobetto and F. Grepioni, *Chem. Commun.*, 2002, 2296.
- 4 N. Kihara and T. Endo, *Macromolecules*, 1994, **27**, 6239; N. Kihara and T. Endo, *J. Chem. Soc., Chem. Commun.*, 1994, 937.
- 5 B. Ochiai, T. Iwamoto, T. Miyagawa, D. Nagai and T. Endo, *J. Polym. Sci., Part A: Polym. Chem.*, 2004, **42**, 3812.
- 6 B. Ochiai, T. Iwamoto, T. Miyagawa, D. Nagai and T. Endo, *J. Polym. Sci., Part A: Polym. Chem.*, 2004, **42**, 4941.
- 7 B. Ochiai, T. Iwamoto, K. Miyazaki and T. Endo, *Macromolecules*, 2005, **38**, 9939.
- 8 J. H. Golden, B. G. M. Chew, D. B. Zax, F. J. DiSalvo, J. M. J. Fréchet and J. M. Tarascon, *Macromolecules*, 1995, **28**, 3468.
- 9 D. C. Webster, *Prog. Org. Coat.*, 2003, **47**, 77; B. Ochiai and T. Endo, *Prog. Polym. Sci.*, 2005, **30**, 183.
- 10 S. Y. Park, H. Y. Park, H. S. Lee, S. W. Park and D. W. Park, *Opt. Mater.*, 2003, **21**, 331.
- 11 N. Kihara, N. Hara and T. Endo, *J. Org. Chem.*, 1993, **58**, 6198.
- 12 D. J. Darensbourg and M. W. Holtcamp, *Coord. Chem. Rev.*, 1996, **153**, 155.
- 13 Y. Hori, Y. Nagano and K. Tanaka, *Chem. Express*, 1986, **1**, 491.

Removal of ammonium bromide, ammonium chloride, and zinc acetate from ionic liquid/organic mixtures using carbon dioxide

Eric M. Saurer, Sudhir N. V. K. Aki and Joan F. Brennecke*

Received 12th October 2005, Accepted 13th December 2005

First published as an Advance Article on the web 3rd January 2006

DOI: 10.1039/b514486h

Carbon dioxide can be used to remove ammonium salts and zinc acetate from ionic liquid/organic mixtures at 25 °C. The amount of CO₂ required to achieve this separation is minimal.

Recently ionic liquids (ILs) have received a lot of interest due to their non-volatile nature and very unique solvent properties. For example, polar and aromatic organic compounds and organometallic compounds are highly soluble in many ILs. At the other extreme, non-polar organics such as alkanes are immiscible with most ILs. These unique properties have been exploited to effectively perform homogeneously catalyzed reactions, such as hydrogenations, oxidations, and hydroformylations.^{1–5} Since many organometallics have a high affinity for ILs, the catalyst can be effectively sequestered by the ILs and the products can be extracted by alkanes or other non-polar or low polarity solvents. Indeed there have been reports of essentially no catalyst loss in the product recovery step. This eliminates one of the major problems frequently encountered when using common organic solvents for homogeneous catalysis. As a further development, our group has shown that organic compounds can be extracted from ILs without contaminating the extracted product using CO₂.^{6,7} IL/CO₂ biphasic systems have been found to be effective as reaction media for performing homogeneously catalyzed reactions with little or no loss of catalyst during the product extraction.^{3,4,8,9}

The potential drawback with the use of ILs for homogeneous catalysis is the separation of the catalyst from the solvent when the catalyst is deactivated. Since the ILs are non-volatile, typical separation techniques such as distillation cannot be used. Liquid–liquid extraction with alkanes is not likely to be a viable option since typical homogeneous catalysts are not soluble in non-polar solvents. Therefore new methods need to be developed to recover the valuable catalysts from the IL and remove spent catalysts so the IL can be reused. We have initiated a program to address this particular issue and this Communication presents our initial results. We have found that CO₂ can be used to recover solid inorganic salts, such as NH₄Cl and NH₄Br, as well as zinc acetate (Zn(CH₃CO₂)₂), from ILs. In this Communication, the solid–liquid–vapor equilibrium for the systems dimethyl sulfoxide (DMSO)–NH₄Cl–CO₂, 1-hexyl-3-methylimidazolium bis(trifluoromethylsulfonyl) imide ([hmim][Tf₂N])–DMSO–NH₄Cl–CO₂, [hmim][Tf₂N]–acetonitrile–NH₄Br–CO₂, [hmim][Tf₂N]–DMSO–Zn(CH₃CO₂)₂–CO₂, and [hmim][Tf₂N]–acetonitrile–Zn(CH₃CO₂)₂–CO₂ at 25 °C is

presented. Here we report for the first time a method to recover solids from IL/organic mixtures using CO₂.

[hmim][Tf₂N] was synthesized in our laboratory according to the published procedures.¹⁰ The IL was dried at 70 °C under high vacuum before use and the water content in the IL was found to be <160 ppm using Karl–Fisher titration. Coleman instrument grade CO₂ was purchased from Mittler Supply, Inc. Acetonitrile (spectrophotometric grade, 99.5+%) and DMSO (AldraSORB, 99.8%) purchased from Aldrich Chemical Co., Inc., were dried over molecular sieves and used without further purification. NH₄Br (99.99+%), NH₄Cl (99.998%), and Zn(CH₃CO₂)₂ (99.99%) were purchased from Aldrich Chemical Co., Inc., and were used as received. The solid–liquid–vapor equilibrium measurements were made in a high pressure static phase equilibrium apparatus, the details of which were given elsewhere.¹⁰ The solutions were made in the following manner. Initially, an IL/organic mixture of the required composition was prepared in a sample vial under a dry nitrogen atmosphere. To this homogeneous solution, the required amount of solid of interest was added and the solution was stirred for several hours. In a typical experiment a known amount of this sample mixture was loaded into a sapphire cell under a dry nitrogen atmosphere, filtering the solution using a 0.2 µm syringe filter if required to remove any undissolved solid. The cell was then connected to the phase equilibrium apparatus and was maintained at 25 °C in a constant temperature water bath. CO₂ was added to the solution slowly while stirring the liquid solution vigorously and continuously monitoring the liquid solution for the presence of solid particles. A boroscope connected to a video monitor was used to identify the presence of solid particles in the solution.

The various phases observed upon addition of CO₂ to the liquid solution is depicted in Fig. 1. As the homogeneous solution consisting of the solid/IL/organic mixture is exposed to CO₂, the solution starts expanding. CO₂ is added until the nucleation pressure, *i.e.*, the pressure at which solid particles are observed for

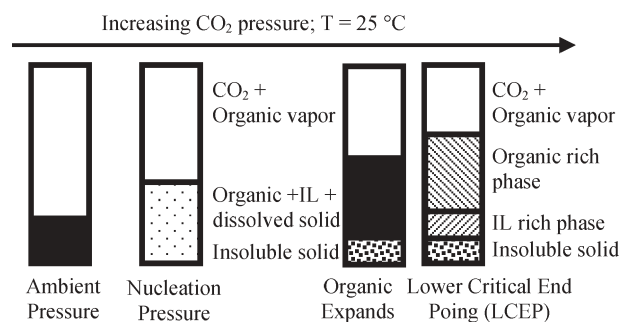


Fig. 1 Schematic representation of the solid removal process.

182 Fitzpatrick Hall, Department of Chemical and Biomolecular Engineering, University of Notre Dame, Notre Dame, USA.
E-mail: jfb@nd.edu; Fax: +1 574-631-8366; Tel: +1 574-631-5847

the first time, is reached. The solubility of the solid in the IL/organic/CO₂ mixture is less than in the IL/organic mixture. Precipitation occurs when the solubility of the solid in the IL/organic/CO₂ solution has decreased to the concentration of solid initially placed in the solution. Further increase in the pressure leads to the precipitation of more particles with an increase in the liquid volume. For the systems studied here CO₂ can be added to the solution until the lower critical end point, *i.e.*, the pressure at which the liquid phase splits into two liquid phases, is reached. We have previously reported such behavior for IL/organic/CO₂ systems.¹¹ Therefore, after the separation of solid from the liquid, one could then recover the IL from the organic by further addition of CO₂.

The solid–liquid–vapor equilibrium for the system [hmim][Tf₂N]–DMSO–NH₄Cl–CO₂ at 25 °C will be described first. Even though NH₄Cl is not a homogeneous catalyst, we chose to study this system for two particular reasons. First, the solubility of this compound in organics and in organic/IL mixtures is relatively high compared to other solid salts. This makes visual identification of the first crystals of solid at the nucleation pressure quite easy. Second, NH₄Cl is a common byproduct formed during the synthesis of ILs, which is relatively difficult to remove from the IL, especially if the IL is hydrophilic. Therefore, antisolvent precipitation with CO₂ could be a possible technique for byproduct removal from ILs. The effect of IL and salt concentration on the nucleation pressure was studied and the results are shown in Fig. 2 and Table 1. The results were compared with those obtained for the system DMSO–NH₄Cl–CO₂, *i.e.*, the same system but without the IL present. Since the nucleation pressure is the pressure at which the first crystals appear, the solubility of the NH₄Cl at the nucleation pressure is the composition listed in the first column. In other words, this is the amount of solid still remaining in the solution at that pressure. Additional solid can be removed by increasing the pressure, which decreases the solubility and causes more solid to precipitate. As expected, the nucleation pressure decreased with an increase in the NH₄Cl concentration under all conditions. For example, in the absence of IL, the nucleation pressure decreased from 33 bar to 8.1 bar as the NH₄Cl concentration increased from 6.9 to 18.4 mol%. Similar trends have been observed previously for the DMSO–NH₄Cl–CO₂

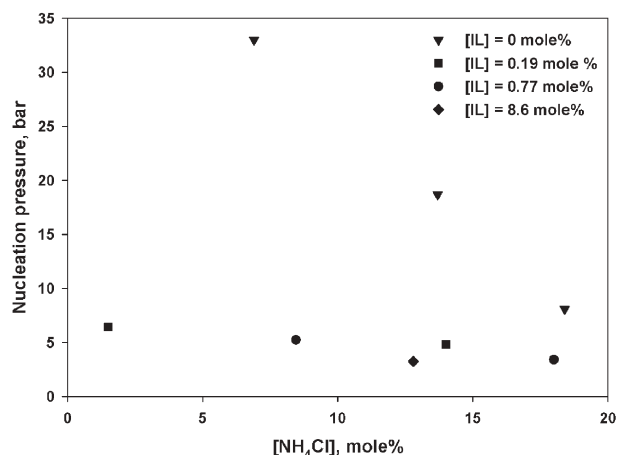


Fig. 2 Dependence of nucleation pressure on the concentration of NH₄Cl and [hmim][Tf₂N] in dimethyl sulfoxide at 25 °C.

Table 1 Dependence of nucleation pressure on the type of salt, ionic liquid, and organic compound in the presence of CO₂ at 25 °C

Salt (mol%)	IL (mol%)	Nucleation pressure/bar	x_{CO_2} (mole fr.)
NH ₄ Cl/[hmim][Tf ₂ N]/dimethyl sulfoxide/CO ₂ system			
6.9	0	33	0.28
13.7	0	18.7	0.095
18.4	0	8.1	0.055
1.5	0.19	6.44	0.038
14	0.19	4.83	0.019
18	0.77	3.41	0.029
8.45	0.77	5.23	0.028
12.8	8.61	3.24	0.044
NH ₄ Br/[hmim][Tf ₂ N]/acetonitrile/CO ₂ system			
<0.026	9.56	3.34	0.034
Zinc acetate/[hmim][Tf ₂ N]/acetonitrile/CO ₂ system			
0.0079	0	10.8	0.15
0.0024	6.8	8.52	0.10
0.0035	10.1	8.9	0.11
0.007	20	10.6	0.16
0.012	34	11.6	0.22
Zinc acetate/[hmim][Tf ₂ N]/dimethyl sulfoxide/CO ₂ system			
18.6	0.17	35.8	0.25

system but the nucleation pressures reported were much greater¹² than those found in the current work. One possible reason for these differences could be the presence of water. We have found the nucleation pressure to be very sensitive to the presence of water, as one would expect for a solid solute that is highly soluble in water. For instance, the addition of 9 wt% water to a 10 mol% NH₄Cl in DMSO solution increased the nucleation pressure from 18.7 bar to 37.4 bar. A dramatic decrease in the nucleation pressure was observed for a particular NH₄Cl concentration when dealing with the DMSO/IL mixtures. For instance, the nucleation pressure decreased from 18.7 bar to 4.8 bar as the IL concentration was increased from 0 to just 0.19 mol% at a NH₄Cl concentration of ~14 mol%. This is no doubt due to the fact that NH₄Cl is much less soluble in the IL than in DMSO, yet the significant reductions in nucleation pressures with the addition of such small amounts of IL is remarkable. Note that the mixtures investigated (0.19–8.6 mol% IL in DMSO) actually contain a fair amount of IL on a mass basis, due to the large difference in the molecular weight of the IL and the DMSO. Another interesting result is the very small amount of CO₂ required to precipitate NH₄Cl from the solution in the presence of IL. Even the presence of a few bar of CO₂ is sufficient to remove ammonium chloride from the solution.

Although we do not sample and analyze the solid precipitate, we are reasonably confident that it is NH₄Cl, and not NH₄Tf₂N or [hmim][Cl], even though ion exchange is certainly possible. The reason is that inorganic chloride salts are much less soluble (*i.e.*, orders of magnitude less) in DMSO and [hmim][Tf₂N] than [Tf₂N] salts. We confirmed this by qualitative measurements of the solubility of LiTf₂N and LiCl in [hmim][Tf₂N].

Similarly, we found that NH₄Br can be removed from a solution of [hmim][Tf₂N]/acetonitrile, as indicated in Table 1. NH₄Br is just sparingly soluble in both the IL and acetonitrile. Once again, just a minimal amount of CO₂ was sufficient to induce the precipitation of the solid.

Also, we have studied the ability of CO₂ to remove Zn(CH₃CO₂)₂, an inexpensive model compound of a homogeneous catalyst, from IL/organic solutions. Other acetates, specifically Pd(CH₃CO₂)₂² and Rh₂(CH₃CO₂)₄,¹³ have been used as homogeneous catalysts for a wide variety of reactions in ILs,

although we note that some of these differ structurally from the $\text{Zn}(\text{CH}_3\text{CO}_2)_2$. We used DMSO and acetonitrile as the organic solvents and [hmim][Tf₂N] as the IL, and the results are shown in Table 1. The concentration of $\text{Zn}(\text{CH}_3\text{CO}_2)_2$ in pure acetonitrile was measured both gravimetrically and using the ICP-OES technique, with good agreement, and the value is shown in Table 1. The concentrations of $\text{Zn}(\text{CH}_3\text{CO}_2)_2$ in the IL/organic mixtures were measured solely with ICP-OES. $\text{Zn}(\text{CH}_3\text{CO}_2)_2$ is significantly more soluble in [hmim][Tf₂N] than in acetonitrile so the presence of increasing amounts of IL in the IL/acetonitrile mixtures increases the initial loading of $\text{Zn}(\text{CH}_3\text{CO}_2)_2$ that we can use. The concentration of $\text{Zn}(\text{CH}_3\text{CO}_2)_2$ in DMSO and the DMSO/IL mixture was measured gravimetrically.

As shown, $\text{Zn}(\text{CH}_3\text{CO}_2)_2$ can be removed from both [hmim][Tf₂N]/acetonitrile and [hmim][Tf₂N]/DMSO mixtures. The nucleation pressure increased slightly with an increase in both the IL and $\text{Zn}(\text{CH}_3\text{CO}_2)_2$ concentration in the mixture. At all conditions, the amount of CO_2 required to induce the nucleation is very small. This is no doubt due to the fact that the concentrations of $\text{Zn}(\text{CH}_3\text{CO}_2)_2$ were not far below the solubility limit in the mixture at ambient pressure. We would expect at a given concentration of IL the nucleation pressure to increase with a decrease in $\text{Zn}(\text{CH}_3\text{CO}_2)_2$ concentration in the solution. Nonetheless, very low pressures of CO_2 , with the associated rather small degree of volume expansion, are required to induce precipitation in the samples examined. Furthermore, it is relatively easy to remove $\text{Zn}(\text{CH}_3\text{CO}_2)_2$ from acetonitrile compared to DMSO. Once again, this is simply because the solubility of $\text{Zn}(\text{CH}_3\text{CO}_2)_2$ in acetonitrile is much lower than in DMSO. However, it should be noted that we have been unsuccessful in removing NH_4Cl , NH_4Br , or $\text{Zn}(\text{CH}_3\text{CO}_2)_2$ from pure [hmim][Tf₂N] (*i.e.*, no organic) using CO_2 pressure, even when the IL appears to be saturated with the solid solute at ambient conditions. We attribute this in part to the relatively small volume expansion of pure ILs even with the addition of large amounts of CO_2 .¹⁰ This is consistent with our observation that CO_2 addition does not significantly change the solvent strength of ILs.¹⁴ In addition, we have found that CO_2 was unable to induce the separation of chromium acetylacetonate, iron acetylacetonate, NaCl, naphthalene or benzoic acid from methanol/1-butyl-3-methylimidazolium hexafluorophosphate solutions. Perhaps this is due to the fact that methanol does not expand as much as DMSO and acetonitrile with CO_2 addition, with a corresponding smaller change in solvent strength. Whatever the case, it points out that

solid solute precipitation from IL/organic mixtures using CO_2 depends on the solute, IL and organic liquid, and the ability of CO_2 to swell the IL/organic solution, which is necessary for decreasing its solvent strength. However, we are aware of one other report of CO_2 -induced solid precipitation from an IL mixture.¹⁵

Conclusions

We have shown that CO_2 can be used to recover several different inorganic and metal containing compounds from IL/acetonitrile and IL/DMSO solutions.

Acknowledgements

The financial support from the donors of the Petroleum Research Fund, administered by American Chemical Society, is greatly appreciated.

Notes and references

- 1 *Ionic Liquids in Synthesis*, ed. P. Wasserscheid and T. Welton, Wiley-VCH Verlag GmbH & Co., Weinheim, 2003.
- 2 C. M. Gordon, *Appl. Catal. A: Gen.*, 2001, **222**, 101–117.
- 3 M. Solinas, A. Pfaltz, P. G. Cozzi and W. Leitner, *J. Am. Chem. Soc.*, 2004, **126**, 16142–16147.
- 4 P. B. Webb, M. F. Sellin, T. E. Kunene, S. Williamson, A. M. Z. Slawin and D. J. Cole-Hamilton, *J. Am. Chem. Soc.*, 2003, **125**, 15577–15588.
- 5 T. Welton, *Chem. Rev.*, 1999, **99**, 2071–2083.
- 6 L. A. Blanchard, D. Hancu, E. J. Beckman and J. F. Brennecke, *Nature*, 1999, **399**, 28–29.
- 7 L. A. Blanchard and J. F. Brennecke, *Ind. Eng. Chem. Res.*, 2001, **40**, 287–292.
- 8 M. T. Reetz, W. Wiesenhofer, G. Francio and W. Leitner, *Adv. Synth. Catal.*, 2003, **345**, 1221–1228.
- 9 Z. S. Hou, B. X. Han, L. Gao, T. Jiang, Z. M. Liu, Y. H. Chang, X. G. Zhang and J. He, *New J. Chem.*, 2002, **26**, 1246–1248.
- 10 S. Aki, B. R. Mellein, E. M. Saurer and J. F. Brennecke, *J. Phys. Chem. B*, 2004, **108**, 20355–20365.
- 11 A. M. Scurto, S. Aki and J. F. Brennecke, *J. Am. Chem. Soc.*, 2002, **124**, 10276–10277.
- 12 S. D. Yeo, J. H. Choi and T. J. Lee, *J. Supercrit. Fluids*, 2000, **16**, 235–246.
- 13 J. S. Yadav, B. V. S. Reddy and P. N. Reddy, *Adv. Synth. Catal.*, 2004, **346**, 53–56.
- 14 C. P. Fredlake, M. J. Muldoon, S. N. V. K. Aki, T. Welton and J. F. Brennecke, *Phys. Chem. Chem. Phys.*, 2004, **6**, 3280–3285.
- 15 A. Shariati, M. C. Kroon, K. Gutkowski, V. A. Toussaint, L. J. Florusse, J. van Spronsen, G. J. Wikkamp, R. A. Sheldon and C. J. Peters, in *International Symposium on Supercritical Fluids*, Orlando, FL, 2005.

Mesoporous polymer–silica catalysts for selective hydroxylation of phenol

Amit Dubey, Minkee Choi and Ryong Ryoo

Received 29th September 2005, Accepted 6th December 2005

First published as an Advance Article on the web 3rd January 2006

DOI: 10.1039/b513845k

Mesoporous polymer–silica nanocomposite materials with redox functional groups such as ferrocene were synthesized *via* controlled radical co-polymerization inside mesoporous silicas and exhibited very high activity and selectivity towards catalytic hydroxylation of phenol.

Introduction

Following the discovery of mesoporous materials, a strong desire to use more environmental friendly processes has been universally acknowledged and much effort has been devoted to this area during the last two decades.¹ This is due to their outstanding advantages such as extremely large surface area combined with large and well-defined pore sizes. In particular, the wide pore size range (2–20 nm) of ordered mesoporous silicas compared to microporous zeolites enables one to incorporate multifunctional organic moieties within the well-defined porous structures.^{1,2} The organic moiety can be functionalized to achieve the active centers for various applications in catalysis, adsorption, ion-exchangers, *etc.*, to design the new required materials. So far, co-condensation of organosilanes during the synthesis^{1,3,4} or direct grafting of the organosilanes into the as-synthesized mesoporous materials⁵ are the most common methods employed to obtain the organo–silica hybrid materials. In particular, the synthesis of novel organic–inorganic hybrid mesoporous materials with an homogeneous distribution of organic fragments and inorganic oxide within the framework was reported.³ However, the limited scope and density of the functional groups achievable and relatively low hydrothermal stability of the siloxane bond under reactive conditions limit the practical utilization. Choi and Ryoo⁶ have disclosed the synthetic strategy towards ordered nanoporous organic polymers using mesoporous carbon as the retaining framework and the design of silica polymer-composite material through controlled radical polymerization of monomers postfunctionalized with sulfonic acid groups for adsorption and acid catalysis.⁷ In this communication, we report the synthesis of new mesopore polymer–silica (KIT-6 with cubic *Ia3d* symmetry) composite materials through *in-situ* radical controlled polymerization of vinylmonomers (styrene and vinyl ferrocene as a functional monomer) inside the silica mesopores for hydroxylation of phenol. The endeavor of incorporating the polymer (styrene) is to make the nature of the surface more hydrophobic that may result in the desired selective products. The use of H₂O₂ as oxidant over

titanosilicate by Enichem has opened vistas for environmentally benign approaches for selective oxidation/hydroxylation reactions.⁸ In continuation, many recent efforts have been emphasized for metal oxides, supported metal complexes, metallosilicates, hydrotalcites, heteropoly-compounds and Cu-exchanged zeolites.⁹ Recently, direct grafting of ferrocene into SBA-15 material was reported for oxidation of benzene.¹⁰ Recently, ferrocene immobilization in MCM-41 types of material was used for hydroxylation/polymerization of phenol wherein only traces of hydroxylated products were formed leading to the polymerization of phenol.¹¹

Experimental

The synthesis methodology involves the incorporation of vinyl monomers, cross linkers and radical initiators into the KIT-6 mesopore walls *via* the wet-impregnation method and equilibrated under reduced pressure to achieve a uniform distribution. The monomers adsorbed on the mesopore walls were subsequently polymerised with temperature programmed heating. Typically, for 30 wt% polymer loading, 0.114 g of styrene (80 mol%), 0.0358 g divinylbenzene (20 mol%), 0.0065 g of AIBN, *a,a'*-azoisobutyronitrile (3% relative to the total vinyl group) and 0.01143 g of vinyl ferrocene (9 : 1 wt ratio; styrene : vinyl ferrocene) were dissolved into 2 ml of solvent (dichloromethane). The role of styrene is to solubilize vinyl ferrocene and to make the nature of the surface more hydrophobic. After impregnating the solution, the sample was heated to 40 °C to remove the dichlorobenzene and subjected to freeze–vacuum–thaw to remove the residual solvent and air. The sample was sealed in a pyrex tube and subjected to controlled temperature programming for polymerization. The temperature scheme follows 45 °C for 24 h, 60 °C for 4 h, 100 °C, 120 °C and 150 °C for 1 h. Two different amounts (3 and 7 wt% vinyl ferrocene : styrene) were selected to synthesize the samples.

Results and discussions

The powder X-ray diffraction pattern (PXRD) of the polymer composite materials (Fig. 1) recorded on a Rigaku X-ray diffractometer ($\lambda = 1.5418 \text{ \AA}$, Cu K α) showed an increase in the intensity of the characteristic peak compared to KIT-6 due to the polymer formation inside the mesopores of silica materials resulting in an increase in the apparent density of the mesopore walls.⁷ The organic nanopores thus obtained exhibit high thermal stability due to the interpenetrating composite frameworks between the cross-linked polymers and silica material. N₂ adsorption isotherms were measured at 77 K using a Quantachrome AS-IMP volumetric adsorption analyzer. Before the adsorption measurements, all samples were outgassed for 12 h at 353 K in the

Center for Functional Nanomaterials, Department of Chemistry, Korea Advanced Institute of Science and Technology, Daejeon, 305-701, South Korea. E-mail: amitdubey75@yahoo.com

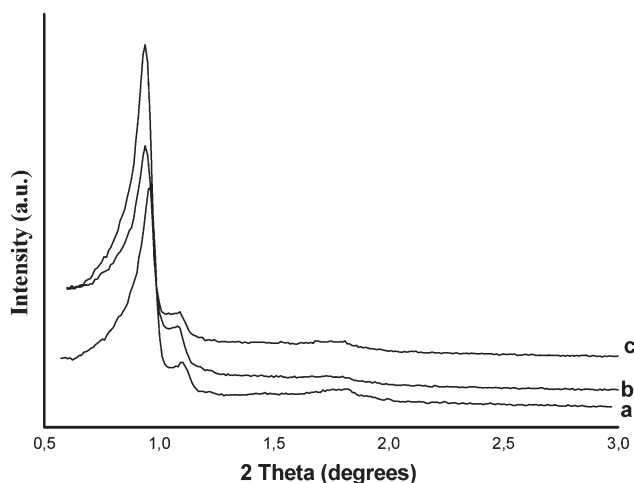


Fig. 1 PXRD pattern of (a) KIT-6, (b) 0.12% Fe/KIT-PS and (c) 0.35% Fe/KIT-PS.

degas port of the adsorption analyzer. The N_2 adsorption–desorption isotherm of KIT-6 shows a type IV adsorption isotherm.

Fig. 2 shows N_2 adsorption–desorption isotherms according to IUPAC classification, with a sharp capillary condensation step at relatively high pressure with an H1 hysteresis loop indicative of well-defined cylindrical pores. The total pore volume, pore size and surface area of the composite materials were reduced compared to the pure KIT-6 and reveals that the mesopores are filled with the polymers (Table 1).

The samples were named as x Fe/KIT-PS, where x presents the percentage of Fe content in vinyl ferrocene (Table 1), PS indicates the polymer composite. The elemental analysis was carried out by ICP-AAS. The thermogravimetric analysis indicated that 99% of the monomers were converted to polymers. The details of the synthetic methodology of KIT-6 has been published elsewhere.¹² Catalytic hydroxylation of phenol is carried out in a two-neck 50 ml glass reactor equipped with a condenser and septum using water as the solvent. 1 g of phenol is dissolved in the solvent containing 50 mg of the catalyst to the magnetically stirred solution kept at a desired temperature (2–65 °C) using H_2O_2 (substrate : oxidant molar ratio = 3 and 5) as an oxidant. A small amount of the samples was periodically withdrawn from the reaction mixture and analyzed by GC5890 equipped with a packed SE-30 column. The identification of the products was carried out by injecting the authentic samples after considering their response factors and using the internal standard, in this case 2-propanol. Catechol (CAT) and hydroquinone (HQ) were observed as the major products on all the catalysts and no benzoquinone was observed under our experimental conditions. Fig. 3 shows the

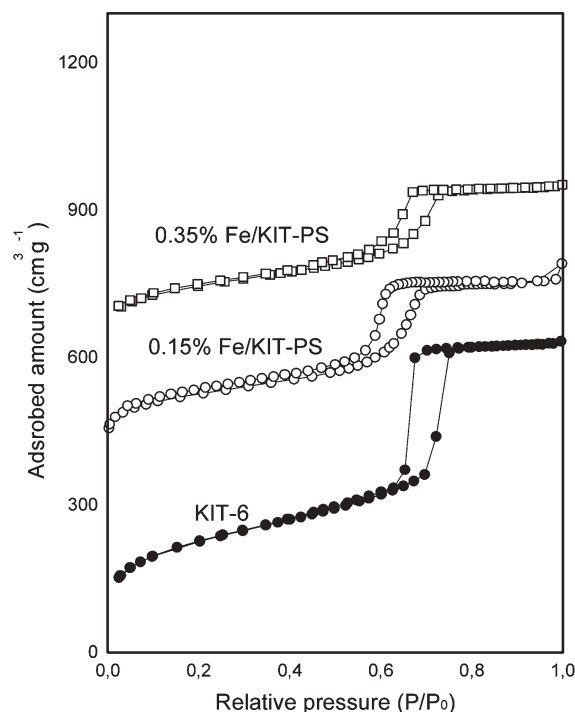


Fig. 2 N_2 adsorption–desorption isotherms for KIT-6, 0.12% Fe/KIT-PS and 0.35% Fe/KIT-PS samples. The isotherms are offset vertically by 400 and 600 cm^3 STP g^{-1} for 0.12 and 0.35% Fe/KIT-PS, respectively.

activity of the 0.35% Fe/KIT-PS (catalyst selected for detailed study) at 20 °C. The results indicated that nearly 30% conversion of phenol and 25.4% conversion based on the dihydroxybenzenes (Cat : HQ ratio = 3.4) with around 76.2% selectivity of H_2O_2 based on products was achieved in 24 h of the reaction time in the ferrocene-derived polymer materials. It should be mentioned here that no catalytic activity was observed for pure KIT-6 and KIT-PS, indicating that the catalytic activity is essentially due to the presence of Fe acting as the active center for this reaction. These results are quite different from some of the iron-containing mesoporous materials (ferrocene immobilization in MCM-41 type materials) where no hydroxylated products were observed under the same reaction conditions. This difference in the higher activity and selectivity of polymeric-derived materials for dihydroxylated product formation may be attributed to the different hydrophobic nature of the surface after the incorporation of polymer. To see the influence of amount of H_2O_2 , the experiments were performed using even lower concentration of H_2O_2 (5 : 1). The results obtained were quite interesting as 14.2% selective conversion to catechol was observed for 0.35%Fe/KIT-PS. This is the highest ever conversion of phenol, product selectivity and the selectivity of H_2O_2 on dihydroxybenzenes among the Fe-containing catalysts at

Table 1 Structural parameters of the samples^a

Catalyst	Surface area/ $m^2 g^{-1}$	Pore volume/ $ml g^{-1}$	Pore size/nm	^b Conversion (wt%)	H_2O_2 selectivity (%)
KIT-6 (silica)	821.74	0.97	8.3	0	0
0.12% Fe/KIT-PS	451.82	0.55	6.2	20.7	62.1
0.35% Fe/KIT-PS	432.32	0.54	5.1	25.4	76.2

^a Phenol (1 g), Catalyst (0.35% Fe/KIT-PS) 50 mg, solvent—water, oxidant— H_2O_2 , Phenol : H_2O_2 (molar ratio 3 : 1), reaction temp—293 K.

^b Conversion based on dihydroxybenzenes.

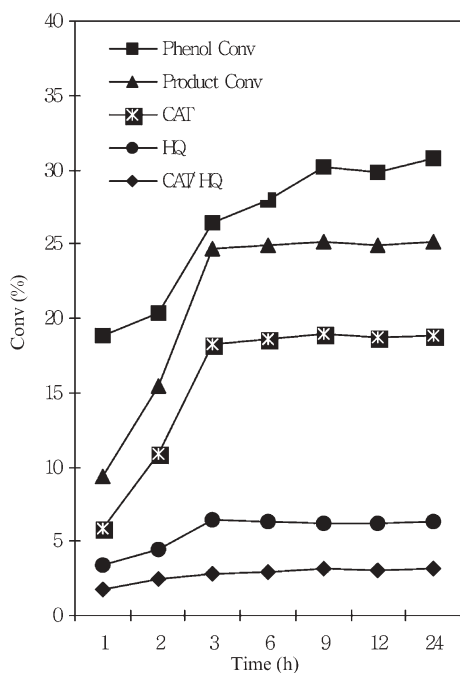


Fig. 3 Variation of conversion of phenol with time over 0.35% Fe/KIT-PS.

low temperature using water as a solvent. The interaction of the H_2O_2 with the catalyst generates hydroxyl radicals, thought to be active centres involved in the reaction, which subsequently attack at the *o*- and *p*-position to produce the desired dihydroxybenzenes. These results are quite significant for industrial perspectives and clearly corroborate the role of polymer incorporation on product selectivity. In order to check the reusability of the materials, the catalyst was centrifuged after the completion of the reaction, washed thoroughly with water several times until the filtrate becomes clear and subjected to fresh reaction. It was observed that 22.1% conversion of phenol was observed and the catalyst was recycled five times without any further decrease in the conversion.

Conclusion

In summary, we have synthesized large pore silica polymer nanocomposite materials through a radical polymerization technique for selective hydroxylation of phenol. The higher conversion of phenol on dihydroxybenzenes and selectivity of H_2O_2 using water as a solvent at 293 K may indicate the promising use of these materials for industrial applications. Further efforts are currently underway for the use of these materials in other applications.

Acknowledgements

This work was supported in part by the Creative Research Initiative Program of the Korean Ministry of Science and Technology, and by the School of Molecular Science through the Brain Korea 21 project.

References

- 1 A. P. Wight and M. E. Davis, *Chem. Rev.*, 2002, **102**, 3589–3614 and references therein.
- 2 W. C. Mplenkamp, M. Watanabe, H. Miyata and S. H. Tolbert, *J. Am. Chem. Soc.*, 2004, **126**, 4476–4477.
- 3 S. Inagaki, S. Guan, Y. Fukushima, T. Ohsuna and O. Terasaki, *J. Am. Chem. Soc.*, 1999, **121**, 9611–9614.
- 4 T. Asefa, J. M. MacLachlan, T. Asefa and G. A. Ozin, *Chem.–Eur. J.*, 2000, **6**, 2507.
- 5 J. H. Clark and D. J. Macquarrie, *Chem. Commun.*, 1998, 853–860.
- 6 M. Choi and R. Ryoo, *Nat. Mater.*, 2003, **2**, 473–476.
- 7 M. Choi, F. Kleitz, D. Liu, H. Y. Lee, W. S. Whn and R. Ryoo, *J. Am. Chem. Soc.*, 2005, **127**, 1924–1932.
- 8 M. Taramasso, G. Perego and B. Notari, *US Pat.*, 4410501, 1983.
- 9 (a) C. Xiong, Q. Chen, W. Lu, H. Gao, W. Lu and Z. Gao, *Catal. Lett.*, 2000, **69**, 231–236; (b) A. Thangaraj, R. Kumar and P. Ratnasamy, *J. Catal.*, 1991, **131**, 294–297; (c) A. Tuel and Y. Ben Taarit, *Appl. Catal., A: General*, 1993, **102**, 69–77; (d) M. Allian, A. Germain, T. Cseri and F. Figueras, *Stud. Surf. Sci. Catal.*, 1993, **78**, 455; (e) J. A. Martens, P. Buskens and P. A. Jacobs, *Appl. Catal., A: General*, 1993, **99**, 71–74; (f) S. Kannan, A. Dubey and H. Knozinger, *J. Catal.*, 2005, **231**, 381–392; (g) J. Wang, J. Park, X. Y. Wei and C. W. Lee, *Chem. Commun.*, 2003, 628–629.
- 10 L. Lee, J. L. Shi, J. Yan, X. Zhao and H. G. Chen, *Appl. Catal., A: General*, 2004, **263**, 213–217.
- 11 M. Trejda and M. Ziolek, *Catal. Today*, 2005, **101**, 109–116.
- 12 F. Kleitz, S. H. Choi and R. Ryoo, *Chem. Commun.*, 2003, 2136–2137.

Use of ionic liquids to improve whole-cell biocatalytic asymmetric reduction of acetyltrimethylsilane for efficient synthesis of enantiopure (*S*)-1-trimethylsilylethanol

Wen-Yong Lou,^a Min-Hua Zong^{*a} and Thomas J. Smith^b

Received 21st October 2005, Accepted 12th December 2005

First published as an Advance Article on the web 13th January 2006

DOI: 10.1039/b514999a

The two typical ionic liquids (ILs), one hydrophobic (BMIM·PF₆) and one hydrophilic (BMIM·BF₄), were tested as solvents for use in the asymmetric reduction of acetyltrimethylsilane (ATMS) to enantiopure (*S*)-1-trimethylsilylethanol {(*S*)-1-TMSE} catalyzed by immobilized *Saccharomyces cerevisiae* cells. The results demonstrate that BMIM·PF₆ and BMIM·BF₄ can markedly boost the activity and the stability of the immobilized cells. To better understand the reaction performed in these IL-containing systems, various variables that influenced the performance of the reaction were examined. The optimal buffer pH, reaction temperature and substrate concentration were 7.3, 30 °C and 84 mM, respectively, for the BMIM·PF₆/buffer (1/6, v/v) biphasic system, and 7.5, 30 °C and 77 mM, respectively, for the 10% (v/v) BMIM·BF₄-buffer co-solvent system. Under the optimal conditions, the initial reaction rate, maximum yield and product *e.e.* were 63.4 mM h⁻¹, 99.9% and >99.9% with the former system, while those with the latter system were 74.5 mM h⁻¹, 99.2% and >99.9%, respectively, which were much higher than those achieved with either *n*-hexane/buffer (2/1, v/v) biphasic system or aqueous buffer. It was also found that the optimal pH and substrate concentration changed when *n*-hexane was replaced by BMIM·PF₆ or BMIM·BF₄. Although the optimal reaction temperature remained the same in the four kinds of reaction systems, the temperature profile of the reaction varied from case to case. Additionally, BMIM·BF₄ and especially BMIM·PF₆ exhibited greater biocompatibility with *Saccharomyces cerevisiae* than *n*-hexane, and could be used repeatedly for economically interesting whole-cell biocatalytic processes with *in situ* coenzyme regeneration.

Introduction

Organosilicon compounds are a group of non-natural compounds that show unique chemical and physical characteristics compared to conventional organic compounds because of the particular properties of the silicon atom, such as its larger atomic radius and smaller electronegativity compared to the carbon atom. Organosilicon compounds not only play a crucial role in asymmetric synthesis and functional materials, but also many are bioactive and can be employed as silicon-containing drugs, such as Zifosilone,¹ Cisobitan² and TAC-101 {4-[3,5-bis(trimethylsilyl)benzamido]benzoic acid},³ with greater pharmaceutical activity, higher selectivity and lower toxicity than their carbon counterparts, though little has been discovered about the mechanisms involved.⁴ Therefore, the replacement of certain specific carbon atoms in drugs by silicon seems to be a useful and efficient strategy in drug design, and should be regarded as a complementary tool in the development of new drugs.⁵ As a result, the preparation of silicon-containing compounds is becoming increasingly

important. Most traditional chemical methods used for synthesis of organosilicon compounds can ensure chiral purity only by using chiral feedstock chemicals, owing to the difficulty and high cost of racemate resolution. Accordingly, the economic asymmetric synthesis of enantiopure organosilicon compounds *via* biocatalytic routes has become a subject of great interest. In recent years, many investigations have been carried out to test the potential of biotransformations to produce useful enantiopure silicon-containing amino acids and peptides,^{6,7} alcohols^{8–11} and cyanohydrins,^{12–14} as well as to explore in detail the mechanism of enzymatic catalysis.¹⁵ In particular, the asymmetric bioreduction of silicon-containing ketones to enantiopure organosilyl alcohols (the silicon counterparts of chiral, enantiopure alcohols, which are key synthons for a large number of pharmaceuticals) has been the goal of extensive studies where both isolated dehydrogenases and whole cells have been used as the biocatalysts. For example, horse liver alcohol dehydrogenase¹⁶ and whole cell of *Rhodotorula* sp. AS2.2241¹¹ were successfully used as biocatalysts in our previous work for the synthesis of optically active silicon-containing alcohols. Since such reactions often require stoichiometric amounts of nicotinamide cofactors (usually NADPH), the use of whole cells rather than isolated enzymes is preferred to avoid the need for enzyme purification and cofactor regeneration.¹⁷ The tremendous potential of whole cells of yeast as practical biocatalysts in the field of

^aSouth China University of Technology, Wushan Street 1, Guangzhou 510640, China. E-mail: wylou@scut.edu.cn; btmhzong@scut.edu.cn; Fax: +86-20-2223-6669; Tel: +86-20-8711-1452

^bBiomedical Research Centre, Sheffield Hallam University, Owen Building, Howard Street, Sheffield, UK S1 1WB. E-mail: t.j.smith@shu.ac.uk

asymmetric synthesis of enantiopure alcohols has been well recognized owing to their high bioavailability, ease of use, low environmental pollution, low cost, high efficiency and mild reaction conditions.¹⁸ However, problems arise with substrates and products that are poorly soluble in the aqueous phase and/or display inhibitory or toxic effects on the biocatalyst. Two-phase systems, consisting of a cell-containing aqueous phase and a second water-immiscible phase (usually an organic solvent) that acts as a reservoir for the equilibrium-based delivery of substrate to the microorganisms, have been established to overcome these limitations.¹⁹ Recently, we reported the use of a UV-generated mutant strain of *Saccharomyces cerevisiae* for asymmetric reduction of acylsilane that yielded improved results in an aqueous/organic biphasic system as compared to those achieved in a single-phase aqueous system.¹⁰ It was found, however, that the operational stability of the yeast cells was poor. Furthermore, the use of conventional organic solvents in such applications is problematic because they are often toxic to the cells, sometimes explosive and usually environmentally harmful. The volatile nature of such solvents is also a serious threat to the operator, particularly when they are employed on a large scale. Thus, there is currently a growing need for green solvents such as supercritical fluids and ionic liquids (ILs) as alternatives to organic solvents, in order to minimize harm to environment and operator, at the same time as allowing highly efficient catalysis using whole cells.²⁰

Ionic liquids (ILs) have recently emerged as novel green solvents for a great variety of biocatalytic transformations, and are becoming more and more attractive in such applications.^{21,22} These solvents display no measurable vapor pressure, eliminating the possibility of gaseous emissions, and therefore are more environmentally friendly than volatile organic solvents. ILs are capable of dissolving a wide range of substrates including highly polar and non-polar organic, inorganic and polymeric compounds. Also, their non-flammability makes them safer in practice than conventional organic solvents. Another obvious advantage is the possibility of designing a solvent with specific properties (including the polarity, hydrophobicity, viscosity and solvent miscibility) by modifying the cation, anion, or attached substituent of the IL.²³ In recent years, there have been many reports of using IL-containing systems for enzymatic reactions.^{21,22,24} In many cases, enzymes, especially lipases and proteases, not only work well in the IL systems, but also exhibit excellent activity, selectivity and stability.^{25–29} Recently, we have reported the successful enzyme-catalyzed asymmetric hydrolysis and ammonolysis of D,L-*p*-hydroxyphenylglycine methyl ester in IL-containing systems with markedly improved results.^{30–32} To date, the possibility of whole-cell catalysis in the presence of ILs remains largely unexplored, with only a few published accounts. Cull *et al.*³³ first reported the use of a 1-butyl-3-methylimidazolium hexafluorophosphate (BMIM·PF₆)/aqueous buffer biphasic system for the biotransformation of 1,3-dicyanobenzene to 3-cyanobenzamide, catalyzed by whole cells of *Rhodococcus* R312. The IL acted as a reservoir for the poorly water-soluble substrate and product, thereby decreasing substrate and product inhibition observed in a single-phase aqueous system. In addition, the IL showed less damage to the

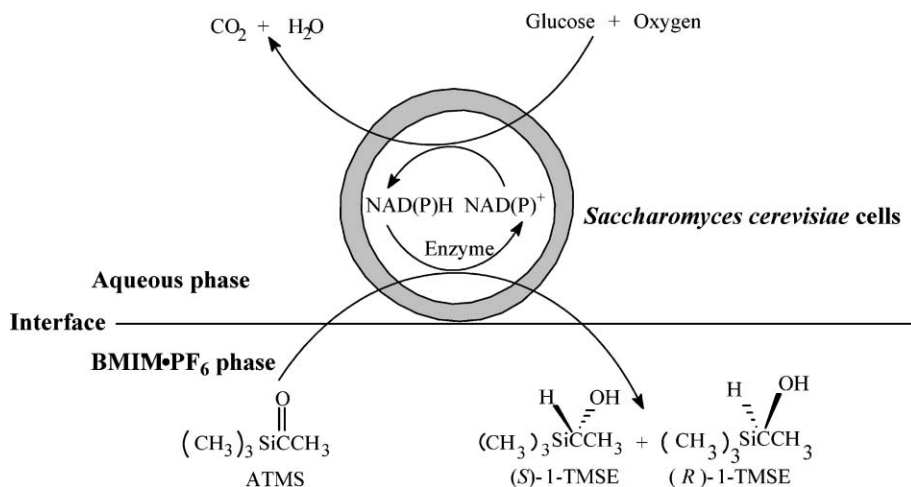
microbial cells than the toluene originally used as the co-solvent. Howarth *et al.*³⁴ attempted the asymmetric reduction of prochiral ketones by baker's yeast in the presence of wet BMIM·PF₆; the yield and enantioselectivity were fair for some substrates but not others. The use of dry BMIM·PF₆ gave very poor results possibly due to enzyme inactivation. The efficient whole-cell biotransformation in an IL/aqueous biphasic system described by Pfruender *et al.*³⁵ involved the enantioselective reduction of 4-chloroacetophenone to (*R*)-1-(4-chlorophenyl)ethanol by *Lactobacillus kefir* cells in the absence of cofactor supplements, with high product yield. Very recently, the biodegradation of phenol catalyzed by *Pseudomonas putida* ATCC 1172 cells has been shown to operate successfully in an aqueous/phosphonium IL biphasic partitioning bioreactor.³⁶

Here, for the first time, we describe the use of the two typical ILs, hydrophobic BMIM·PF₆ and hydrophilic BMIM·BF₄, for the synthesis of enantiopure (*S*)-1-trimethylsilylethanol {(*S*)-1-TMSE} via asymmetric reduction of acetyltrimethylsilane (ATMS) with immobilized *Saccharomyces cerevisiae* cells, which may become a novel and efficient route for the preparation of chiral, enantiopure organosilyl alcohols.

Results and discussion

Generally, economically attractive whole-cell-catalyzed redox reactions require a solvent that is nontoxic for the biocatalyst and the environment, that permits efficient cofactor regeneration, and that dissolves poorly water-soluble substrates and/or products. ILs, rather than organic solvents, have been shown to be preferable solvents for cell-based systems. Therefore, two typical ILs, one hydrophobic (BMIM·PF₆) and the other hydrophilic (BMIM·BF₄), were tested in the present study for their performance as solvent system components for the asymmetric reduction of ATMS catalyzed by immobilized *Saccharomyces cerevisiae* cells.

Initially, we focused on the water-immiscible BMIM·PF₆ as the second liquid phase, which can act as a reservoir of substrate and product. The cellular cofactor regeneration system is active in the presence of the IL. ATMS is reduced to enantiopure (*S*)-1-TMSE while converting NAD(P)H to NAD(P)⁺ (Scheme 1). Glucose is simultaneously oxidized to CO₂, regenerating NAD(P)H from NAD(P)⁺. Additionally, the biphasic system can efficiently overcome the limitation of substrate and the product inhibition often observed during the bioreduction of carbonyl compounds in a monophasic system,³⁷ and consequently a high product yield can be achieved without cofactor supplements. For a better understanding of the bioreduction of ATMS conducted in the novel system, the effects of several influential variables on the reaction were studied (Fig. 1). It has been reported that the effect of volume ratio of two phases on biocatalytic reactions varies widely and unpredictably, so the initial rate, the product yield and the product *e.e.* of the reaction were determined in various biphasic systems with the volume of BMIM·PF₆ phase fixed (0.25 mL) and that of the aqueous buffer phase varied from 125 μL to 2.5 mL. As can be seen in Fig. 1a, the volume ratio of the aqueous phase to the IL phase (V_{aq}/V_{IL} , mL/mL) clearly influenced the initial reaction rate and the product



Scheme 1 The asymmetric reduction of ATMS to enantiopure (S)-1-TMSE catalyzed by *Saccharomyces cerevisiae* cells in an BMIM·PF₆/buffer biphasic system.

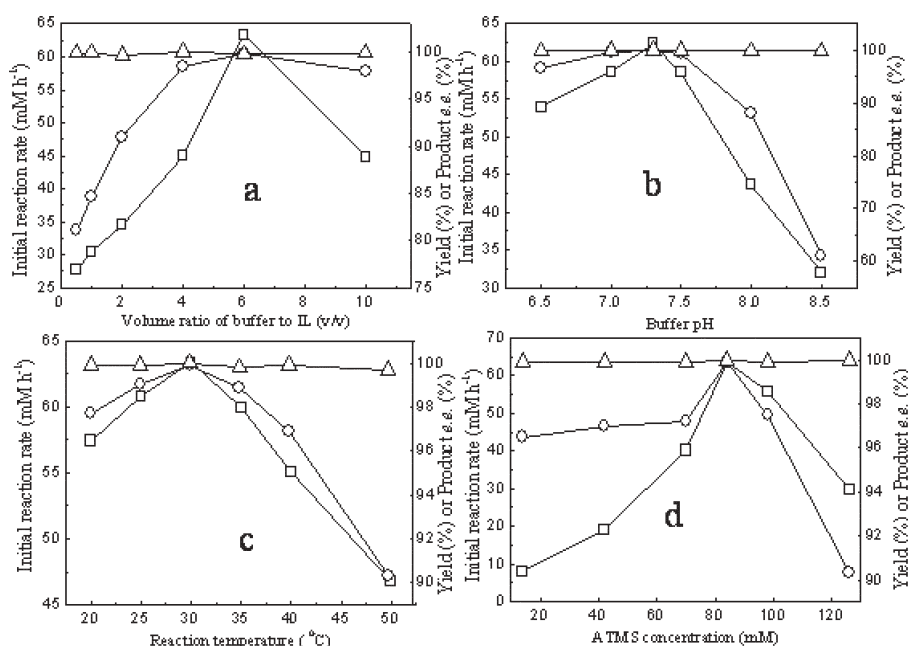


Fig. 1 The asymmetric reduction of ATMS mediated by immobilized *Saccharomyces cerevisiae* cells in a BMIM·PF₆/buffer biphasic system. (a) Effect of volume ratio of aqueous phase to IL phase (buffer pH 7.3; 30 °C; 84 mM ATMS). (b) Effect of buffer pH {BMIM·PF₆/buffer volume ratio: 1/6 (v/v); 30 °C; 84 mM ATMS}. (c) Effect of reaction temperature {BMIM·PF₆/buffer volume ratio: 1/6 (v/v); buffer pH 7.3; 84 mM ATMS}. (d) Effect of substrate concentration {BMIM·PF₆/buffer volume ratio: 1/6 (v/v); buffer pH 7.3; 30 °C}. Symbols: (□) initial reaction rate; (○) product yield; (Δ) product e.e.

yield, but had no appreciable effect on the product e.e. Enzymes and active cells are commonly inactivated by direct contact with the interface between the aqueous and non-aqueous phases and so the obvious enhancement in initial rate and product yield with the increase of $V_{\text{aq}}/V_{\text{IL}}$ up to 6/1 is easily explained because as the $V_{\text{aq}}/V_{\text{IL}}$ value increases it becomes less likely that the cells will contact the IL. Further rise in the $V_{\text{aq}}/V_{\text{IL}}$ ratio led to a sharp decline in the initial rate, possibly owing to inefficient transfer of substrate to the aqueous phase when very little IL was present. From Fig. 1a it is clear that the optimum ratio of buffer to BMIM·PF₆ ($V_{\text{aq}}/V_{\text{IL}}$) under the conditions of this experiment is 6/1.

Buffer pH influences not only enzymatic selectivity and activity, but also the regeneration of the coenzyme present in the microbial cells, which in turn affects the reaction rate. Different isoenzymes capable of catalyzing the reaction have different optimum pHs. As a result, there exists an optimum pH at which the desired reductases are most active, and the undesired isoenzymes show the lowest activity or even no activity. Fig. 1b depicts the significant effect of buffer pH in the IL/buffer biphasic system on the asymmetric reduction of ATMS catalyzed by immobilized *Saccharomyces cerevisiae* cells. The cells lost their activity dramatically at pH of above 7.3, leading to poor reaction rate and product yield. The

reaction accelerated with increasing buffer pH from pH 6.5 to 7.3, and the product yield increased to some extent. Within the pH range tested, the *e.e.* of the product was consistently above 99%, indicating that there was no problem with activity of undesired isoenzymes within this range of pH. Taking into account the initial rate and the product yield, pH 7.3 appeared to be the optimal buffer pH for the reaction. As shown in Fig. 1c, a rise in reaction temperature clearly boosted both the initial rate and the product yield up to 30 °C. However, the reaction rate and the product yield dropped sharply when the temperature was above 30 °C, although temperature showed little effect on the product *e.e.* within the range examined. Obviously, 30 °C was the optimal temperature for the reaction.

As shown in Fig. 1d, the initial rate and the product *e.e.* clearly increased with increasing concentration of substrate up to 80 mM, beyond which further increase in substrate concentration gave rise to a substantial decrease in the reaction rate and product yield, suggesting substrate inhibition at high concentrations of substrate. Throughout the range of substrate concentrations, however, the product *e.e.* showed no variation. Thus, the optimal substrate concentration was 80 mM. After a reaction time of 12 h under the optimum conditions described above, the immobilized yeast cell-catalyzed asymmetric reduction of prochiral ATMS in the BMIM·PF₆/buffer biphasic system produced (*S*)-1-TMSE with a yield of 99.9% and an *e.e.* greater than 99%.

The other IL that was investigated, BMIM·BF₄, is hydrophilic in nature and miscible with water in all proportions. In our previous reports,^{31,32} it has been demonstrated that IL content in co-solvent systems markedly affects enzyme activity, selectivity and stability. Accordingly, it was considered to be important to examine the effect of the concentration of BMIM·BF₄ in the aqueous buffer on the cell-mediated bioreduction. As expected, BMIM·BF₄ concentration showed an obvious effect on the initial rate and the product yield (see Fig. 2a). Clear increases in the reaction rate, the product yield and the product *e.e.* were observed with the increase of BMIM·BF₄ content up to 10% (v/v), and further increase in IL content led to a sharp decline in the initial rate and the yield. Relative to the reaction conducted in neat aqueous buffer, the reaction was accelerated to some extent on the addition of small amounts (5–20%, v/v) of BMIM·BF₄, but became significantly slower than the reaction in the neat aqueous medium upon addition of the IL above 30% (v/v). When the IL concentration in the co-solvent mixture reached 50% (v/v), the immobilized cells displayed very low activity, resulting in poor reaction rate and yield. This is possibly because a high concentration of IL causes not only high ionic strength of the reaction medium that might inactivate the cells or the enzymes present in the cells (leading to lower activity), but also high viscosity of the reaction mixture, which limits the diffusion of substrates and products to and from the immobilized cells, resulting in a drop in initial rate. Such an effect of solvent viscosity on the reaction is consistent with the obvious variation of the initial reaction rate with the shaking rate at very high concentration of BMIM·BF₄ observed in our previous experiments.³¹ As evident from the results presented here, the presence of the IL BMIM·BF₄ at an appropriate concentration can boost the activity and the enantioselectivity

of the cell-mediated reduction of ATMS, and the optimal content of BMIM·BF₄ in the co-solvent system under the conditions used was 10% (v/v). For a better understanding of the effect of IL concentration on the reaction, the apparent pH of the co-solvent system was measured at various concentrations of BMIM·BF₄. When BMIM·BF₄ content was above 30% (v/v), the pH of the mixed solvent was clearly lowered with increasing concentration of the IL. No appreciable variation of the pH, however, was observed in the cases where BMIM·BF₄ concentration was below 20% (v/v), which is similar to our previous observations.³¹ In order to optimize the reaction further, the initial rate, product yield and product *e.e.* were investigated in the 10% (v/v) BMIM·BF₄-buffer co-solvent system as a function of buffer pH, reaction temperature and substrate concentration (see Fig. 2b–d). All of these variables significantly influenced the initial rate and the product yield, but had only slight effects on the product *e.e.* within the ranges explored. The optimal buffer pH, reaction temperature and substrate concentration were 7.5, 30 °C and 77 mM, respectively; under these optimal conditions both the product yield and the product *e.e.* were above 99%, and the initial rate was as high as 74.54 mM h⁻¹.

It has been reported that a variety of enzymes and microbial cells in IL-containing systems show catalytic activities that are generally comparable with or higher than those observed in systems containing conventional organic solvents.^{38–41} From both a practical and a theoretical viewpoint, it is of particular interest to compare the asymmetric reduction of ATMS catalyzed by immobilized *Saccharomyces cerevisiae* cells in IL-containing systems with that in organic solvent-containing systems. In our previous report,¹⁰ *n*-hexane was shown to be the best organic phase when the reduction reaction was performed in an aqueous/organic biphasic system, owing to its relatively low toxicity for the cells and faster product extraction rate as compared to other organic solvents examined. Therefore, a comparative study was made here of the cell-catalyzed asymmetric reduction of ATMS in the *n*-hexane/buffer biphasic system, in IL-containing systems (BMIM·PF₆/buffer biphasic system, BMIM·BF₄-buffer co-solvent system) and in aqueous buffer. From the data summarized in Table 1, the optimal pH and substrate concentration for the reaction changed when BMIM·PF₆/buffer biphasic system or BMIM·BF₄-buffer co-solvent system was used as the reaction medium instead of *n*-hexane/buffer biphasic system or pure buffer. Although the optimal reaction temperature remained the same in the four kinds of media, the temperature profile of the reaction varied from case to case. Changes in the optimal pH might possibly be because the ILs and *n*-hexane have different influences on buffer pH, though little has been known about the underlying mechanisms. The different partition coefficients of ATMS in the BMIM·PF₆/buffer biphasic system and in the *n*-hexane/buffer biphasic system could partly account for the difference in optimum substrate concentration between these two systems. The detailed reasons for these differences require further study and are the subject of ongoing investigation in our laboratory. As shown in Table 1, under the optimal conditions for each medium, the initial rate was more than 44 times greater in the BMIM·PF₆/buffer biphasic system than

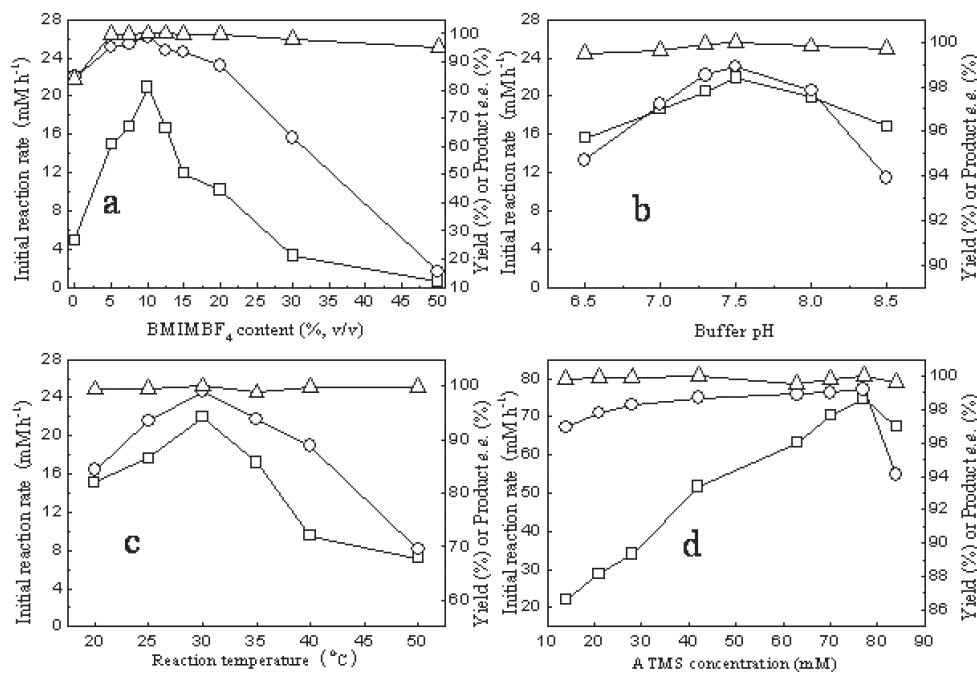


Fig. 2 The asymmetric reduction of ATMS mediated by immobilized *Saccharomyces cerevisiae* cells in a BMIM·BF₄-buffer co-solvent system. (a) Effect of IL content in the co-solvent system (buffer pH 7.5; 30 °C; 14 mM ATMS). (b) Effect of buffer pH {10% (v/v) BMIM·BF₄; 30 °C; 14 mM ATMS}. (c) Effect of reaction temperature {10% (v/v) BMIM·BF₄; buffer pH 7.5; 14 mM ATMS}. (d) Effect of substrate concentration {10% (v/v) BMIM·BF₄; 30 °C; buffer pH 7.5}. Symbols: (□) initial reaction rate; (○) product yield; (△) product *e.e.*

Table 1 Comparison of asymmetric reduction of ATMS catalyzed by immobilized yeast cells in various media

Medium	Optimal reaction conditions						
	pH ^c	Temperature /°C	ATMS concentration/mM	V _o /mM h ⁻¹	t/h ⁻¹	Yield (%)	<i>e.e.</i> (%)
<i>n</i> -Hexane/buffer biphasic system (2/1, v/v) ^a	8.0	30	42	1.45	48	97.4	95.4
BMIM·PF ₆ /buffer biphasic system (1/6, v/v) ^a	7.3	30	84	63.38	12	99.9	>99.9
Aqueous buffer	7.3	30	14	4.88	12	84.1	82.7
BMIM·BF ₄ -buffer co-solvent system (10%,v/v) ^b	7.5	30	77	74.54	12	99.2	>99.9

^a The optimum volume ratio of *n*-hexane or BMIM·PF₆ to aqueous buffer in a biphasic system. ^b The optimum volume concentration of BMIM·BF₄ in a co-solvent system. ^c The optimum pH of Tris-HCl buffer before addition of IL or *n*-hexane to the reaction system.

in the *n*-hexane/buffer biphasic system and was 15-fold faster in the BMIM·BF₄-buffer co-solvent system than in pure buffer. Moreover, both of the IL-containing systems outperformed the pure buffer and *n*-hexane/buffer biphasic system in terms of yield and product *e.e.* The success of the IL-containing systems in this application may be attributable to one or more of the following: (1) the IL might interact with charged groups on cell membrane, causing changes in the ionic states of substrate and cell membrane, and making it easier for substrate to permeate through the cell membrane; (2) since the IL is an organic salt, it might activate the enzyme responsible for the bioreduction of ATMS to (*S*)-1-TMSE (the desired enzyme) and inhibit isoenzymes with undesirable activities present in the cells; (3) compared to *n*-hexane, BMIM·PF₆ could favourably alter the partition coefficient of the substrate (ATMS) between the two phases; (4) IL shows much lower toxicity and greater biocompatibility with *Saccharomyces cerevisiae* cells than organic solvents.

It is well known that the partitioning behavior of substrates and products is of great importance for the thermodynamics

of reactions in two-phase systems.⁴² Thus, the partition coefficients for ATMS and 1-TMSE between BMIM·PF₆ or *n*-hexane and buffer were measured, and the results are listed in Table 2. The partition coefficient for ATMS in the BMIM·PF₆/water biphasic system was much higher than that observed in the *n*-hexane/water biphasic system, suggesting that the IL BMIM·PF₆ is more suitable than *n*-hexane for the delivery of ATMS to the aqueous phase. This is probably responsible for the improved initial rate and yield observed when *n*-hexane was replaced by BMIM·PF₆ in the biphasic

Table 2 Partition coefficients for ATMS and 1-TMSE

Solute	Partition coefficients between the two phases	
	BMIM·PF ₆ /buffer (1/6, v/v) ^a	<i>n</i> -hexane/buffer (2/1, v/v) ^a
ATMS	55.1	10.9
1-TMSE	8.8	9.2

^a The optimum volume ratio of BMIM·PF₆ or *n*-hexane to aqueous buffer in a biphasic system for the reaction

system, as indicated in Table 1. Additionally, the partition coefficients for 1-TMSE in the BMIM·PF₆/water and *n*-hexane/water biphasic systems are both quite high (8.8 and 9.2, respectively), implying that BMIM·PF₆ and *n*-hexane are almost equally effective in extracting the product 1-TMSE from the aqueous phase and thus reducing product inhibition.

It has been reported that in a BMIM·PF₆/water biphasic system, *Rhodococcus* R312 cells were not actively growing, although the viability of the cells was assessed over only 90 min of exposure to the IL and so it is not possible to assess whether the IL used in this case was highly biocompatible with the strain.³³ Indeed, Pernak *et al.*⁴³ demonstrated that ILs could display significant antimicrobial activity against bacteria and fungi. The biocompatibility of phosphonium ILs with three xenobiotic-degrading bacteria, *Pseudomonas putida*, *Achromobacter xylosoxidans*, and *Sphingomonas aromaticivorans*, has recently been tested in order to establish an efficient degradation of phenol in an IL-containing biphasic system.³⁶ These reports suggest that the demonstration of IL biocompatibility is not a trivial matter, and it must be established before an IL can be fully exploited as a delivery phase in a two phase for a whole-cell biocatalytic process. Fig. 3 depicts the cell growth profiles of *Saccharomyces cerevisiae* in IL- and *n*-hexane-containing systems. Cell concentrations (g L⁻¹) were measured based on the cell dry weight and the ability of cells to grow in the presence of each compound was taken as an estimate of its biocompatibility. Reduced cell concentration relative to the positive control (no IL and *n*-hexane) was also regarded as an indicator of toxicity.⁴⁴ As evident from the data in Fig. 3, the cell growth of *Saccharomyces cerevisiae* was hardly affected by BMIM·PF₆, showing the excellent biocompatibility of this compound. Although affecting the cell growth to some extent, BMIM·BF₄ displayed greater biocompatibility than *n*-hexane. Compared with the two ILs, substantially reduced cell concentration relative to the control was observed with *n*-hexane, implying that *n*-hexane shows higher toxicity for the cells than BMIM·PF₆ and BMIM·BF₄, which is in good accordance with the observations that the cells show

greatly enhanced catalytic activity in IL-containing systems compared to *n*-hexane/buffer biphasic system (Table 1).

To gain a deeper insight into the effect of ILs on the whole-cell biocatalytic processes, it is essential to make a comparative study on the stability of the cells used in IL-containing systems and other systems. The operational stability of the immobilized *Saccharomyces cerevisiae* cells was therefore examined by incubating them in the BMIM·PF₆/buffer (1/6, v/v) biphasic system, 10% (v/v) BMIM·BF₄-buffer co-solvent system, *n*-hexane/buffer (2/1, v/v) biphasic system and pure Tris-HCl buffer (50 mM, pH 7.3), for a specified period of time at 30 °C under the optimal conditions of each system, followed by the measurement of their remaining activity. Because the reaction was much slow in the *n*-hexane-containing system, a longer time per cycle in the *n*-hexane/buffer biphasic system than that in the systems involving ILs (48 h vs. 12 h) was needed to make it go to completion. The relative activity of the immobilized cells employed for the first batch cycle was defined as 100%. After operating repeatedly for eight batches (12 h per batch, 96 h in total) in the BMIM·PF₆/buffer (1/6, v/v) biphasic system and the 10% (v/v) BMIM·BF₄-buffer co-solvent system, the relative activities of the immobilized cells were approximately 81% and 63%, respectively (Fig. 4). In contrast, the immobilized cells employed for the same period (two batches, 48 h per batch, 96 h in total) in the *n*-hexane/buffer (2/1, v/v) biphasic system retained only 48% of their initial activity. Similarly, the immobilized cells in neat aqueous buffer retained only 51% of their initial activity after eight batches (12 h per batch, 96 h in total). Clearly, the operational stability of the immobilized cells was considerably enhanced in the IL-containing systems, relative to the *n*-hexane-containing system and aqueous buffer system, and the cells had the greatest operational stability in the BMIM·PF₆-containing system. The ILs' lower toxicity for the microbial cells than *n*-hexane, as was demonstrated in Fig. 3, could partly account for these observations. The coating and protection of the cells by the IL⁴⁵ may also be important and improved interactions

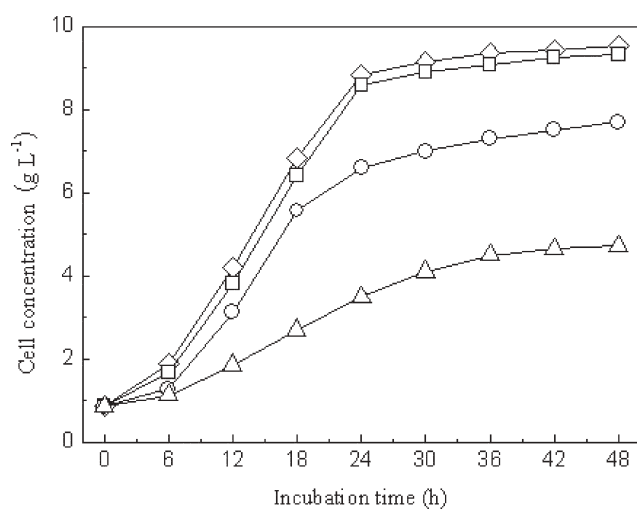


Fig. 3 Effect of ILs and *n*-hexane on the growth of *Saccharomyces cerevisiae* cultures. Symbols: (◇) control experiment with no IL or *n*-hexane; (□) BMIM·PF₆; (○) BMIM·BF₄; (△) *n*-hexane.

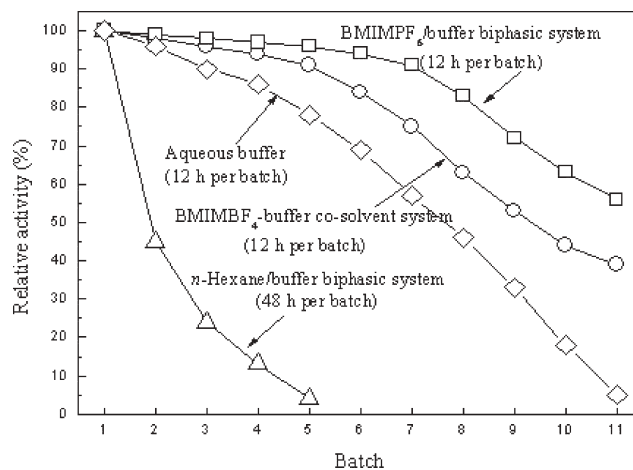


Fig. 4 Operational stability of immobilized *Saccharomyces cerevisiae* cells in various reaction systems. Symbols: (□) BMIM·PF₆/buffer (1/6, v/v) biphasic system; (○) 10% (v/v) BMIM·BF₄-buffer co-solvent system; (△) *n*-hexane/buffer (2/1, v/v) biphasic system; (◇) aqueous buffer.

between ILs and the carrier (calcium alginate) used for immobilization of *Saccharomyces cerevisiae* cells may contribute to the good stability of the immobilized cells in the IL-containing systems. The immobilized cells showed only about 23% remaining activity after they had been re-used for three batches (48 h per batch, total time in operation 144 h) and no significant activity for five batches in the presence of *n*-hexane, and displayed extremely low activity after re-use for eleven batches (12 h per batch, total 132 h) in aqueous buffer. However, after being re-used for eleven batches (12 h per batch, total 132 h) in the presence of BMIM·PF₆ and BMIM·BF₄, the immobilized cells still retained around 56% and 40%, respectively, of their original activity even after this prolonged period of use. Obviously, the *n*-hexane-containing system was the poorest in terms of the catalytic efficiency of the immobilized cells because, although the biocatalyst was moderately stable in terms of time, the reaction rate was so low that the catalytic activity was lost before the catalyst could convert as much substrate as the catalyst in IL-containing system or aqueous system could.

Thus, the whole-cell biocatalytic asymmetric reduction of ATMS for the synthesis of enantiopure (*S*)-1-TMSE on analytic scales took place more efficiently in the system involving IL than in the organic solvent/buffer or pure buffer system with respect to the reaction rate, the chemical yield, the product *e.e.*, and the stability of whole-cell biocatalyst. To show that the bioreductions in the presence of IL are useful and practical for industrial production of valuable fine chemicals, it is essential to explore the reactions performed on a larger scale. Accordingly, we also conducted a preparative scale asymmetric reduction of ATMS to (*S*)-1-TMSE catalyzed by immobilized *Saccharomyces cerevisiae* cells as a 154 mL batch process in the BMIM·PF₆/Tris-HCl buffer (1/6, v/v) biphasic system under the optimal conditions described above. The reaction process was monitored by GC analysis. The product was extracted from the reaction mixture with *n*-hexane once the substrate was no longer detectable. Although slightly lower than that obtained on the 2.0 mL analytical scale, the isolated yield (95.1%) is much higher than that reported so far for whole-cell-mediated reductions of ketones in systems involving ILs^{34,35} and the product *e.e.* was >99.9%. Furthermore, no emulsification of the two-phase system was observed, so the phases could be separated readily by centrifugation. No by-products accumulated in the IL phase, and the IL may consequently be easily recycled. Also, the reaction required no additional cofactor NAD(P)H. Thus, the overall costs of the whole-cell biocatalytic process in the presence of the IL on an industrial scale appear to be very promising and competitive.

Conclusions

The typical ILs BMIM·PF₆ and BMIM·BF₄ can markedly boost the activity, stereoselectivity and stability of immobilized *Saccharomyces cerevisiae* cells in the asymmetric reduction of ATMS to enantiopure (*S*)-1-TMSE. In addition, BMIM·PF₆ exhibits excellent solvent properties for ATMS and 1-TMSE and very good biocompatibility with *Saccharomyces cerevisiae*. Accordingly, BMIM·PF₆ could be used effectively as a substrate

reservoir and for *in situ* extraction of product, for commercially interesting whole-cell biocatalytic processes without the need for a separate system for cofactor regeneration.

Experimental

Biological and chemical materials

Yeast, *Saccharomyces cerevisiae*, was from the collection of the Division of Industrial Microbiology, College of Biological Sciences & Biotechnology, South China University of Technology (China). Wort medium was obtained from the Institute of Microbiology of Guangdong Province (China). Acetyltrimethylsilane (ATMS, 97% purity), (*S*)-1-trimethylsilylethanol {(*S*)-1-TMSE, 98% purity}, (*R*)-1-trimethylsilylethanol {(*R*)-1-TMSE, 98% purity} and *n*-nonane (>99% purity) were purchased from Aldrich-Fluka (USA). The two ionic liquids (ILs) used in this work, 1-butyl-3-methylimidazolium hexafluorophosphate (BMIM·PF₆) and 1-butyl-3-methylimidazolium tetrafluoroborate (BMIM·BF₄), were purchased from Aldrich-Fluka (USA) and were both of over 97% purity. ILs were dried at 200 °C for 48 h prior to use. Solvents were dried over Zeolite CaA (Uetikon, activated at 400 °C for 24 h before use). All other chemicals were from commercial sources and were of analytical grade.

Cultivation of *Saccharomyces cerevisiae* cells

Saccharomyces cerevisiae cells were cultivated in wort medium containing 2% (w/v) malt extract, 2% (w/v) glucose, 1% (w/v) peptone and 0.5% (w/v) yeast extract. The medium was adjusted to pH 6.8 with 2 M NaOH solution and autoclaved for 30 min. A preculture was prepared by inoculation of 100 mL of the complex medium with fresh cells from an agar plate culture. Incubation was performed in a 400 mL Erlenmeyer shaking-flask, which was shaken at 150 rpm and 30 °C. After 16 h incubation the cells were in the exponential growth phase and were collected by centrifugation (3500 rpm, 15 min), washed twice with distilled water, and separated from the aqueous medium by centrifugation to give a cell wet mass (cwm) of 2–5 g per 400 mL batch. The ratio 'cell wet mass'/cell dry mass' of around 4.0 was determined by lyophilization of samples of wet cells. The wet cells were immobilized on calcium alginate as described below.

Immobilization of *Saccharomyces cerevisiae* cells

A homogenous cell/sodium alginate suspension was prepared at 25 °C by adding 10 g of a suspension containing fresh cells (5 g wet cells in 5 mL water) into 30 mL of a homogeneous aqueous sodium alginate solution (2%, w/v), which was prepared by dissolving sodium alginate in deionized water, heating and stirring vigorously. The suspension was added dropwise by means of an injector to a gently stirred CaCl₂ solution (2%, w/v), where the calcium alginate pearls with a load of 13.2% (w/w) of *Saccharomyces cerevisiae* cells (based on cwm) precipitated. The pinhole size of injector and the drop rate were adjusted in such a way that the diameter of the pearls was about 1 mm. The pearls were kept in the CaCl₂ solution for another 1 h at 25 °C and collected by filtration, washed with water and re-suspended in an aqueous solution of

20% (w/v) glucose, 0.9% (w/v) NaCl and 0.05% (w/v) CaCl₂. They were stored at 4 °C for later use.

General procedure for the asymmetric reduction of ATMS with immobilized *Saccharomyces cerevisiae* cells in IL-containing systems

In a typical experiment, the mixture (2.0 mL) of the IL BMIM·PF₆ or BMIM·BF₄ and Tris-HCl buffer (50 mM) containing 0.15 g mL⁻¹ immobilized *Saccharomyces cerevisiae* cells, 20% (w/v) glucose and 0.05% (w/v) CaCl₂ was pre-incubated in a 10 mL Erlenmeyer flask capped with a septum for 5 min at 180 rpm and the appropriate temperature, and the reaction was initiated by adding a fixed amount of ATMS to the mixture. Aliquots (10 µL) were withdrawn at specified time intervals from the IL phase for the BMIM·PF₆/buffer biphasic system or from the co-solvent mixture for the BMIM·BF₄-buffer co-solvent system. Then, the product and residual substrate were extracted with *n*-hexane (50 µL) containing 5.6 mM *n*-nonane (internal standard) before GC analysis. Details about the volume ratio of buffer to BMIM·PF₆ in a biphasic system or BMIM·BF₄ content in a co-solvent system, ATMS concentration, buffer pH and reaction temperature are specified for each case.

The preparative scale biocatalytic reduction of ATMS to (*S*)-1-TMSE was performed by adding 23 g of immobilized *Saccharomyces cerevisiae* cells and 1.50 g (12.93 mmol) of ATMS to 154 mL of BMIM·PF₆/Tris-HCl buffer (50 mM, pH 7.3) biphasic system (1/6, v/v), containing 20% (w/v) glucose and 0.05% (w/v) CaCl₂ in the aqueous phase, and shaking at the rate of 180 rpm and at 30 °C until the substrate was no longer detectable by GC analysis. The immobilized cells were removed by filtration, and then the products were extracted from the reaction mixture with *n*-hexane. The product *e.e.* and yield were determined by GC analysis and the product was confirmed to be (*S*)-enantiomer of 1-TMSE by comparing its retention time with that of the standard (*S*)-1-TMSE under the same GC analysis conditions.

Determination of partition coefficients

The partition coefficients ($K_{IL/aq}$, $K_{or/aq}$) were determined by dissolving a known amount of ATMS or 1-TMSE (42 mM) in the biphasic system of BMIM·PF₆ or *n*-hexane and aqueous Tris-HCl buffer (50 mM, pH 7.3) (the volume ratio of IL to the aqueous buffer and the volume ratio of *n*-hexane to the aqueous buffer were 1/6 and 2/1, respectively, being the optimal volume ratio of the two phases for the reaction), with shaking (180 rpm), for 48 h at 25 °C. The concentration of ATMS or 1-TMSE in the BMIM·PF₆ or *n*-hexane phase was then analyzed by GC and the partition coefficient was determined *via* mass balance.

Biocompatibility of IL and organic solvent with *Saccharomyces cerevisiae* cells

The biocompatibility fermentations were conducted at 100 mL scale with wort medium and 5% (v/v) liquid inocula of *Saccharomyces cerevisiae* cells. Immediately after inoculation, 3 mL of IL (BMIM·PF₆, or BMIM·BF₄) or *n*-hexane was

added to each flask (except for a control flask containing no IL or *n*-hexane). Cultivation was carried out under the conditions described above. Samples (10 mL) were taken at specified time intervals from each flask and centrifuged (3500 rpm, 15 min) to remove the supernatant. *Saccharomyces cerevisiae* cells were washed three times with distilled water, and dried at 80 °C under vacuum. Then, the cell dry weight was determined in order to measure the cell growth of the *Saccharomyces cerevisiae* culture, which was generally taken as an indicator of biocompatibility.

Operational stability of immobilized *Saccharomyces cerevisiae* cells

In order to assess the operational stability of the yeast cells, the re-use of immobilized *Saccharomyces cerevisiae* cells was investigated in the mixture of BMIM·PF₆, BMIM·BF₄ or *n*-hexane, respectively, and Tris-HCl buffer (50 mM) containing 20% (w/v) glucose and 0.05% (w/v) CaCl₂. Initially, aliquots (0.3 g) of the immobilized cells were added into separate screw-capped vials each containing 2 mL of the appropriate medium {BMIM·PF₆/buffer (volume ratio: 1/6, v/v) biphasic system, BMIM·BF₄-buffer (volume ratio: 1/9, v/v) co-solvent system, or *n*-hexane/buffer (volume ratio: 2/1, v/v) biphasic system}, together with the optimal amount of ATMS for this reaction conducted in various media. Then, the reaction was repeated over 11 cycles (12 h per cycle) in IL-containing systems or over 5 cycles (48 h per cycle) in the *n*-hexane/buffer biphasic system at 30 °C and 180 rpm. Between cycles the immobilized cells were filtered from the reaction mixture, washed twice with fresh water, and added to a fresh batch of substrate solution, followed by the assay of the residual ATMS reduction activity. The relative activity of the immobilized cells employed for the first batch cycle was defined as 100%.

GC analysis

The reaction mixtures were assayed by a Shimadzu GC 2010 model with a flame ionization detector and a chiral column (20% permethylated β -cyclodextrin 30 m \times 0.25 mm \times 0.25 μ m) from Hewlett Packard (USA). The split ratio was 100 : 1. The injector and the detector were both kept at 250 °C. The column temperature was held at 64 °C for 1 min and was increased to 71 °C at a rate of 1 °C min⁻¹, and then kept constant for 1 min. The carrier gas was nitrogen and its flow rate in the column was 2.5 mL min⁻¹. The retention-times for ATMS, *n*-nonane, (*R*)-1-TMSE and (*S*)-1-TMSE were 3.53 min, 6.09 min, 6.74 min and 7.35 min, respectively. Quantitative data were obtained after integration on a Shimadzu GC integrator. An internal standard method was used for the calculations. The average error for this determination was less than 1.0%. All reported data are averages of experiments performed at least in duplicate.

Acknowledgements

The authors thank the National Natural Science Foundation of China (Grant No. 20376026), the Key Project of Chinese Ministry of Education (Grant No. 104147), the Research Fund

for the Doctoral Program of Chinese Higher Education (Grant No. 20030561017), BBSRC China Partering Award (Grant No. PA1519) and the Natural Science Foundation of SCUT (South China University of Technology) (Grant No. G02E5051010) for financial support.

References

- X. D. Zhu, E. Giacobini and J. M. Hornsperger, *Eur. J. Pharmacol.*, 1995, **276**, 93–99.
- L. Nicander, *Acta Pharmacol. Toxicol.*, 1975, **36**, 40–54.
- J. Shibata, K. Murakami, K. Wierzba, Y. Aoyagi, A. Hashimoto, M. Sano, T. Toko and Y. Yamada, *Anticancer Res.*, 2000, **20**, 3169–3176.
- R. Tacke, M. Merget, R. Bertermann, M. Bernd, T. Beckers and T. Reissmann, *Organometallics*, 2000, **19**, 3486–3497.
- W. Bains and R. Tacke, *Curr. Opin. Drug Discovery Dev.*, 2003, **6**, 526–543.
- T. Kawamoto, H. Yamanaka and A. Tanaka, *Appl. Biochem. Biotechnol.*, 2000, **88**, 17–22.
- H. Ishikawa, H. Yamanaka, T. Kawamoto and A. Tanaka, *Appl. Microbiol. Biotechnol.*, 1999, **53**, 19–22.
- M.-H. Zong, T. Fukui, T. Kawamoto and A. Tanaka, *Appl. Microbiol. Biotechnol.*, 1991, **36**, 40–43.
- P. Zani, *J. Mol. Catal. B: Enzym.*, 2001, **11**, 279–285.
- W.-Y. Lou, M.-H. Zong, Y.-Y. Zhang and H. Wu, *Enzyme Microb. Technol.*, 2004, **35**, 190–196.
- D.-H. Luo, M.-H. Zong and J.-H. Xu, *J. Mol. Catal. B: Enzym.*, 2003, **24**, 83–88.
- N. Li, M.-H. Zong, H.-S. Peng, H.-C. Wu and C. Liu, *J. Mol. Catal. B: Enzym.*, 2003, **22**, 7–12.
- R. Xu, M.-H. Zong, Y.-Y. Liu, J. He, Y.-Y. Zhang and W.-Y. Lou, *Appl. Microbiol. Biotechnol.*, 2004, **66**, 27–33.
- S.-R. Huang, S.-L. Liu, M.-H. Zong and R. Xu, *Biotechnol. Lett.*, 2005, **27**, 79–82.
- R. J. Smith, M. Pietzsch, T. Waniek, C. Syldatk and S. Bienz, *Tetrahedron: Asymmetry*, 2001, **12**, 157–65.
- W.-Y. Lou, M.-H. Zong, H. Wu and W.-J. Fang, *Prog. Biochem. Biophys.*, 2003, **30**, 431–434.
- J. D. Stewart, *Curr. Opin. Biotechnol.*, 2000, **11**, 363–368.
- T. R. Gervais, G. Carta and J. L. Gainer, *Biotechnol. Prog.*, 2003, **19**, 389–395.
- R. Leon, P. Fernandes, H. M. Pinheiro and J. M. S. Cabral, *Enzyme Microb. Technol.*, 1998, **23**, 483–500.
- K. R. Seddon, *J. Chem. Technol. Biotechnol.*, 1997, **64**, 351–356.
- F. van Rantwijk, R. M. Lau and R. A. Sheldon, *Trends Biotechnol.*, 2003, **21**, 131–138.
- Z. Yang and W. Pan, *Enzyme Microb. Technol.*, 2005, **37**, 19–28.
- T. Welton, *Chem. Rev.*, 1999, **99**, 2071–2083.
- U. Kragl, M. Eckstein and N. Kaftzik, *Curr. Opin. Biotechnol.*, 2002, **13**, 565–571.
- J. L. Kaar, A. M. Jesionowski, J. A. Berberich, R. Moulton and A. J. Russell, *J. Am. Chem. Soc.*, 2003, **125**, 4125–4131.
- M. Persson and U. T. Bornscheuer, *J. Mol. Catal. B: Enzym.*, 2003, **22**, 21–27.
- R. A. Sheldon, R. M. Lau, M. J. Sorgedraeger and F. van Rantwijk, *Green Chem.*, 2002, **4**, 147–151.
- S. Wallert, K. Drauz, I. Grayson, H. Gröger, P. D. de Maria and C. Bolm, *Green Chem.*, 2005, **7**, 602–607.
- K.-W. Kim, B. Song, M.-Y. Chio and M.-J. Kim, *Org. Lett.*, 2001, **3**, 1507–1509.
- W.-Y. Lou, M.-H. Zong and H. Wu, *Biocatal. Biotransform.*, 2004, **22**, 171–176.
- W.-Y. Lou, M.-H. Zong and H. Wu, *Biotechnol. Appl. Biochem.*, 2005, **41**, 151–156.
- W.-Y. Lou, M.-H. Zong, H. Wu, R. Xu and W.-J. Fang, *Green Chem.*, 2005, **7**, 500–506.
- S. G. Cull, J. D. Holbrey, V. Vargas-Mora, K. R. Seddon and G. J. Lye, *Biotechnol. Bioeng.*, 2000, **69**, 227–233.
- J. Howarth, P. James and J. F. Dai, *Tetrahedron Lett.*, 2001, **42**, 7517–7519.
- H. Pfruender, M. Amidjojo, U. Kragl and D. Weuster-Botz, *Angew. Chem., Int. Ed.*, 2004, **43**, 4529–4531.
- M. D. Baumann, A. J. Daugulis and P. G. Jessop, *Appl. Microbiol. Biotechnol.*, 2005, **67**, 131–137.
- P. Huber, S. Bratovanov, S. Bienz, C. Syldatk and M. Pietzsch, *Tetrahedron: Asymmetry*, 1996, **7**, 69–78.
- R. M. Lau, F. van Rantwijk, K. R. Seddon and R. A. Sheldon, *Org. Lett.*, 2000, **2**, 4189–4191.
- P. Lozano, T. de Diego, S. Gmouh, M. Vaultier and J. L. Iborra, *Biotechnol. Prog.*, 2004, **20**, 661–669.
- M.-J. Kim, H. M. Kim, D. Kim, Y. Ahe and J. Park, *Green Chem.*, 2004, **6**, 471–474.
- R. Irimescu and K. Kato, *Tetrahedron Lett.*, 2004, **45**, 523–525.
- M. Eckstein, M. V. Filho, A. Liese and U. Kragl, *Chem. Commun.*, 2004, 1084–1085.
- J. Pernak, K. Sobaszekiewicz and I. Mirska, *Green Chem.*, 2003, **5**, 52–56.
- H. A. Vronis, A. M. Kropinski and A. J. Daugulis, *Biotechnol. Bioeng.*, 2002, **79**, 587–594.
- T. Itoh, S. Han, Y. Matsushita and S. Hayase, *Green Chem.*, 2004, **6**, 437–439.

Biodegradable ionic liquids

Part III.† The first readily biodegradable ionic liquids

Nicholas Gathergood,^{‡a} Peter J. Scammells*^a and M. Teresa Garcia*^b

Received 15th November 2005, Accepted 13th December 2005

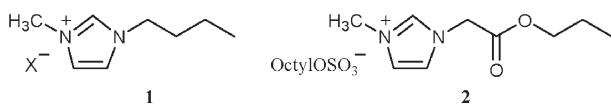
First published as an Advance Article on the web 13th January 2006

DOI: 10.1039/b516206h

Further research toward the discovery of biodegradable ionic liquids (ILs) is described herein. The biodegradability of the target ILs was evaluated using the 'Closed Bottle' and 'CO₂ Headspace' tests (OECD 301D and ISO 14593). This research has identified the first ILs which can be classified as 'readily biodegradable' under aerobic conditions.

Introduction

Although ionic liquids have created a great deal of interest as green reaction media, the first reports regarding their biodegradability have only appeared relatively recently.^{1–3} In these studies the biodegradability of the common 1-butyl-3-methylimidazolium ionic liquids (general structure **1**) was assessed using the Closed Bottle test (OECD 301D). The ionic liquid was added to an aerobic aqueous medium inoculated with wastewater microorganisms and the depletion of dissolved molecular oxygen was measured for 28 days and expressed as a percentage of the theoretical maximum. In general the 1-butyl-3-methylimidazolium ionic liquids performed very poorly in this test with all but one of the series undergoing little or no degradation after 28 days. 1-Butyl-3-methylimidazolium octylsulfate was the only ionic liquid that underwent a significant level of degradation (25%), but was well short of achieving the pass level for this test (60%).



In an analogous approach to that used to prepare biodegradable detergents, dialkylimidazolium ionic liquids that contained metabolisable side chain moieties were prepared and evaluated. The incorporation of an ester in the side chain of the imidazolium cation was found to confer higher biodegradability with all of the anions that were tested. The combination of the 3-methyl-1-(propyloxycarbonyl)imidazolium cation and the octyl sulfate anion afforded the most biodegradable compound in the series (compound **2**: 49% degradation in the Closed Bottle test). Although this represents

a considerable improvement, this compound was still short of the mark required for classification as 'readily biodegradable'.

The aims of this current study were (i) to confirm the findings of our earlier work using an independent test protocol, and (ii) to incorporate additional structural modifications to improve biodegradability. More specifically, a 2-methyl group was incorporated to provide an additional site for metabolism. It is known that 2-methylimidazole is significantly more biodegradable than imidazole.⁴ It has been postulated that the catabolic pathways for compounds of this type may be similar to that of urocanate, the first metabolite in the biodegradation pathway of histidine.⁴ In this enzymatic mechanism, the imidazole ring is activated to attack by electron donating substituents such as alkyl groups attached to the ring carbon atoms. Furthermore, 1,3-dialkylimidazolium ionic liquids are known to form carbenes following deprotonation at the 2-position, which limits their suitability as a medium for certain base catalysed reactions.⁵ Thus, the presence of a 2-methyl may have some additional advantages for applications where carbene formation is deleterious.

Results and discussion

The panel of ionic liquids included in the biodegradation study is outlined in Table 1. This panel includes compounds with 1-(alkoxycarbonyl)-3-methylimidazolium cations and the corresponding 1-alkoxycarbonyl-2,3-dimethyl analogs. The biodegradability of 1-(alkoxycarbonyl)-3-methylimidazolium ionic liquids has been reported to increase slightly with increasing alkyl chain length, with a plateau at C₄.² In this current study, C₃ and C₅ analogs were included in the test set. Both bromide and octyl sulfate anions were evaluated.

The 1-(alkoxycarbonyl)-3-methylimidazolium bromide (**3** and **5**) and octyl sulfate (**2** and **8**) ionic liquids were prepared using a standard approach, as described in Parts I and II of this series.^{2,3} All of these compounds are liquids at room temperature. 1-(Alkoxycarbonyl)-2,3-dimethylimidazolium bromides (**4** and **6**) were prepared in high yield by reacting propyl and pentyl bromoacetate with 1,2-dimethylimidazole. Conversion to the octyl sulfate derivatives (**7** and **9**) was performed analogously to the disubstituted examples. All of the dimethyl derivatives are solids at room temperature, with melting points above 100 °C.

^aDepartment of Medicinal Chemistry, Victorian College of Pharmacy, Monash University, Parkville 3052, Australia.

E-mail: peter.scammells@vcp.monash.edu.au; Fax: +61 3 99039582; Tel: +61 3 9903 9542

^bDepartment of Surface Technology, IQAB-CSIC, Jordi Girona 18-26, 08034, Spain. E-mail: mtgbet@iqab.csic.es; Fax: +34 93 204 5904; Tel: +34 93 400 6100

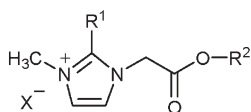
† For Part II see ref. 3.

‡ Current address: National Institute for Cellular Biotechnology, School of Chemical Sciences, Dublin City University, Glasnevin, Dublin 9, Ireland. E-mail: Nick.Gathergood@dcu.ie; Fax: +353 1 700 5503; Tel: +353 1 700 7860.

Table 1 Test panel of 1-(alkoxycarbonyl)-3-methylimidazolium ionic liquids

No.	X	R ₁	R ₂	Closed Bottle (%)	CO ₂ Headspace (%)
3	Br	H	C ₃ H ₇	24	24
4	Br	CH ₃	C ₃ H ₇	23	n.d.
5	Br	H	C ₅ H ₁₁	32	41
6	Br	CH ₃	C ₅ H ₁₁	33	n.d.
2	C ₈ H ₁₇ OSO ₃	H	C ₃ H ₇	49	64
7	C ₈ H ₁₇ OSO ₃	CH ₃	C ₃ H ₇	55	62
8	C ₈ H ₁₇ OSO ₃	H	C ₅ H ₁₁	54	67
9	C ₈ H ₁₇ OSO ₃	CH ₃	C ₅ H ₁₁	56	61

^a n.d. = not determined.



Aerobic ultimate biodegradability of the ionic liquids was evaluated applying two standard methods: the Closed Bottle test (OECD 301D) and the CO₂ Headspace test (ISO 14593). Both tests are included in the European Regulation (EC) No 648/2004 on biodegradability of detergent surfactants, the CO₂ Headspace test (ISO 14593) being the reference method for laboratory testing of ultimate biodegradability.

In the Closed Bottle and CO₂ Headspace tests, the compound to be evaluated was added to an aerobic aqueous medium inoculated with wastewater microorganisms and the depletion of dissolved O₂ or the CO₂ evolution, respectively, was periodically measured and reported as a percentage of the theoretical maximum. Sodium *n*-dodecyl sulfate (SDS) was used as reference substance. An ionic liquid will be considered as “readily biodegradable” and, therefore it will be assumed that such a chemical will be rapidly and completely biodegraded in aquatic environments under aerobic conditions, if the biodegradation level measured according to one of the described tests is higher than 60% within 28 days.

Data obtained from the Closed Bottle test showed significant differences of the biodegradability of the tested ionic liquids depending on their molecular structure (Fig. 1). Regarding the extent of biodegradation reached by the ionic liquids (Table 1), three groups can be considered: (i) conventional ionic liquids based on 1-butyl-3-methylimidazolium core (bmimBr and bmimBF₄) which showed a negligible extent of biodegradation (0–1%), (ii) ionic liquids with an ester group in the side chain which reached biodegradation extents of 23–33% and (iii) ionic liquids with an ester bond in the side chain and the octyl sulfate as counter ion which presented the higher biodegradation values (49–56%). The incorporation of an ester group in the side chain clearly improves the biodegradation properties of the ionic liquids. ILs with different alkyl esters in the side chain presented similar biodegradation profiles (Fig. 1) but the biodegradation values slightly increased with increasing the alkyl chain length as previously reported.² The addition of a 2-methyl group (comparison of compounds 3 and 4, 5 and 6, 2 and 7, 8 and 9) had no significant effect on the biodegradation results. Finally, the incorporation of a biodegradable organic counter

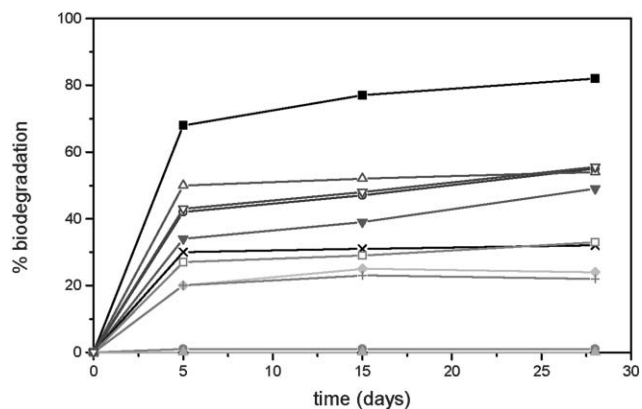


Fig. 1 Biodegradation curves (Closed Bottle test): (●) bmimBr (1a), (▲) bmimBF₄ (1b), (◆) 3-methyl-1-propoxycarbonylimidazolium-Br (3), (+) 2,3-dimethyl-1-propoxycarbonylimidazolium-Br (4), (×) 3-methyl-1-pentoxycarbonylimidazolium-Br (5), (□) 2,3-dimethyl-1-pentoxycarbonylimidazolium-Br (6), (▼) 3-methyl-1-propoxycarbonylimidazolium-OctSO₄ (2), (○) 2,3-dimethyl-1-propoxycarbonylimidazolium-OctSO₄ (7), (△) 3-methyl-1-pentoxycarbonylimidazolium-OctSO₄ (8), (▽) 2,3-dimethyl-1-pentoxycarbonylimidazolium-OctSO₄ (9), reference substance: SDS (■).

ion increased the extent to which the ionic liquids underwent biodegradation.

The biodegradation curves obtained for the ionic liquids applying the CO₂ Headspace test are shown in Fig. 2. These biodegradation data (Table 1) are consistent with those obtained using the Closed Bottle test and confirm the above mentioned remarks on the effect of the different structural parameters on the biodegradability of ILs, *i.e.* a null biodegradation of the bmimBr and bmimBF₄ ionic liquids (0–3%), a significant increase on biodegradability of the ionic liquids containing an ester bond in the side chain (24–41%) and the best results for those containing both an ester group in the

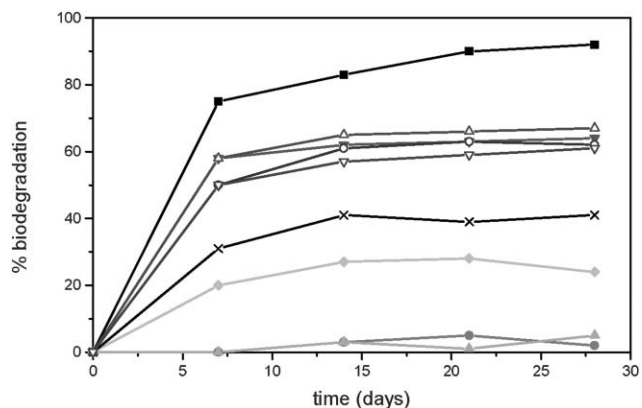


Fig. 2 Biodegradation curves (CO₂ Headspace test): (●) bmimBr (1a), (▲) bmimBF₄ (1b), (◆) 3-methyl-1-propoxycarbonylimidazolium-Br (3), (×) 3-methyl-1-pentoxycarbonylimidazolium-Br (5), (▼) 3-methyl-1-propoxycarbonylimidazolium-OctSO₄ (2), (○) 2,3-dimethyl-1-propoxycarbonylimidazolium-OctSO₄ (7), (△) 3-methyl-1-pentoxycarbonylimidazolium-OctSO₄ (8), (▽) 2,3-dimethyl-1-pentoxycarbonylimidazolium-OctSO₄ (9), reference substance: SDS (■).

side chain and octyl sulfate as counter ion (60–67%), as well as a minor effect of the alkyl side chain length and the number of methyl groups. However, biodegradation values obtained are somewhat higher than those obtained by applying the Closed Bottle test. Such differences, probably related to the differences in cell density of the two biodegradation tests, are particularly important for the group of ionic liquids with both an ester bond and an organic counter ion because it allows them to be classified as “readily biodegradable”, *i.e.* to assume that these compounds will be rapidly mineralized/biodegraded in aquatic environments under aerobic conditions.

The most commonly used ionic liquids are based on the 1-butyl-3-methylimidazolium core. Two ionic liquids belonging to this group, bmimBr and bmimBF₄, were tested for aerobic ultimate biodegradation by the Closed Bottle and CO₂ Headspace tests and were found to show negligible biodegradation rates (Table 1).

The biodegradation data obtained should be interpreted with caution taking into account the features of both biodegradation tests and the chemicals studied. Many quaternary ammonium salts are potential biocides and could inhibit growth of microorganisms capable of degrading them.^{6,7} Screening methods have been used in many studies on the biodegradability of quaternary ammonium compounds, namely surfactants such as alkyltrimethyl ammonium salts and alkylbenzyltrimethyl ammonium salts.^{8,9} The non-biodegradation of quaternary ammonium salts with a long alkyl chain may be caused by the relatively high concentration necessary in these tests.^{10,11} Since imidazolium compounds are similarly charged ammonium ion-species the potential toxicity of the ILs might also have an negative effect on their biodegradation.

Recent studies on the biological effects of dialkylimidazolium ionic liquids have shown that the toxicity of these ILs is higher than that of common volatile organic solvents^{3,12,13} and lower than that of the conventional quaternary ammonium surfactants.³ The length of the alkyl chains was found to influence the toxicity of the dialkylimidazolium ILs, with longer chain lengths proving to be more toxic.^{3,12} The toxicity of the dialkylimidazolium ionic liquids was mainly determined by the hydrophobic character of the imidazolium cation whereas the nature of the inorganic anion had a negligible effect.

In order to determine if the lack of biodegradability of bmimX compounds could be due to their toxicity on the aerobic microorganisms, biodegradation tests with binary mixtures of a bmimX compound (X = Br or BF₄) and a reference substance (SDS) were carried out. Similar biodegradation rates were obtained for the reference substance alone and mixed with the ionic liquid. Therefore, bmimBr and bmimBF₄ at the tested concentrations (2 and 40 mg L⁻¹ in the Closed Bottle and the CO₂ Headspace tests, respectively) did not inhibit the degrading activity of the microorganisms. In other words, the null biodegradability of dialkylimidazolium salts in the screening test appears not to be related to the toxicity of these compounds on the bacterial populations.

Conclusions

These findings support our earlier conclusion that (i) the octyl sulfate anion is considerably more biodegradable than the

other commonly used anions, and (ii) the introduction of an ester group in the side chain of the 1,3-dialkylimidazolium cation leads to biodegradation values very close to the pass level of the Closed Bottle test. This is particularly significant taking into account the stringent conditions of the biodegradation test applied. Regarding other structural parameters (as the length of the cation side chain or the number of methyl groups) no significant effects have been observed. In the CO₂ Headspace test, all of these ionic liquids with an octyl sulfate anion (compounds **2**, **7**, **8**, **9**) were readily biodegradable compounds under aerobic conditions. The incorporation of a methyl group in the 2-position of imidazolium cation had no significant effect on biodegradability. The commonly used 1-butyl-3-methylimidazolium core showed negligible levels of degradation in the CO₂ Headspace test. This result is consistent with the data previously obtained using the Closed Bottle test. The possible inhibitory effect of bmimX compounds on the aerobic microorganisms has been checked with mixtures of bmimX and a readily biodegradable compound. No toxic effects were detected at the test concentration. The elevated melting point may limit the synthetic utility of the trisubstituted ILs, however their expected improved stability may lead to their application in specialized cases. The ILs **2** and **8** are both readily biodegradable in the CO₂ Headspace test and are liquids at room temperature.

Experimental

Synthesis

The synthesis of compounds **2**, **3** and **5** were described in Part I and II of this series. NMR spectra of ILs were recorded in CD₃CN (Aldrich 15,180–7, 99.8 atom%D) on a Bruker Avance DPX 300 spectrometer. ¹H and ¹³C NMR spectra were recorded at 300 MHz and 75.4 MHz respectively. Melting points are uncorrected. A study of glass transition temperatures was not attempted with these materials. Determination of the physical properties of the ionic liquids prepared is still in progress (*e.g.* solubility, thermal stability, viscosity, density and stability to hydrolysis) and will be reported in due course.

2,3-Dimethyl-1-(propoxycarbonylmethyl)imidazolium bromide (**4**)

To a stirred solution of 1,2-dimethylimidazole (4.80 g, 50 mmol) in THF (50 mL) at –5 °C under a nitrogen atmosphere was added dropwise propyl bromoacetate (10.9 g, 7.8 mL, 60 mmol). The reaction mixture was stirred vigorously at –5 °C for 1 h, then at rt for 4 h. A white precipitate formed which was collected by suction filtration and washed with dry diethyl ether (3 × 15 mL). The product was dried at 60 °C at 0.01 mmHg for 72 h to give a white solid in 95% yield (13.13 g, 47.4 mmol). Mp = 128–130 °C. ¹H NMR (300 MHz, CD₃CN) δ 7.69 (d, *J* = 2.0 Hz, 1H), 7.54 (d, *J* = 2.0 Hz, 1H), 5.27 (s, 2H), 4.13 (t, *J* = 6.6 Hz, 2H), 3.82 (s, 3H), 2.57 (s, 3H), 1.64 (qt, *J* = 7.5, 6.6 Hz, 3H), 0.92 (t, *J* = 7.5 Hz, 3H). ¹³C NMR (75 MHz, CD₃CN) δ 166.37, 145.96, 122.28, 122.21, 67.63, 49.16, 35.23, 21.50, 9.69, 9.50. MS (ESI): *m/z*, 169.1 [M–Br⁻]⁺; MS (ESI): *m/z*, 79 and 81 [Br⁻].

2,3-Dimethyl-1-(pentoxycarbonylmethyl)imidazolium bromide (6)

To a stirred solution of 1,2-dimethylimidazole (1.69 g, 17.6 mmol) in THF (25 mL) at $-0\text{ }^{\circ}\text{C}$ under a nitrogen atmosphere was added dropwise pentyl bromoacetate (4.30 g, 20.6 mmol). The reaction mixture was stirred vigorously at rt for 4 h. The THF was decanted and the IL washed with dry diethyl ether ($3 \times 10\text{ mL}$), then residual solvent removed *in vacuo*. The product was dried at $60\text{ }^{\circ}\text{C}$ at 0.01 mmHg for 72 h to give a clear viscous hygroscopic oil, which crystallized on standing at room temperature, in 96% yield (5.16 g, 16.9 mmol). Mp = $45\text{--}47\text{ }^{\circ}\text{C}$. ^1H NMR (300 MHz, CD_3CN) δ 7.67 (d, $J = 2.2\text{ Hz}$, 1H), 7.53 (d, $J = 2.2\text{ Hz}$, 1H), 5.24 (s, 2H), 4.17 (t, $J = 6.6\text{ Hz}$, 2H), 3.82 (s, 3H), 2.56 (s, 3H), 1.70–1.58 (m, 2H), 1.35–1.25 (m, 4H), 0.88 (t, $J = 7.2\text{ Hz}$, 3H). ^{13}C NMR (75 MHz, CD_3CN) δ 167.75, 147.37, 123.71, 123.63, 67.64, 50.58, 36.66, 29.18, 28.92, 23.27, 14.60, 11.10. MS (ESI): m/z , 225.1 $[\text{M}-\text{Br}]^+$; MS (ESI): m/z , 79 and 81 $[\text{Br}]^-$.

2,3-Dimethyl-1-(propoxycarbonylmethyl)imidazolium octyl-sulfate (7)

The title compound was prepared according to a literature procedure¹⁴ using 2,3-dimethyl-1-(propoxycarbonylmethyl)imidazolium bromide (4) (3.00 g, 10.8 mmol) and $\text{Na}(n\text{-C}_8\text{H}_{17}\text{O}-\text{SO}_3)$ (2.14 g, 9.23 mmol) in distilled water (5 mL) in 93% yield (3.49 g, 8.6 mmol) as a white solid. Mp = $118\text{--}120\text{ }^{\circ}\text{C}$. ^1H NMR (300 MHz, CD_3CN) δ 7.41 (d, $J = 2.2\text{ Hz}$, 1H), 7.37 (d, $J = 2.2\text{ Hz}$, 1H), 5.01 (s, 2H), 4.15 (t, $J = 6.6\text{ Hz}$, 2H), 3.79 (t, $J = 6.6\text{ Hz}$, 2H), 3.77 (s, 3H), 2.51 (s, 3H), 1.68 (qt, $J = 7.5, 6.6\text{ Hz}$, 2H), 1.60–1.50 (m, 2H), 1.40–1.20 (m, 10H), 0.94 (t, $J = 7.5\text{ Hz}$, 3H), 0.88 (t, $J = 7.5\text{ Hz}$, 3H). ^{13}C NMR (75 MHz, CD_3CN) δ 167.87, 147.55, 123.94, 123.80, 69.32, 67.83, 50.42, 36.64, 33.11, 30.96, 30.63, 30.53, 27.34, 23.90, 23.09, 14.92, 11.07, 10.78. MS (ESI): m/z , 196.9 $[\text{M}-\text{OctOSO}_3]^-$; MS (ESI): m/z , 209.1 $[\text{OctOSO}_3]^-$.

3-Methyl-1-(pentoxycarbonylmethyl)imidazolium octyl-sulfate (8)

The title compound was prepared according to a literature procedure¹⁴ using 3-methyl-1-(pentoxycarbonylmethyl)imidazolium bromide (6) (2.03 g, 6.9 mmol) and $\text{Na}(n\text{-C}_8\text{H}_{17}\text{O}-\text{SO}_3)$ (1.36 g, 5.85 mmol) in distilled water (4 mL) in 75% yield (1.85 g, 4.4 mmol) as a very viscous oil. ^1H NMR (300 MHz, CD_3CN) δ 8.91 (s, 1H), 7.50 (s, 1H), 7.44 (s, 1H), 5.10 (s, 2H), 4.18 (t, $J = 6.6\text{ Hz}$, 2H), 3.89 (s, 3H), 3.81 (t, $J = 6.6\text{ Hz}$, 2H), 1.70–1.50 (m, 4H), 1.40–1.25 (m, 14H), 0.92 (t, $J = 7.5\text{ Hz}$, 3H), 0.88 (t, $J = 7.5\text{ Hz}$, 3H). ^{13}C NMR (75 MHz, CD_3CN) δ 167.50, 138.95, 124.69, 124.34, 67.35, 67.24, 50.70, 37.04, 32.54, 30.37, 30.04, 29.95, 28.80, 28.55, 26.95, 23.32, 22.92, 14.35, 14.20. MS (ESI): m/z , 211.0 $[\text{M}-\text{OctOSO}_3]^-$; MS (ESI): m/z , 209.1 $[\text{OctOSO}_3]^-$.

2,3-Dimethyl-1-(pentoxycarbonylmethyl)imidazolium octyl-sulfate (9)

The title compound was prepared according to a literature procedure¹⁴ using 2,3-dimethyl-1-(pentoxycarbonylmethyl)imidazolium bromide (6) (2.34 g, 7.66 mmol) and

$\text{Na}(n\text{-C}_8\text{H}_{17}\text{O}-\text{SO}_3)$ (1.52 g, 6.55 mmol) in distilled water (5 mL) in 44% yield (1.25 g, 2.88 mmol) as a white solid. Mp = $134\text{--}135\text{ }^{\circ}\text{C}$. ^1H NMR (300 MHz, CD_3CN) δ 7.38 (d, $J = 2.4\text{ Hz}$, 1H), 7.35 (d, $J = 2.4\text{ Hz}$, 1H), 4.98 (s, 2H), 4.19 (t, $J = 6.6\text{ Hz}$, 2H), 3.79 (t, $J = 6.9\text{ Hz}$, 2H), 3.77 (s, 3H), 2.51 (s, 3H), 1.72–1.60 (m, 2H), 1.60–1.50 (m, 2H), 1.40–1.25 (m, 14H), 0.91 (t, $J = 7.0\text{ Hz}$, 3H), 0.89 (t, $J = 7.0\text{ Hz}$, 3H). ^{13}C NMR (75 MHz, CD_3CN) δ 167.33, 147.10, 123.50, 123.34, 67.48, 67.25, 50.00, 36.21, 32.68, 30.57, 30.20, 30.10, 28.93, 28.70, 26.93, 23.47, 23.04, 14.47, 14.32, 10.35. MS (ESI): m/z , 225.2 $[\text{M}-\text{OctOSO}_3]^-$; MS (ESI): m/z , 209.1 $[\text{OctOSO}_3]^-$.

Closed Bottle test¹⁵

The biodegradability of the test compounds was evaluated using the ‘‘Closed Bottle’’ test (OECD 301 D). In this method, the chemical being evaluated is added to an aerobic aqueous medium inoculated with wastewater microorganisms and the depletion of dissolved molecular oxygen is measured for a defined period of time and reported as a percentage of the theoretical maximum. Compounds which reach a biodegradation level higher than 60% are referred to as ‘‘readily biodegradable’’. Sodium *n*-dodecyl sulfate (SDS) was used as reference substance. Solutions containing 2 mg L^{-1} of the test ionic liquids and the reference chemical as sole sources of organic carbon were prepared, separately, in previously aerated mineral medium. The solutions were then inoculated with secondary effluent collected from an activated sludge treatment plant and each well-mixed solution was carefully dispensed into a series of biochemical oxygen demand (BOD) bottles so that all the bottles were completely full. A control with inoculum, but without test chemicals was run parallel for the determination of oxygen blanks. Duplicate bottles of each series were analysed immediately for dissolved oxygen and the remaining bottles were incubated at $20\text{ }^{\circ}\text{C} \pm 1\text{ }^{\circ}\text{C}$ in the dark. Bottles of all series were withdrawn in duplicate for dissolved oxygen analysis over the 28 day incubation period. The biodegradation after *n* days was expressed as the ratio of the BOD to the chemical oxygen demand (COD) both of them expressed as mg O_2 per mg compound. The chemical oxygen demand was determined by the dichromate reflux method (APHA, 1985).¹⁶ For the calculation of the biochemical oxygen demand the determined oxygen depletions were divided by the concentration of ionic liquid.

CO₂ Headspace test¹⁷

To evaluate the biodegradability of the test ionic liquids, the ‘‘CO₂ Headspace’’ test (ISO 14593) was also applied. This method allows the evaluation of the ultimate aerobic biodegradability of an organic compound in aqueous medium at a given concentration of microorganisms by analysis of inorganic carbon. The test ionic liquid, as the sole source of carbon and energy, was added at a concentration of 40 mg L^{-1} to a mineral salt medium. These solutions were inoculated with activated sludge collected from an activated sludge treatment plant, washed and aerated prior to use and incubated in sealed vessels with a headspace of air. Biodegradation (mineralization to carbon dioxide) was determined by measuring the net increase in total organic carbon (TOC) levels over time

compared with unamended blanks. Sodium *n*-dodecyl sulfate (SDS) was used as reference substance. The tests ran for 28 days. The extent of biodegradation was expressed as a percentage of the theoretical amount of inorganic carbon (ThIC) based on the amount of test compound added initially.

References

- 1 N. Gathergood and P. J. Scammells, *Aust. J. Chem.*, 2002, **55**, 557.
- 2 N. Gathergood, M. T. Garcia and P. J. Scammells, *Green Chem.*, 2004, **6**, 166.
- 3 M. T. Garcia, N. Gathergood and P. J. Scammells, *Green Chem.*, 2005, **7**, 9.
- 4 E. Rorije, F. Germa, B. Philipps, B. Schink and D. B. Beimbom, *SAR QSAR Environ. Res.*, 2002, **1**, 199.
- 5 (a) V. K. Aggarwal, I. Emme and A. Mereu, *Chem. Commun.*, 2002, 1612; (b) P. Formentin, H. Garcia and A. Leyva, *J. Mol. Catal. A: Chem.*, 2004, **214**, 137; (c) P. J. Scammells, J. L. Scott and R. D. Singer, *Aust. J. Chem.*, 2005, **58**, 155 and references therein.
- 6 R. M. Ventullo, *Appl. Environ. Microbiol.*, 1986, **51**, 356.
- 7 D. M. Tubbing and W. Admiraal, *Appl. Environ. Microbiol.*, 1991, **57**, 3616.
- 8 C. G. Van Ginkel and M. Kolvenbach, *Chemosphere*, 1991, **23**, 281.
- 9 M. T. García, I. Ribosa, T. Guindulain, J. Sánchez-Leal and J. Vives-Rego, *Environ. Pollut.*, 2001, **111**, 169.
- 10 R. J. Larson, *Residue Rev.*, 1983, **85**, 159.
- 11 C. G. Van Ginkel, in *Biodegradability of Surfactants*, ed. D. R. Karsa and M. R. Porter, Blackie Academic & Professional, Glasgow, 1995.
- 12 J. Ranke, K. Mölter, F. Stock, U. Bottin-Weber, J. Poczobutt, J. Hoffmann, B. Ondruschka, J. Filser and B. Jastorff, *Ecotoxicol. Environ. Saf.*, 2004, **58**, 396.
- 13 R. J. Bernot, M. A. Brueseke, M. A. Evans-White and G. A. Lamberti, *Environ. Toxicol. Chem.*, 2005, **24**, 87.
- 14 P. Wasserscheid, R. van Hal and A. Bosmann, *Green Chem.*, 2002, **4**, 400.
- 15 OECD Chemical Group, Ready Biodegradability: Closed Bottle Test. Method 301 D, *OECD Revised Guidelines for Tests for Ready Biodegradability*, Paris, France, 1993.
- 16 APHA (American Public Health Association), AWWA (American Water Works Association), and WPCF (Water Pollution Control Federation), Method 508 B, *Standard Methods for the Examination of Water and Wastewater*, Washington, 16th edn, 1985, pp. 532–537.
- 17 ISO 14593: Water quality. Evaluation of ultimate aerobic biodegradability of organic compounds in aqueous medium. Method by analysis of inorganic carbon in sealed vessels (CO₂ headspace test), 1999.

A critical assessment of electrochemistry in a distillable room temperature ionic liquid, DIMCARB

Anand I. Bhatt,^a Alan M. Bond,^{*a} Douglas R. MacFarlane,^a Jie Zhang,^a Janet L. Scott,^b Christopher R. Strauss,^b Philip I. Iotov^{†a} and Sasha V. Kalcheva^{†a}

Received 30th August 2005, Accepted 11th November 2005

First published as an Advance Article on the web 13th December 2005

DOI: 10.1039/b512263e

Ionic liquids are frequently advocated as green media for electrochemical studies. However, they are non-volatile and hence difficult to purify or recover. In this paper the electrochemical behaviour of a 'distillable' room temperature ionic liquid, DIMCARB, has been investigated. This ionic liquid is unusual because it is readily prepared, in large quantities and at low cost, by mixing of gaseous carbon dioxide with dimethylamine and also easily recovered by decomposition back into its gaseous components followed by reassociation. Almost ideal reversible voltammetry is observed for the $Cc^{+/0}$ process (Cc = cobalticinium), which therefore is recommended for reference potential calibration. Another IUPAC recommended reference potential process, $Fc^{+/0}$ (Fc = ferrocene), is only reversible at fast scan rates and occurs near the positive potential limit available. However, decamethylferrocene ($DmFc$) is reversibly oxidised and behaves ideally as for the reduction of Cc^+ . The small diffusion coefficients of $1.2 \times 10^{-7} \text{ cm}^2 \text{ s}^{-1}$ (Cc^+) and $5.0 \times 10^{-8} \text{ cm}^2 \text{ s}^{-1}$ ($DmFc$) at 20 °C are attributed to the relatively high viscosity. The potential window of *ca.* -1.50 V to $+0.50 \text{ V}$ vs. SHE indicates that DIMCARB is more suitable for electrochemical studies of reductive rather than oxidative processes. Voltammetric studies in DIMCARB reveal a series of reversible reductive processes for the Keggin $[\alpha\text{-SiW}_{12}\text{O}_{40}]^{4-}$ polyoxometallate. Comparison of reversible potential data reported in other media indicate that the polarity of DIMCARB is intermediate between that of MeCN and the conventional ionic liquid [BMIM][PF₆]. The deposition of metallic Pb also has been studied and reveals that Pb(II) is reduced in a single irreversible 2-electron step to the metallic state *via* a nucleation/growth mechanism. Overall, these studies show that DIMCARB is highly suitable for electrochemical studies, but that it is a potentially reactive medium.

Introduction

Room temperature ionic liquids (RTILs) have advantageous chemical, physical and 'green' properties related to negligible vapour pressure, low toxicity, high chemical and thermal stability, high conductivities and significant electrochemical stability, as well as the ability to dissolve a wide range of organic and inorganic compounds.¹ From an electrochemical perspective, RTILs have been advocated for use in metal deposition, battery electrolytes and electrosynthesis (for reviews on RTIL electrochemistry see ref. 2 and 3). However, there are problems associated with their use. For example, separation of RTIL soluble synthesised products from the bulk RTIL (and/or reactants) mixture post electro-synthesis is difficult. Recovery of the non-volatile RTILs for further use or disposal also is problematical, as conventional solvent distillation techniques are not available for this

purpose. Although the thermal decomposition of RTILs (often at high temperatures) could, in theory, be used to separate solvent and products, this also could prove problematical if the product decomposes at temperatures below that of the RTIL decomposition.

A possible alternative approach to avoid this reaction product–ionic liquid separation problem is to use *N,N*-dialkylammonium *N',N'*-dialkylcarbamate based melts (dialcarbs). Dialcarbs are liquids composed of significant proportions of ionic moieties but have the advantageous property of being distillable. These so called 'distillable' ionic liquids have similar properties to RTILs, but are easily recovered and separated from products by low temperature distillation.⁴ Dialcarbs are mixtures of adducts of CO₂ and dialkylamines of the general formula R'RNH (where R and R' = alkyl group).⁴ Additionally, dialcarbs also have advantages associated with low cost of synthesis and high, tuneable conductivities achieved by varying the R'RNH : CO₂ ratio. In the very simple case where R = R' = methyl, a series of liquids containing the dimethylcarbamate ion is produced.

In the case of DIMCARB, which is of interest in this study, the ability to 'distill' this largely ionic liquid medium at low temperature, by decomposition to its constituent gases followed by reassociation, provides a simple means to recover

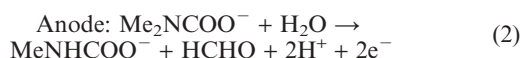
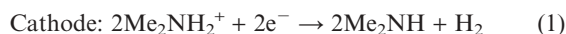
^aSchool of Chemistry, Monash University, Clayton, Victoria 3800, Australia. E-mail: alan.bond@sci.monash.edu.au; Fax: +61 3 9905 4597; Tel: +61 3 9905 1338

^bARC Special Research Centre for Green Chemistry, Monash University, Clayton, Victoria 3800, Australia

[†] On leave from the University of Chemical Technology and Metallurgy, 8 Kl. Ohridski Blvd., 1756 Sofia, Bulgaria.

products of bulk electrolysis and recycle the electrolyte/solvent. In addition, the use of a single medium (DIMCARB) as both electrolyte and solvent avoids the use of mixtures, again providing for ease of recovery and recycling. While dimethylamine is not without hazards, the incorporation of this gas into DIMCARB provides a huge reduction in vapour pressure of this component.

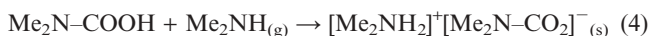
The stoichiometric compound *N,N*-dimethylammonium *N,N'*-dimethylcarbamate ($[\text{Me}_2\text{NH}_2]^+[\text{Me}_2\text{N}-\text{CO}_2]^-$) has a melting point around 35 °C and is not convenient for room temperature work. As the $\text{Me}_2\text{NH} : \text{CO}_2$ ratio drops below 2 : 1 the melting point falls below room temperature. Typically, in previous work, a ratio of 1.8 : 1 has been used.⁴ This highly conductive, stable liquid, otherwise referred to as DIMCARB, has been used in organic synthesis as a solvent and to provide a convenient and safe source of dimethylamine.⁴ With respect to electrochemical applications, Schäfer *et al.* have used a mixture of DIMCARB and acetonitrile to anodically dissolve Zn metal and hence form a $[\text{Zn}_2(\text{O}_2\text{CNMe}_2)_5]^-$ complex,⁵ while Hess *et al.* employed pure $[\text{Me}_2\text{NH}_2]^+[\text{Me}_2\text{N}-\text{CO}_2]^-$ in the molten state for galvanic electrolysis, utilising the distillable nature of $[\text{Me}_2\text{NH}_2]^+[\text{Me}_2\text{N}-\text{CO}_2]^-$ to separate the ionic liquid/electrolyte from products.⁶ At a more fundamental level Maschmeier and Baltruschat have investigated the limiting electrochemical processes and found that the potential range available was governed by the following reactions:⁷



The aim of this study was to determine the feasibility of using voltammetric techniques in this 'distillable' ionic liquid medium as an alternative to the use of RTILs. Although these studies focussed upon DIMCARB, the scope may be extended to include other dialcarbs. Herein, we describe the voltammetry of the IUPAC recommended reference potential standards ferrocene and the cobalticinium cation. Their data enable comparison of potentials reported in DIMCARB with data obtained in other solvents. In addition, we describe voltammetric data obtained with decamethylferrocene, a polyoxometalate that exhibits a series of reduction processes, and the deposition of lead to provide a survey of the types of electrochemical experiment that can be conducted within this medium. These processes allow a broad based assessment to be made of this distillable ionic liquid for use in voltammetric studies.

Properties of DIMCARB relevant to electrochemical use

DIMCARB is formed by mixing of CO_2 and Me_2NH at 0 °C, according to the following reactions:



Notably reaction (4) is limited by the insufficiency of $\text{Me}_2\text{NH}(\text{g})$ in the DIMCARB liquid and hence DIMCARB is

best thought of, at a first level of approximation, as a mixture of $[\text{Me}_2\text{NH}_2]^+[\text{Me}_2\text{N}-\text{CO}_2]^-$ and $\text{Me}_2\text{N}-\text{COOH}$. At a higher level of detail, the liquid contains equilibrium amounts of all five of the species in reactions (3) and (4); these are, in turn, in equilibrium with the vapour phase. The liquid, whilst being synthesised from dry gases, need not be rigorously protected from water and in these circumstances can yield further ionic species, reaction (5), as well as the ions derived from carbonic acid:



The conductivity of DIMCARB is usually in the order of $1 \times 10^{-3} \text{ S cm}^{-1}$ and hence comparable with that of conventional organic solvents with a supporting electrolyte.³ The conductivity, viscosity and density may be altered by varying the $\text{CO}_2 : \text{Me}_2\text{NH}$ ratio. This allows a degree of tunability of the physical properties of this medium. The conductivity is attributed to the high proportion of ionic moieties present in the liquid. Clearly there are a series of equilibria⁸ between the neutral and ionic moieties (as well as associated species) in reactions (3), (4) and (5). The structurally related dialkylammonium carbamates ($[\text{NH}_2\text{R}_2]^+[\text{NR}_2\text{CO}_2]^-$, where R = H or alkyl group) are excellent for the dissolution and complexation of inorganic species in aqueous and non-aqueous solutions,⁹ and have been studied for use in transition metal catalysis.¹⁰ Therefore, DIMCARB is expected to be an excellent medium for dissolution of a wide range of inorganic and organic compounds.

Table 1 provides dissociation temperatures of DIMCARB and other selected dialcarbs. Upon heating DIMCARB to about 60 °C, it reverts to its gaseous components. This property facilitates the separation of DIMCARB from any dissolved species, (assuming that dissolved species are thermally stable and non-volatile up to 60 °C). Importantly, cooling the separated gaseous products allows reassociation and provides an easy route to recovery and hence recycling of DIMCARB *via* a process analogous to distillation.

As well as DIMCARB behaving as an advantageous solvent–electrolyte ionic liquid, it is miscible with organic solvents, such as benzene, dichloromethane, diethyl ether, acetonitrile, dimethylformamide, dioxane and methanol and mixed solvent (dialcarb electrolyte) combinations can exhibit high conductivities.⁸ Thus, DIMCARB is also a potential supporting electrolyte in a wide range of organic media. The fact that the bulk melt (or electrolyte when dissolved in organic solvents) is volatile, implies that *in situ* identification of bulk electrolysis products may be facilitated by direct injection of

Table 1 Melting point and dissociation temperature of selected dialcarbs^{4,8}

R ₁	R ₂	Melting point/°C	Dissociation temperature/°C
Me	Me	30–45 ^a	60–61
Me	Et	—	62
Et	Et	17–33	62–63
Me	<i>n</i> -Pr	—	70–71
-(CH ₂) ₄ -	—	55–80	105

^a For the salt containing exactly 2 : 1 ratio of $\text{Me}_2\text{NH} : \text{CO}_2$.

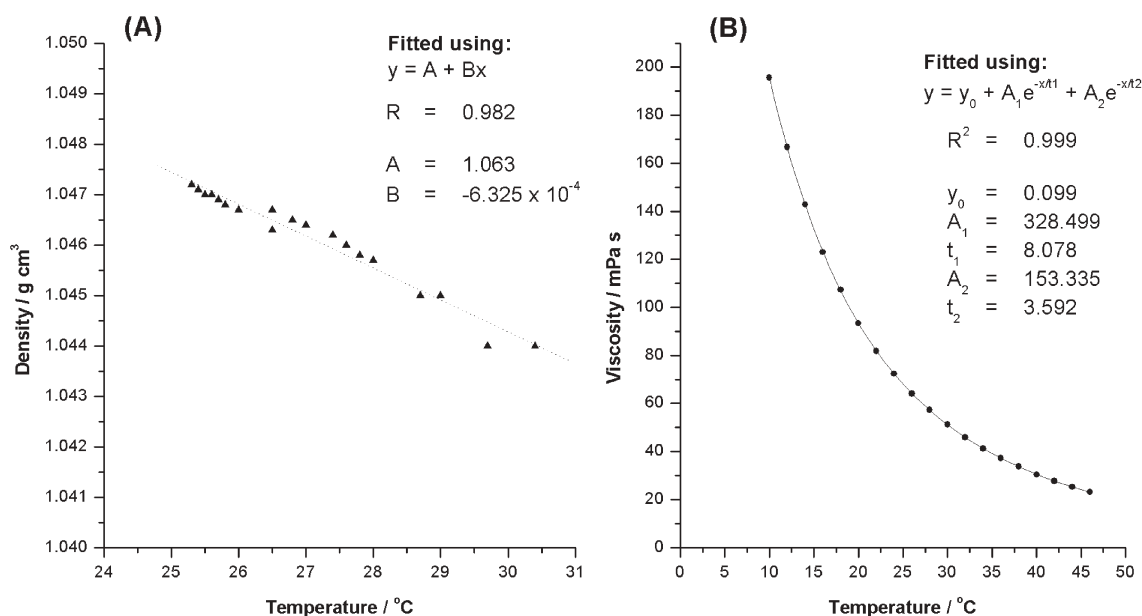


Fig. 1 Effect of temperature on viscosity and density of DIMCARB. A: Density change as a function of temperature; B: viscosity change as a function of temperature.

DIMCARB into an electrospray mass spectrometer or gas chromatograph. In contrast, conventional solvent (electrolyte) combinations produce salt residues, an aspect that is detrimental to their use in combination with mass spectrometry or chromatography.

Results and discussion

Synthesis and properties of DIMCARB

As shown in Table 1, at a 2 : 1 ratio of $\text{Me}_2\text{NH} : \text{CO}_2$, the melting point of DIMCARB is between 30–45 °C. However, the aforementioned synthetic procedure⁸ forms a mixture with an equilibrium $\text{Me}_2\text{NH} : \text{CO}_2$ ratio of 1.8 : 1. The excess Me_2NCOOH , relative to the stoichiometric salt, acts to lower its melting point to below 0 °C; decrease the viscosity; and increase the Brønsted acidity of the mixture. The acidity is of particular significance in this work since it will influence the cathodic limit of the mixture.

The effect of temperature on density and viscosity of DIMCARB has also been investigated. Density measurements (Fig. 1) show a linear relationship between density (ρ) and temperature (T). It should be noted that although there is some correlation between ρ and T , ρ only varies by *ca.* 0.3% over the measured range (or *ca.* 3.6% from 0–60 °C calculated from the data obtained). Thus, to a first approximation, ρ can be considered to be constant over the working range of 0–60 °C.

The viscosity does exhibit a marked dependence on temperature, as is shown in Fig. 1, and the viscosity ranges between 190 and 23 mPa s between 10 and 46 °C. Wilkes *et al.* have previously investigated the temperature effect on viscosity for a series of dialkylimidazolium chloroaluminate systems.¹¹ Their results show that the temperature dependence

of viscosity for ionic liquids is best described by the Vogel–Tammann–Fulcher (VTF) relationship:¹²

$$\eta = A_\eta T^{1/2} e^{k_\eta/(T - T_0)} \quad (6)$$

where η = dynamic viscosity, A_η = constant, T = temperature, k_η = constant characteristic of the material (and $k_\eta = \Delta E_{\text{visc}}/R$, where ΔE_{visc} is the activation energy of viscosity) and T_0 = ideal glass transition temperature.

Attempts to fit the measured viscosity data to the VTF equation have not been made due to the narrow temperature range of experimental data points measured making determinations of T_0 unreliable. A plot of $\ln \eta$ vs. $1/T$ is shown in Fig. 2

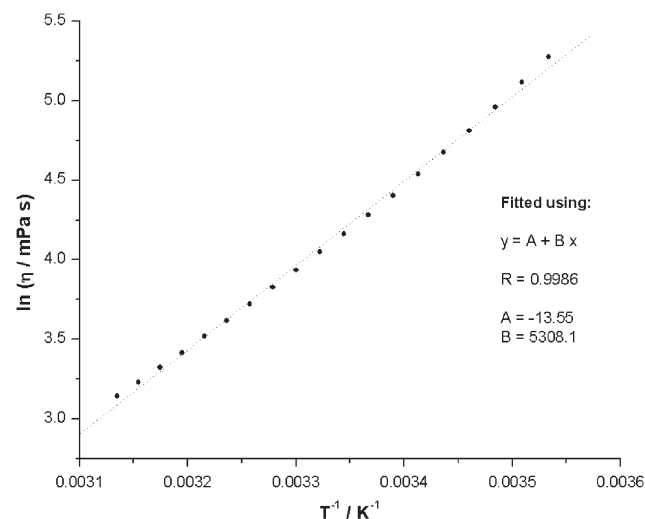


Fig. 2 Plot of $\ln \eta$ vs. $1/T$ for DIMCARB.

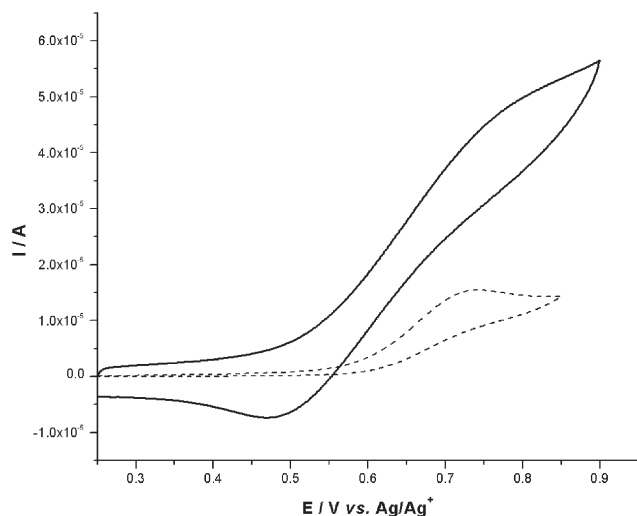


Fig. 3 Cyclic voltammograms of ferrocene in DIMCARB (5 mM) at 20 °C and scan rates of 0.1 V s⁻¹ (dashed line) and 10 V s⁻¹ (solid line).

and has some curvature, reflecting the influence of a non-zero T_0 . That is if T_0 is equal to zero, then eqn (6) would predict a linear relationship between $\ln \eta$ and $1/T$. The fact that a curvature is observed in the plot suggests that T_0 has a non-zero value *i.e.* DIMCARB forms a glass upon cooling. To a first approximation, a linear fit can nonetheless be found for this data set *i.e.* that over short region of temperature change:

$$\eta = \eta_0 \exp\left(\frac{-E_{\text{app}}}{RT}\right) \quad (7)$$

where η_0 is a pre-exponential constant and E_{app} is an apparent activation energy.

A value for E_{app} of *ca.* 40 kJ mol⁻¹ has been calculated from the slope. It should be stated that this value is not regarded as

highly accurate, but instead gives an idea of the magnitude of ΔE_{visc} . The temperature dependence of viscosity (and related transport properties) is probably more complex than predicted by the VTF equation because of the complex equilibria involved in this system.

Development of a potential reference scale in DIMCARB

It is most common to use the ferrocene/ferrocinium couple as an internal standard for voltammetry.¹³ However, ferrocene (Fc) is not a suitable internal standard in DIMCARB since the Fc^{0/+} process is very close to the positive limit of the potential window and is not reversible under all conditions. Fig. 3 provides cyclic voltammetric data for the Fc^{0/+} process *vs.* the Ag wire quasi reference electrode (QRE). Only for scan rates above 10 V s⁻¹, does the Fc^{0/+} process exhibit partial chemical reversibility. The reversible potential calculated from the average of the oxidation and reduction peak positions at fast scan rates is *ca.* 0.63 V *vs.* Ag wire QRE. The voltammetric waveshapes, in addition to the scan rate dependence, indicate that Fc⁺ reacts with the DIMCARB system. Additionally, UV/vis/nIR spectra of a Fc⁺ salt dissolved in DIMCARB confirm that the Fc⁺ cation is not stable in this solvent (see below). Further investigations to establish the full nature of the chemical reaction between Fc⁺ and DIMCARB have not been conducted.

In most solvents, the penta-methyl substituted metallocene, decamethylferrocene, (bis(pentamethylcyclopentadienyl)iron(II)-[(Me₅Cp)₂Fe], DmFc), is known to have a reversible potential ($E^{0'}$) value that is *ca.* 500 mV more negative than Fc¹⁴ which, if also true in DIMCARB, should provide a potential well removed from the solvent oxidation. The DmFc^{0/+} process was therefore investigated as an alternative reference process in DIMCARB. A voltammogram obtained for DmFc at 20 °C at a scan rate of 0.1 V s⁻¹ is

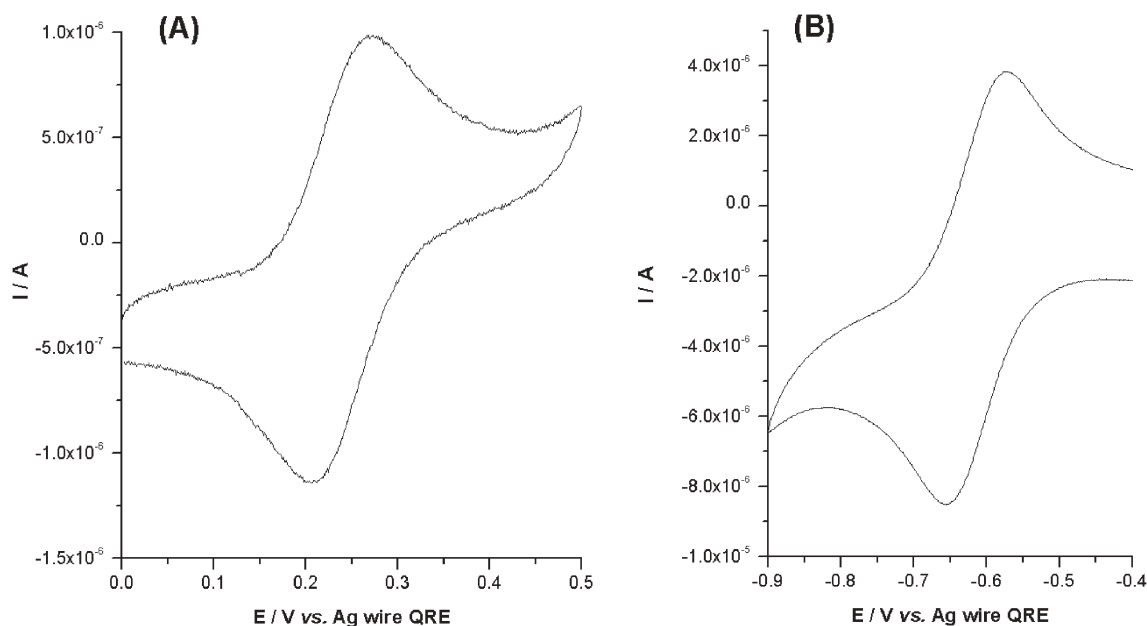


Fig. 4 Cyclic voltammograms of metallocenes in DIMCARB. A: 1.8 mM DmFc at 0.1 V s⁻¹ scan rate and 20 °C; B: 4.7 mM Cc⁺ at 0.1 V s⁻¹ scan rate and 26 °C.

Table 2 Cyclic voltammetry parameters for decamethylferrocene (1.8 mM) and cobaltocinium hexafluorophosphate (4.7 mM) in DIMCARB. All potentials quoted vs. Ag wire quasi reference electrode

Scan rate/mV s ⁻¹	Decamethylferrocene				Cobaltocinium hexafluorophosphate			
	E_p^{red} /mV	E_p^{ox} /mV	ΔE_p /mV	E^0 /mV	E_p^{red} /mV	E_p^{ox} /mV	ΔE_p /mV	E^0 /mV
200	206	271	65	239	-646	-558	88	-602
180	208	270	62	239	-656	-562	94	-609
160	206	271	65	239	-650	-561	89	-606
140	208	272	64	240	-608	-538	70	-573
120	207	270	63	239	-647	-567	80	-607
100	206	270	64	238	-654	-572	82	-613
80	207	270	63	239	-645	-565	80	-605
60	210	269	59	240	-636	-563	73	-600
40	210	270	60	240	-641	-571	70	-606
20	212	269	57	241	-642	-577	65	-610
10	211	269	58	240	-629	-566	63	-598
2	205	270	65	238	-629	-561	68	-595

shown in Fig. 4(A). Clearly this process is well removed from oxidation of DIMCARB and is chemically reversible since the magnitude of the ratio of the oxidation peak current (I_p^{ox}) to reduction peak current (I_p^{red}) is very close to unity.

Data obtained for oxidation of DmFc in DIMCARB as a function of scan rate are summarised in Table 2. At all scan rates, peak–peak separations *i.e.* the difference in oxidation (E_p^{ox}) and reduction (E_p^{red}) potentials or ΔE_p -values are in the range 57 to 65 mV (Table 2), which is close to the theoretical separation of 55 mV expected for a one electron reversible couple at 20 °C. Importantly, E^0 , defined as $(E_p^{\text{ox}} + E_p^{\text{red}})/2$, is independent of scan rate, as required for a reversible potential and as needed for a reversible couple.¹⁵ Apparently, uncompensated resistance effects do not pose a significant problem in DIMCARB under these low scan rate cyclic voltammetric conditions.

A plot of i_p vs. square root of scan rate exhibits a linear dependence, as expected for a diffusion controlled process. Using the Randles–Sevcik relationship¹⁵ (eqn (8)) the diffusion coefficient for DmFc was calculated to be $5.0 \times 10^{-8} \text{ cm}^2 \text{ s}^{-1}$ at 20 °C.

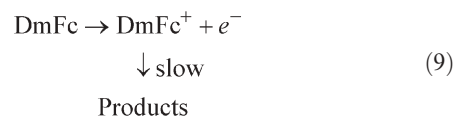
$$i_p = 0.4463 \sqrt{\frac{n^3 F^3}{RT}} A C D^{1/2} v^{1/2} \quad (8)$$

where i_p = peak current, n = number of electrons transferred, F = Faraday constant, R = gas constant, T = temperature, A = electrode area, C = bulk concentration, D = diffusion coefficient and v = scan rate.

DmFc⁺, unlike Fc⁺, is stable on the voltammetric timescale in DIMCARB. Controlled potential bulk oxidative electrolysis of DmFc was carried out on a 25 mL volume scale to ascertain if DmFc⁺ was stable on the synthetic timescale. Electrolysis under these conditions required 26 h to go to completion. The long experimental time is attributed to slow mass transport rates ($D = 5.0 \times 10^{-8} \text{ cm}^2 \text{ s}^{-1}$) associated with the high viscosity of DIMCARB. Slow bulk electrolysis in RTILs has previously been observed by Seddon *et al.* who reported that 65 h was required for the complete bulk electrolysis of Fc in an even higher viscosity ionic liquid.¹⁶ Coulometric analysis of data, confirm that the oxidation is a 1.0 electron process and hence equates to formation of DmFc⁺. However, voltammetric experiments after bulk oxidative electrolysis did not exhibit the expected DmFc⁺ + e⁻ \rightleftharpoons DmFc reduction close to the

reversible potential of the DmFc^{0/+} couple, suggesting that the DmFc⁺ cation generated electrochemically is not stable in this medium on the hours time scale of these bulk electrolysis experiments.

Spectroelectrochemical studies were conducted to investigate the stability of electrogenerated DmFc⁺ cation on a timescale intermediate between that of voltammetry and bulk electrolysis. To minimise problems with slow mass transport rates, a thin layer cell was used. In this experiment, the distance between the meshed electrode to the cell wall was 0.1 mm or less. Consequently, the time required for diffusion to occur within this cell is <1000 s when $D = 5.0 \times 10^{-8} \text{ cm}^2 \text{ s}^{-1}$ as calculated from the equation $\delta = \sqrt{2Dt}$ (where δ = diffusion layer thickness and t = time).¹⁵ Prior to electrochemical oxidation, a DmFc absorption band was detected at 425 nm.¹⁷ During the initial stages of electrolysis, the intensity of the DmFc absorbance decreased and a new absorption band emerged at 325 nm, which is assigned to the generation of the DmFc⁺ cation (Fig. 5). However, after *ca.* 45 min, the DmFc⁺ absorption band also decreased in intensity (Fig. 5), consistent with instability of electrochemically generated DmFc⁺ in DIMCARB. This and the instability of oxidised ferrocene on the synthetic timescale was confirmed by addition of Fc⁺ and DmFc⁺ salts to DIMCARB and studying the decomposition by UV/vis/nIR spectroscopy. Spectroscopic data with Fc⁺ indicate that it decomposes very rapidly in DIMCARB (reaction had occurred in-between sample preparation and measurement). With DmFc⁺, reaction with DIMCARB is much slower as shown by examination of the plot of time vs. absorbance (Fig. 5) for the DmFc⁺ band at 425 nm. All of the above data imply that on the long time scale of bulk electrolysis in DIMCARB, oxidation of DmFc is represented by the reaction scheme:



For DmFc, the rate of the chemical step following its oxidation is sufficiently slow to enable the DmFc^{0/+} process to be detected as a reversible process on the voltammetric time scale. In contrast, in the case of Fc, we propose an analogous reaction scheme, with the difference being that the rate of the chemical step (Fc⁺ $\xrightarrow{\text{fast}}$ products) is comparable to the voltammetric timescale.

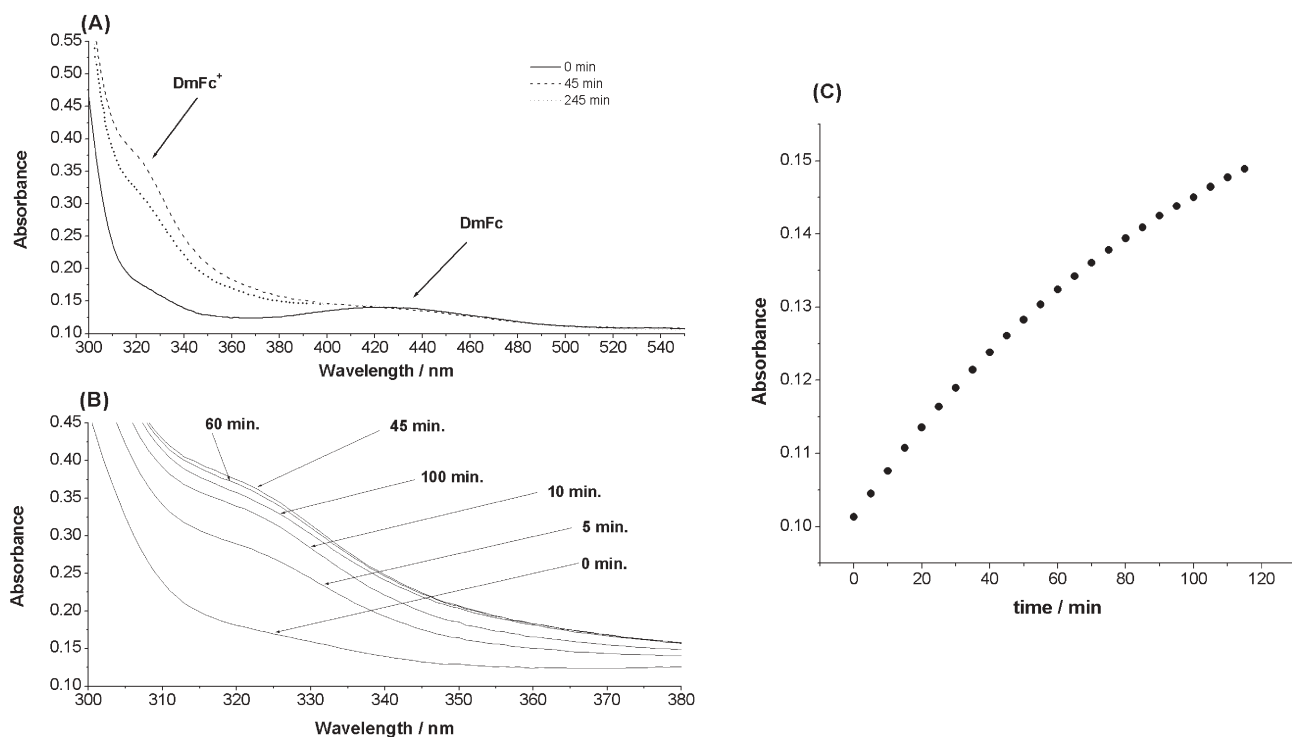


Fig. 5 UV/vis spectral monitoring of the electrochemical reduction of DmFc in DIMCARB. A: spectra measured at time = 0 (solid line), 45 (dashed line) and 245 minutes (dotted line); B: UV/vis spectra showing initial increase in DmFc⁺ absorption, then decrease in intensity after 45 min; C: Plot of peak absorbance as a function of time for the DmFc absorption band at 425 nm for DmFcBF₄ dissolved in DIMCARB.

The cobalticinium/cobaltocene (Cc⁺/Cc) couple, like the Fc⁰⁺ process, is recommended by IUPAC for use as a reference potential scale standard.¹³ Cyclic voltammetric data shown in Fig. 4 and Table 2 confirm that the one electron Cc⁺/Cc redox couple is almost ideal in DIMCARB at scan rates up to 1 V s⁻¹ (limit of scan rate examined). ΔE_p values found from reduction of Cc⁺ in DIMCARB showed a small (63 to 94 mV) dependence on scan rate, but were again close to the ideal value of 56 mV predicted by theory for a one electron reversible process. In this case small differences between the experimental and theoretical values for a reversible process were attributed to a small level of IR drop (ΔE_p less at lower Cc⁺ concentration thus, as for the DmFc/DmFc⁺ case, solution resistance does not pose a significant problem). The difference between the reversible potentials for the Cc^{+/0} and the Fc⁰⁺ processes is ca. 1.30 V and is comparable to that found in acetonitrile at a glassy carbon electrode.¹⁸ The plot of i_p vs. $v^{1/2}$ for the reduction of Cc⁺ was found to be linear, again indicative of a purely diffusion controlled process. Using eqn (8), the diffusion coefficient for Cc⁺ was found to be 2.0×10^{-7} cm² s⁻¹ at 26 °C which is slightly larger than that observed for DmFc (5.0×10^{-8} cm² s⁻¹). The product of the Cc^{+/0} process, cobaltocene, was found to be reactive in DIMCARB when added as a solid. Thus, again, stability is only established on the voltammetric rather than synthetic timescale.

The diffusion coefficient of Cc⁺ was also measured using a 11 μ m diameter carbon fibre microdisc electrode and use of eqn (10):¹⁵

$$i_{ss} = 4nFDcR \quad (10)$$

where i_{ss} = steady state current, r = electrode radius and other symbols have their usual meanings

In order to achieve a near steady-state response, a slow scan rate of 1 mV s⁻¹ was employed. However, even under these conditions, the small peak observed at -0.7 V (see Fig. 6) suggests that a minor transient component is still associated with this voltammogram. Transient behaviour, observed under conditions where steady state voltammograms are conventionally obtained, has also been observed previously in other ionic liquid media,¹⁹ and is a consequence of the diffusion coefficient of redox species in DIMCARB being much smaller than found in conventional organic solvents.

The steady-state currents used to calculate the diffusion coefficient using eqn (10) were measured at -0.9 V vs. Ag wire to ensure that the influence of this transient behaviour was negligible. A diffusion coefficient value of $1.2 \pm 0.1 \times 10^{-7}$ cm² s⁻¹ was obtained *via* measurement of these currents over a concentration range of 5–250 mM. No contribution of electron hopping²⁰ to the apparent diffusion coefficient was observed under these conditions even though the diffusion coefficient of Cc⁺ is very low. The smaller value of D obtained from the steady state method compared to cyclic voltammetry (1.2×10^{-7} cm² s⁻¹ *cf.* 2.0×10^{-7} cm² s⁻¹) is due to the difference in temperature at which experiments were conducted (20 °C for the microdisc and 26 °C for CV) and the concomitant difference in viscosities (93.4 mPa s *cf.* 64.1 mPa s, respectively). It should be noted that the value of D obtained (1.2×10^{-7} cm² s⁻¹) is close to that predicted by the Stokes–Einstein equation¹⁵ of 1.3×10^{-7} cm² s⁻¹ (calculated using $D = 2.0 \times 10^{-7}$ cm² s⁻¹ and η -values of 93.4 mPa s for 20 °C and 64.1 mPa s for 26 °C).

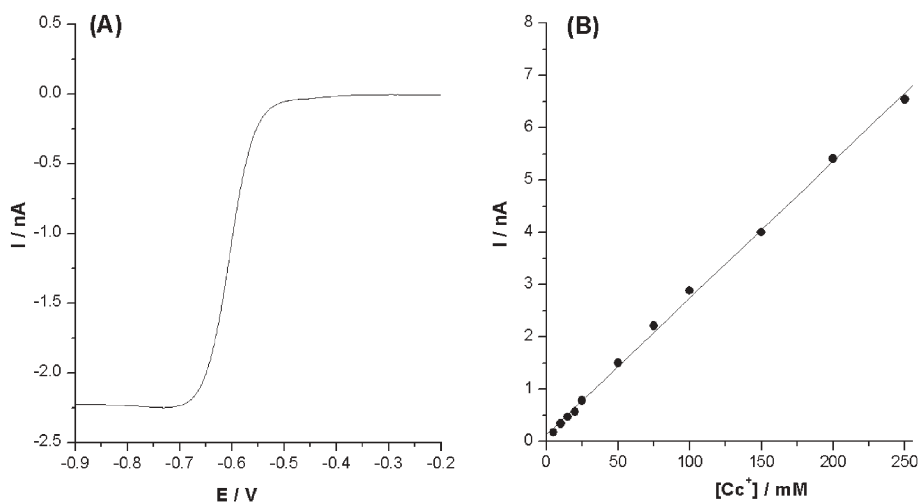


Fig. 6 Steady state cyclic voltammograms obtained at a 11 μm glassy carbon microdisk electrode for 75 mM cobaltocenium hexafluorophosphate (Cc^+) at 1 mV s^{-1} (graph A) and the dependence on steady state limiting current as function of Cc^+ concentration (graph B) at 20°C .

Reduction of oxygen in DIMCARB

Unless DIMCARB solutions were degassed with CO_2 or N_2 , two waves were observed when the voltammetry of Cc^+ was being studied at a rotating disk electrode (RDE) as shown in Fig. 7(A,B). The process at about $-0.7 \text{ V vs. Ag wire}$ is due to the $\text{Cc}^{+/0}$ reaction, whereas the process observed at about $-0.5 \text{ V vs. Ag wire}$ is assigned to the reduction of O_2 . To support this conclusion, cyclic voltammograms were recorded in DIMCARB after bubbling air through the solution. They exhibit an irreversible process with a reduction peak at *ca.*

$-0.45 \text{ V vs. Ag wire QRE}$ (Fig. 7(C)). A plot of i_p vs. $v^{1/2}$ shows a linear relationship, consistent with the reduction of O_2 in DIMCARB being diffusion controlled at the peak potential. On bubbling CO_2 through the system (Fig. 7(D)), the decrease in reduction peak intensity, detected at a glassy carbon electrode, with time, suggests that the CO_2 gas displaces O_2 from DIMCARB. Cyclic and RDE voltammetric data are consistent with O_2 being irreversibly reduced in DIMCARB. However, no evidence for a reversible $\text{O}_2^{0/-}$ process involving formation of the superoxide was found when using scan rates of 20 mV s^{-1} to 5 V s^{-1} , as previously observed in some other

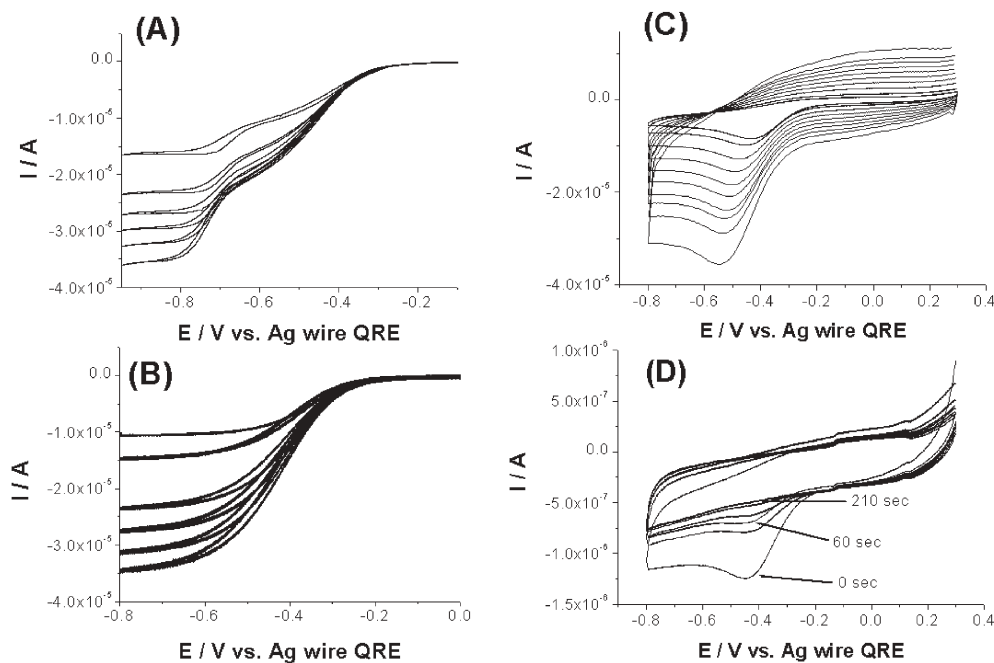


Fig. 7 Cyclic voltammograms of O_2 in DIMCARB at stationary and rotating disk electrodes. A: Steady state CV obtained at a glassy carbon rotating disk electrode for a solution of 5 mM Cc and O_2 at 5 mV s^{-1} scan rate and 500–3000 rpm; B: Steady state CVs obtained at a glassy carbon rotating disk electrode for O_2 in DIMCARB at 5 mV s^{-1} scan rate and 500–3000 rpm; C: Cyclic voltammograms of O_2 in DIMCARB from 50 mV s^{-1} to 1 V s^{-1} ; D: Effect of bubbling CO_2 through the O_2 /DIMCARB mixture (bubbling time labelled).

ionic liquids.²¹ Presumably the reduced O₂ species reacts very rapidly in DIMCARB so that an electrochemically irreversible process is detected in this medium, under the conditions examined. It has been shown previously that O₂⁻ can react with CO₂.²² Therefore, it seems likely that the origin of the electrochemical irreversibility arises from the reaction of the reduced O₂ with the CO₂ present in DIMCARB (eqn (3)–(5)).

For many electrochemical experiments it is desirable to work under conditions where O₂ is not present. This can be accomplished by degassing the electrochemical cell/solution with an inert gas *e.g.* N₂ or Ar. In the case of DIMCARB, a complex set of equilibria exists between CO₂/Me₂NH gases and other species of which DIMCARB is composed (eqn (3)–(5)). Thus, addition of other gases could, in theory, displace CO₂ (or Me₂NH) from the system and thereby change the DIMCARB composition. Our observations have shown that on the voltammetric timescale, addition of small quantities of either N₂ or CO₂ does not appear to significantly change either composition or volume of DIMCARB solutions. However, care should be exercised upon degassing DIMCARB over long timescales. Further studies on possible consequences of degassing are currently in progress in our laboratories.

Potential limits in DIMCARB

In order to compare voltammetric data obtained in DIMCARB with that found in other media, it is necessary to either introduce a reference electrode of known potential against a standard (*e.g.* against the standard hydrogen electrode) or else reference data to a reversible process whose potential is assumed to be independent of solvent. Since a well defined reference electrode is not available for use in DIMCARB, we will employ a Ag wire QRE and IUPAC recommended reference potential couples. This approach enables the potential window range to be defined *versus* that in other solvents. Thus, under conditions of cyclic voltammetry at a glassy carbon electrode (0.1 V s⁻¹ scan rate), the potential window of DIMCARB was found to be -1.50 V to +0.50 V *vs.* SHE (-0.50 V to +1.50 V *vs.* Cc⁺⁰). Under the same conditions, but using the DmFc⁺⁰ process as a standard, the potential window was shown to be -1.50 V to +0.50 V *vs.* SHE (-1.40 V to +0.60 V *vs.* DmFc).

The potential window of DIMCARB is comparable to that of [Me₂NH₂]⁺[Me₂N-CO₂]⁻ in the molten state reported by Hess *et al.*,⁶ where the authors report a potential window at a glassy carbon electrode of -1.0 V to +0.7 V *vs.* SHE (-1.25 V to +0.5 V *vs.* SCE). The slightly larger potential window obtained for DIMCARB is attributed to the differences in composition between [Me₂NH₂]⁺[Me₂N-CO₂]⁻ and DIMCARB.

The calculated potential range *vs.* SHE, imply that DIMCARB is unlikely to be a suitable solvent for widespread investigation of oxidation processes. Indeed, the Fc^{0/+} process occurs at 0.40 V *vs.* SHE and is at the limit of the electrochemical window. In contrast, the relatively wide negative potential limit in DIMCARB indicates that this medium will be suitable for reductive studies.

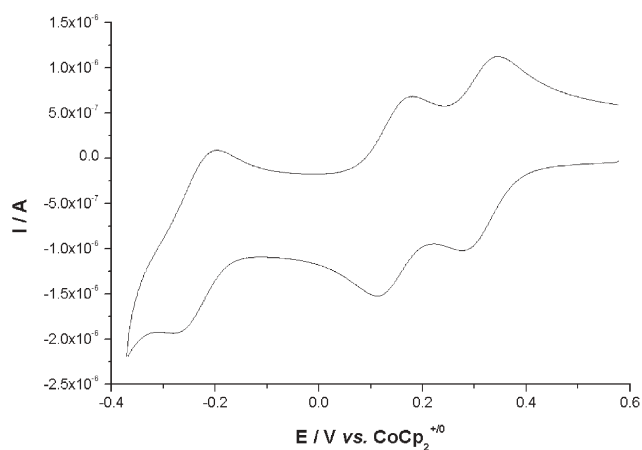


Fig. 8 CV of Keggin [α-SiW₁₂O₄₀]⁴⁻ in DIMCARB (5 mM) showing the [α-SiW₁₂O₄₀]^{4-/-5-/-6-/-7-} processes ($E_{1/2}$ = 0.310, 0.147 and -0.239 V, respectively), scan rate = 0.1 V s⁻¹, temperature = 20 °C.

Voltammetry of [α-SiW₁₂O₄₀]⁴⁻

Polyoxometallates (POM) are known to exhibit an extensive series of reduction processes in many media. Therefore, the voltammetric properties of the Keggin polyoxometallate [α-SiW₁₂O₄₀]⁴⁻ has been investigated in DIMCARB. Three well-defined, reversible, one-electron transfer processes are observed under conditions of cyclic voltammetry with $E^{0'}$ -values of 0.310, 0.147 and -0.239 V *vs.* Cc⁺⁰ that are assigned to the [α-SiW₁₂O₄₀]^{4-/-5-/-6-/-7-} processes,²³ respectively (Fig. 8). A further [α-SiW₁₂O₄₀]^{7-/-8-} process is detected at the solvent limit. The $E^{0'}$ value for the first [α-SiW₁₂O₄₀]^{4-/-5-} process of 0.310 V *vs.* Cc⁺⁰ is more positive than the value of 0.240 V *vs.* Cc⁺⁰ obtained in MeCN (0.1 M Bu₄NClO₄),²³ but much less positive than the value of 0.614 V *vs.* Cc⁺⁰ observed in the ionic liquid [BMIM][PF₆] (where BMIM⁺ is the 1-butyl,3-methylimidazolium cation).²⁴ Defining the polarity of ionic liquids is complicated due to the number of differing interactions present.²⁵ $E^{0'}$ values can be used for this purpose and our voltammetric results for [α-SiW₁₂O₄₀]⁴⁻ suggest that the polarity of DIMCARB lies between that of MeCN and [BMIM][PF₆]. For further details on DIMCARB polarity see ref. 26. The diffusion coefficient of the Keggin [α-SiW₁₂O₄₀]⁴⁻ in DIMCARB was calculated to be 1.8×10^{-8} cm² s⁻¹.

Reduction of Pb(II) in DIMCARB

The standard reduction potential for the Pb(II)/Pb(0) process in water is -0.12 V *vs.* SHE,²⁷ and it is likely that Pb(II) should also be reduced electrochemically to the metallic state in DIMCARB. In order to confirm that this reaction occurs in DIMCARB, the electrochemical behaviour of Pb(CH₃COO)₂·3H₂O was investigated by both voltammetry and bulk electrolysis methods. Cyclic voltammograms of Pb(II) consist of a broad reduction peak at *ca.* -0.90 V *vs.* DmFc (assigned to the Pb²⁺/Pb⁰ reduction), and a sharper oxidation peak at *ca.* -0.47 V *vs.* DmFc (assigned to the Pb⁰/Pb²⁺ oxidation) as shown in Fig. 9. The wavelshapes and behaviour are as expected for the deposition of an insoluble substance (in this case Pb metal) onto the glassy carbon electrode surface

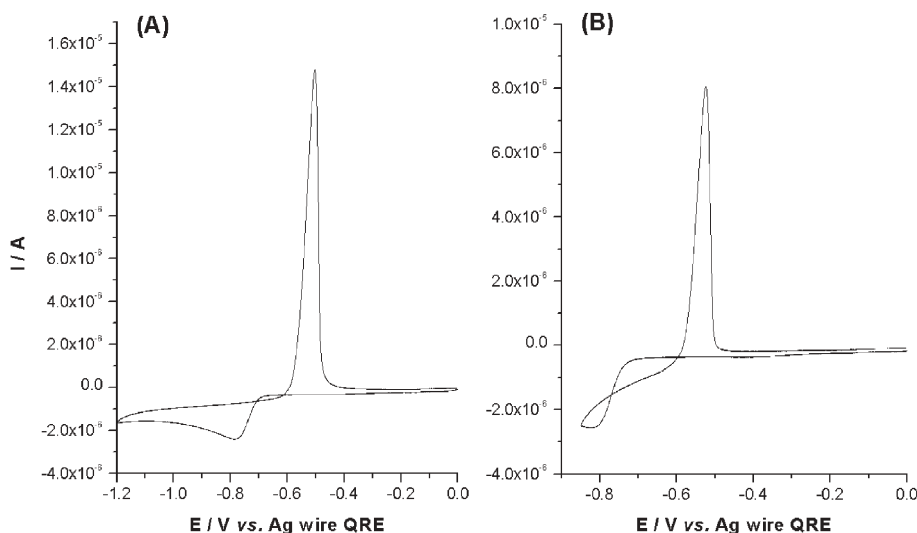


Fig. 9 Reduction of $\text{Pb}(\text{CH}_3\text{COO})_2 \cdot 3\text{H}_2\text{O}$ in DIMCARB. A: cyclic voltammogram of 5 mM $\text{Pb}(\text{CH}_3\text{COO})_2 \cdot 3\text{H}_2\text{O}$ at 40 mV s^{-1} scan rate and 25°C ; B: cyclic voltammogram of $\text{Pb}(\text{CH}_3\text{COO})_2 \cdot 3\text{H}_2\text{O}$ at 40 mV s^{-1} scan rate and 25°C showing nucleation loop.

followed by stripping of the metal when the scan direction is reversed. The reduction of $\text{Pb}(\text{II})$ in DIMCARB at a glassy carbon electrode proceeds *via* a nucleation and growth mechanism, as is evident by the nucleation loops observed in the voltammogram in Fig. 9.

In order to confirm that $\text{Pb}(\text{II})$ was indeed being reduced to the metallic state, bulk electrolysis at a platinum electrode was carried out with the potential being held at $-1.2 \text{ V vs. Ag wire QRE}$ for 35 min. After electrolysis was complete, a dark grey deposit was observed on the electrode surface. The powder X-ray diffraction pattern obtained from this solid analysed for Pb metal and a very small quantity of PbO . It is tentatively suggested that $\text{Pb}(\text{II})$ ions are reduced to the metallic state to form the Pb metal in DIMCARB and that a subsequent reaction with air/moisture produces PbO .

Conclusions

Voltammetric studies undertaken on model electrode processes confirm that, the distillable ionic liquid, DIMCARB is highly suitable for studies of reduction processes *e.g.* $\text{Cc}^{+/0}$ and $[\alpha\text{-SiW}_{12}\text{O}_{40}]^{4-/-5-/-6-/-7-/-8-}$. Studies with the IUPAC recommended Fc/Fc^+ potential scale reference couple show that the couple lies on the positive potential solvent limit and that Fc^+ rapidly reacts with DIMCARB. However, the more easily oxidised DmFc ($\text{DmFc}^{0/+}$ process) as well as the $\text{Cc}^{+/0}$ process can be used for reference potential calibration purposes as they exhibit close to ideal, reversible voltammetry, with minimal problems from uncompensated resistance. The diffusion coefficients of DmFc and Cc^+ have been determined to be 5.0×10^{-8} and $1.2 \times 10^{-7} \text{ cm}^2 \text{ s}^{-1}$ at 20°C , respectively, with the smaller values relative to those found in conventional organic solvents being attributed to the high viscosity of DIMCARB. Reaction of Fc^+ , DmFc^+ and Cc with the DIMCARB medium has been detected on voltammetric (Fc^+), bulk electrolysis (DmFc^+) and synthetic timescales (Fc^+ , DmFc^+ and Cc), implying that this is a potentially reactive medium.

The reversible voltammetric responses of the $[\alpha\text{-SiW}_{12}\text{O}_{40}]^{4-/-5-/-6-/-7-/-8-}$ processes are analogous to processes previously reported in MeCN (0.1 M Bu_4NClO_4) and in the ionic liquid $[\text{BMIM}][\text{PF}_6]$. However, $E^{0'}$ values in these media suggest that the polarity of the DIMCARB lies between that of MeCN and $[\text{BMIM}][\text{PF}_6]$.²⁶

Voltammetric reduction of $\text{Pb}(\text{II})$ in DIMCARB results in deposition of metallic lead at both glassy carbon and Pt electrodes. The metal can in turn be stripped from the surface by oxidative electrolysis. The $\text{Pb}(\text{II})/\text{Pb}(0)$ is an electrochemically irreversible, but chemically reversible process. The $\text{Pb}(\text{II})$ reduction in DIMCARB at a glassy carbon surface proceeds *via* a nucleation growth mechanism. A full description of the $\text{Pb}(\text{II})$ deposition will be published elsewhere and we have recently published a detailed account of the voltammetry of the Keggin polyoxometallate $[\alpha\text{-SiW}_{12}\text{O}_{40}]^{4-}$ in DIMCARB.²⁶

Oxygen, dissolved in DIMCARB, has been detected by voltammetric measurements. However, degassing with Ar or N_2 to remove O_2 needs careful thought as these gases could also displace CO_2 from the melt, thus modifying the composition of DIMCARB. Degassing with CO_2 gas may therefore be the preferred option for removal of oxygen.

In summary, the present investigations demonstrate that DIMCARB provides an ideal solvent medium for voltammetry (linear sweep, cyclic, hydrodynamic and microelectrode), bulk electrolysis and spectroelectrochemistry. The wide negative potential range shows that DIMCARB is particularly useful for studies of reduction processes. However, the medium is potentially reactive as it consists of a complex mixture of species that exhibit Brønsted acid–base properties and this needs to be taken into consideration if DIMCARB is to be used for electrochemical studies.

Experimental

Reagents and chemical

All chemicals used were commercially available and used as supplied. Bis(pentamethylcyclopentadienyl)iron(II)

(decamethylferrocene, DmFc), bis(cyclopentadienyl)cobalt(II) (cobaltocene, Cc) and dimethylamine were supplied by Aldrich. CO₂ was supplied by BOC gases, Pb(CH₃COO)₂·3H₂O was supplied by BDH, cobaltocinium hexafluorophosphate (Cc⁺) was supplied by Strem and [Bu₄N]₄[α-SiW₁₂O₄₀] synthesised as previously reported.²⁸

Synthesis of DIMCARB

A 250 mL 3-necked round bottom flask was equipped with a water condenser and two gas purge tubes connected to CO₂ and dimethylamine (DMA) gas cylinders and the entire setup placed into a ice bath. After cooling the reaction vessel to 0 °C, CO₂ and DMA were passed into the vessel, at a slow rate, allowing the two gas streams to mix. The exothermic reaction was allowed to progress until ca. 200 mL of clear colourless liquid DIMCARB, comprising Me₂NH : CO₂ in a 1.8 : 1 ratio, was formed (ca. 4 h). The DIMCARB was collected and stored at 5 °C until use.

Electrochemical instrumentation and techniques

Voltammetric studies were undertaken with a VoltaLab PGZ301 potentiostat (Radiometer Analytical) operated by VoltaLab Software, version 4 or a BAS100B potentiostat (BioAnalytical Systems). Rotating disk electrode (RDE) voltammograms were obtained by combining the VoltaLab system with a Metrohm 628-10 RDE assembly. All voltammetric data was obtained in a conventional 3-electrode cell. In the case of cyclic voltammograms, a glassy carbon working electrode (0.0314 cm²), Pt counter electrode (0.0628 cm²) and a silver wire quasi reference electrode (QRE) were used. For RDE studies, a glassy carbon electrode (0.0314 cm²) and the aforementioned counter and reference electrodes were used. Unless otherwise stated, oxygen dissolved in DIMCARB was removed by degassing with nitrogen or carbon dioxide.

Optically transparent thin-layer electrolysis (OTTLE) experiments were carried out at a Pt gauze electrode placed into a 1 mm thick quartz cuvette, a Pt counter electrode and a Ag wire reference electrode. Electrolysis was conducted using a BAS100A potentiostat and UV/vis/nIR spectra measured using a Varian Cary 5 UV/vis/nIR spectrometer.

Bulk electrolysis was achieved by placing 25 mL of DIMCARB solution into a cell equipped with a Pt gauze working electrode, Pt gauze counter electrode and an Ag wire QRE.

Viscosity and density measurements

Density measurements were made with a Anton Paar DMA35n density-specific gravity concentration meter. Experiments were performed by placing 1 mL of DIMCARB heated to 40 °C within the sample chamber and simultaneously recording both temperature and density at regular intervals as the DIMCARB cooled to room temperature. Viscosity measurements were conducted using a Anton Paar AMVn automated micro viscometer with flow times in the order of minutes, thus uncertainties in time measurements were negligible. Measurements at varying temperature were made by heating or cooling the sample in the viscometer cell and

allowing the temperature to equilibrate for 5 min prior to measurements.

Acknowledgements

The authors express appreciation to Rio Tinto for financial support and Mr R. Mackie for assistance with powder XRD measurements. The award of a Royal Society Fellowship to AIB also is gratefully acknowledged.

References

- 1 T. Welton, *Chem. Rev.*, 1999, **99**, 2071; P. Wasserchied and W. Kiem, *Angew. Chem., Int. Ed.*, 2000, **39**, 3772; A. Blanchard, D. Hancu, E. J. Beckman and J. F. Brenecke, *Nature*, 1999, **399**, 28; *Ionic Liquids in Synthesis*, ed. P. Wasserchied and T. Welton, Wiley VCH, Germany, 2003.
- 2 M. C. Buzzeo, R. G. Evans and R. G. Compton, *ChemPhysChem*, 2004, **5**, 1106; F. Endres, *ChemPhysChem*, 2002, **13**, 144; D. R. MacFarlane, J. M. Pringle and S. A. Forsyth, *Aust. J. Chem.*, 2004, **57**, 113.
- 3 J. Zhang and A. M. Bond, *Analyst*, 2005, **130**, 1132.
- 4 U. P. Kreher, A. E. Rosamilia, C. L. Raston, J. L. Scott and C. R. Strauss, *Molecules*, 2004, **9**, 387; U. P. Kreher, A. E. Rosamilia, C. L. Raston, J. L. Scott and C. R. Strauss, *Org. Lett.*, 2003, **5**, 3107.
- 5 J. Klunker, M. Biedermann, W. Schäfer and H. Hartung, *Z. Anorg. Allg. Chem.*, 1998, **624**, 1503.
- 6 C. -P. Maschmeier, J. Krahnstöver, H. Matschiner and U. Hess, *Electrochim. Acta*, 1990, **35**, 769.
- 7 C. -P. Maschmeier and H. Baltruschat, *Electrochim. Acta*, 1992, **37**, 759.
- 8 R. Radeaglia, J. Andetsch and W. Schroth, *Z. Naturforsch., B: Chem. Sci.*, 1989, **44**, 181.
- 9 D. D. Dell'Amico, F. Calderazzo, L. Labella, F. Marchetti and G. Pampaloni, *Chem. Rev.*, 2003, **103**, 3857.
- 10 D. M. Roundhill, *Chem. Rev.*, 1992, **92**, 1.
- 11 A. A. Fannin, Jr., D. A. Floreani, L. A. King, J. S. Landers, B. J. Piersma, D. J. Stech, R. L. Vaughn, J. S. Wilkes and J. L. Williams, *J. Phys. Chem.*, 1984, **88**, 2614.
- 12 G. S. Fulcher, *J. Am. Ceram. Soc.*, 1925, **8**, 339.
- 13 G. Gritzner and J. Kuta, *Pure Appl. Chem.*, 1982, **54**, 1527; G. Gritzner and J. Kuta, *Pure Appl. Chem.*, 1984, **56**, 461.
- 14 I. Noviadri, K. N. Brown, D. S. Fleming, P. T. Gulyas, P. A. Lay, A. F. Masters and L. Phillips, *J. Phys. Chem. B*, 1999, **103**, 6713.
- 15 A. J. Bard and L. R. Faulkner, *Electrochemical Methods: Fundamentals and Applications*, John Wiley & Sons Inc., New York, 2001.
- 16 M. C. Lagunas, W. R. Pitner, J. van den Berg and K. R. Seddon, in *Ionic liquids as Green Solvents: Progress and Prospects*, ed. R. D. Rogers and K. R. Seddon, American Chemical Society, Washington, D.C., 2003.
- 17 J. L. Robbins, N. Edelstein, B. Spencer and J. C. Smart, *J. Am. Chem. Soc.*, 1982, **104**, 1882.
- 18 R. S. Stojanovic and A. M. Bond, *Anal. Chem.*, 1993, **65**, 56.
- 19 J. Zhang and A. M. Bond, *Anal. Chem.*, 2003, **75**, 2694; D. L. Boxall, J. J. O'Dea and R. A. Osteryoung, *J. Electrochem. Soc.*, 2002, **149**, E468.
- 20 M. Majda, in *Molecular Design of Electrode Surfaces*, ed. R. W. Murray, Wiley & Sons, New York, 1992, pp. 159–206 and references therein.
- 21 I. M. AlNashef, M. L. Leonard, M. A. Matthews and J. W. Weidner, *Ind. Eng. Chem. Res.*, 2002, **41**, 4475; M. C. Buzzeo, O. V. Klymenko, J. D. Wadhawan, C. Hardacre, K. R. Seddon and R. G. Compton, *J. Phys. Chem. A*, 2003, **107**, 8872; R. G. Evans, O. V. Klymenko, S. A. Saddoughi, C. Hardacre and R. G. Compton, *J. Phys. Chem. B*, 2004, **108**, 7878.
- 22 C. Amatore and J.-M. Saveant, *J. Am. Chem. Soc.*, 1981, **103**, 5021; C. E. W. Hahn, H. McPeak, A. M. Bond and D. Clark, *J. Electroanal. Chem.*, 1995, **393**, 61; C. E. W. Hahn, H. McPeak and A. M. Bond, *J. Electroanal. Chem.*, 1995, **393**, 69.

- 23 J. Zhang, A. M. Bond, P. J. S. Richardt and A. G. Wedd, *Inorg. Chem.*, 2004, **43**, 8263.
- 24 J. Zhang, A. M. Bond, D. R. MacFarlane, S. A. Forsyth, J. M. Pringle, A. W. A. Mariotti, A. F. Glowinski and A. G. Wedd, *Inorg. Chem.*, 2005, **44**, 5123.
- 25 C. Reichardt, *Green Chem.*, 2005, **7**, 339.
- 26 J. Zhang, A. I. Bhatt, A. M. Bond, A. G. Wedd, J. L. Scott and C. R. Strauss, *Electrochem. Commun.*, 2005, **7**, 1283–1290.
- 27 T. F. Sharpe, in *Encyclopaedia of Electrochemistry of the Elements*, ed. A. J. Bard, Marcel Dekker, Inc., New York, 1973.
- 28 A. Tézé and G. Hervé, *Inorg. Synth.*, 1990, **27**, 85.

Chemical Science

An exciting news supplement providing a snapshot of the latest developments across the chemical sciences



Free online and in print issues of selected RSC journals!*

Research Highlights – newsworthy articles and significant scientific advances

Essential Elements – latest developments from RSC publications

Free access to the original research paper from every online article

*A separately issued print subscription is also available

03003519

RSC Publishing

www.rsc.org/chemicalscience

Density and viscosity of several pure and water-saturated ionic liquids

J. Jacquemin, P. Husson, A. A. H. Padua and V. Majer

Received 19th September 2005, Accepted 6th December 2005

First published as an Advance Article on the web 19th December 2005

DOI: 10.1039/b513231b

Densities and viscosities were measured as a function of temperature for six ionic liquids (1-butyl-3-methylimidazolium hexafluorophosphate, 1-butyl-3-methylimidazolium tetrafluoroborate, 1-butyl-3-methylimidazolium bis(trifluoromethylsulfonyl)imide, 1-ethyl-3-methylimidazolium bis(trifluoromethylsulfonyl)imide, 1-ethyl-3-methylimidazolium ethylsulfate and butyltrimethylammonium bis(trifluoromethylsulfonyl)imide). The density and the viscosity were obtained using a vibrating tube densimeter from Anton Paar and a rheometer from Rheometrics Scientific at temperatures up to 393 K and 388 K with an accuracy of 10^{-3} g cm $^{-3}$ and 1%, respectively. The effect of the presence of water on the measured values was also examined by studying both dried and water-saturated samples. A qualitative analysis of the evolution of density and viscosity with cation and anion chemical structures was performed.

Introduction

Room temperature ionic liquids (ILs) constitute a new class of substances that are considered as potential substitutes to many traditional organic solvents in reaction and separation systems.^{1,2} The great interest of these organic salts, composed of bulky ions, is their negligible vapour pressure, low melting point and good thermal stability which make them liquid over a large temperature range (typically 300 K) including ambient temperature. Furthermore, they are non-flammable and easy to recycle. These properties make them very attractive especially in the emerging field of green chemistry.

Even if the number of articles on ILs is increasing exponentially, there is still a lack of data on their thermodynamic and thermophysical properties. The first reason for that is the wide variety of ILs. Indeed, in order to obtain these liquids with properties suitable for a particular industrial application (in terms of chemical reactivity and process engineering), new ILs are being continuously designed. The aim is to achieve exactly the desired chemical and physical properties by a judicious combination of an anion and a cation. Furthermore, although different ways of synthesizing this new class of liquid are better understood and controlled, it still remains difficult to obtain them with a high purity or at least with well defined admixtures. The identification of the impurities in the samples is of importance as their presence has a strong impact on the physico-chemical properties of ILs.³ Thus the comparison of data sets obtained with samples of different origins is not always concluding and can lead to confusion. Finally, many physico-chemical data presented in the literature are collected mainly to characterise an IL after synthesis work and are thus often of limited reliability. In this context, our aim is to study closely two key thermophysical properties, density and viscosity, for several ILs with special

attention paid to the influence of the presence of a major impurity: water.

A considerable amount of data on the density of ILs are available in the literature (many in communications dedicated primarily to synthesis) as it is a typical property for characterising a substance. A recent review of density measurements of ILs has been published by Mantz and Trulove.⁴ By far the most studied liquids are those containing imidazolium and, to a lesser extent, pyridinium-based cations. Usually the influence of the alkyl chain length in these cations on the density is studied as well as the effect of different anions (chloride Cl $^{-}$, tetrafluoroborate BF $_4^{-}$, hexafluorophosphate PF $_6^{-}$, bis(trifluoromethylsulfonyl)imide NTf $_2^{-}$). Several authors^{5,6} have worked on other types of cation (ammonium, pyrrolidinium) but only at 298 K. The most frequently studied IL was 1-butyl-3-methylimidazolium hexafluorophosphate Bmim $^{+}$ PF $_6^{-}$. The interest has, however, weakened over the last few years as it has been shown that this IL can degrade in the presence of water at temperatures above 323K⁷ leading to formation of HF. ILs are generally denser^{4,8,9} than either organic solvents and water, with typical values of densities ranging from 1 to 1.6 g cm $^{-3}$. The density generally decreases with increasing length of an alkyl chain in a cation or anion as was documented for imidazolium-based cations.^{8,10,11} The density values are often reported at a single temperature, usually 293 K or 298 K. Knowledge of the temperature dependence of this property is, however, very useful and several recent studies^{10,12-15} present data as a function of temperature. They have reported an approximately linear decrease of density with temperature, corresponding to typical values¹⁴ for the thermal expansion coefficient near 5×10^{-4} K $^{-1}$ which is about twice higher compared to water and three times lower compared to common organic solvents (such as methanol, acetone, benzene and n-hexane). Sun *et al.*⁶ and Gu and Brennecke¹⁴ examined also the variation of the density of ILs with pressure. They came to a conclusion of an isothermal compressibility comparable with water and lower than that for organic solvents.

Laboratoire de Thermodynamique des Solutions et des Polymères,
Université Blaise Pascal Clermont-Ferrand/CNRS, 63 177 Aubière,
France

The knowledge of the viscosity of ILs is of prime importance from an engineering point of view as it plays a major role in stirring, mixing and pumping operations; in addition, it also affects other transport properties such as diffusion. Nevertheless, the viscosity is much less investigated than the density and only limited data are available in the literature. Most of the studies^{10,15–18} concern imidazolium-based ILs, differing in the length and ramification of the alkyl chains. Okoturo *et al.*¹⁸ have also studied pyrrolidinium cations. ILs are generally viscous liquids^{8,9} with viscosities ranging typically from 10 to 500 mPa s at ambient temperature. This is comparable with the values obtained for oils, that is to say two or three orders of magnitude higher than viscosities of traditional organic solvents. This is obviously a real disadvantage for their industrial application and it explains the quest for new ILs exhibiting lower viscosity. The influence of temperature on viscosity is much more important than on density: a strong decrease is observed with increasing temperature^{10,15,17,18} making ILs easier to apply at super-ambient conditions.

Both for densities and viscosities, a comparison of all the data presented in the literature allows one to make some general qualitative conclusions about trends, but a detailed analysis indicates that a quantitative description is much more difficult to make. Particularly, the effect of impurities present in the samples on the measured physico-chemical properties of ILs was put forward by Marsh *et al.*⁸ An exhaustive study of this problem was published by Seddon *et al.*³ with a focus on the influence of chloride and water. The presence of this latter component in an IL sample can indeed greatly modify both the values of thermophysical properties and the reactivity. Even so, very few authors have identified the water quantity in their samples before performing physicochemical measurements. This information is lacking and makes comparison of literature data difficult. Huddleston *et al.*¹⁷ have studied at 298 K water-saturated and dried samples in order to report the effect of the presence of water on several properties of the ILs (melting point, thermal stability, viscosity, surface tension, density...). They have examined how sensitive the physicochemical properties studied are on the water content, an effect that sometimes shifts the results by an order of magnitude. In this context, the preparation of ILs of well-defined purity is absolutely necessary and the development of analytical techniques to quantify major impurities in samples appears to be crucial. Furthermore, care should be taken to avoid contamination of the samples during measurement. For example, Okoturo *et al.*¹⁸ have conducted viscosity measurements in an atmosphere with oxygen and water controlled levels in order to minimise inaccuracies in the measured properties caused by the presence of air or moisture. Without this meticulous analytical work, no definitive conclusions on property-structure relationship in ILs will ever be found.

Scope and objectives of the study

Our aim was to obtain original and highly accurate data on density (ρ) and viscosity (η) as a function of temperature for several ILs and to examine the effect of water content on the

results. Six ILs were chosen for this study: 1-butyl-3-methylimidazolium hexafluorophosphate ($\text{Bmim}^+\text{PF}_6^-$), 1-butyl-3-methylimidazolium tetrafluoroborate ($\text{Bmim}^+\text{BF}_4^-$), 1-butyl-3-methylimidazolium bis(trifluoromethylsulfonyl)imide ($\text{Bmim}^+\text{NTf}_2^-$), 1-ethyl-3-methylimidazolium bis(trifluoromethylsulfonyl)imide ($\text{Emim}^+\text{NTf}_2^-$), 1-ethyl-3-methylimidazolium ethylsulfate ($\text{Emim}^+\text{EtSO}_4^-$) and butyltrimethylammonium bis(trifluoromethylsulfonyl)imide ($\text{N}_{4111}^+\text{NTf}_2^-$).

The first two ILs are commercially available and widely investigated. They were chosen in order to compare our results with numerous data in the literature that present, however, an important dispersion. The NTf_2^- -containing ILs are hydrophobic and chemically stable. They exhibit a wide liquid range even if a recent study of Fox *et al.*¹⁹ indicates that decomposition temperatures were overestimated in previous thermal studies. However, the relatively high cost of the NTf_2^- -containing ILs is a limiting factor for their industrial use. The presence of fluorine in anions that can decompose is, similarly as for PF_6^- and BF_4^- , a real disadvantage for components referred to as green. The hydrophilic ILs containing the EtSO_4^- anion belong to a new generation of fluorine-free ILs valued from an environmental point of view. The imidazolium-based cations were here considered because they are among the most promising ions for applications despite their cost and their somewhat poor chemical stability in the presence of impurities. Finally, one IL with an alkylammonium cation was included as a representative of another class of salt for which very few data are available in the literature. Its higher viscosity compared to ILs with imidazolium ions is, however, a limitation. This selection should allow one to study on one hand the effect of the cation structure for the NTf_2^- -based ILs and, on the other hand, the effect of the anion structure for the imidazolium-based ILs.

Finally, given the importance impurities can have on the physico-chemical properties, the influence of water on the density and the viscosity was also systematically investigated. The experiments were thus performed first with samples carefully dried and then for the four hydrophobic ILs ($\text{Emim}^+\text{NTf}_2^-$, $\text{Bmim}^+\text{NTf}_2^-$, $\text{Bmim}^+\text{PF}_6^-$, $\text{N}_{4111}^+\text{NTf}_2^-$) also with samples saturated with water.

Experimental

Samples

The $\text{Bmim}^+\text{BF}_4^-$ sample was purchased from Sigma Aldrich with a minimum stated mole fraction purity of 0.97 and $\text{Bmim}^+\text{PF}_6^-$ was obtained from Acros Organics with a minimum stated mole fraction purity of 0.999. As they were synthesized from Bmim^+Cl^- , chloride can remain in the samples. The quantity of this anion, measured following the Mohr method, was of 0.01% in mass. The samples of the four other ILs (minimum stated purity of 0.99 in mole fraction) were supplied by the group of P. Wasserscheid (University of Erlangen-Nürnberg, Germany). The $\text{Bmim}^+\text{NTf}_2^-$ and $\text{Emim}^+\text{NTf}_2^-$ were synthesized *via* ion exchange from Bmim^+Cl^- and Emim^+Br^- respectively and have contents of chloride and bromide respectively lower than 50 ppm. The last two samples ($\text{N}_{4111}^+\text{NTf}_2^-$ and $\text{Emim}^+\text{EtSO}_4^-$) do not contain any chloride or bromide ions.

In the following sections, an IL sample treated for 15 h at 323 K under vacuum will be referred to as 'dried sample'. It was then conditioned under a nitrogen atmosphere. This inert gas was chosen because of its very low solubility in the ILs investigated.²⁰ To avoid any contact of the sample with atmosphere, a schlenk and a syringe equipped with a luer lock valve were used to measure the water quantity and to load the samples into the instruments. A coulometric Karl–Fisher titration (Mettler Toledo DL31) on water was performed before and after each series of measurements and it was found that there was no variation of the water quantity in the samples. The water-saturated samples were obtained by adding water to the conditioned ILs until the second (aqueous) phase appeared and the water composition in the IL, measured by coulometric Karl–Fisher titration, was constant (typically after 5 days of a gently stirring).

The water contents of the dried and saturated samples are presented in Table 1. Given the high molar masses of the ILs, the water quantity expressed in mole fraction is at least one order of magnitude higher than the corresponding mass fraction. The water quantities in the dried samples are of the order 10^{-4} and 10^{-3} in mass and mole fraction, respectively. The water-saturated samples contain typically between 10^{-2} and 3×10^{-2} of water in mass fraction which corresponds to mole fractions up to 3×10^{-1} .

Measurements

Densities were measured using a U-shape vibrating-tube densimeter (Anton Paar, model DMA 512) operating in a static mode. The temperature was maintained constant to 0.01 K by means of a recirculating bath equipped with a PID temperature controller (Julabo FP40-HP). For measuring temperature a 100 Ω platinum resistance thermometer (precision 0.02 K, accuracy 0.04 K) was used. Its calibration was performed against a 100 Ω platinum resistance Hart Scientific model 1502A. The measured period of vibration (τ) of a U tube is related to the density (ρ) according to: $\rho = A\tau^2 + B$ where A and B are parameters that are a function of temperature. They were determined in the range between 293 and 393 K using air, tridistilled water and aqueous solutions of NaCl (molalities of 1 M and 3 M). These latter two fluids were chosen in order to cover a range of densities corresponding to the density of ILs studied. Measurements were performed with a step of 10 K and at least three independent values were obtained at each temperature. The precision of the density measurement is of the order 10^{-4} g cm⁻³, the results are expected to be accurate to 10^{-3} g cm⁻³.

Table 1 Molar masses (M_{IL}) and water content in mass fractions (w_w) and mole fractions (x_w) of the dried and water saturated ILs

	$M_{\text{IL}}/\text{g mol}^{-1}$	$w_w \times 10^3$		$x_w \times 10^3$	
		Dried	Saturated	Dried	Saturated
Bmim ⁺ PF ₆ ⁻	284.18	0.19	26.8	3.00	303
Bmim ⁺ NTf ₂ ⁻	419.37	0.05	19.9	1.20	321
Bmim ⁺ BF ₄ ⁻	226.03	0.70	Miscible	8.60	Miscible
N ₄₁₁₁ ⁺ NTf ₂ ⁻	396.38	0.07	14.3	1.50	242
Emim ⁺ NTf ₂ ⁻	391.31	0.05	19.8	1.10	305
Emim ⁺ EtSO ₄ ⁻	236.29	0.10	Miscible	1.30	Miscible

The rheometer used (Rheometrics Scientific, SR200) allows measurements from 293 to 393 K at atmospheric pressure and in a wide viscosity range (from 1 to 3000 mPa s) depending on the geometry of the vessel used. A couette geometry (concentric cylinders) was chosen for this study. Temperature was maintained constant to 0.01 K by means of a recirculating bath similar to that used for the densimeter and was measured with the same accuracy. To avoid any water contamination of the sample during the measurement, the rheometer was placed inside a glove-box in an isolating atmosphere of purified and dried air. The rheometer was calibrated with an oil of known viscosity (viscosity standard oil from Brookfield, 95 mPa s at 298 K). Measurements were performed with a step of 10 K and at least three independent values were obtained at each temperature. A statistical analysis of our results indicates a precision in the viscosities of 0.2% and an expected overall uncertainty lower than 1%.

Results and discussion

Densities

The densities of the six dried samples were first obtained as a function of temperature from 293 K to 393 K. The four hydrophobic ILs were then saturated with water, as described above, and their density was remeasured from 293 K to 343 K. We have decided not to measure the density of these samples at higher temperatures to avoid changes in the composition of the sample due to the vaporization of water. Below 343 K, the vapor pressure of water is sufficiently low (less than 0.031 MPa) to consider this change in composition as negligible. For the six ILs studied, the experimental densities of the dried and saturated samples are presented in Table 2.

For the dried ILs, the values vary typically from 1.20 to 1.53 g cm⁻³ at 293 K and from 1.13 to 1.43 g cm⁻³ at 393 K. As expected, the densities are related to the molar masses of the ions and ILs containing heavy atoms are in general denser as is observed for those composed of NTf₂⁻ when compared to those with PF₆⁻. Similarly, the IL containing the latter is denser compared to that containing BF₄⁻. This is not however valid for strongly asymmetric cations; the density decreases with increasing length of the alkyl chain on the imidazolium cation. Such trends are well documented in the literature.^{8,10,15,21,22}

The densities of the water-saturated ILs are somewhat lower when compared with the dried samples; the observed difference, of 1 to 2%, is almost negligible from the practical point of view. This minor change in density with water content appears to be largely independent of temperature.

In the temperature range studied, the density decreases linearly with temperature for both dried and water-saturated ILs. Fig. 1 illustrates this for the dried samples. A linear equation was used to express the correlation with temperature:

$$\rho \text{ (g cm}^{-3}\text{)} = a + b(T/\text{K} - 273.15) \quad (1)$$

The characteristic parameters a and b for temperature in K are given in Table 3.

It is also of interest to express the volumetric behaviour of ILs in terms of molar volume $V_m = M/\rho$ reflecting the size of

Table 2 Experimental densities (ρ) of dried and water saturated ILs as a function of temperature at atmospheric pressure

Bmim ⁺ PF ₆ ⁻				Bmim ⁺ NTf ₂ ⁻				Bmim ⁺ BF ₄ ⁻	
Dried		Saturated		Dried		Saturated		Dried	
T/K	$\rho/\text{g cm}^{-3}$	T/K	$\rho/\text{g cm}^{-3}$	T/K	$\rho/\text{g cm}^{-3}$	T/K	$\rho/\text{g cm}^{-3}$	T/K	$\rho/\text{g cm}^{-3}$
292.87	1.3705	292.88	1.3539	292.88	1.4431	292.9	1.4279	292.89	1.2048
302.73	1.3620	302.63	1.3451	302.80	1.4334	302.81	1.4178	302.77	1.1975
312.69	1.3535	312.53	1.3358	312.79	1.4239	312.79	1.4071	312.71	1.1900
322.69	1.3451	322.49	1.3278	322.81	1.4144	322.77	1.3980	322.72	1.1830
332.65	1.3370	332.44	1.3194	332.54	1.4048	332.50	1.3881	332.71	1.1760
342.58	1.3287	342.32	1.3114	342.72	1.3949	342.67	1.3791	342.67	1.1694
352.31	1.3209			352.31	1.3866			352.31	1.1611
373.34	1.3043			373.34	1.3668			373.33	1.1465
391.27	1.2902			391.28	1.3510			391.28	1.1345
N ₄₁₁₁ ⁺ NTf ₂ ⁻				Emim ⁺ NTf ₂ ⁻				Emim ⁺ EtSO ₄ ⁻	
Dried		Saturated		Dried		Saturated		Dried	
T/K	$\rho/\text{g cm}^{-3}$	T/K	$\rho/\text{g cm}^{-3}$	T/K	$\rho/\text{g cm}^{-3}$	T/K	$\rho/\text{g cm}^{-3}$	T/K	$\rho/\text{g cm}^{-3}$
292.97	1.3966	292.86	1.3892	292.79	1.5235	292.87	1.5042	292.8	1.2430
302.84	1.3878	302.62	1.3800	302.68	1.5134	302.64	1.4936	302.71	1.2369
312.82	1.3788	312.50	1.3701	312.64	1.5034	312.54	1.4827	312.66	1.23050
322.81	1.3701	322.47	1.3616	322.62	1.4932	322.47	1.4728	322.65	1.2241
332.75	1.3613	332.43	1.3527	332.58	1.4834	332.21	1.4627	332.61	1.2176
342.67	1.3528	342.32	1.3441	342.49	1.4738	342.33	1.4529	342.51	1.2111
352.31	1.3422			352.32	1.4638			352.30	1.2075
373.33	1.3249			373.33	1.4429			373.33	1.1946
391.27	1.3104			391.29	1.4263			391.27	1.1838

the ions. The molar volumes of the dried and water-saturated samples, obtained from the densities calculated *via* eqn (1), are presented at 293 K and 343 K in Table 4.

In the case of samples saturated with water the molar mass of the ILs ($M_{\text{IL}}^{\text{sat}}$) was corrected because of the presence of water as:

$$M_{\text{IL}}^{\text{sat}} = M_{\text{IL}}(1 - x_w) + M_w x_w \quad (2)$$

where M_w is the molar mass of water. The values vary between 190 and 300 $\text{cm}^3 \text{mol}^{-1}$ for the dried samples and are 20 to 30% lower in the case of water-saturated samples, depending

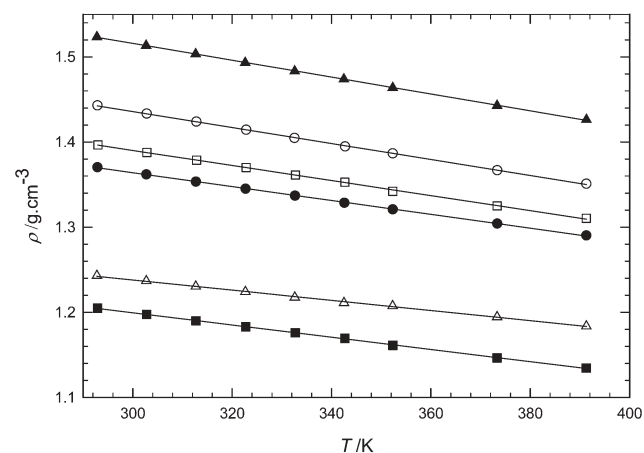


Fig. 1 Experimental densities of the dried ILs as a function of temperature: (●), Bmim⁺PF₆⁻; (○), Bmim⁺NTf₂⁻; (■), Bmim⁺BF₄⁻; (□), N₄₁₁₁⁺NTf₂⁻; (▲), Emim⁺NTf₂⁻; (△), Emim⁺EtSO₄⁻. The lines correspond to the fit of the data by eqn (1).

on the water content. When comparing the molar volumes of the different dried ILs studied it is obvious that the molar mass governs the molar volume. Indeed, Bmim⁺NTf₂⁻ having the highest molar mass ($M_{\text{IL}} = 419.4 \text{ g mol}^{-1}$) exhibits the highest molar volume among the investigated ILs.

Both in the cases of the dried and water-saturated ILs, a logical increase of V_m with increasing temperature was observed. The evolution of the volumetric properties with temperature can be expressed by calculating the coefficient of thermal expansion, α_p , defined as

$$\alpha_p = \frac{1}{V} \left(\frac{\partial V}{\partial T} \right)_p = - \frac{1}{\rho} \left(\frac{\partial \rho}{\partial T} \right)_p \quad (3)$$

Table 3 Correlation parameters a and b and standard deviation σ for the density of dried and water-saturated ILs as a function of temperature determined from measurements between 293 K and 393 K for the dried samples and between 293 K and 343 K for the water-saturated samples

		$a/\text{g cm}^{-3}$	$b/10^{-4} \text{ g cm}^{-3} \text{ K}^{-1}$	$\sigma/10^{-4} \text{ g cm}^{-3}$
Bmim ⁺ PF ₆ ⁻	Dried	1.3859	-8.15	5
	Saturated	1.3703	-8.60	4
Bmim ⁺ NTf ₂ ⁻	Dried	1.4610	-9.38	6
	Saturated	1.4469	-9.80	5
Bmim ⁺ BF ₄ ⁻	Dried	1.2186	-7.17	5
	Saturated	1.4067	-9.10	4
N ₄₁₁₁ ⁺ NTf ₂ ⁻	Dried	1.4139	-8.85	8
	Saturated	1.5425	-9.90	4
Emim ⁺ NTf ₂ ⁻	Dried	1.5242	-10.40	4
	Saturated	1.2541	-5.98	8

$$a \sigma = \left(\frac{\sum (\rho_i^{\text{exp}} - \rho_i^{\text{cal}})^2}{n - v} \right)^{0.5} \quad \text{where } n \text{ is the number of experimental points, } v \text{ the number of adjustable parameters.}$$

Table 4 Calculated molar volumes ($V_m/\text{cm}^3 \text{mol}^{-1}$) and the coefficients of the thermal expansion ($\alpha_p/\text{cm}^3 \text{mol}^{-1}$) of dried and water-saturated ILs at 293.15 K and 343.15 K

T/K	Bmim ⁺ PF ₆ ⁻				Bmim ⁺ NTf ₂ ⁻				Bmim ⁺ BF ₄ ⁻	
	$V_m/\text{cm}^3 \text{mol}^{-1}$		$\alpha_p/10^{-4} \text{K}^{-1}$		$V_m/\text{cm}^3 \text{mol}^{-1}$		$\alpha_p/10^{-4} \text{K}^{-1}$		$V_m/\text{cm}^3 \text{mol}^{-1}$	$\alpha_p/10^{-4} \text{K}^{-1}$
	Dried	Saturated	Dried	Saturated	Dried	Saturated	Dried	Saturated	Dried	
293.15	207	150	5.95	6.35	291	204	6.51	6.90	188	5.95
343.15	214	155	6.13	6.55	301	211	6.72	7.15	193	6.13
T/K	N ₄₁₁₁ ⁺ NTf ₂ ⁻				Emim ⁺ NTf ₂ ⁻				Emim ⁺ EtSO ₄ ⁻	
	$V_m/\text{cm}^3 \text{mol}^{-1}$		$\alpha_p/10^{-4} \text{K}^{-1}$		$V_m/\text{cm}^3 \text{mol}^{-1}$		$\alpha_p/10^{-4} \text{K}^{-1}$		$V_m/\text{cm}^3 \text{mol}^{-1}$	$\alpha_p/10^{-4} \text{K}^{-1}$
	Dried	Saturated	Dried	Saturated	Dried	Saturated	Dried	Saturated	Dried	
293.15	284	220	6.34	6.56	257	185	6.50	6.91	190	4.82
343.15	293	227	6.55	6.78	266	191	6.72	7.16	195	4.94

The values of α_p for the dried and saturated samples calculated at 293 K and 343 K from the fitted densities are presented in Table 4. Since the densities decrease linearly with temperature it is obvious that α_p values are positive increasing with temperature. The values obtained vary between 5×10^{-4} and $7 \times 10^{-4} \text{K}^{-1}$ in the case of dried samples, and are up to 7% higher for the water-saturated samples. Values for α_p of the same order of magnitude ($5\text{--}6 \times 10^{-4} \text{K}^{-1}$) were reported by Gu and Brennecke¹⁴ for several ILs containing BF₄⁻ and PF₆⁻ anions and imidazolium and pyridinium-based cations. The trends observed for the densities can be also noticed in the thermal expansion coefficients. The imidazolium-based ILs exhibit a higher thermal expansion than the ammonium-based IL. The results also suggest that the presence of the NTf₂⁻ anion strongly increases the thermal expansion coefficient compared to the other anions. The presence of the EtSO₄⁻ anion seems to yield a smaller thermal expansion coefficient, the difference between α_p for Emim⁺ NTf₂⁻ and Emim⁺EtSO₄⁻ being about 30%.

Viscosities

A second series of measurements, analogous to those for densities, allowed us to obtain dynamic viscosities of dried and water-saturated samples. For the ILs studied we have first observed that the viscosity remains constant with increasing shear rates (from 0 to 200 s⁻¹). This linear relationship between the shear stress and the shear rate corresponds to a Newtonian behaviour. This seems to be consistent with the findings of Huddleston *et al.*¹⁷ and Seddon *et al.*¹⁰ They reported a Newtonian behaviour for ILs of alkylimidazolium BF₄⁻ family (with the alkyl chain length between 4 and 8 carbon atoms) while the ILs with longer alkyl chains (number of carbon atoms typically 12) are thixotropic fluids whose viscosity decreases when increasing the shear rate.

In Table 5 are presented the experimental viscosities of the dried samples from 293 K to 388 K and those of the water-saturated samples from 293 K to 343 K. The viscosity was not measured at higher temperatures on these samples since the results would be affected by vaporization of water. The trends in the evolution of viscosity with the structure of the cations and the anions are in many aspects inverse to those observed for density. The NTf₂⁻ anion lowers the viscosity compared to

the other investigated anions. Particularly the contribution of the PF₆⁻ anion to the viscosity increase is exceptionally strong. On the basis of a similar analysis to that for density, it can be concluded that the EtSO₄⁻ anion increases viscosity compared to the BF₄⁻ anion. These differences in viscosities are one of the reasons behind the recent development of many NTf₂⁻-based ILs which are relatively less viscous compared to ILs containing other anions.

The alkylammonium-based IL exhibits a higher viscosity than the imidazolium-based ILs with the same anion; furthermore, the viscosity of the latter ILs increases with the length of the alkyl chain on the imidazolium ring. This is a somewhat surprising result, since one would expect at first view that, as the side-chain length increases, the overall contribution of the strong, associating, electrostatic (and hydrogen-bond) terms to the interactions diminishes, while the contribution of weaker, non-associating, dispersion forces increases. As a consequence, it could be anticipated that the viscosity would decrease as the size of the non-polar part of the cations becomes larger. Evidently, this is not the case and this observation has been discussed in the literature by several authors.^{11,16} The justification put forward by Bonhôte *et al.*¹⁶ is that it is the increase in the van der Waals interactions due to the presence of a long alkyl chain that leads to higher viscosities. However, this argument seems to come from a simple correlation of what is observed, not having a strong molecular basis. The study of Tokuda *et al.*¹¹ is more profound, since it relates the behaviour of the transport properties, viscosity and diffusion, to a ratio of ionic conductivities that can be interpreted as a measure of ionic dissociation or “ionicity”. These authors observe that the “ionic dissociation” is directly related to the diffusion coefficient, and inversely related to the viscosity, and they attribute this to a preponderance of the effect of the Van der Waals interactions over electrostatic terms. Computer simulations performed in our group²³ would lead to a different interpretation of the reasons behind this dependence on the alkyl chain length. Simulations have shown that imidazolium ILs with side chains above butyl (and up to C₁₂) exist in the pure liquid phases as microstructured fluids, in which non-polar domains are formed by the alkyl chains and, at the same time, the charged parts form ionic domains which tend to be continuous (channels). Such microstructuring has been

Table 5 Experimental viscosities (η) of dried and water saturated ILs as a function of temperature at atmospheric pressure

Bmim ⁺ PF ₆ ⁻				Bmim ⁺ NTf ₂ ⁻				Bmim ⁺ BF ₄ ⁻	
Dried		Saturated		Dried		Saturated		Dried	
T/K	η /mPa s	T/K	η /mPa s	T/K	η /mPa s	T/K	η /mPa s	T/K	η /mPa s
293.59	375.9	296.73	84.8	293.40	59.8	293.33	32.0	293.67	109.2
302.61	209.1	302.97	60.9	302.93	40.6	302.84	22.4	303.22	75.4
312.21	135.0	312.34	41.5	312.45	28.7	312.41	17.0	312.74	50.0
321.95	91.6	322.03	30.8	321.88	21.5	322.00	13.3	322.00	35.1
331.45	60.3	331.49	23.8	331.12	16.2	331.26	10.9	331.56	24.9
340.94	43.1	340.92	17.7	340.66	12.4	340.73	8.7	341.04	19.1
350.29	32.0			350.47	9.6			350.47	14.8
360.16	24.2			359.66	7.5			359.81	11.8
369.55	16.8			368.87	6.2			369.15	9.4
378.90	14.0			377.93	5.1			378.38	7.4
388.19	12.8			387.51	4.2			388.04	5.8
N ₄₁₁₁ ⁺ NTf ₂ ⁻				Emim ⁺ NTf ₂ ⁻				Emim ⁺ EtSO ₄ ⁻	
Dried		Saturated		Dried		Saturated		Dried	
T/K	η /mPa s	T/K	η /mPa s	T/K	η /mPa s	T/K	η /mPa s	T/K	η /mPa s
293.79	140.7	293.77	72.6	293.39	40.1	296.06	21.9	296.80	107.7
303.31	85.5	303.00	43.4	303.48	28.7	303.47	16.8	303.52	78.5
312.91	56.5	312.24	29.8	313.03	21.1	312.85	13.4	313.05	52.2
322.54	40.0	321.68	21.7	322.59	16.2	322.06	10.8	322.51	36.3
331.91	29.1	331.29	15.6	332.12	12.7	331.51	8.7	331.97	26.6
341.39	21.0	341.25	13.3	341.45	10.3	341.32	7.2	341.41	20.3
350.72	16.0			350.79	8.5			350.81	15.8
359.86	12.9			360.16	7.2			360.20	12.6
368.90	10.7			369.23	6.2			369.06	10.6
378.15	8.4			378.90	5.0			378.90	8.6
388.51	6.6			388.19	4.1			388.19	7.2

suggested by Dupont *et al.*^{24,25} to explain the properties of ILs containing dissolved water. The dual nature of the interactions (nonpolar-dispersive and ionic domains) has also been reported connected to the use of ILs as stationary phases for gas chromatography.²⁶

This segregation into domains is not observed for Emim⁺-based ILs,²³ since the non-polar part is too small, and in structural terms these just show charge ordering like "simple molten salts".²⁷ The formation of the microstructures is likely to be responsible for the increase in viscosity and for the decrease in ion mobility (meaning a decrease in conductivity and in diffusion). Therefore, it is not a strong interaction between the non-polar parts that is giving rise to a more viscous fluid. In ILs with longer side-chains, the non-polar parts are being driven into domains, excluded by the strong electrostatic attraction between the anions and charged parts of the cations.

The presence of water strongly decreases the viscosity of the sample (see Table 5). This phenomenon is particularly dramatic in the case of the more viscous IL, Bmim⁺PF₆⁻ for which the viscosity at 293 K is four times lower in the saturated sample compared to the viscosity in the dried one. For the other ILs investigated the viscosity drops roughly twice.

As illustrated in Fig. 2, in the temperature range studied, the viscosity drastically decreases with increasing temperature. It is again most striking for dried Bmim⁺PF₆⁻, 30 times more viscous at 293 K than at 388 K. At room temperature we can observe great differences in the data measured for the investigated ILs (from 40 to 376 mPa s at 293 K for the dried samples and from 22 to 85 mPa s at the same temperature for

the water-saturated samples) whereas at higher temperature all the ILs tend to have closer viscosities (from 4 to 13 mPa s at 388 K for the dried samples). Thus it is obvious that as the viscosity decreases with temperature the effect of water is much less important, as documented in Table 5.

The most commonly used equation to correlate the variation of viscosity with temperature is the Arrhenius-like law:

$$\eta = \eta_{\infty} \exp(-E_a/RT) \quad (4)$$

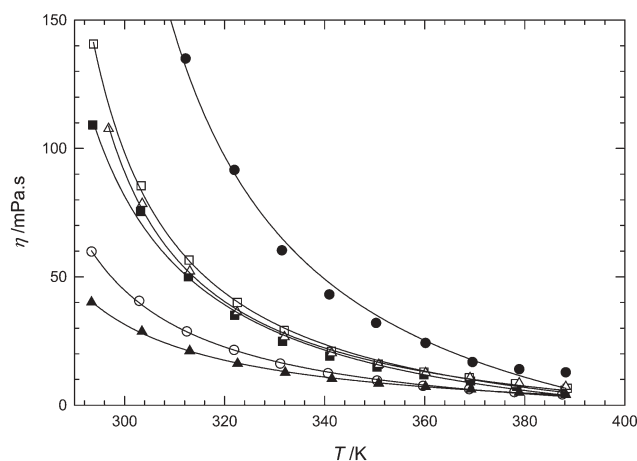


Fig. 2 Experimental viscosities of the dried ILs as a function of temperature: (●), Bmim⁺PF₆⁻; (○), Bmim⁺NTf₂⁻; (■), Bmim⁺BF₄⁻; (□), N₄₁₁₁⁺NTf₂⁻; (▲), Emim⁺NTf₂⁻; (△), Emim⁺EtSO₄⁻. The lines correspond to the fit of the data by eqn (5).

Table 6 Correlation parameters of the Arrhenius equation (η_∞ , E_a), and of the VFT equation (k , A and T_0) with the deviations of the fit σ_r for the viscosity of dried and water saturated ILs as a function of temperature determined from measurements between 293 K and 388 K

		Arrhenius eqn (4)			VFT eqn (5)			
		$\eta_\infty/10^{-4}$ mPa s	$-E_a/kJ$ mol $^{-1}$	σ_r	k/K	$A/10^{-3}$ mPa s K $^{-1/2}$	T_0/K	σ_r
Bmim $^+$ PF $_6^-$	Dried	2.72	34.1	0.08	1320	2.43	148	0.04
	Saturated	6.24	29.0	0.04	512	27.6	198	0.02
Bmim $^+$ NTf $_2^-$	Dried	10.59	26.6	0.02	2240	0.21	62.7	0.01
	Saturated	31.20	22.4	0.03	579	15.1	173	0.01
Bmim $^+$ BF $_4^-$	Dried	6.62	29.2	0.04	1970	0.41	89.6	0.02
	Saturated	5.70	30.1	0.06	1340	1.75	135	0.02
N $_{4111}^+$ NTf $_2^-$	Dried	3.10	30.0	0.07	290	56.1	227	0.02
	Saturated	43.39	22.2	0.03	1620	1.11	81.8	0.02
Emim $^+$ NTf $_2^-$	Dried	54.62	20.3	0.02	591	13.7	165	0.02
	Saturated	10.81	28.1	0.06	945	5.68	162	0.01

$^a \sigma_r = \left(\frac{\sum ((\eta_i^{\text{exp}} - \eta_i^{\text{cal}})/\eta_i^{\text{cal}})^2}{n - v} \right)^{0.5}$ where n is the number of experimental points, v the number of adjustable parameters.

Viscosity at infinite temperature (η_∞) and the activation energy (E_a) are characteristic parameters generally adjusted from experimental data. According to Seddon *et al.*,¹⁰ the Arrhenius law can generally be applied when the cation presents only a limited symmetry. If it is not the case, and especially in the presence of small and symmetrical cations with low molar mass, the Vogel–Fulcher–Tamman (VFT) equation, an empirical extension of eqn (4), is recommended:^{9,10,18}

$$\eta = AT^{0.5} \exp(k/T - T_0) \quad (5)$$

where A , k and T_0 are adjustable parameters. Table 6 lists the parameters for both equations with the standard relative deviation of the fits (σ_r) which indicates clear improvement of the data fit when using the VFT equation both for dried and saturated samples independently of the ion structure. However, as can be seen both in Table 6 and in Fig. 2, the data fit by the VFT equation is not quite satisfactory for the dried Bmim $^+$ PF $_6^-$.

Comparison with the literature data

As stated above the observed trends in the evolution of density and viscosity are generally consistent with information available in the literature. For a more detailed comparison, we have focused on two ILs: Bmim $^+$ PF $_6^-$ and Bmim $^+$ NTf $_2^-$. The first was selected as it is the most intensively studied IL in the past, and for which multiple data sources are available. The second was examined as an IL frequently considered for various practical applications and popular in theoretical studies. The relative deviations of the densities and viscosities reported by different authors from the fits of our experimental values (eqns (1) and (5)) for the dried samples are presented in Fig. 3 to 6. The deviations are also plotted for our water-saturated samples. All the authors claim to have dried their samples before the measurements; the quantity of water is not, however, always specified. As expected the literature data are generally closer to our data for the dried samples than to those for the wet ILs. Yet it is apparent that in certain cases the differences between the literature data can be attributed to the presence of water.

In the case of Bmim $^+$ PF $_6^-$, both for densities and viscosities, the data presented by Seddon *et al.*¹⁰ on samples containing 76 ppm (w/w) of water, agree reasonably well with our results for the dried sample: they are 0.2 to 0.3% higher for densities and about 10% lower for viscosities. Except for the higher values of Suarez *et al.*²¹ and Blanchard *et al.*,³⁰ all the densities for Bmim $^+$ PF $_6^-$ are within $\pm 0.5\%$ from our data set for the dried samples. Gu and Brennecke¹⁴ have obtained lower densities, which is consistent with the larger amount of water (1500 ppm) they reported for their samples. Furthermore, they estimate the uncertainty of their data to be 0.008 g cm $^{-3}$, so our results are within this error margin. The densities of Bmim $^+$ NTf $_2^-$ that are in better agreement with our results are those presented by Fredlake *et al.*¹² and by Krummen *et al.*²⁸ ($\pm 0.1\%$ from our data set for the dried sample). The densities reported by Dzyuba and Bartsch¹⁵ for both ILs are lower than our data and the difference is increasing with temperature. The quantity of water in the samples is not specified in their paper. In the case of Bmim $^+$ NTf $_2^-$ data of the same authors at 323 K are closer to our values for the water-saturated samples than to

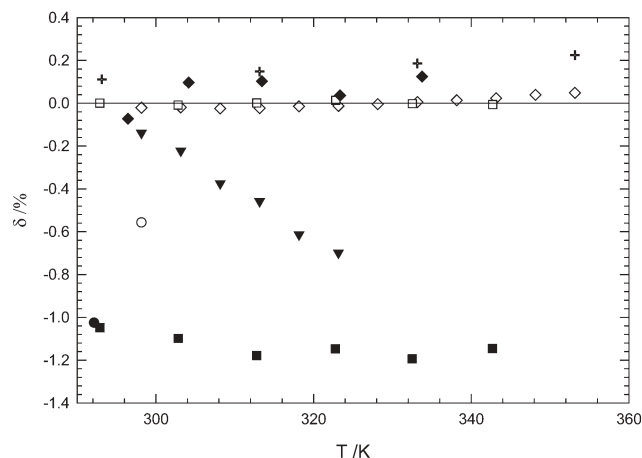


Fig. 3 Relative deviations ($100(\rho_{\text{lit}} - \rho_{\text{fit}})/\rho_{\text{fit}}$) of the literature densities for Bmim $^+$ NTf $_2^-$ from our fitted data for the dried sample: (●), Bonhote *et al.*;¹⁶ (○), Huddleston *et al.*;¹⁷ (◇), Krummen *et al.*;²⁸ (▼), Dzyuba *et al.*;¹⁵ (◆), Fredlake *et al.*;¹² (+), Tokuda *et al.*;¹¹ (■), this work—water saturated IL; (□), this work—dried IL.

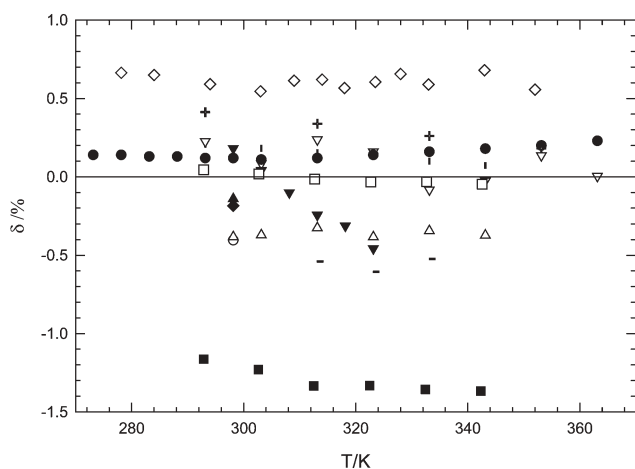


Fig. 4 Relative deviations ($100(\rho_{\text{lit}} - \rho_{\text{fit}})/\rho_{\text{fit}}$) of the literature densities for $\text{Bmim}^+\text{PF}_6^-$ from our fitted data for the dried sample: (\diamond), Suarez *et al.*;²¹ (\circ), Huddleston *et al.*;¹⁷ (\blacktriangle), Hyun *et al.*;²⁹ (\triangle), Gu *et al.*;¹⁴ ($-$), Blanchard *et al.*;³⁰ (\square), Seddon *et al.*;³¹ (∇), Seddon *et al.*;¹⁰ (\blacktriangledown), Dzyuba *et al.*;¹⁵ (\bullet), Harris *et al.*;³² ($+$), Tokuda *et al.*;¹¹ (\blacksquare), this work—water saturated IL; (\square), this work—dried IL.

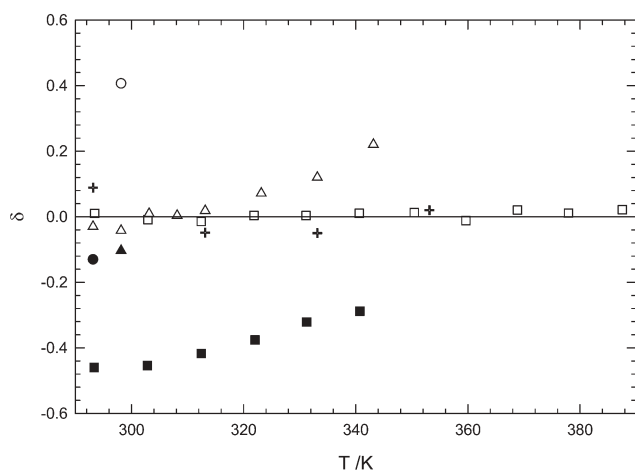


Fig. 5 Relative deviations ($(\eta_{\text{lit}} - \eta_{\text{fit}})/\eta_{\text{fit}}$) of the literature viscosities for $\text{Bmim}^+\text{NTf}_2^-$ from our data fitted with VFT equation for the dried sample: (\bullet), Bonhote *et al.*;¹⁶ (\circ), Huddleston *et al.*;¹⁷ (\blacktriangle), Hyun *et al.*;²⁹ (\triangle), Okoturo *et al.*;¹⁸ ($+$), Tokuda *et al.*;¹¹ (\blacksquare), this work—water saturated IL; (\square), this work—dried IL.

those for the dried ones. This could be due to an increase of the water quantity in their samples, kept in contact with atmosphere during measurements.

Concerning the viscosities, for both ILs important differences between individual authors are observed, especially for $\text{Bmim}^+\text{PF}_6^-$ at low temperatures. Considering the strong dependence of viscosity on temperature, the discrepancies could be also attributed (beside the presence of water) to problems of temperature control and its determination. For example, Okoturo *et al.*¹⁸ reported a viscosity of 201 mPa s for $\text{Bmim}^+\text{NTf}_2^-$ at 293 K compared to 378 mPa s for our dried sample, which corresponds to a difference of 47%. At higher temperatures, these differences are generally reduced to 20% or so. At low temperatures, Okoturo *et al.*¹⁸ obtains for $\text{Bmim}^+\text{PF}_6^-$ the data which are between the values for our

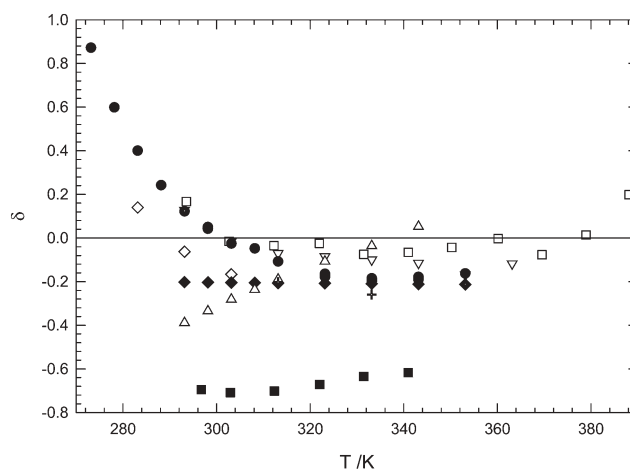


Fig. 6 Relative deviations ($(\eta_{\text{lit}} - \eta_{\text{fit}})/\eta_{\text{fit}}$) of the literature viscosities for $\text{Bmim}^+\text{PF}_6^-$ from our data fitted with VFT equation for the dried sample: (∇), Seddon *et al.*;¹⁰ (\diamond), Branco *et al.*;³³ (\blacklozenge), Fadeev *et al.*;³⁴ (\triangle), Okoturo *et al.*;¹⁸ (\bullet), Harris *et al.*;³² ($+$), Tokuda *et al.*;¹¹ (\blacksquare), this work—water saturated IL; (\square), this work—dried IL.

dried and water-saturated samples, while at higher temperatures their viscosities cross our data and eventually become higher. Finally, the lower densities and higher viscosities reported by Huddleston *et al.*¹⁷ suggest the presence of a higher quantity of chloride in their samples.

Due to this comparison with a wide variety of data sources for $\text{Bmim}^+\text{PF}_6^-$ and for $\text{Bmim}^+\text{NTf}_2^-$ it can be supposed that our results for all of the investigated salts are free of important systematic errors and our uncertainty estimates are realistic. At the same time we have quantified the effect of water on the density and viscosity results.

Conclusion

This paper presents a collection of experimental densities and viscosities for a selection of six hydrophobic and hydrophilic ILs. The aim was to provide practical information on the evolution of these two properties with temperature and with the water presence in the samples, the relationship property–ion structure was also examined qualitatively. In the temperature range investigated, the densities are little affected by the temperature while viscosities decrease dramatically when increasing temperature. While the evolution of the volumetric properties of ILs with the presence of water is almost negligible (1–2%), it strongly decreases the viscosity of the samples. It was also found that some analogies can be drawn in the changes of density, thermal expansivity and viscosity with the structure of cations and anions. Finally, this study highlighted the disparity in the experimental data presented in the literature, that is mainly due to the differences in the sample purities.

Acknowledgements

The authors thank the group of P. Wasserscheid from Erlangen-Nurnberg University for supplying the IL samples and the MSD-Chibret company for the donation of the rheometer. This study is a part of a CNRS–DFG cooperation

project between France and Germany and is also supported by the ADEME France (PhD grant of J.J.).

References

- P. Wasserscheid and T. Welton, *Ionic Liquids in Synthesis*, Wiley-VCH, 2003.
- R. E. Baltus, R. M. Counce, B. H. Culbertson, H. Luo, D. W. DePaoli, S. Dai and D. C. Duckworth, *Sep. Sci. Technol.*, 2005, **40**, 525–541.
- K. R. Seddon, A. Stark and M. J. Torres, *Pure Appl. Chem.*, 2000, **72**, 12, 2275.
- R. A. Mantz and P. C. Trulove, in *Ionic Liquids in Synthesis*, ed. P. Wasserscheid and T. Welton, Wiley-VCH, 2003, pp. 56–68.
- H. Matsumoto, M. Yanagida, K. Tanimoto, M. Nomura, Y. Kitagawa and Y. Miyazaki, *Chem. Lett.*, 2000, 922.
- J. Sun, M. Forsyth and D. R. MacFarlane, *J. Phys. Chem. B*, 1998, **102**, 8858.
- P. Scovazzo, A. E. Visser, J. H. Davis, R. D. Rogers, C. A. Koval, D. L. Dubois and R. D. Noble, Supported Ionic Liquid Membranes and Facilitated Ionic Liquid Membranes, ed. R. D. Rogers and K. R. Seddon, *Ionic Liquids: Industrial Applications to Green Chemistry*, ACS Symposium Series 818, Washington, DC, 2002, pp. 69–87.
- K. N. Marsh, J. A. Boxall and R. Lichtenthaler, *Fluid Phase Equilib.*, 2004, **219**, 93.
- J. S. Wilkes, *J. Mol. Catal. A: Chem.*, 2004, **214**, 11.
- K. R. Seddon, A. S. Stark and M.-J. Torres, Viscosity and density of 1-alkyl-3-methylimidazolium ionic liquids, ed. R. D. Rogers and K. R. Seddon, *Ionic Liquids III: Fundamentals, Progress, Challenges, and Opportunities*, ACS Symposium Series 901, Washington DC, 2004.
- H. Tokuda, K. Hayamizu, K. Ishii, Md. A. B. H. Susan and M. Watanabe, *J. Phys. Chem. B*, 2005, **109**, 6103.
- C. P. Fredlake, J. M. Crosthwaite, D. G. Hert, S. N. V. K. Aki and J. F. Brennecke, *J. Chem. Eng. Data*, 2004, **49**, 954.
- G. J. Kabo, A. V. Blokhin, Y. U. Paulechka, A. G. Kabo, M. P. Shymanovich and J. W. Magee, *J. Chem. Eng. Data*, 2004, **49**, 453.
- Z. Gu and J. F. Brennecke, *J. Chem. Eng. Data*, 2002, **47**, 339.
- S. V. Dzyuba and R. A. Bartsch, *ChemPhysChem*, 2002, **3**, 161.
- P. Bonhôte, A.-P. Dias, N. Papageorgiou, K. Kalyanasundaram and M. Gratzel, *Inorg. Chem.*, 1996, **35**, 1168.
- J. G. Huddleston, A. E. Visser, W. M. Reichert, H. D. Willauer, G. A. Broker and R. D. Rogers, *Green Chem.*, 2001, **3**, 156.
- O. O. Okoturo and T. J. VanderNoot, *J. Electroanal. Chem.*, 2004, **568**, 167.
- D. M. Fox, W. H. Awad, J. W. Gilman, P. H. Maupin, H. C. De Long and P. C. Trulove, *Green Chem.*, 2003, **5**, 6, 724.
- J. Jacquemin, M. F. Costa Gomes, P. Husson and V. Majer, *J. Chem. Thermodyn.*, 2006 in press.
- P. A. Z. Suarez, S. Einloft, J. E. L. Dullius, R. F. de Souza and J. Dupont, *J. Chim. Phys.*, 1998, **95**, 1626.
- H. Tokuda, K. Hayamizu, K. Ishii, Md. A. B. H. Susan and M. Watanabe, *J. Phys. Chem. B*, 2004, **108**, 16593.
- A. A. H. Pádua, Solvation in ionic liquids: conformations, interactions and liquid structure by molecular simulation, 1st Int. Congress on Ionic Liquids (COIL), Salzburg, Austria, June 19–22, 2005.
- U. Schröder, J. D. Wadhawan, R. G. Compton, F. Marken, P. A. Z. Suarez, C. S. Consorti, R. F. de Souza and J. Dupont, *New J. Chem.*, 2000, **24**, 1009.
- J. Dupont, *J. Braz. Chem. Soc.*, 2004, **15**, 341.
- J. L. Anderson and D. W. Armstrong, *Anal. Chem.*, 2003, **75**, 4851.
- J. P. Hansen and I. R. McDonald, *Theory of Simple Liquids*, Academic Press, London, 2nd edn, 1986.
- M. Krummen, P. Wasserscheid and J. Gmehling, *J. Chem. Eng. Data*, 2002, **47**, 1411.
- B. R. Hyun, S. V. Dzyuba, R. A. Bartsch and E. L. Quitevis, *J. Phys. Chem. A*, 2002, **106**, 7579.
- L. A. Blanchard, Z. Gu and J. F. Brennecke, *J. Phys. Chem. B*, 2001, **105**, 2437.
- K. R. Seddon and M. J. Torres, *Clean Solvents*, ed. L. Moens and M. A. Abrahams, ACS Symposium Series, 2001, p. 819.
- K. R. Harris, L. A. Woolf and M. Kanakubo, *J. Chem. Eng. Data*, 2005, **50**, 1777.
- L. C. Branco, J. N. Rosa, J. J. Moura Ramos and C. A. M. Afonso, *Chem.—Eur. J.*, 2002, **8**, 16, 3671.
- A. G. Fadeev and M. M. Meagher, *Chem. Commun.*, 2001, 295.

An organic solvent free process for the demethylation of 4-(4-methoxyphenyl)butanoic acid

Laurent Delhaye,^a Khalid Diker,^a Thomas Donck^{†,b} and Alain Merschaert^{*a}

Received 26th August 2005, Accepted 21st November 2005

First published as an Advance Article on the web 8th December 2005

DOI: 10.1039/b512176k

A mild and efficient organic solvent free process has been developed for the synthesis of 4-(4-hydroxyphenyl)butanoic acid, a key intermediate in the synthesis of LY518674. Thus we have achieved the demethylation of 4-(4-methoxyphenyl)butanoic acid with only a slight excess of aqueous HBr and without phase transfer catalysis. In addition, 4-(4-hydroxyphenyl)butanoic acid is easily obtained by direct crystallization from the reaction mixture.

An efficient large scale process was recently reported for the synthesis of 4-(4-hydroxyphenyl)butanoic acid **2** via demethylation of the corresponding methyl ether **1** with pyridine hydrochloride at 195–200 °C¹ (Fig. 1).

Although a high yield of **2** is obtained, that process suffers from the need to use elevated temperatures and the production of large amounts of aqueous pyridine as waste. A well-known alternative procedure utilizes hydrobromic acid in acetic acid or water at reflux to perform the ether cleavage.² On the other hand, Rolla *et al.* have recently reported a milder protocol that involves phase transfer catalysis.³ A common feature of these methods is the use of a large excess of hydrobromic acid, the environmental impact of which is problematic. We have recently revisited the demethylation of 4-(4-methoxyphenyl)butanoic acid **1** in order to (i) reduce the acid waste stream, (ii) find reaction conditions more compatible with classical pilot plant equipments, (iii) reduce overall production cost, and (iv) improve recovery of the title compound from the reaction mixture.

Our initial screening was aimed to replace hexadecyltributylphosphonium bromide with a cheaper and more readily available phase transfer catalyst.⁴

As illustrated in Table 1, we did not observe dramatic kinetic differences between most of the classical phase transfer catalysts tested. We noticed however that a cheap and readily available catalyst like TBAB (entry 1) gave better results than the previously reported hexadecyltributylphosphonium bromide. More interestingly, a similar result was also observed in the uncatalyzed control reaction (entry 12).

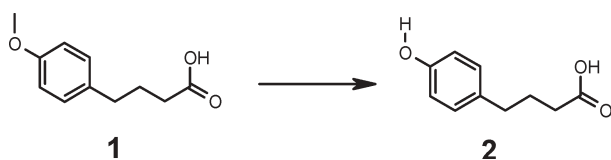


Fig. 1 Synthesis of 4-(4-hydroxyphenyl)butanoic acid.

^aLilly Development Centre S.A., rue Granbonpre 11, 1348, Mont-saint-Guibert, Belgium. E-mail: merschaert_alain@lilly.com; Fax: +32 10 47 63 15; Tel: +32 10 47 70 21

^bHaute Ecole Lucia De Brouckere, Institut Meurice, Avenue Emile Gryzon, 1, B-1070-Bruxelles, Belgium

[†] Present address: av. Albert Béchet 5, 1950, Kraainem, Belgium. E-mail: thomas.donck@standform.be; Tel: +32 27 67 79 01.

We therefore decided to perform a DoE study with the aim to:

- reduce the excess of HBr (major driver of process cost)
- evaluate the utility of phase transfer catalysis

Based on our initial screenings, the limits for the reaction parameters were set as follows:

- *T*^o: between 100 and 115 °C
- excess of 48% aqueous HBr: between 1.1 and 1.5 equiv.
- amount of TBAB: from 0 to 5 mol%

Our objective was to reach more than 98% conversion of **1** within 8 h with less than 2% area total related substances formed. As shown in the DoE summary illustrated below (Chart 1 and Chart 2), these results were achieved using 1.5 equiv. of 48% aqueous HBr at 115 °C. The reaction could also be run with 1.1 equiv. of HBr but in that case, a higher level of an ester by-product was formed (Fig. 2).

The other key conclusion of the DoE study is that the utilization of TBAB does not offer any advantage over the uncatalyzed reaction. The reaction is even more efficient without phase transfer catalyst.

We have then successfully validated the best operating conditions identified in the above DoE study at a larger scale using an overhead stirrer. These reactions gave us also the opportunity to start evaluating the work-up of the reaction and the recovery of **2**. The extractive procedure reported previously by Schmid *et al.*¹ was initially successfully

Table 1 Comparison of phase transfer catalysts (PTC)^a

Entry	PTC ^b	Conversion (%) ^c
1	Tetrabutylammonium bromide	79
2	Tetraethylammonium bromide	62
3	Tetraoctylammonium bromide	51
4	Tetrahexylammonium bromide	69
5	Tetrabutylammonium chloride	50
6	Tetrabutylammonium iodide	39
7	Benzyltriethylammonium bromide	33
8	Benzyltributylammonium chloride	62
9	Hexadecyltributylphosphonium bromide	64
10	Tetrabutylphosphonium bromide	69
11	Tetraphenylphosphonium bromide	44
12	None	61

^a All reactions were run with 10 molar equiv. of 48% aqueous HBr at 100 °C under nitrogen for 2 h using a Radleys[®] carousel.

^b 10 mol%. ^c Area phenol/(area phenol + area ether) at 220 nm.

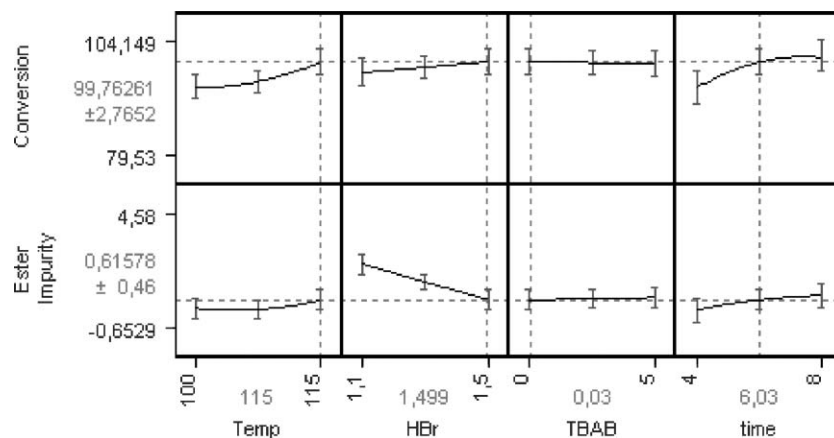


Chart 1 Effects of factors on conversion and impurity.

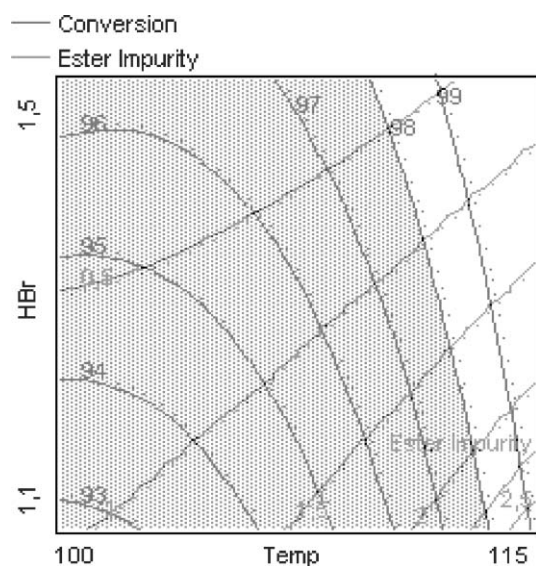


Chart 2 Response surfaces of conversion and impurity after 7 h.

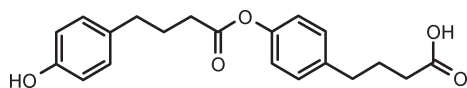


Fig. 2 Major impurity.

reproduced. Thus after extraction with MTBE and stripping with toluene, the desired compound was obtained by crystallization in 95% yield (98.54% area purity). However, we quickly observed that **2** could easily be obtained by direct crystallization after dilution of the reaction mixture with water. Similar results were obtained with a 95 : 5 water/acetone mixture (91% yield, 98.83% area purity) or with water alone (94% yield, 98.5% area purity). Further scale-up of the reaction to 50 g methyl ether gave reproducible results (90–91% yield; 98.5–98.7% area purity).

We have also shown that the highly toxic methylbromide formed in the reaction can be recovered efficiently if a dry-ice trap is added at the outlet of the reactor.

In conclusion, we have developed a greener process potentially useful for the large scale production of

4-(4-hydroxyphenyl)butanoic acid **2**, a key intermediate for the synthesis of LY518674. Up to 95% isolated yield was obtained without using any phase transfer catalyst and organic solvent. We have more recently observed that the procedure is generalisable to other substrates and that work will be reported in due course.

Experimental procedure (50 g). 49.87 g (0.257 mol) of 4-(4-methoxyphenyl)butanoic acid are introduced into a 1 L double-jacketed reactor pre-heated to 75 °C and equipped with a T° controller, anchor stirrer, nitrogen inlet and dry-ice trap. Once the solid is totally melted, 48% aqueous HBr (60 mL, 0.53 mol) is added slowly and the resulting biphasic mixture is heated to 110 °C for 6 h (the reaction is monitored by HPLC). After the reaction is complete, the solution is cooled to 80 °C and diluted with water (465 mL). The solution is seeded with pure 4-(4-hydroxyphenyl)butanoic acid at 45 °C and slowly cooled to 0 °C for 1 h before filtration on a double-jacketed refrigerated filter. The white crystals are washed with cold water (75 mL) and dried at 40 °C under vacuum for 24 h (43.5 g, 94% yield, 98.5% HPLC area purity, ¹H NMR identical to a reference spectrum: ¹H NMR (500 MHz, DMSO-d₆) δ 1.70 (m, 2 H), 2.15 (t, 2 H), 2.45 (t, 2 H), 3.33 (s, 1 H), 6.65 (d, 2 H), 6.95 (d, 2 H). ¹³C NMR (125 MHz, DMSO-d₆) δ 26.5, 32.5, 33.5, 114.6, 129.0, 131.2, 155.3, 174.2).

Acknowledgements

The authors would like to thank Dr Christopher Schmid, Research Advisor Lilly Research Laboratories, for useful discussions and advice.

References

- C. R. Schmid, C. A. Beck, J. S. Cronin and M. A. Staszak, *Org. Process Res. Dev.*, 2004, **35**, 3523.
- M. V. Bhatt and S. U. Kulkarni, *Synthesis*, 1983, 249–282; B.C. Ranu and S. Bhar, *Org. Prep. Proced. Int.*, 1996, **28**, 371–409; D. Papa, E. Schwenk and H. Hankin, *J. Am. Chem. Soc.*, 1947, **69**, 3018–3022; C. S. Yi, L. C. Martinelli and C. DeWitt Blanton, *J. Org. Chem.*, 1978, **43**, 405–407.
- D. Landini, F. Montanari and F. Rolla, *Synthesis*, 1978, 771–773.
- (n-Hexadecyl)tri-n-butylphosphonium bromide: >\$1200 kg⁻¹ (>\$600 mol⁻¹), Lancaster synthesis catalog. Tetra-n-butylammonium bromide: \$145 kg⁻¹ (\$47 mol⁻¹), Lancaster synthesis catalog.

Catalytic pyrolysis of several kinds of bamboos over zeolite NaY

W. Y. Qi, C. W. Hu,* G. Y. Li, L. H. Guo, Y. Yang, J. Luo, X. Miao and Y. Du

Received 25th July 2005, Accepted 6th December 2005

First published as an Advance Article on the web 21st December 2005

DOI: 10.1039/b510602h

The catalytic pyrolysis of four kinds of bamboo, *Neosinocalamus affinis*, *Pubescens*, *Bambusa rigida* and *Dendrocalamus latiflorus*, was performed in a fixed bed reactor in an inert atmosphere of nitrogen at 773 K and 873 K for 10 h using zeolite NaY as catalyst. For *Neosinocalamus affinis* and *Pubescens*, the influence of pyrolysis temperature on the product distribution was also studied over the temperature range of 573–873 K at an interval of 50 K. As the pyrolysis temperature increases, the yield of gaseous products increases, while the yield of liquid products goes through a maximum value, and the amount of residue reduces. For the four kinds of samples, the liquid yield at 873 K increases to 64.1–68.8 wt% in the presence of NaY catalyst, in compared to that of 19.7–53.3 wt% from direct pyrolysis. In addition, the non-catalytic liquid contains numerous species including mainly carboxylic, carbonylic, lactonic, phenolic and furan compounds, while the catalytic liquid contains markedly reduced number of species composed mainly of carboxylic and carbonylic compounds, of which acetic acid is the major component. Scanning Electron Microscopy (SEM), X-Ray Diffraction (XRD) and X-ray Photoelectron Spectroscopy (XPS) were used to characterize the catalysts before and after use at 873 K. The results show that during the pyrolysis the NaY catalyst interacts with the primary pyrolysis intermediates of bamboos and thus leads to *in situ* reconstruction involving the impairment of [111] and [220] planes, and the enhancement of the [311] plane.

1 Introduction

Biomass, including raw materials from the forest, by-products from the timber industry and agricultural waste, is a renewable carbon resource. The use of biomass as a resource to produce simple monomeric compounds will provide a sustainable approach for chemical industry. The consumption of these compounds will cause almost zero or very low net CO₂ emission since the same amounts of carbon and energy are fixed during the biomass growth.^{1–8} Among the available forestry resources capable of providing hydrocarbons, bamboo shows promise for industrial exploitation and utilization because of their worldwide distribution. Furthermore, the growth period of bamboo is usually one year, and this provides an abundant and sustainable supply of raw materials. In addition, bamboo is rich in cellulose which is favorable for the formation of carbonaceous compounds.

Biomass can be converted to useful simple monomeric chemicals by biological or thermo-chemical processes like gasification or pyrolytic liquefaction.⁹ Pyrolysis is a form of hydrocarbon recovery process which potentially produces char, oil and gaseous products, all of which have a potential end use.^{4,10} Pyrolysis oil as a high-value energy carrier and value-added chemicals obtained through thermo-chemical conversion processes are expected to play an important role in future energy and chemical supply. However, the bio-oil

obtained from direct pyrolysis of biomass is highly oxygenated, highly viscous with a poor calorific value, corrosive, thermally unstable, and complex in composition.^{11,12} Thus, the direct substitution of biomass-derived pyrolysis oil for petroleum fuel and chemical feedstock may be limited. Upgrading of bio-oil has been proposed for several years.^{13–16} Zeolites, silica–alumina, molecular sieves and the like were used as cracking catalysts,^{17,18} and the type of zeolite catalyst plays a significant role. The final products obtained depend on the characteristics of the catalyst used: aromatic hydrocarbon products are obtained mostly when strong acid, shape selective HZSM-5 zeolites are used, whereas aliphatic hydrocarbons are produced mostly when HY zeolites and silica–alumina are used.¹¹

In the present work, NaY type zeolite was used as a catalyst for the pyrolysis of bamboo. Four different kinds of typical bamboo, *Neosinocalamus affinis*, *Pubescens*, *Bambusa rigida* and *Dendrocalamus latiflorus* collected from the Sichuan Province of China were selected as raw materials for the experiment.

2 Experimental

2.1 Preparation of solutions for the analysis of the main components of bamboo

HNO₃–HAc mixed solution: 10 ml 65% nitric acid was added to the 100 ml 80% HAc solution, and mixed well.

0.2% C₆H₅NHC₆H₄COOH indicator: 1.0 g C₆H₅NHC₆H₄COOH was put into a mortar, and 5 ml 0.1 M NaOH solution was added and triturated. The mixture was transferred into a 50 ml volumetric flask and diluted with water to the 50 ml scale.

Key Laboratory of Green Chemistry and Technology (Sichuan University), Ministry of Education, College of Chemistry, Sichuan University, Chengdu, Sichuan 610064, China.
E-mail: gchem@scu.edu.cn; chwehu@mail.sc.cninfo.net;
Fax: +86 28 85411105; Tel: +86 28 85411105

Oxalic acid–sulfuric acid mixed solution: 60 g oxalic acid was put into a 1000 ml glass beaker and 800 ml distilled water was added. Then 70 ml 98% H₂SO₄ solution was added and diluted with distilled water to 1000 ml.

Solution A: 75 g Na₂CO₃ was put into a 1000 ml glass beaker and dissolved with 400 ml distilled water. 12 g CuSO₄·5H₂O and 21.5 g tartaric acid were put into another 1000 ml glass beaker and also dissolved with 400 ml distilled water. The mixture in the latter glass beaker was added to the former gradually with stirring. 0.89 g KIO₃ and 8.0 g KI were added to the above mixture and stirred to mix well. The mixture was transferred into a 1000 ml volumetric flask, diluted with water to the scale. The mixture was transferred into a 2000 ml glass beaker and heated for 5 min in boiling water-bath. Then the mixture was left standing for 24 h before use.

2.2 Analysis of the main components of bamboo

The main components of biomass are cellulose, hemi-cellulose and lignin. The contents of cellulose, hemi-cellulose and lignin have a close relationship to the products from the pyrolysis of biomass.¹⁹ The components of bamboo were analyzed using the classical methods as follows:

2.2.1 Determination of cellulose content. The air-dried bamboo samples were milled into powder of 40–60 mesh. Sample (0.05–0.06 g) was put into a centrifuge tube, and then 5 ml HNO₃–HAc mixed solution was added. The mixture was heated in boiling water for 25 min with stirring. Then the mixture was centrifuged. The supernatant was decanted, and the precipitate was washed with distilled water for three times. The washed precipitate was added to 10 ml 0.5 M K₂Cr₂O₇ and 8 ml 98% H₂SO₄ solution before heating in boiling water for 10 min with stirring. Then the reaction mixture was cooled to room temperature, and then transferred into a 250 ml Erlenmeyer flask. Three drops of 0.2% C₆H₅NHC₆H₄COOH indicator was added, and then the mixture was titrated with 0.1 M (NH₄)₂SO₄·FeSO₄ solution to the end point. A blank experiment was also performed. The cellulose content, *x*%, in the bamboo sample was calculated as follows

$$K = 25 \times 0.1/m \quad (1)$$

$$x\% = 0.675 \times K(a - b)/n \quad (2)$$

where *K* is the titer of 0.1 M (NH₄)₂SO₄·FeSO₄ solution, *m* is the volume of 25 ml 0.1 M K₂Cr₂O₇ standard solution for demarcating titer, *a* is the volume of 0.1 M (NH₄)₂SO₄·FeSO₄ solution for the blank experiment, *b* is the volume of 0.1 M (NH₄)₂SO₄·FeSO₄ solution for the sample, and *n* is the sample weight.

2.2.2 Determination of hemi-cellulose content. 0.1–0.2 g air-dried bamboo powder was put into a 100 ml glass beaker to which 15 ml 80% Ca(NO₃)₂ solution was added. Then the glass beaker was covered and heated for 5 min on a hot plate. The reaction mixture was centrifuged. The supernatant was decanted, and the precipitate was washed with hot distilled water for three times. The precipitate was added to 10 ml 2 M HCl solution and heated in a boiling water-bath for 45 min

with stirring. The mixture was centrifuged again to separate the supernatant and the precipitate, which was washed with distilled water for three times, and then the mixture solution, *i.e.*, the supernatant and the three washes, was transferred into a 100 ml volumetric flask after neutralization with 2 M NaOH solution, diluted with water to the 100 ml scale, and then filtered. To an aliquot of 10 ml filtrate, Solution A was added, and heated in a boiling water-bath for 15 min. Then, 5 ml mixed solution of oxalic acid and sulfuric acid solution and 0.5 ml 5% starch were added before titrated with 0.01 M Na₂S₂O₃ solution to the end point. A blank experiment was also performed. The hemi-cellulose content, *x*%, in the bamboo sample was calculated as

$$x\% = 0.9 \times 100 [248 - (a - b)](a - b)/10000 \times \frac{10}{n} \quad (3)$$

where *a* is the volume of 0.01 M Na₂S₂O₃ solution for the blank experiment, *b* is the volume of 0.01 M Na₂S₂O₃ solution for the sample, and *n* is the sample weight.

2.2.3 Determination of lignin content. 0.05–0.10 g air-dried bamboo powder was put into a centrifuge tube and 10 ml 1% acetic acid solution was added. Then, the mixture was centrifuged. The supernatant was decanted, and the precipitate was washed with 5 ml 1% acetic acid and 3 ml acetone thrice. The precipitate was dispersed on the wall of the centrifuge tube and dried in the water-bath. 3 ml 73% H₂SO₄ was added to the dried precipitate with stirring, and the mixture was left to stand for 24 h. Then, 10 ml distilled water was added to the mixture before it was heated for 5 min in boiling water. The mixture was cooled to room temperature, and then 0.5 ml 10% BaCl₂ solution was added and stirred to mix well. Then the mixture was centrifuged, the supernatant was decanted, and the precipitate was washed with distilled water twice. The washed precipitate was added to 10 ml 0.5 M K₂Cr₂O₇ and 8 ml 98% H₂SO₄ solution before heating in boiling water for 15 min with stirring. Then the mixture was cooled to room temperature again, and transferred into a 250 ml Erlenmeyer flask. Three drops of 0.2% C₆H₅NHC₆H₄COOH indicator was added, then titrated with 0.1 M (NH₄)₂SO₄·FeSO₄ solution to the end point. A blank experiment was also performed. The lignin content, *x*%, in the bamboo sample was calculated as

$$K = 25 \times 0.1/m \quad (1)$$

$$x\% = 0.433 \times K(a - b)/n \quad (4)$$

where *K* is the titer of 0.1 M (NH₄)₂SO₄·FeSO₄ solution, *m* is the volume of 25 ml 0.1 M K₂Cr₂O₇ standard solution for demarcating titer, *a* is the volume of 0.1 M (NH₄)₂SO₄·FeSO₄ solution for the blank experiment, *b* is the volume of 0.1 M (NH₄)₂SO₄·FeSO₄ solution for the sample, and *n* is the sample weight.

2.3 Pyrolysis procedure

The pyrolysis of the samples was performed in a fixed bed reactor. Bamboo powder of *Neosinocalamus affinis* or *Pubescens* was heated from room temperature to 573 K, 623 K,

673 K, 723 K, 773 K, 823 K and 873 K, respectively, and kept for 10 h. The catalytic pyrolysis of the four kinds of samples was performed at 773 K and 873 K using the NaY catalyst. The temperature ramp was 10 K min⁻¹ controlled with Temperature Control Specialists (SKW-1000). The volatile products were swept out by nitrogen at a flow rate of 28 ml min⁻¹ and analyzed on-line by packed column gas chromatography (GC7890T: column temp.: 353 K; inlet temp.: 363 K; detector temp.: 393 K). The pyrolysis oil was collected in an ice trap and analyzed by gas chromatography-mass spectrometry (Agilent 5973N GC/MS: column: DB-5; inlet temp.: 523 K; detector temp.: 523 K; He Flow: 0.8 ml min⁻¹; mode: split).

2.4 Characterization of the catalysts

SEM (JEOL-5900, Tokyo, Japan), XRD (X'Pert Pro MPD, Philips, Netherlands) and XPS (XSAM 800, Kratos, England) were used to characterize the fresh and used catalysts. The surface morphology of the catalysts was observed by SEM operated at 20 kV and 20 mA. The distributions of crystallite size of zeolite NaY catalysts were determined by the broadening effect of the XRD patterns. The continuous scanning mode with 0.02 interval and 0.5 s of set time was used to collect the XRD patterns using Cu K α (0.15405 nm) radiation operated at 40 mA and 40 kV over 5–60° in 2-theta. The software based on Warren–Averbach Fourier Transform (W–A/FT) method was used to calculate the distribution of crystallite size of the zeolite NaY. The crystalline structures of NaY were refined with Rietveld method to calculate a series of structure parameters, such as, cell lattice parameters, *a*. The degree of disordering, *A*, of all samples was calculated with the method of Erika Godđólková *et al.*²⁰ In the present work, the fresh sample is assumed to be the reference and assuming its disordering degree to be zero. XPS measurements were performed using Al K α X-ray source at 12 kV and 12 mA.

3 Results and discussion

3.1 The main components of bamboo

Table 1 shows the composition of the main components of the four kinds of bamboo. The content of either cellulose or hemi-cellulose in *Neosinocalamus affinis* is the highest in all the samples, while the lignin content in *Bambusa rigida* is higher than those in the others. Both the content of cellulose and the total content of the three components are the lowest in *Pubescens*. The content of cellulose in *Neosinocalamus affinis* is up to 44.8 wt%, being the highest among the four samples. The total content of the three components varies from about

Table 1 Main components of different kinds of samples/wt%

Sample	Cellulose	Hemi-cellulose	Lignin	Σ^a	Σ^b
<i>Neosinocalamus affinis</i>	44.8	21.8	11.9	66.6	78.5
<i>Bambusa rigida</i>	42.9	15.6	21.7	58.5	80.2
<i>Dendrocalamus latiflorus</i>	40.8	10.5	21.5	51.3	72.8
<i>Pubescens</i>	28.8	19.4	15.3	48.2	63.5

^a The total content of cellulose and hemi-cellulose. ^b The total content of the three components.

64 wt% to 80 wt% in the four kinds of samples. The values are close to the corresponding Σ^a and Σ^b values of 63.7 wt% and 82.9 wt% in rice husk.⁴

3.2 The effect of pyrolysis temperature on the distribution of products

The products from the pyrolysis of *Neosinocalamus affinis* at different final temperatures (573 K, 623 K, 673 K, 723 K, 773 K, 823 K and 873 K) are given in Fig. 1. An increase in yield of the gaseous products is observed with increasing pyrolysis temperature. This is consistent with those reported previously using rice husks, wood and Greek wood as pyrolysis materials.^{4,21,22} It could be attributed predominately to the secondary cracking of the pyrolysis vapour at higher temperature. However, the gaseous products from the pyrolysis of rice husks⁴ consisted largely of CO and CO₂ with lower concentrations of H₂, CH₄, and other hydrocarbons. Whilst in the present work, the gaseous products from the pyrolysis of *Neosinocalamus affinis* consist largely of H₂ with lower concentrations of CO, CO₂ and CH₄. The main products obtained from the pyrolysis of cellulose, hemi-cellulose and lignin at different temperatures have been reported in ref. 19. At lower temperature, the products of CO₂, CO and H₂O were mainly due to the decomposition of hemi-cellulose and the initial stages of cellulose decomposition, while the products of more char, also less CO₂, CO, H₂O and tar were originated from the decomposition of lignin. At higher temperature, the products of oil and other hydrocarbons were due to the later stages of cellulose decomposition and the decomposition of residual hemi-cellulose, while H₂ and CO were produced mainly from lignin. In the present work, H₂ constitutes the main component of the gaseous products with small amounts of CH₄ and CO₂. This implies that the decomposition process of cellulose, hemi-cellulose and lignin in *Neosinocalamus affinis* is different from that in pine wood reported in ref. 19. Though the values of Σ^a and Σ^b in *Neosinocalamus affinis* are near to those of rice husks, the main gaseous products are different. This indicates that the pyrolysis of *Neosinocalamus affinis* may provide more H₂ than other materials.

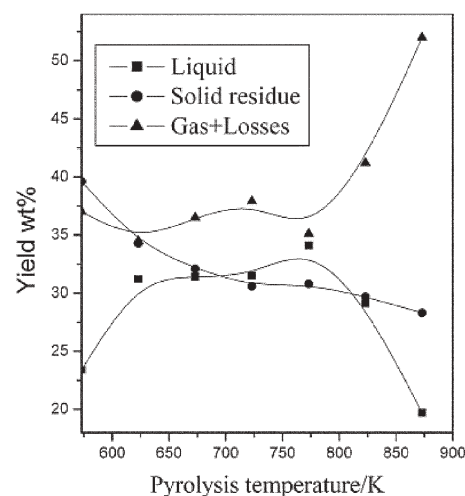


Fig. 1 Yield of products from the pyrolysis of *Neosinocalamus affinis* at different temperatures.

The yield of liquid also depends strongly on the pyrolysis temperature under the selected experimental conditions. Below 623 K, the yield of liquid is low. Above the temperature range of 623 K–773 K, an increase is observed with increasing pyrolysis temperature, and the highest yield of 34.1 wt% is obtained at 773 K. Above 773 K, however, the yield of pyrolytic liquid decreases markedly. The amount of residue reduces gradually (from 39.6 wt% at 573 K to 28.3 wt% at 873 K) with increasing pyrolysis temperature. The decrease in the amount of residue with increasing temperature maybe due to the secondary decomposition of the solid residues from the pyrolysis of *Neosinocalamus affinis* at higher temperatures giving non-condensable gaseous products which will contribute to the increase in gaseous yield.

The compositions of the main components of the pyrolytic liquid obtained from *Neosinocalamus affinis* at different temperature determined by GC/MS are given in Table 2. The results indicate that the content of acetic acid is the highest among the various components obtained, especially over the temperature range of 623–673 K. Over the temperature range tested, the content of acetic acid is the highest compared to that of the other main components. The content of the main components other than acetic acid is generally higher over the temperature range of 623 K–723 K than below 623 K or above 723 K. Comparison of the above data with those reported in the literature²³ shows that the acetic acid content in the pyrolytic liquid of *Neosinocalamus affinis* at lower temperature is more than two times as high as those of rice husks and wood.

A comparison of the influence of temperature on the pyrolytic products from *Neosinocalamus affinis* with those from *Pubescens* is given in Fig. 2 and Fig. 3. The yield of pyrolytic liquid of *Neosinocalamus affinis* is lower than that of *Pubescens* below 623 K; but from 623 K to 773 K, both of them are about 31–34 wt%, and at 823 K, the liquid yield of *Pubescens* reaches its highest value of 37.0 wt%. It shows that the liquid products are more easily to be obtained from *Pubescens*, especially at higher temperatures. For the maximum liquid yield, the optimal temperature for the pyrolysis of *Neosinocalamus affinis* is 773 K while that for *Pubescens* is 823 K. The optimal pyrolysis temperature for the formation of liquid or certain compounds has been reported.^{24,25} For example, the optimal temperature for the pyrolysis of cellulose was 673 K²⁴ to obtain macromolecules; at the optimal pyrolysis temperature of 823 K,²⁵ the liquid product yield from the pyrolysis of rice straw had a highest value of 27.26 wt%. This indicates that both the raw material and the

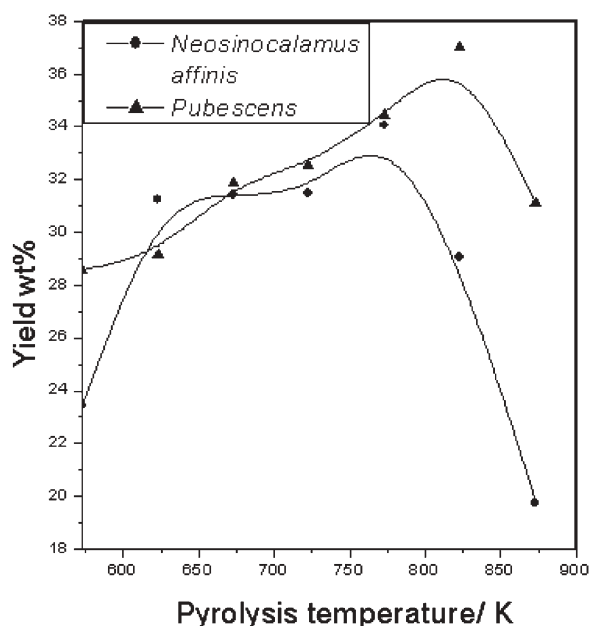


Fig. 2 Yield of liquid from the pyrolysis of *Neosinocalamus affinis* and *Pubescens* at different temperatures.

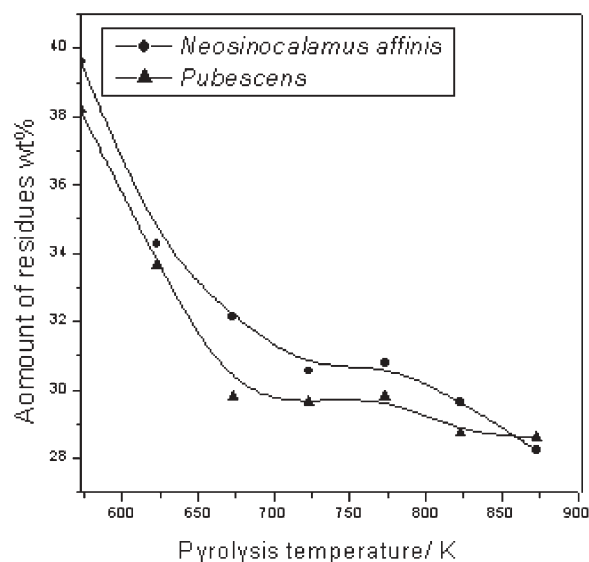


Fig. 3 Amount of residue from the pyrolysis of *Neosinocalamus affinis* and *Pubescens* at different temperatures.

Table 2 Compositions of the main compositions of the liquid from the pyrolysis of *Neosinocalamus affinis* at different pyrolysis temperature (%)^a

Component (%) ^a	Pyrolysis temperature/K						
	573	623	673	723	773	823	873
C ₂ H ₄ O ₂ (Acetic acid)	10.7	41.1	41.5	37.1	29.2	14.7	38.0
C ₃ H ₆ O ₂ (1-Hydroxy-2-propanone)	2.2	7.6	9.4	9.1	6.5	3.3	8.0
C ₄ H ₈ O ₂ (1-Hydroxy-2-butanone)	1.3	4.7	4.6	4.6	3.4	5.1	3.8
C ₅ H ₄ O ₂ (Furfural)	1.1	4.6	5.3	4.2	3.4	1.9	2.7
C ₅ H ₆ O ₂ (2-Furanmethanol)	—	4.6	4.4	11.5	8.9	3.8	5.0
C ₈ H ₈ O (2,3-Dihydro-benzofuran)	2.1	8.6	7.1	7.8	6.0	—	2.5
C ₈ H ₁₀ O ₃ (2,6-Dimethoxyphenol)	1.8	9.4	7.7	9.2	6.8	—	4.7

^a The amount (%) of the products was evaluated through the peak area; no response factors were introduced.

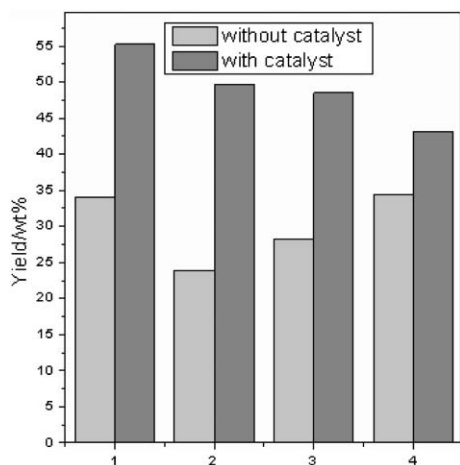


Fig. 4 Liquid yields from the pyrolysis of the four samples with and without catalyst at 773 K for 10 h of (1), *Neosinocalamus affinis* (2), *Bambusa rigida* (3), *Pubescens* and (4), *Dendrocalamus latiflorus*.

pyrolysis temperature affect the products. Different raw materials have different optimal temperatures for the maximum liquid yield or the formation of certain components.

The amount of the solid residue obtained from the pyrolysis of the two samples above is shown in Fig. 3. With increasing final pyrolysis temperature the amount of solid residue decreases for both *Neosinocalamus affinis* and *Pubescens*, but the amount of solid residue of *Neosinocalamus affinis* is higher than that of *Pubescens* over the temperature range tested. It indicates that the direct pyrolysis of *Neosinocalamus affinis* is not as complete as that of *Pubescens*.

3.3 The effects of the NaY catalyst on the liquid products

Fig. 4 and Fig. 5 show the yield of the liquid products from the direct pyrolysis and catalytic pyrolysis of the four kinds of bamboo samples at 773 K and 873 K, respectively. Before catalysis, the derived liquid from the pyrolysis of the four

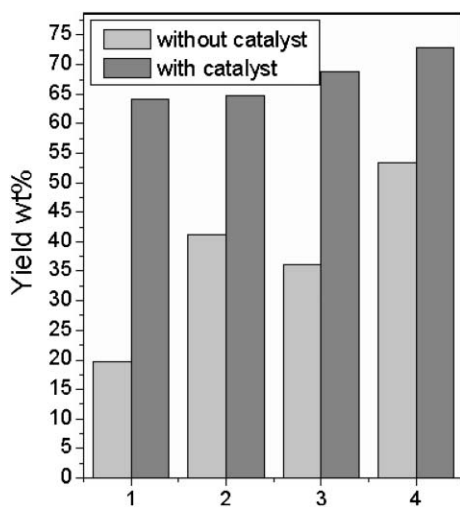


Fig. 5 Liquid yields from the pyrolysis of the four samples with and without catalyst at 873 K for 10 h of (1), *Neosinocalamus affinis* (2), *Bambusa rigida* (3), *Pubescens* and (4), *Dendrocalamus latiflorus*.

samples is brown in colour, while after catalysis the liquid is light brown in colour consisting of a single phase. Fig. 4 shows a significant increase in liquid yield for all the four samples at 773 K in the presence of NaY catalyst, especially the liquid yield for *Bambusa rigida* increases from 23.9 wt% before catalysis to 49.6 wt% after catalysis. Fig. 5 indicates that the yields of pyrolytic liquid obtained at 873 K all increase markedly to 64.1–68.8 wt% in the presence of catalyst, from 19.7–53.3 wt% in the absence of catalyst for the four kinds of samples. In particular, the liquid yield from the catalytic pyrolysis of *Neosinocalamus affinis* is more than three times as high as that from the corresponding non-catalytic pyrolysis. The yields of liquid products from the direct pyrolysis and catalytic pyrolysis at 873 K are higher compared to the corresponding values obtained at 773 K for all samples except *Neosinocalamus affinis*. So, the catalyst samples are treated at 873 K for further characterization.

Vitolo *et al.*¹¹ reported that the upgraded liquid obtained over zeolite HY catalyst consisted of a single phase in which the organic components are both dispersed and dissolved in water while the upgraded liquid obtained using zeolite HZSM-5 consisted of an organic and an aqueous layer. It implies that the character of zeolite has an influence on the property of liquid products and the performance of NaY catalyst in the present work acting as an *in situ* upgrading catalyst may be similar to HY used by Vitolo *et al.*¹¹ In addition, the yield of bio-oil from the catalytic pyrolysis of rice husks over zeolite ZSM-5 catalyst was markedly reduced,⁴ while those from the catalytic pyrolysis of the bamboo samples over zeolite NaY catalyst increase significantly in the present work. This shows that there may exist an accommodation between the kinds of biomass and the catalyst used.

Before catalysis the compositions of the main liquid components of the samples at 773 K and 873 K are given in Table 3. The pyrolysis oil of bamboo in the absence of catalyst contains mainly carboxylic, carbonylic, lactonic, phenolic and furan compounds, such as acetic acid, propanoic acid, 1-hydroxy-2-propanone, 1-hydroxy-2-butanone, butyrolactone, phenol, 2,6-dimethoxyphenol, furfural, 2-furanmethanol, and 2,3-dihydrobenzofuran. The content of acetic acid is observed to be the highest in all pyrolytic liquids. The total contents of acetic acid, 1-hydroxy-2-propanone, 2-furanmethanol and 2,3-dihydrobenzofuran are in the range of 30–60% in the pyrolytic liquids of samples at 773 K. The pyrolysis of different bamboo gives similar liquid products, the composition of which varies from one to another. For example, the content of cyclopropanol obtained from the pyrolysis of *Bambusa rigida* is the highest at 773 K among the various values from the four samples, while the content of 2,6-dimethoxyphenol from *Pubescens* at 873 K is the highest. Furthermore, the pyrolysis of *Pubescens*, *Neosinocalamus affinis* and *Bambusa rigida* produces butyrolactone but *Dendrocalamus latiflorus* does not. Comparison of the major components of bamboo with the compositions of pyrolytic liquid shown in Tables 1 and 3 may suggest that the different contents of cellulose, hemi-cellulose and lignin in the four samples are strongly related to the distribution of the components from the pyrolytic liquid of the samples. Pouwels²⁶ reported the strong relation between the origin of the low

Table 3 Compositions of the main components of the liquid from the pyrolysis of bamboo at 773 K and 873 K (%)^a

Component (%) ^a	<i>Pubescens</i>		<i>Neosinocalamus affinis</i>		<i>Bambusa rigida</i>		<i>Dendrocalamus latiflorus</i>	
	773K	873K	773K	873K	773K	873K	773K	873K
Acetic acid	30.4	30.8	28.0	38.0	25.4	18.5	15.6	15.0
1-Hydroxy-2-propanone	6.9	8.4	6.4	8.0	10.8	6.2	3.9	2.9
Propanoic acid	2.4	—	2.7	1.4	6.9	1.8	—	0.8
1-Hydroxy-2-butanone	5.3	6.3	3.5	3.8	7.7	2.9	2.5	1.4
Furfural	2.1	—	3.2	2.7	—	3.0	6.7	5.4
2-Furanmethanol	6.6	7.3	8.4	5.0	6.4	3.3	4.5	2.5
Butyrolactone	3.0	3.3	3.1	2.5	5.3	2.5	—	—
Phenol	2.0	3.1	4.3	1.7	—	1.1	—	0.9
Cyclopropanol	5.3	6.4	5.3	5.8	18.2	—	3.2	1.5
2-Methoxyphenol	2.6	3.2	3.8	1.5	—	2.1	—	1.3
2,3-Dihydrobenzofuran	8.2	11.4	6.5	2.5	—	4.2	6.3	5.0
2,6-Dimethoxyphenol	2.2	13.4	7.2	4.7	9.1	6.5	8.0	4.0

^a The amount (%) of the products was evaluated through the peak area; no response factors were introduced.

molecular weight products from the pyrolysis of biomass and the content of cellulose. It was shown that the pyrolysis of cellulose produced a great variety of primary and secondary products, acetone, acetic acid, butanone, furfural, and other products. However, in the present work, just acetic acid, furfural and 2,3-dihydrobenzofuran are obtained from the pyrolysis of cellulose in the four samples, while other products such as acetone and butanone are not detected under the selected conditions. That is to say that the kinds of cellulose contained in bamboo may not produce these compounds in the pyrolysis or the amount of them is too small to be detected.

After catalysis the composition of the main liquid components of the samples at 773 K and 873 K are shown in Table 4. Acetic acid is also observed to be the main component and its content is more than two times higher than that from non-catalytic pyrolysis, and the content of carbonylic compounds decreases markedly. In addition, 1,4-dioxane as a new compound is detected in the liquid from *Pubescens*, *Bambusa rigida* and *Dendrocalamus latiflorus* at 873 K. The high content of acetic acid in liquid products is consistent with the high concentration of hydrogen gas in gaseous products from the pyrolysis of the samples, since oxygen in the bamboo is transferred to the molecule of acetic acid.

According to the data in ref. 14 and 27 the presence of zeolite HZSM-5 catalyst was favorable for the formation of highly aromatic oil with high concentrations of monocyclic aromatic hydrocarbons while zeolite HY catalyst was favorable for the formation of aliphatic hydrocarbons. Zeolite NaY catalyst is found in this work to be favorable for the formation of carboxylic compounds. Also, it is effective in increasing the liquid yield, reducing the number of species and producing new compound species with use of the NaY catalyst. This

indicates that different catalysts act differently in the pyrolysis process, thus resulting in different composition of the liquid products. In the present work, zeolite NaY, may interact with the primary pyrolytic intermediates, and then plays a role of *in situ* upgrading catalyst during the process, thus changing the distribution of the catalytic products. In addition, the raw materials also play an important role in the type and distribution of the products obtained.

3.4 Characterization of zeolite NaY catalysts

The SEM micrograph of the zeolite NaY catalyst with or without treatment shows no pre-orientation. This indicates that the peak intensities of the XRD patterns are correct and the sampling of the zeolite for XRD measurement has no influence on these intensities.

XRD results give a significant difference between the fresh catalyst and the catalyst after calcination (heating alone) or used in the catalytic reaction at 873 K. A series of parameters calculated from the XRD data and 3D crystal model of the zeolite are listed in Table 5. In Table 5, the No. 1–No. 6 samples represent the fresh catalyst, the calcined (heating alone) catalyst at 873 K, and those used in the catalytic pyrolysis of *Dendrocalamus latiflorus*, *Neosinocalamus affinis*, *Bambusa rigida* and *Pubescens*, respectively. After calcination, an increase of peak intensities from 5° to 40° in 2-theta is observed obviously compared with those of the fresh catalyst, especially the patterns for the [111], [220], [311] and [440] planes. In addition, the reduction of the values of the lattice parameter and the disordering degree, and the increase of crystalline size could be attributed to the condensation of the crystal cell and the improvement of the crystal structure.

Table 4 Compositions of the main components of the liquid from the catalytic pyrolysis of bamboo over the NaY catalyst at 773 K and 873 K (%)^a

Component (%) ^a	<i>Pubescens</i>		<i>Neosinocalamus affinis</i>		<i>Bambusa rigida</i>		<i>Dendrocalamus latiflorus</i>	
	773K	873K	773K	873K	773K	873K	773K	873K
Acetic acid	84.6	62.4	76.3	88.7	75.2	54.6	100	60.2
2-Methylpropyl ester fomic acid	—	26.7	—	—	—	31.2	—	—
1-Hydroxy-2-propanone	4.9	—	6.8	—	—	—	—	5.9
Propanoic acid	10.5	—	7.0	6.8	—	—	—	6.3
1,4-Dioxane	—	10.8	—	—	—	14.2	—	3.4

^a The amount (%) of the products was evaluated through the peak area; no response factors were introduced.

Table 5 Parameters corresponding to XRD patterns of the zeolite catalysts. No. 1–No. 6 samples represent the fresh catalyst, the calcined (heating alone) catalyst at 873 K, and those used in the catalytic pyrolysis of *Dendrocalamus latiflorus*, *Neosinocalamus affinis*, *Bambusa rigida* and *Pubescens*, respectively

Sample	Lattice parameter (a)/nm	Disordering degree (A)	Crystalline size/nm
No. 1	2.4669 ± 0.0002	0	23.9 ± 0.2
No. 2	2.4645 ± 0.0001	−9.1	27.0 ± 0.3
No. 3	2.4711 ± 0.0002	29.4	26.9 ± 0.1
No. 4	2.4682 ± 0.0002	11.1	27.6 ± 0.2
No. 5	2.4677 ± 0.0001	32.1	27.2 ± 0.2
No. 6	2.4762 ± 0.00001	32.7	26.7 ± 0.3

Changes in the above parameters imply that the zeolite structure can be influenced strongly by heating alone.

After use in the reaction, the peak intensities of the catalyst also increase sharply compared with that of the fresh sample, especially the peaks corresponding to [111], [220] and [311] planes. However, the disordering degree of all the used catalysts increases compared to that of No. 1, and the disordering degree of No. 3, No. 5 or No. 6 sample is more than two times as high as that of No. 4 sample (Table 5). In addition, the variation of the *a*-value is significant for the zeolite of the cubic crystal system which varies from 2.4669 nm for the fresh catalyst to 2.4762 nm for the used catalyst, due to the expansion of the crystal cell after use in the catalytic pyrolysis. The variation of the corresponding parameters such as the disordering degree is significantly different from that of heating alone. In fact, the variation of parameters after catalytic pyrolysis is a combination of the interaction of the samples with the catalyst and the effect of heating. The above data indicate that both heating and the kind of bamboo act on the reconstruction of the zeolite structure concomitantly during the pyrolysis process.

The reconstruction of the catalyst during the catalytic process involves the increase of the disordering degree and the expansion of the crystal cell. In addition, the XPS study also provides evidence of the interaction of the NaY catalyst with the primary intermediates of the pyrolysis process of bamboo. The profiles of high resolution Si and C are both asymmetric and have an obvious shoulder peak, respectively. The new C–Si bond (BE = 282.69 eV for C_{1s}, BE = 101.72 eV for Si_{2p} in the XPS spectra of the used catalyst in the catalytic pyrolysis of *Pubescens*) is formed in the surface layer for all the used catalysts with different relative intensities. This is in good agreement with the XRD results.

4 Conclusions

The contents of cellulose, hemi-cellulose, and lignin are high in the four kinds of bamboo tested.

Both pyrolysis temperature and the kinds of raw materials influence the liquid yields and the distribution of the components. Acetic acid is observed to be the main component in the pyrolytic liquids of the four kinds of bamboo. The optimal temperature for the maximum liquid yield of *Neosinocalamus affinis* is found to be 773 K, while that of *Pubescens* is 823 K.

Zeolite NaY catalyst is not only effective in increasing the yield of liquid product but also condenses the species formed during the pyrolysis. The components of pyrolytic liquids in the absence of the catalyst are mainly carboxylic, carbonylic, lactonic, phenolic and furan compounds, while in the presence of the catalyst the liquid obtained just consists of carboxylic and carbonylic compounds mainly. In particular, the content of acetic acid is observed to be the main component and its content is more than two times higher than that from a non-catalytic process, and the content of carbonylic compounds decreases markedly.

XRD diagrams, XPS spectra and SEM micrographs show that during the pyrolysis processes the NaY catalyst interacts with the primary pyrolytic intermediates of bamboo. The catalyst endures reconstruction involving the impairment of [111] and [220] planes, and the enhancement of the [311] plane as a result of the combination of the above interactions and thermal effects.

Acknowledgements

This work is supported by the National Natural Science Foundation of China (No. 20576086), and the Special Research Fund for the Doctoral Program of Higher Education of China (No. 20050610013), the Teaching Research Award Program for Outstanding Young Teachers in Higher Education Institutions of MOE, P. R. C (2002), the Science Foundation of Sichuan Province and the Funds for Innovative Research of Sichuan University. The supervision of Prof. Qingshi Zhu is highly acknowledged.

References

- H. Komiyama, T. Mitsumorib, K. Yamajic and K. Yamadad, *Fuel*, 2001, **80**, 707.
- V. Minkova, S. P. Marinoy, R. Zanzi, E. Björnbo, T. Budinova, M. Stefanova and L. Lakov, *Fuel Process. Technol.*, 2000, **62**, 45.
- J. M. Ekmann, J. C. Winslow, S. M. Smouse and M. Ramezan, *Fuel Process. Technol.*, 1998, **54**, 171.
- P. T. Williams and N. Nugranad, *Energy*, 2000, **25**, 493.
- V. Minkova, M. Razvigorova, E. Björnbo, R. Zani, T. Budinova and N. Petrov, *Fuel Process. Technol.*, 2001, **70**, 53.
- G. Chen, J. Andries and H. Spliethoff, *Renewable Energy*, 2003, **28**, 985.
- C. P. Liao, C. Z. Wu, Y. J. Yan and H. T. Huang, *Biomass Bioenergy*, 2004, **27**, 119.
- C. Courson, E. Makaga, C. Petit and A. Kiennemann, *Catal. Today*, 2000, **63**, 427.
- K. Engelen, Y. H. Zhang, D. J. Draelants and G. V. Baron, *Chem. Eng. Sci.*, 2003, **58**, 665.
- P. A. Horne and P. T. Williams, *Fuel*, 1996, **75**, 1051.
- S. Vitolo, M. Seggiani, P. Frediani, G. Ambrosini and L. Politi, *Fuel*, 1999, **78**, 1147.
- N. Islam and F. N. Ani, *Bioresour. Technol.*, 2000, **73**, 67.
- S. P. Zhang, Y. J. Yan, T. C. Li and Z. W. Ren, *Bioresour. Technol.*, 2005, **96**, 545.
- J. D. Adjave and N. N. Bakhshi, *Fuel Process. Technol.*, 1995, **45**, 161.
- P. T. Williams and P. A. Horne, *Fuel*, 1995, **74**, 1839.
- J. D. Adjave, S. P. R. Katikaneni and N. N. Bakhshi, *Fuel Process. Technol.*, 1996, **48**, 115.
- I. K. Basily, E. Ahmed and N. N. Ibraheem, *J. Anal. Appl. Pyrolysis*, 1995, **32**, 221.
- K. Kuroda and D. R. Dimmel, *J. Anal. Appl. Pyrolysis*, 2002, **62**, 259.

- 19 P. T. Williams and S. Besler, *Renewable Energy*, 1996, **7**, 233.
 20 E. Godoňková, P. Baláž and E. Boldižárová, *Hydrometallurgy*, 2002, **65**, 83.
 21 O. Beaumont and Y. Schwob, *Ind. Eng. Chem. Process Des. Dev.*, 1984, **23**, 637.
 22 M. C. Samolada, T. Stoicos and I. A. Vasalos, *J. Anal. Appl. Pyrolysis*, 1990, **18**, 127.
 23 H. Jiang, *PhD Thesis*, Hefei: University of Science and Technology of China, 2003.
 24 R. Marbot, *J. Anal. Appl. Pyrolysis*, 1997, **39**, 97.
 25 A. E. Pütün, E. Apaydn and E. Pütün, *Energy*, 2004, **29**, 2171.
 26 A. Pouwels, *PhD Thesis*, University of Amsterdam, 1989.
 27 J. D. Adjaye and N. N. Bakhshi, *Fuel Process. Technol.*, 1995, **45**, 185.

Find a SOLUTION

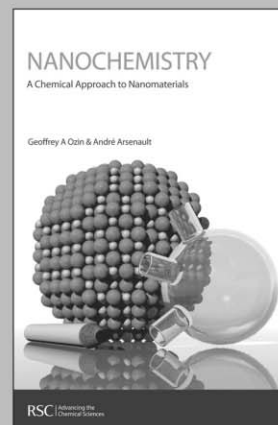
... with books from the RSC

Choose from exciting textbooks, research level books or reference books in a wide range of subject areas, including:

- Biological science
- Food and nutrition
- Materials and nanoscience
- Analytical and environmental sciences
- Organic, inorganic and physical chemistry

Look out for 3 new series coming soon ...

- RSC Nanoscience & Nanotechnology Series
- Issues in Toxicology
- RSC Biomolecular Sciences Series



28040542

RSC Publishing

www.rsc.org/books

In(OTf)₃-catalyzed thiolysis of 1,2-epoxides by arylthiols under SFC. A new approach for the synthesis of thiazolopyridinium ionic liquids

Francesco Fringuelli, Ferdinando Pizzo,* Simone Tortoioli, Cristiano Zuccaccia and Luigi Vaccaro*

Received 27th October 2005, Accepted 6th December 2005

First published as an Advance Article on the web 22nd December 2005

DOI: 10.1039/b514979g

The efficiency of In(III)-catalyzed thiolysis of safrole oxide (**1**) by phenylthiol (**2a**) under SFC or in an organic medium, strongly depends on its associated counterion. In(OTf)₃ has proven to be a very efficient catalyst and the use of solvent-free condition (SFC) results in the highest catalytic efficiency. In the presence of 2 mol% of this salt the reactions of 1,2-epoxides **1**, **5**, and **8** by thiols **2a–f**, have allowed the corresponding β-hydroxy sulfides to be obtained at 30 °C in generally short times, high yields and with C-β-regioselectivity. In addition two representatives of a new class of [1,3]thiazolo[3,2-*a*]pyridin-4-ium-based ionic liquids, **11** and **12**, have been prepared by a simple one-pot procedure by using as a key step the thiolysis of 1,2-epoxyhexane (**5**) by 2-mercaptopyridine **2f**.

New synthetic methodologies must be developed to face the need for environmentally responsible organic chemistry. To reach this goal, the use of green reaction media, reagents and catalysts should be investigated. By applying alternative reaction conditions, more efficient processes and new catalysts can be discovered allowing the preparation of innovative materials.¹

We have been contributing to the development of a green organic synthesis proving that water as reaction medium,² solvent-free condition (SFC),³ or their combination⁴ can be efficiently used for accessing target molecules. We are currently involved in a project aimed at the synthesis of new ionic liquids (ILs) starting from 1,2-epoxides.^{3d} ILs are a promising alternative to common organic solvents and they have proved to be highly efficient reaction media for organic transformations.⁵ Recently the synthesis of a new class of thiazolium salts has been disclosed, opening the route to the use of ILs containing the thioether functionality.⁶ Considering that 1,2-epoxides are easily accessible in both racemic and enantiopure form,⁷ we believe that the thiolysis of this heterocyclic nucleus by an appropriate biaptic thiol under SFC, is an efficient synthetic tool for the regio- and stereoselective preparation of S-containing heterocyclic ILs.

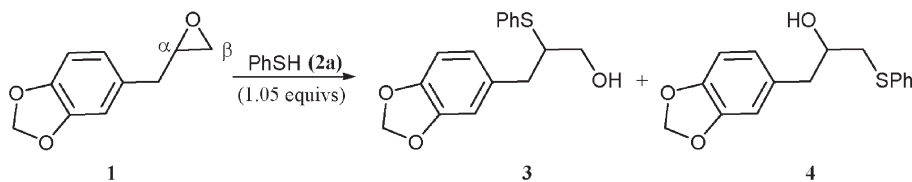
Thiolysis of 1,2-epoxides in organic solvents has been widely investigated and a variety of Lewis acids have been used to promote this process.⁸ We have already developed various protocols for the thiolysis of 1,2-epoxides in water catalyzed by various Lewis acids,^{2b,f,g} but we found that by using multi-dentate nucleophiles these catalysts form stable complexes making the ring-opening of 1,2-epoxides impossible to be realized.^{2g} We intend to use SFC to solve this problem and to define a new protocol for the synthesis of new S-containing ILs, with the best chemically efficiency and environmental

compatibility. To achieve this goal we have studied in detail the thiolysis of 1,2-epoxides by examining (a) the most suitable In(III) salt and the role of the counterion on its catalytic efficiency, (b) the limits posed by the thiol on the process feasibility, and (c) the influence of the reaction medium. This paper illustrates the results of this study. In organic solvents the efficiency of a metal catalyst is generally influenced by the coordinating character of the associated counterion,⁹ but this relationship has never been outlined in the case of thiolysis of 1,2-epoxides under SFC. For this purpose we investigated the counterion effect on the catalytic activity of In(III) salts in the reaction of safrole oxide (**1**) with phenylthiol (**2a**). 1,2-epoxide **1** was chosen as a representative substrate due to its low reactivity in the uncatalyzed thiolysis and with the intention of extending the catalyzed process to functionalized 1,2-epoxides. The thiolysis of **1** was carried out at 30 °C under SFC and in MeCN and dichloromethane (DCM) as reaction media and in the presence of a variety of commonly used In(III) salts (5 mol%). The results are illustrated in Table 1.

In(OTf)₃ was the most efficient catalysts under SFC (Table 1, entry 8) allowing in only 10 min a complete conversion of **1** to a 5 : 95 mixture of β-hydroxy sulfides **3** and **4**.¹⁰ Among the indium halides, InF₃ was the least efficient (Table 1, entry 2 vs. 3, vs. 6). InCl₃ and InI₃ showed a good catalytic efficiency but 2 and 6% of the corresponding chlorohydrin and iodohydrin were respectively formed (Table 1, entries 3 and 6). In₂(SO₄)₃ showed a catalytic effect comparable to that of InCl₃ but much smaller than In(OTf)₃ (Table 1, entry 7 vs. 3 and 8). The catalytic activity of In(III) salts increased as the basicity and the coordinating ability of the associated counterion decreased. Under SFC In(OTf)₃ was so efficient that only 2 mol% of this salt was sufficient to complete the thiolysis of **1** with **2a** still in a short time (Table 1, entry 9).

In organic solvents In(OTf)₃ showed an acceptable catalytic efficiency only when it was soluble in the reaction medium (e.g. MeCN, Table 1, entries 11 vs. 10) while InCl₃ always gave discouraging results (Table 1, entries 4 and 5). Phenylthiol (**2a**)

CEMIN—Centro di Eccellenza Materiali Innovativi Nanostrutturati, Dipartimento di Chimica, Università di Perugia, Via Elce di Sotto, 8 06123, Perugia, Italy. E-mail: luigi@unipg.it; pizzo@unipg.it; Fax: +39 075 5855560; Tel: +39 075 5855558

Table 1 Lewis-acid-catalyzed thiolysis of safrole oxide (**1**) by phenylthiol (**2a**) at 30 °C

Entry	Medium	Catalyst (5 mol%)	<i>t</i> /h	<i>C</i> ^a (%)	3/4 ^a
1	SFC	—	24	2	—
2	SFC	InF ₃	24	99	5/95
3	SFC	InCl ₃	5	93	7/93 ^b
4	CH ₂ Cl ₂	InCl ₃	5	40	5/95
5	CH ₃ CN	InCl ₃	5	5	5/95
6	SFC	InI ₃	3	90	5/95 ^c
7	SFC	In ₂ (SO ₄) ₃	5	99	5/95
8	SFC	In(OTf) ₃	0.17	99	5/95
9	SFC	In(OTf) ₃ ^d	0.70	99	5/95 ^e
10	CH ₂ Cl ₂	In(OTf) ₃	0.17	10	5/95
11	CH ₃ CN	In(OTf) ₃	0.17	85	5/95

^a Reaction conversions and ratios determined by GLC analyses. ^b 2% of the corresponding β -chlorohydrin was formed and determined by ¹H NMR analysis. ^c 6% of the corresponding β -iodohydrin was formed and measured by ¹H NMR analysis. ^d 2 mol% of catalyst was used. ^e α -Regioisomer **3** and β -regioisomer **4** were isolated in 4 and 86% yields respectively.

prevalently attacked safrole oxide (**1**) at the C- β position both in organic solvents and under SFC. To evaluate to what extent a multidentate thiol can influence the catalytic efficiency of In(OTf)₃, the thiolysis of 1,2-epoxyhexane (**5**) by phenylthiol (**2a**) and a variety of poly-functionalized arylthiols (**2b–f**) was studied. The results are illustrated in Table 2.

Under SFC and 30 °C in the absence of catalyst, phenylthiol (**2a**) and arylthiols **2b–d** and **2f** reacted slowly with 1,2-epoxyhexane (**5**) giving the corresponding β -hydroxy sulfides in unsatisfactory yields (Table 2, entries 1, 3, 5, 7, and 11). The only exception was 2-mercaptophenol (**2e**) which completed thiolysis of **5** after 4 h (Table 2, entry 9). The catalytic efficiency of In(OTf)₃ in the SFC thiolysis of **5** by **2a** was very high, only 2 mol% of this salt was able to promote the complete formation of β -hydroxy sulfides **6a** (C- α) and **7a** (C- β) (in a 13/87 ratio) in only 5 min (Table 2, entry 2). When biaptic thiols **2b–f** were used (Table 2, entries 4, 6, 8, 10, and 12), In(OTf)₃ was still a very good catalyst allowing one to complete the reactions in short times. β -Adducts **7** were the sole or the main reaction products and were isolated in good to excellent yields with the exception of **7b**, because the thiolysis of **5** by **2b** gave 27% of bis-adduct coming from both S- and N-attacks. (Table 2, entry 4). In(OTf)₃-catalyzed protocol was extended to the thiolysis of *trans*-2,3-epoxyhexanol (**8**) by phenylthiol (**2a**) and thiols **2d** and **2f** (Scheme 1). The corresponding sulfides **9/10a, d, f** were isolated in good yields proving that In(OTf)₃ was an efficient catalyst also for the thiolysis of 2,3-epoxyalcohols an important and widely studied class of 1,2-epoxides.

In all cases the reactions proceeded to give exclusively *anti*-adducts **9** and **10** in 7/3 ratio.^{2f,g} The main thiolysis reaction products **9a, d, f** were isolated, purified and characterized.

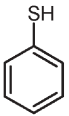
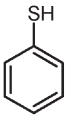
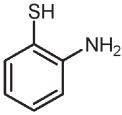
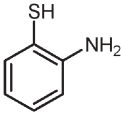
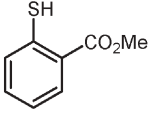
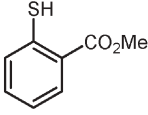
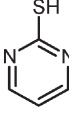
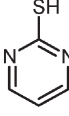
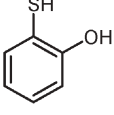
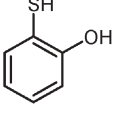
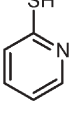
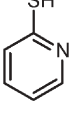
The results obtained were finally exploited for the preparation of two representative thiazolium-based ILs (**11** and **12**). The crude β -hydroxy sulfide **7f** coming from the

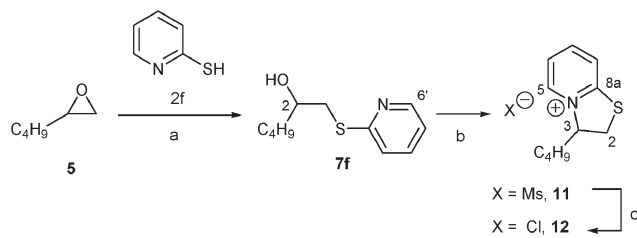
In(OTf)₃-catalyzed reaction of 1,2-epoxyhexane (**5**) with 2-mercapto-pyridine (**2f**) under SFC and obtained in 99% yield, was dissolved in CH₂Cl₂ and treated with 2.0 equiv. of methanesulfonyl chloride (MsCl) and triethylamine (Et₃N) at 0 °C, and after 6 h the corresponding 3-butyl-2,3-dihydro-[1,3]thiazolo[3,2-*a*]pyridin-4-ium methyl sulfate (**11**) was isolated in 86% yield. After treatment with a Cl⁻-exchange resin, **11** was converted into the corresponding chloride **12** in 85% yield (Scheme 2).

¹H NMR chemical shifts of protons at position C-5 of **11** and **12** resonate at 9.28 and 9.77 ppm respectively. These values are consistent with ¹H NMR downfield shift of pyridine protons expected when the positive charge is localized on the nitrogen atom but we retain that this effect cannot be used to prove that cyclization of **7f** has occurred. In fact ¹H NMR chemical shifts of pyridinium salts significantly change by varying solvent, counterion or substituent on nitrogen.^{11,14} To unequivocally confirm the cyclic nature of **11** and **12**, we searched for the presence of ¹³C-¹H long-range coupling between protons H-3 and H-5 and carbons C-3 and C-5. These long-range correlations are easily detectable in **11** and **12** (see Scheme 3), while in the starting β -hydroxy sulfide **7f**, the corresponding correlations between protons H-2 and H-6' and carbons C-2 and C-6' are not present.

In conclusion thiolysis of 1,2-epoxides **1**, **5**, and **8** by thiols **2a–f** has been investigated under SFC and in organic solvents, in the presence and in the absence of a Lewis-acid catalyst. The best results have been obtained by performing the reactions under SFC and in the presence of 2 mol% of In(OTf)₃. As less basic or coordinating counterions were used as much the catalytic efficiency of this metal catalyst was increased. The In(OTf)₃-catalyzed thiolysis of 1,2-epoxides under SFC is a new, efficient and environmentally-friendly synthetic tool which was used to prepare thiazolopyridinium salts **11** and **12** as representatives of a new class of ILs.

Table 2 Thiolysis of 1,2-epoxyhexane (**5**) by thiols **2a–f** at 30 °C

Entry	Thiol	Catalyst (2 mol%)	<i>t</i> /h	<i>C</i> ^a (%)	6/7 ^a	<i>Y</i> ^b (%)
1		—	200	7	—	—
2		In(OTf) ₃	0.08	99	13/87	80
3		—	70	10	1/99	—
4		In(OTf) ₃	6	95	1/99	40 ^c
5		—	170	10	10/90	—
6		In(OTf) ₃ ^d	24	90	19/81	75
7		—	120	55	1/99	—
8		In(OTf) ₃	20	95	1/99	75
9		—	4	98	1/99	95
10		In(OTf) ₃	2	96	20/80	—
11		—	80	80	1/99	—
12		In(OTf) ₃	0.75	99	1/99	95

^a Reaction conversions and ratios were measured by GLC analyses.^b Isolated yield of the product **7**. ^c 67% overall yield, including 40% of **7b** and 27% of bis-adduct coming from both S- and N-attack.^d 5 mol% of catalyst was used.(a) In(OTf)₃ (2 mol%), **2f** (1.05 equivs), SFC, 30 °C, 0.75 h; (b) MsCl (2.0 equivs.), Et₃N (2.0 equivs.), CH₂Cl₂, 0 °C, 6 h, 86%; (c) Cl-exchange resin, MeOH/H₂O (1/1), 85%.**Scheme 2** Synthesis of thiazolopyridinium salts **11** and **12**.

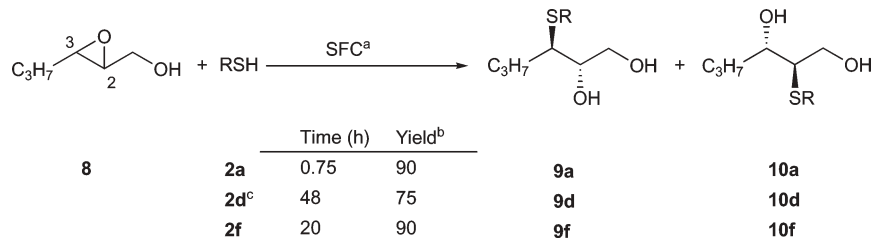
Experimental

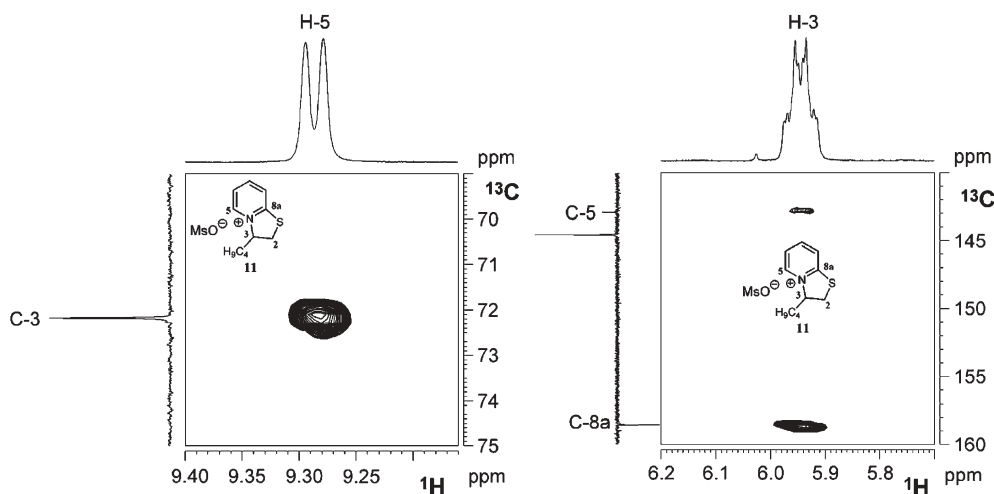
General

All chemicals were purchased and used without any further purification. ¹H NMR and ¹³C NMR spectra were recorded at 200 MHz or 400 MHz, and at 50.3 or 100.6 MHz respectively, using a convenient deuterated solvent (reported below) and the residual peak as internal standard, or TMS in the case of CDCl₃. All melting points are uncorrected. Thin layer chromatography analyses were performed on silica gel on aluminium plates. Column chromatography were performed by using silica gel 230–400 mesh. β-Hydroxy sulfides **6a**, **7a**, **9a**, **10a** are known compounds,^{2f,g} **3**, **4**, **6c**, **6e**, **7b–f**, **9d**, **9f**, **10d**, **10f**, **11** and **12** are new compounds and are described below.

Typical experimental procedure. In an oven-dried screw-capped vial a suitable thiol (**2a–f**) (1.05 mmol) was stirred with the catalyst (2–5 mol%) for 10 min at 30 °C. The appropriate 1,2-epoxide was then added (1.0 mmol) and the resulting mixture stirred for the time reported in the tables. The crude reaction mixture was then diluted with Et₂O, washed with water to remove and recover the Lewis-acid catalyst. The ethereal layer was dried over Na₂SO₄ and evaporated under vacuum. The crude reaction products were purified by silica gel column chromatography.

3-(Benzo[d][dioxol-5'-yl)-2-(phenylthio)propan-1-ol (3). Chromatography eluent: 6/4-petroleum ether/Et₂O; oil; yield: 4%; R_f: 0.34 (7/3 Et₂O/petroleum ether); (Table 1, entry 9); ¹H NMR δ = 2.85–2.87 (m, 2H), 3.35–3.41 (m, 1H), 3.53 (dd, *J* = 5.5, 11.5 Hz, 1H), 3.62 (dd, *J* = 4.5, 11.5 Hz, 1H), 5.93 (s, 2H), 6.68–6.75 (m, 3H), 7.26–7.42 (m, 5H); ¹³C NMR δ = 37.4, 53.7, 62.4, 100.9, 108.2, 109.5, 122.2, 127.6, 129.1, 132.2, 132.7,

^a RSH (1.05 equivs), In(OTf)₃ (2 mol%), 30 °C, SFC. ^b isolated yield of the 7/3 C-3/C-2 mixture of regioisomers. ^c 5 mol% of In(OTf)₃, 50 °C**Scheme 1** Thiolytic ring-opening of *trans*-2,3-epoxyhexan-1-ol.



Scheme 3 ^{13}C - ^1H long range correlations in compound **11**.

134.7, 146.2, 147.6; IR (CHCl_3): $\nu = 3042$ (m), 3012 (s), 2880 (s), 1714 (s), 1578 (m), 1489 (s), 1441 (m), 1107 (m) cm^{-1} ; GC-EIMS $m/z = 288$ (M^+ , 33), 153 (8), 135 (100), 109 (10), 91 (7), 77 (12), 65 (6); anal. calcd. for $\text{C}_{16}\text{H}_{16}\text{O}_3\text{S}$ (288.4): C 66.64; H 5.69; found: C 66.90; H 5.83.

1-(Benzo[d]dioxol-5'-yl)-3-(phenylthio)propan-2-ol (4). Chromatography eluent: 6/4-petroleum ether/ Et_2O ; oil; yield: 86%; R_f : 0.30 (7/3 Et_2O /petroleum ether); (Table 1 entry 9); ^1H NMR $\delta = 2.75$ (dd, $J = 7.3, 13.8$ Hz, 1H), 2.81 (dd, $J = 5.5, 13.9$ Hz, 1H), 2.90 (dd, $J = 8.0, 13.7$ Hz, 1H), 3.12 (dd, $J = 3.9, 13.7$ Hz, 1H), 3.84–3.90 (m, 1H), 5.92 (s, 2H), 6.64–6.74 (m, 3H), 7.25–7.35 (m, 5H); ^{13}C NMR $\delta = 40.8, 41.9, 70.5, 100.9, 108.2, 109.7, 122.3, 126.5, 129.0, 129.8, 131.3, 135.2, 146.2, 147.7$; GC-EIMS $m/z = 288$ (M^+ , 39), 161 (37), 135 (100), 109 (14), 77 (25); anal. calcd. for $\text{C}_{16}\text{H}_{16}\text{O}_3\text{S}$ (288.4): C 66.64; H 5.69; found: C 66.81; H 5.90.

1-[(2'-(2'-Hydroxyhexyl)amino)phenyl]thio]hexan-2-ol (bis-adduct from **5 and **2b**).** Chromatography on silica gel deactivated with Et_3N , eluent: 7/3- Et_2O /petroleum ether; oil; yield: 27%; (Table 2, entry 4); ^1H NMR $\delta = 0.85$ (t, $J = 7.0$ Hz, 3H), 0.91 (t, $J = 7.0$ Hz, 3H), 1.21–1.56 (m, 12H), 2.62 (ddd, $J = 7.1, 9.4, 14.0$ Hz, 1H), 2.89 (ddd, $J = 2.9, 4.9, 13.5$ Hz, 1H), 3.03 (ddd, $J = 4.4, 8.5, 12.8$ Hz, 1H), 3.29 (dt, $J = 2.7, 12.2$ Hz, 1H), 3.50–3.55 (m, 1H), 3.81–3.86 (m, 1H), 4.30 (br s, 1H), 6.56–6.64 (m, 2H), 7.12–7.15 (m, 2H); ^{13}C NMR $\delta = 13.9, 14.0, 22.6, 22.7, 27.8, 35.9, 36.0, 45.5, 49.7, 69.6, 70.1, 115.2, 117.4, 118.2, 136.6, 148.5$; IR (CHCl_3): $\nu = 3385$ (s), 3070 (w), 2933 (s), 2867 (s), 1590 (s), 1505 (s), 1453 (s), 1313 (m), 1038 (m), 890 (w) cm^{-1} ; GC-EIMS $m/z = 325$ (M^+ , 50), 238 (100), 220 (29), 208 (10), 150 (41), 136 (63), 124 (20), 109 (14), 94 (17); anal. calcd. for $\text{C}_{18}\text{H}_{31}\text{NO}_2\text{S}$ (325.5): C, 66.42, H, 9.60; N, 4.30; found: C, 66.50; H, 9.51; N, 4.25.

2-[(2'-(Carboxymethyl)phenylthio)hexan-1-ol (6c). Chromatography eluent: 9/1-petroleum ether/ EtOAc ; oil; yield: 14%; (Table 2, entry 6); ^1H NMR $\delta = 0.91$ (t, $J = 7.1$ Hz, 3H), 1.30–1.48 (m, 4H), 1.57–1.61 (m, 2H), 2.60 (br s, 1H), 2.91 (dd, $J = 8.5, 13.5$ Hz, 1H), 3.18 (dd, $J = 3.5, 13.2$ Hz,

1H), 3.76–3.82 (m, 1H), 3.92 (s, 3H), 7.18–7.22 (m, 1H), 7.40–7.45 (m, 2H), 7.90–7.92 (m, 1H); ^{13}C NMR $\delta = 14.0, 22.6, 27.8, 36.1, 40.8, 52.2, 69.3, 124.7, 127.5, 129.2, 131.0, 132.2, 139.6, 167.1$; IR (CHCl_3): $\nu = 3468$ (s), 2940 (s), 1699 (s), 1466 (s), 1300 (s), 1056 (s), 909 (m), 655 (w) cm^{-1} ; GC-EIMS $m/z = 268$ (M^+ , 2), 236 (11), 182 (100), 167 (28), 150 (75), 136 (22), 122 (40), 108 (11); anal. calcd. for $\text{C}_{14}\text{H}_{20}\text{O}_3\text{S}$ (268.4): C, 62.66, H, 7.51; found: C, 62.10; H, 7.45.

2-[(2'-(Hydroxyphenyl)thio)hexan-1-ol (6e). Characterized by using a chromatographically enriched mixture also containing **7e**, eluent: 4/6- Et_2O /petroleum ether; oil; (Table 2, entry 10); ^1H NMR $\delta = 0.83$ (m, 3H), 1.21–1.50 (m, 6H), 2.83–2.86 (m, 1H), 3.43 (dd, $J = 7.7, 11.3$ Hz, 1H), 3.60–3.64 (m, 1H), 5.69 (br s, 1H), 6.75–6.86 (m, 1H), 6.94–6.97 (m, 1H), 7.22–7.29 (m, 1H), 7.43–7.48 (m, 1H); ^{13}C NMR $\delta = 13.7, 22.3, 27.4, 28.9, 53.3, 63.7, 115.7, 119.0, 120.6, 131.3, 135.2, 156.5$; GC-EIMS $m/z = 226$ (M^+ , 23), 195 (29), 139 (10), 126 (100), 97 (10).

1-[(2'-(Aminophenyl)thio)hexan-2-ol (7b). Chromatography on silica gel deactivated with Et_3N , eluent: 7/3- Et_2O /petroleum ether; oil; yield: 40%; (Table 2, entry 4); ^1H NMR $\delta = 0.84$ –0.91 (m, 3H), 1.24–1.53 (m, 6H), 2.64 (dd, $J = 8.8, 13.5$ Hz, 1H), 2.93 (dd, $J = 3.2, 13.5$ Hz, 1H), 3.51–3.61 (m, 1H), 4.07 (br s, 2H), 6.57–6.73 (m, 2H), 7.12–7.14 (m, 1H), 7.38–7.40 (m, 1H); ^{13}C NMR $\delta = 13.9, 22.6, 27.9, 35.6, 42.9, 69.7, 115.2, 117.3, 119.0, 130.0, 136.2, 148.2$; IR (CHCl_3): $\nu = 3331$, (s), 2936 (s), 1905 (w), 1593 (m), 1469 (s), 1229 (m), 1034 (m), 831 (w) cm^{-1} ; GC-EIMS $m/z = 225$ (M^+ , 55), 164 (7), 150 (8), 139 (45), 125 (100), 106 (13), 93 (21), 80 (28); anal. calcd. for $\text{C}_{12}\text{H}_{19}\text{NOS}$ (225.4): C, 63.96, H, 8.50; N, 6.22; found: C, 64.05; H, 8.66; N, 6.50.

1-[(2'-(Carboxymethyl)phenylthio)hexan-2-ol (7c). Chromatography eluent: 9/1-petroleum ether/ EtOAc ; oil; yield: 75%; (Table 2, entry 6); ^1H NMR $\delta = 0.91$, (t, $J = 7.3$ Hz, 3H), 1.31–1.79 (m, 6H), 3.36 (dt apparent, $J = 5.5, 11.7$ Hz, 1H), 3.56–3.68 (m, 2H), 3.92 (s, 3H), 7.19–7.28 (m, 1H), 7.39–7.45 (m, 1H), 7.49–7.52 (m, 1H), 7.81–7.83 (m, 1H);

^{13}C NMR δ = 13.9, 22.5, 29.3, 30.9, 51.0, 63.9, 125.7, 130.5, 130.6, 131.0, 131.5, 131.9, 137.6, 167.7; IR (CHCl₃): ν = 3674 (w), 3438 (s), 2933 (s), 2874 (m), 1715 (s), 1589 (w), 1465 (m), 1290 (s), 1110 (m), 1059 (m), 909 (w) cm⁻¹; GC-EIMS: not detectable; anal. calcd. for C₁₄H₂₀O₃S (268.4): C, 62.66, H, 7.51; found: C, 62.22; H, 7.35.

1-(Pyrimidin-2'-ylthio)-hexan-2-ol (7d). Chromatography eluent: 6/4-petroleum ether/EtOAc; oil; yield: 75%; (Table 1, entry 8); ^1H NMR δ = 0.92 (t, J = 7.1 Hz, 3H), 1.32–1.48 (m, 4H), 1.59–1.63 (m, 2H), 3.17 (dd, J = 7.3, 14.5 Hz, 1H), 3.40 (dd, J = 3.2, 14.5 Hz, 1H), 3.92–3.97 (m, 1H), 4.03 (br s, 1H), 7.01 (t, J = 4.9 Hz, 1H), 8.51 (d, J = 4.9 Hz, 2H); ^{13}C NMR δ = 13.9, 22.5, 27.7, 36.2, 38.2, 71.3, 116.6, 157.1, 172.5; IR (CHCl₃): ν = 3666 (w), 3375 (s), 2933 (s), 2462 (w), 1731 (w), 1557 (m), 1459 (w), 1388 (m), 1184 (m), 902 (w) cm⁻¹; GC-EIMS m/z = 212 (M⁺, 1), 155 (20), 126 (100), 113 (20), 80 (24), 68 (8); anal. calcd. for C₁₀H₁₆N₂OS (212.3): C, 56.57, H, 7.60; found: C, 56.75; H, 7.72.)

1-[(2'-(Hydroxyphenyl)thio)hexan-2-ol (7e). Obtained with >98% of purity from the uncatalyzed process; oil; yield: 95%; (Table 2, entry 9); R_f: 0.30 (4/6-Et₂O/petroleum ether); ^1H NMR δ = 0.86 (t, J = 6.9 Hz, 3H), 1.27–1.39 (m, 4H), 1.47–1.51 (m, 2H), 2.68 (dd, J = 8.7, 13.6 Hz, 1H), 2.90 (dd, J = 3.3, 13.6 Hz, 1H), 3.60–3.66 (m, 1H), 6.82–6.86 (m, 1H), 6.96–6.99 (m, 1H), 7.23–7.27 (m, 1H), 7.46–7.48 (m, 1H); ^{13}C NMR δ = 13.9, 22.5, 27.7, 35.9, 44.0, 69.9, 115.5, 118.9, 120.7, 131.1, 136.2, 157.2; IR (CHCl₃): ν = 3597 (m), 3402 (s), 2932 (s), 2868 (m), 1729 (m), 1576 (m), 1470 (s), 1345 (w), 1288 (m), 1210 (s), 1035 (m) cm⁻¹; GC-EIMS m/z = 226 (M⁺, 33), 208 (8), 140 (100), 125 (29), 97 (23), 69 (12); anal. calcd. for C₁₂H₁₈O₂S (226.3): C, 63.68, H, 8.02; found: C, 63.80; H, 8.10.

1-(Pyridin-2'-ylthio)-hexan-2-ol (7f). Obtained with 99% of purity from the work-up; oil; yield: 95%; (Table 2, entry 12); R_f: 0.25 (9/1-petroleum ether/EtOAc); ^1H NMR δ = 0.92 (t, J = 7.1 Hz, 3H), 1.33–1.40 (m, 3H), 1.47–1.64 (m, 3H), 3.16 (dd, J = 7.0, 14.8 Hz, 1H), 3.35 (dd, J = 2.7, 14.7 Hz, 1H), 3.90–3.95 (m, 1H), 7.00–7.04 (m, 1H), 7.27–7.30 (m, 1H), 7.48–7.52 (m, 1H), 8.34–8.36 (m, 1H); ^{13}C NMR δ = 13.7, 22.4, 27.5, 36.2, 38.0, 71.2, 119.4, 122.3, 136.0, 148.4, 158.9; IR (CHCl₃): ν = 3155 (m), 3020 (s), 2931 (s), 2834 (s), 1582 (s), 1458 (s), 1417 (m), 1225 (m), 1128 (m), 1044 (w) cm⁻¹; GC-EIMS m/z = 211 (M⁺, 1), 193 (8), 154 (58), 136 (30), 125 (100), 111 (47), 79 (36), 67 (13); anal. calcd. for C₁₁H₁₇NOS (211.3): C, 62.52; H, 8.11; N, 6.63; found: C, 62.40; H, 8.01; N, 6.55.

Rel(2*S*,3*R*)-3-(pyrimidin-2'-ylthio)-hexane-1,2-diol (9d). Chromatography eluent: 60/38/2-petroleum ether/EtOAc/MeOH; oil; yield: 52% yield; (Scheme 1); ^1H NMR δ = 0.93 (t, J = 7.2 Hz, 3H), 1.45–1.87 (m, 4H), 3.61 (dd, J = 6.9, 11.4 Hz, 1H), 3.69 (dd, J = 4.3, 11.4 Hz, 1H), 3.86–3.94 (m, 1H), 4.05–4.13 (m, 1H), 7.12 (t, J = 4.9 Hz, 1H), 8.55 (d, J = 4.9 Hz, 2H); ^{13}C NMR δ = 15.1, 22.1, 33.5, 49.7, 65.9, 77.0, 118.8, 159.4, 174.4; IR (CHCl₃): ν = 2875 (s), 2462 (w), 1962 (w), 1709 (s), 1656 (s), 1552 (s), 1465 (m), 1384 (m) cm⁻¹; GC-EIMS, not detectable; anal. calcd. for C₁₀H₁₆N₂O₂S (228.3): C, 52.61, H, 7.06, N, 12.27; found: C, 52.45; H, 7.15; N, 12.31.

Rel(2*S*,3*R*)-3-(pyridin-2-ylthio)hexane-1,2-diol (9f). Chromatography eluent: 98/2-Et₂O/MeOH; yield 63% yield; (Scheme 1); ^1H NMR δ = 0.91 (t, J = 7.1 Hz, 3H), 1.40–1.72 (m, 3H), 1.95–2.00 (m, 1H), 3.65–3.79 (m, 3H), 3.91 (dd, J = 3.4, 11.2 Hz, 1H), 4.68 (br s, 2H), 7.03–7.06 (m, 1H), 7.26–7.31 (m, 1H), 7.47–7.52 (m, 1H), 8.33–8.36 (m, 1H); ^{13}C NMR δ = 13.7, 20.2, 32.9, 48.2, 63.6, 74.8, 119.7, 123.2, 136.5, 148.6, 157.1; IR (CHCl₃): ν = 3551 (m), 3251 (s), 2964 (s), 2471 (w), 1730 (m), 1584 (s), 1459 (s), 1417 (m), 1233 (s), 1057 (m), 910 (m) cm⁻¹; GC-EIMS, not detectable; anal. calcd. for C₁₁H₁₇NO₂S (227.3): C, 58.12, H, 7.54, N, 6.16; found: C, 58.02; H, 7.67; N, 6.25.

Rel(2*R*,3*S*)-2-(pyrimidin-2'-ylthio)-hexane-1,3-diol (10d). Characterized by using a chromatographically enriched mixture, eluent: 60/38/2-petroleum ether/EtOAc/MeOH; oil; (Scheme 1); ^1H NMR δ = 0.92–0.95 (m, 3H), 1.37–2.12 (m, 4H), 3.61–3.82 (m, 3H), 4.46–4.48 (m, 1H), 6.99–7.02 (m, 1H), 8.48–8.51 (m, 2H); ^{13}C NMR δ = 14.2, 22.1, 35.4, 55.1, 63.0, 72.4, 116.9, 157.3, 165.8; GC-EIMS, not detectable.

Rel(2*R*,3*S*)-2-(pyridin-2'-ylthio)-hexane-1,3-diol (10f). Chromatography eluent: 98/2-Et₂O/MeOH; oil; yield: 27%; (Scheme 1); ^1H NMR δ = 0.92 (t, J = 6.5 Hz, 3H), 1.26–1.77 (m, 4H), 3.87–3.87 (m, 1H), 3.99–4.09 (m, 3H), 4.42 (br s, 2H), 7.03–7.07 (m, 1H), 7.28–7.31 (m, 1H), 7.51–7.53 (m, 1H), 8.33–8.35 (m, 1H); ^{13}C NMR δ = 15.3, 19.0, 36.9, 54.0, 63.3, 72.7, 120.0, 123.5, 136.6, 148.7, 157.8; IR (CHCl₃): ν = 3390 (s), 2964 (s), 1729 (m), 1582 (s), 1458 (m), 1232 (m), 1127 (m), 1044 (w), 910 (w) cm⁻¹; GC-EIMS, not detectable; anal. calcd. for C₁₁H₁₇NO₂S (227.3): C, 58.12; H, 7.54; N, 6.16; found: C, 58.20; H, 7.66; N, 6.23.

3-*n*-Butyl-2,3-dihydro[1,3]thiazolo[3,2-*a*]pyridin-4-ium methanesulfonate (11). 1.0 mmol of **7f** coming directly from the thiolysis of **5** with **2f**, was dissolved with 2 mL of CH₂Cl₂ and at 0 °C 2 equiv. of Et₃N (0.203 g) and 2 equiv. of MsCl (0.155 mL) were added. After 6 h the reaction mixture was charged on a silica gel column chromatography and eluted with CH₂Cl₂/MeOH 7/3. Salt **11** was obtained as a viscous liquid in 86% overall yield (Scheme 2); ^1H NMR δ = 0.72 (t, J = 7.0 Hz, 3H), 1.21–1.34 (m, 5H), 1.79–1.91 (m, 1H), 2.53 (s, 3H), 3.39 (dd, J = 2.4, 11.6 Hz, 1H), 4.03 (dd, J = 8.1, 11.6 Hz, 1H), 5.94–5.96 (m, 1H), 7.55 (t, J = 6.8 Hz, 1H), 7.82 (d, J = 8.3 Hz, 1H), 8.18 (t, J = 7.9 Hz, 1H), 9.28 (d, J = 6.2 Hz, 1H); ^{13}C NMR δ = 13.4, 21.9, 26.8, 32.9, 34.1, 39.1, 72.1, 122.7, 122.8, 142.7, 144.5, 158.5; IR (CHCl₃): ν = 3415 (s), 3115 (w), 2935 (s), 2465 (m), 1613 (s), 1565 (m), 1479 (s), 1445 (m), 1382 (w), 1290 (m), 1246 (s) cm⁻¹; anal. calcd. for C₁₂H₁₉NO₃S₂ (289.4): C, 49.80; H, 6.62; N, 4.84; found: C, 49.65; H, 6.45; N, 4.70.

3-*n*-Butyl-2,3-dihydro[1,3]thiazolo[3,2-*a*]pyridine-4-ium chloride (12). Obtained by charging **11** on a Amberlite-Ira-400 (Cl) resin column chromatography and eluting with 1/1-H₂O/MeOH; oil; yield: 85% (Scheme 2); ^1H NMR δ = 0.84 (t, J = 6.9 Hz, 3H), 1.19–1.49 (m, 4H), 1.96–2.04 (m, 2H), 3.42 (d, J = 11.8 Hz, 1H), 4.15 (dd, J = 8.0, 11.7 Hz, 1H), 6.43–6.46 (m, 1H), 7.67 (t, J = 6.6 Hz, 1H), 7.87 (d, J = 8.4 Hz, 1H), 8.24 (d,

$J = 7.8$ Hz, 1H), 9.77 (d, $J = 6.1$ Hz, 1H); ^{13}C NMR $\delta = 13.3$, 21.8, 27.0, 32.9, 34.2, 71.7, 122.5, 122.9, 142.6, 144.4, 158.4; IR (CHCl₃): $\nu = 3388$ (s), 2999 (m), 2937 (s), 2463 (w), 1613 (s), 1566 (m), 1481 (s), 1445 (m), 1290 (m), 1234 (s) cm⁻¹; anal. calcd. for C₁₁H₁₆ClNS (229.8): C, 57.50; H, 7.02; Cl, 15.45; N, 6.10; found: C, 57.63; H, 7.11; Cl, 15.51; N, 6.21.

Acknowledgements

The Ministero dell'Istruzione dell'Università e della Ricerca (MIUR) and the Università degli Studi di Perugia (within the funding projects: COFIN, COFINLAB (CEMIN) and FIRB 2001) are thanked for financial support

References

- (a) J. H. Clark, *Green Chem.*, 1999, **1**, 1–8; (b) *Green Chemistry: Challenging Perspectives*, ed. P. Tundo and P. T. Anastas, Oxford Science, Oxford, 1999; (c) Various authours, *Pure Appl. Chem.*, 2001, **73**, 77–199.
- For recent papers see: (a) F. Fringuelli, F. Pizzo and L. Vaccaro, *J. Org. Chem.*, 2001, **66**, 4719–4722; (b) F. Fringuelli, F. Pizzo, S. Tortoioli and L. Vaccaro, *Adv. Synth. Catal.*, 2002, **344**, 379–384; (c) F. Fringuelli, F. Pizzo, M. Rucci and L. Vaccaro, *J. Org. Chem.*, 2003, **68**, 7041–7045; (d) F. Fringuelli, F. Pizzo, S. Tortoioli and L. Vaccaro, *Green Chem.*, 2003, **5**, 436–440; (e) D. Amantini, F. Fringuelli, O. Piermatti, F. Pizzo and L. Vaccaro, *J. Org. Chem.*, 2003, **68**, 9263–9268; (f) D. Amantini, F. Fringuelli, F. Pizzo, S. Tortoioli and L. Vaccaro, *Synlett*, 2003, 2292–2296; (g) F. Fringuelli, F. Pizzo, S. Tortoioli and L. Vaccaro, *J. Org. Chem.*, 2003, **68**, 8248–8251; (h) F. Fringuelli, F. Pizzo and L. Vaccaro, *J. Org. Chem.*, 2004, **69**, 2315–2321.
- (a) D. Amantini, F. Fringuelli, F. Pizzo and L. Vaccaro, *J. Org. Chem.*, 2001, **66**, 6734–6737; (b) F. Fringuelli, F. Pizzo, S. Tortoioli and L. Vaccaro, *Tetrahedron Lett.*, 2003, **44**, 6785–6787; (c) D. Amantini, R. Beleggia, F. Fringuelli, F. Pizzo and L. Vaccaro, *J. Org. Chem.*, 2004, **69**, 2896–2898; (d) F. Fringuelli, F. Pizzo, S. Tortoioli and L. Vaccaro, *J. Org. Chem.*, 2004, **69**, 7745–7747; (e) F. Fringuelli, F. Pizzo, C. Vittorini and L. Vaccaro, *Chem. Commun.*, 2004, 2756–2757; (f) F. Fringuelli, F. Pizzo, S. Tortoioli and L. Vaccaro, *J. Org. Chem.*, 2004, **69**, 8780–8785.
- (a) D. Amantini, F. Fringuelli and F. Pizzo, *J. Org. Chem.*, 2002, **67**, 7238–7243; (b) D. Amantini, F. Fringuelli, O. Piermatti, F. Pizzo and L. Vaccaro, *J. Org. Chem.*, 2003, **68**, 9263–9268.
- (a) J. D. Holbrey and K. R. Seddon, *Clean Prod. Process.*, 1999, **1**, 223–236; (b) T. Welton, *Chem. Rev.*, 1999, **99**, 2071–2083; (c) P. Wasserscheid and W. Keim, *Angew. Chem., Int. Ed.*, 2000, **39**, 3772–3789; (d) C. Baudequin, J. Baudoux, J. Levillain, D. Cahard, A. –C. Gaumont and J. –C. Plaquevent, *Tetrahedron: Asymmetry*, 2003, **14**, 3081–3093.
- J. Levillain, G. Dubat, I. Abrunhosa, M. Gulea and A. –C. Gaumont, *Chem. Commun.*, 2003, 2914–2915.
- Enantiopure monosubstituted 1,2-epoxides are easily prepared in multi-ton quantities by Jacobsen hydrolytic kinetic resolution of racemates: M. Tokunaga, J. F. Larrow, F. Kakiuchi and E. Jacobsen, *Science*, 1997, **277**, 936–938.
- (a) J. M. Chong and K. B. Sharpless, *J. Org. Chem.*, 1985, **50**, 1560–1563[Ti(O-*i*-Pr)₄]; (b) A. E. Vougioukas and H. B. Kagan, *Tetrahedron Lett.*, 1987, **28**, 6065–6068 [Lanthanides complexes]; (c) P. N. Guivisdalsky and R. Bittman, *J. Am. Chem. Soc.*, 1989, **111**, 3077–3079 [BF₃·Et₂O]; (d) J. Iqbal, A. Pandey, A. Shukla, R. R. Srivastava and S. Tripathi, *Tetrahedron*, 1990, **46**, 6423–6432 [CoCl₃]; (e) M. Chini, P. Crotti, E. Giovani, F. Macchia and M. Pineschi, *Synlett*, 1992, 303–305 [LiClO₄]; (f) G. Lin, Z. Shi and C. Zeng, *Tetrahedron: Asymmetry*, 1993, **4**, 1533–1536 [Ti(O-*i*-Pr)₄]; (g) I. W. J. Still and L. P. J. Martin, *Synth. Commun.*, 1998, **28**, 913–923 [SmI₂]; (h) J. S. Yadav, B. V. S. Reddy and G. Baisha, *Chem. Lett.*, 2002, 906–907[InCl₃]; (i) S. Chanrasekar, Ch. R. Reddy, B. N. Babu and G. Chandrasekar, *Tetrahedron Lett.*, 2002, **43**, 3801–3803 [B(C₆F₅)₃]; (j) N. Devan, P. R. Sridhar, K. R. Prabhhu and S. Chandrasekaran, *J. Org. Chem.*, 2002, **67**, 9417–9420 [tetrathiomolybdate]; (k) M. Sasaki, K. Tanino, A. Hirai and M. Miyashita, *Org. Lett.*, 2003, **5**, 1789–1791 [(CH₃O)₃B].
- (a) D. A. Evans, D. M. Barnes, J. S. Johnson, T. Lectka, P. von Matt, S. J. Miller, J. A. Murry, R. D. Norcross, E. A. Shaughnessy and K. R. Campos, *J. Am. Chem. Soc.*, 1999, **121**, 7582–7594; (b) A. Fürstner, M. Libl, C. W. Lehmann, M. Picquet, R. Kunz, C. Bruneau, D. Touchard and P. H. Dixneuf, *Chem. Eur. J.*, 2000, **6**, 1847–1857.
- Also Sc(OTf)₃, Al(OTf)₃, Cu(OTf)₂, Yb(OTf)₃, Hf(OTf)₄ were used as catalysts but a significant conversion of **1** was reached after more than 60 h of reaction time. The only exception was Zn(OTf)₂ which gave complete conversion after 0.5 h.
- It is reported that aromatic protons of *N*-butylpyridinium chloride resonate in the range 8.10–9.23 ppm in d₆-DMSO¹² while *ortho* and *para* protons of the same compound in CD₂Cl₂ resonate at 9.76 and 8.51 ppm respectively.¹³ Furthermore *ortho* and *para* protons of *N*-butylpyridinium hexafluorophosphate resonate at 8.68 and 8.51 ppm in CD₂Cl₂.¹⁴ Summarizing, by simply varying the solvent and/or the counterion significant shifts are observed (e.g., in CD₂Cl₂ 1.08 ppm upfield shift is observed moving from Cl to PF₆ as counterions).
- G. L. Rebeiro and B. M. Khadilkar, *Synthesis*, 2001, 370–372.
- L. Magna, Y. Chauvin, G. P. Niccolai and J. –M. Basset, *Organometallics*, 2003, **22**, 4418–4425.
- A. R. Katritzky, O. Rubio, M. Szajda and B. Nowak-Bydra, *J. Chem. Res. (S)*, 1984, 234–235.

Supported ionic liquids catalysts for fine chemicals: citral hydrogenation†

Jyri-Pekka Mikkola,*^a Pasi Virtanen,^a Hannu Karhu,^b Tapio Salmi^a and Dmitry Yu. Murzin^a

Received 8th June 2005, Accepted 23rd September 2005

First published as an Advance Article on the web 12th October 2005

DOI: 10.1039/b508033a

The quest for new concepts in catalysis involving fine chemicals production is discussed. A new approach for easy preparation of structural, heterogeneous catalysts where the selectivity profile is altered by means of different ionic liquids and the same transition metal species (Pd) is introduced. Furthermore, a novel ionic liquid, [A336][PF₆], derived from a common phase-transfer catalyst, Aliquat336[®], was synthesized and utilized in catalytic hydrogenation of citral.

Introduction

Ionic liquids or room temperature salt melts have received a lot of interest during the last few years. Some of the most important features of these materials are the negligible vapour pressure, wide liquidus range, unique solvation properties, good ion conductivity as well as high catalytic activity and selectivity.^{1–4} They are a novel class of materials that have already been found to perform well in various kinds of catalytic reactions as well as preparation of nanostructured materials and nanoparticles for catalysis.^{5–8} However, the industrial use of ionic liquids is retarded primarily by their still rather high cost and limited knowledge on physico-chemical properties, separation behaviour, biodegradability and ecotoxicology. Therefore, supported ionic liquids with catalytic amounts of ionic liquids attached to industrially easily recyclable solid and structured materials suitable for fixed bed or slurry operations, possess an interesting alternative in heterogenized catalysis. It's worth mentioning that the ionic liquid itself can be catalytically active or the catalytically active species (transition metal salt, complex or even an enzyme) is dissolved into the ionic liquid so that it both stabilizes and immobilizes the nanoscale catalyst, as well as controls the dissolution of the reactants.

Immobilization and supporting of ionic liquids can be carried out in many ways, such as simple impregnation ('incipient wetness'), covalent linking of the cation or the anion, polymerization, sol-gel method *etc.*^{9–12} Undoubtedly, the easiest method involves a kind of impregnation of the support material with the ionic liquid of choice, diluted with a conventional co-solvent, such as acetone. The dilution followed by removal of the co-solvent by evaporation results in a uniform and thin ionic liquid loading. In actual reaction conditions, on the other hand, such a bulk solvent, that is not miscible with the ionic liquid, was chosen.

One of the prominent trends in industry is the quest for alternative, more sophisticated catalytic systems to replace often inefficient traditional slurry or fixed bed concepts. The driving force, naturally, is the search for a more selective and economical process concept. A number of alternatives have been introduced, such as monoliths, Sulzer Katapak[®] elements, various net structures and stirrer structures containing catalytic coating/catalyst elements. A review by Matatov-Meytal and Sheintuch¹³ introduces a series of different types of fibers and cloths for catalytic applications. One of the benefits common for all approaches is the elimination of an often cumbersome and costly catalyst filtration step. Furthermore, more efficient usage of the catalytically active material and improved external mass transfer of reactants to the catalyst have been claimed. However, the capacity and efficiency (performance per time unit) of traditional systems is difficult to achieve with any available structured alternative: the reason is that in the case of *e.g.* slurry systems, a huge overload of catalyst powder usually is loaded into a reactor, whereas the structured systems (such as monoliths or coated static mixers) have macroscopic dimensions which limit the number of units that can be packed into a certain volume. Therefore, an intermediate solution, where a seemingly organized matt structure (Active Carbon Cloth woven from small fibers and containing microscopic features in the pore structure) with high surface area and packed within a reactor tube or attached to a stirrer of a stirred tank, introduces a new perspective.

Experimental

Traditionally, catalytically active transition metal particles have been introduced into the heterogeneous catalysts by means of various impregnation, precipitation, deposition, ALE (atomic layer epitaxy) *etc.* methods—or by means of direct mixing of the metal precursors (salts, organometallic complexes) during the synthesis of the solid material (*i.e.* sol-gel methods, zeolite synthesis *etc.*)—followed by (thermal) decomposition, restructuring and redistribution of the resulting active metal sites during calcination and reduction steps. Consequently, the catalytic properties of the resulting material are largely determined by these post-treatment operations, such as the final temperature during calcinations and reduction, temperature gradients during these processes, reduction method (chemical or molecular hydrogen), oxygen effects,

^aLaboratory of Industrial Chemistry, Process Chemistry Centre, Åbo Akademi University, Biskopsgatan 8, FIN-20500, Åbo/Turku, Finland. E-mail: Jyri-Pekka.Mikkola@abo.fi; Fax: +358 2 215 4479; Tel: +358 2 215 4574

^bDepartment of Physics, Laboratory of Materials Science, 20014 Turun yliopisto - FIN-20014 University of Turku, Turku, Finland

† This work was presented at the Conference on Knowledge-based Materials and Technologies for Sustainable Chemistry, held in Tallinn, Estonia, 1–5 June, 2005.

nature of the precursors *etc.* Moreover, the deactivation behaviour—an important aspect in industrial operations—of a particular catalyst is dependent not only of the process conditions applied but also on the details of the synthesis process and on the precursors used. Therefore, the development of a well-performing heterogeneous catalyst involves a tedious process upon which a huge amount of experimental work and characterization is required. Hereby a strategy for the preparation of structured (as well as non-structured) heterogeneous catalysts by means of an immobilized ionic liquid (IL) layer, into which the metallic transition metal species have been dissolved, is applied. The concept has been previously investigated by a few authors^{5–6,10,12,14–15} but according to our knowledge, until now, not in connection to structured, heterogeneous catalysts. Also, in a study by Anderson *et al.*,¹⁶ hydrogenation of α,β unsaturated aldehydes cinnamaldehyde and citral, Pd on active carbon powder was supported in various ionic liquids.

The sample reaction, hydrogenation of citral, is a challenging reaction: Citral is a multi-unsaturated compound containing both an isolated and conjugated carbon-carbon double-bond as well as a carbonyl group. Upon hydrogenation, numerous parallel and consecutive reactions, such as *cis-trans* isomerization, cyclization, acetalization and decarbonylation, typically take place.^{17–21} A few of the interesting hydrogenation products are citronellal, citronellol and dihydrocitronellal that are utilized in the perfumery industry. A list of a few products and sample applications are listed in Table 1. A reaction scheme for citral hydrogenation is presented in Fig. 1. The selectivity of hydrogenation of α,β -unsaturated aldehydes, such as citral, depends on several factors, although hydrogenation as such, can be carried out over most platinum metal catalysts.^{22,23}

In this study we used an extremely simple preparation methodology, according to which the ionic liquid ([bmim]-[PF₆], Merck, 98%; [bmim][BF₄], Merck, 98% and [A336][PF₆], self-made novel IL the synthesis of which will be described

Table 1 A few fragrances and sample applications

Citronellal	Fragrance in soaps and mosquito-repellant candles
Citronellol	Anti-perspirant, fabric softener, detergent TAED, shampoo, soap
Isopulegol	Oral care, mint flavors, grape, raspberry, lime
Dihydrocitronellal	Fragrance
Nerol	Anti-perspirant, fabric softener, detergent TAED, shampoo, soap
Geraniol	Pesticide and fragrance industry, flavour in alcoholic and non-alcoholic beverages, ice cream, candies and baked goods
Menthols and derivatives	For the use of nature-identical peppermint oils
Tetrahydrogeraniol	A nature identical flavouring substance
Borneol	Artificial flavouring
α -Terpineol	Perfumery industry
Elemene	Incense, potpourri or perfume
<i>p</i> -menthene	Plant growth regulator
Piperitone	Culinary herb and for medicinal purposes
β -Caryophyllene	Flavoring agent, aromatherapy

later) and the transition metal salt (palladium acetylacetonate, Aldrich 99%) were both dissolved in dry acetone (Acros Organics, 50 ppm H₂O), mixed and, thereafter, a pre-dried (105 °C, 1 h) structural solid, high surface area Kynol® active carbon cloth/matt (ACC, Fig. 2) was wetted ('incipient wettness') with the solution. Upon this, the capillary forces instantaneously sucked the liquid into the support, resulting in a seemingly 'dry' texture. The active carbon cloth has excellent mechanical strength (tensile strength 6 kg/50 mm) and high surface area (*ca.* 1500 m² g⁻¹; manufacturer information). In the next step acetone was evaporated from the ACC in an oven at 105 °C (15 min) and cut into pieces that fitted into our tailor-made laboratory autoclave internals (Fig. 3). The amount of ACC-support was approximately 1.1–1.4 g (dry), corresponding to a macroscopic surface area of 4 × 10 cm². The amount of ionic liquids was approximately 0.15–0.17 g and that of Pd(acac) 0.05 g. The exact loading of Pd(acac) as well as ILs on Pd/IL/ACC or SSIL-TM (structured supported ionic liquid-transition metal) catalysts are reported in Table 2. The catalyst was exposed to a flow of hydrogen (Aga Oy, 99.999%) for 1 h at 100 °C, thereby facilitating reduction or complex formation and stabilization of Pd. The reduction treatment is reported to induce the formation of Pd-nanoparticles⁶ or, in the case of a complex formation, molecular size catalytic species. Assessment of the particle size requires direct evidence, such as high resolution transmission electron microscopy (HRTEM), work which is in progress. The immobilization relies on the simple fact that the bulk solvent, *n*-hexane, and the ionic liquids are immiscible with each other.

The leaching of ionic liquids into the bulk solvent (*n*-hexane) was studied by means of high performance liquid chromatography (HPLC). Detection of ionic liquids in citral hydrogenation samples by HPLC was made by reversed-phase HPLC with UV detection under the following conditions: sample injection volume was 3 μ l; eluent 20% acetonitrile, 80% 0.02 M phosphate buffer pH 4.5; flow rate of 1.0 ml min⁻¹; column Hewlett Packard Zorbax eclipse XDB-C8, id (internal diameter) 4.6 mm, length 150 mm; column temperature 40 °C and detection with DAD (diode array detector), qualitatively from UV-spectrum, quantitatively with wavelength 250 nm.

X-ray photoelectron spectroscopy (XPS) was used to study the reduction state of the Pd species residing in the ionic liquid on the ACC support. To the best of our knowledge, XPS has not been previously used to study the reduction state of metal species in ionic liquids. A Perkin-Elmer 5400 ESCA was used for the XPS analysis. The ionic liquid catalyst was analysed *ex-situ* as a residue on Kynol support material after an outgassing of several hours in vacuum. Despite the low vapor pressure of the liquid, it was observed that most of the liquid vaporized in the ultra-high vacuum (UHV) environment and a high pass energy setting (44.75 eV) was necessary to obtain a sufficient rate of photoelectron pulses. In the spent catalyst, the amount of ionic liquid residue in UHV conditions was higher and a lower pass energy value was used to obtain a higher resolution. The binding energies of carbon and oxygen originating from support material were also tabulated as they can be indicative of minor sample charging during X-ray bombardment. Palladium metal, PdO and PdO₂ typically have binding energies of *ca.* 335.1 eV, 336.3 eV and 337.9 eV.²⁴

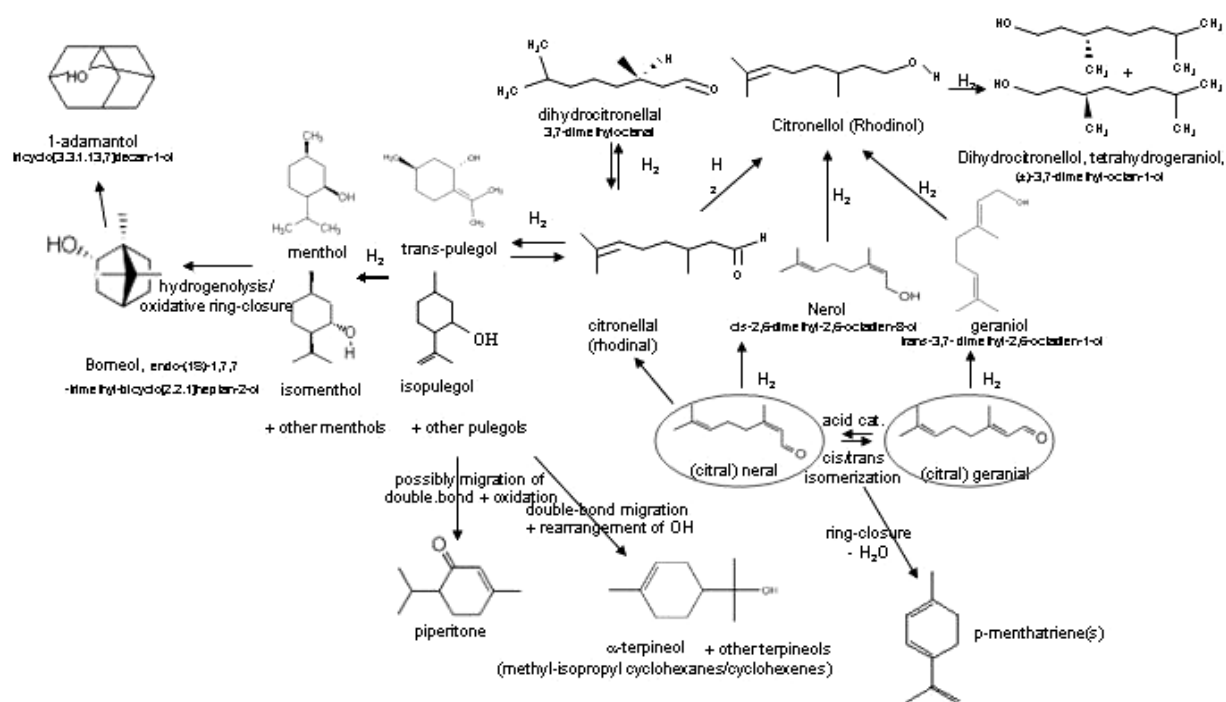


Fig. 1 Plausible reaction network for the hydrogenation of citral and the molecular structure of known impurities in the citral standard.

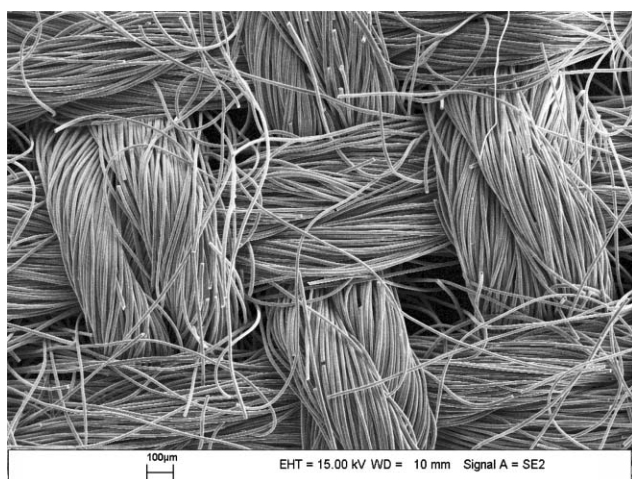


Fig. 2 SEM image of the Kynol™ active carbon cloth support.

In the kinetic experiments, the reactant (*cis/trans* citral, Fluka > 95%, redistilled) dissolved into a 250 ml volume of solvent (hexane, Merck pro-analyti) was bubbled with H₂ to remove dissolved oxygen (2 min) and fed into the preheated reactor. Consequently, the stirring was immediately engaged at

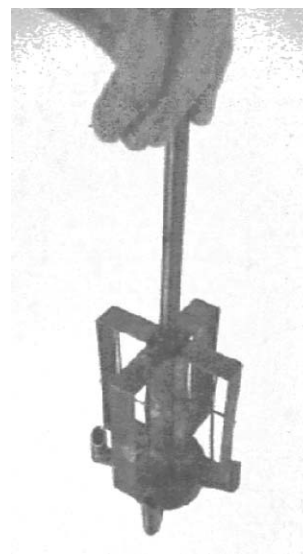


Fig. 3 Integrated gadget of a combined stirrer and catalyst holder.

a rate which ensured that no external mass-transfer limitations prevailed (1500 rpm). Hydrogenation of citral was carried out in a 600 ml (total volume) laboratory autoclave (Parr Inc.,

Table 2 The characteristics of the ionic liquid catalysts

Pd/IL/ACC type (ionic liquid)	[bmim][PF ₆]	[bmim][BF ₄]	[A336][PF ₆]
Weight, ACC support/g	1.11	1.28	1.45
IL loading (wt%) (on ACC)	13.5	11.9	11.7
Pd (metal) loading (wt%) (on IL)	11.5	11.5	10.3
Pd (metal) loading (wt%) (on IL + ACC)	1.3	1.1	1.0

USA) equipped with a heating jacket. The reactor was equipped with a tailor-made internals: the matt-structures were cut into suitable pieces and attached to the stirrer shaft as blades (Fig. 3). The temperature and stirrer controllers used were Parr 4843 (Watlow Controls Series 982). Prior to each experiment, the catalyst and reactor vessel were preheated under hydrogen atmosphere to the desired temperature. In the case of the experiments with active carbon catalysts, a volume of 250 ml of 0.08 M of citral (33.9/66.1 mol% *cis/trans*, Lancaster 5460 or Acros Organics 5392-40-5, 95%) was dissolved in analytical grade hexane (99%, Merck) without any further purification. In the case of the monolith experiments, 0.0195 mol of citral was dissolved in 150 ml of hexane. During the course of the experiment, small samples were withdrawn from the reactor for analysis by means of GC-MS (gas chromatography coupled to a mass spectrometer). At the end of the experiment, the reactor contents were emptied *via* the sampling line and the catalyst stored under hydrogen for the next experiment with recycled catalyst. The experiments were carried out at 2–30 bar of hydrogen pressure. Hydrogen gas used had a purity of 99.999% (AGA). The mass of citral in the experiments was around 3 g.

The samples were analyzed by means of GC. 500 μ l of internal standard (0.021 M cyclohexanone in cyclohexane) was added to the samples withdrawn from the reactor. The column used was a DB-1 with the length 30 m, inner diameter 0.25 mm and the film thickness 0.5 μ m. The following temperature program was applied: 70 $^{\circ}$ C for 1 min, 13 $^{\circ}$ C min⁻¹ to 120 $^{\circ}$ C and continued with 1 $^{\circ}$ C min⁻¹ to 125 $^{\circ}$ C and 0.5 $^{\circ}$ C min⁻¹ to 130 $^{\circ}$ C. At the end the temperature was increased 10 $^{\circ}$ C min⁻¹ to 160 $^{\circ}$ C and kept constant for 5 min. Several minor species, like impurities in the citral standard, were identified with GC-mass spectrometry (GC-MS).

Ionic liquids preparation

Two of the ionic liquids used in this study are, perhaps, the most investigated ones: 1-butyl-3-methylimidazolium hexafluorophosphate, [bmim][BF₆] (IL1), and -tetrafluoroborate, [bmim][BF₄] (IL2). These ionic liquids were used as received. The third one, tricaprilmethylammonium hexafluorophosphate, [A336][PF₆] (IL3), is a novel, self-prepared ionic liquid. This ionic liquid was prepared by the metathesis procedure as follows: 0.0095 mol of Aliquat 336[®] (or tricaprilmethylammonium chloride), a common phase transfer catalyst and an ionic liquid itself (Aldrich), as well as 0.01 mol of NaPF₆ (Aldrich, 98%) were dissolved in 5 ml and 10 ml of extra dry acetone (Acros Organics, <0.005% H₂O), respectively. The

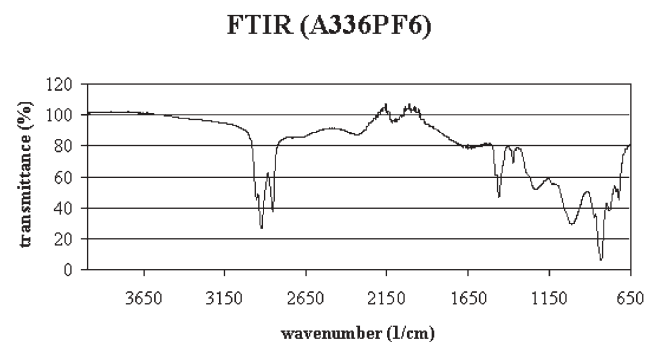
latter solution was added dropwise to a stirred solution of Aliquat, at room temperature, upon which the precipitate of NaCl crystals immediately formed due to the insolubility of NaCl. The solution was decanted, filtered through a Millipore Millex 0.45 μ m filter and heated under high vacuum (rotavapor, 80 $^{\circ}$ C, 8 mbar, 30 min) to remove acetone. Some more sediment was formed since the synthesis was carried out under normal atmosphere and the IL was dissolved in another portion of 5 ml acetone. The decanting–filtration–vacuum treatment procedure was repeated and, again, dissolved in 5 ml absolute ethyl alcohol (Primalco Oy). After yet another decanting–filtration–vacuum treatment procedure, the hydrophobic IL was washed with 20 ml of deionized H₂O and placed in rotary evaporator for drying of the excess moisture (2 h, 90 $^{\circ}$ C, 8 mbar). The resulting ionic liquid, [A336][PF₆], is a clear, colourless IL obtained in quantitative yield.

Results

Ionic liquid [A336][PF₆] characterization

The FTIR spectrum for the novel, hydrophobic ionic liquid [A336][PF₆] is depicted in Fig. 4. On the basis of TGA (thermographic analysis, Fig. 5a) and DSC (digital scanning calorimetry, Fig. 5b) measurements, upon cooling the freezing point was estimated as 62–64 $^{\circ}$ C, upon heating the melting zone as 46–70 $^{\circ}$ C and decomposition temperature as 274 $^{\circ}$ C. It is a rather viscous liquid below 80 $^{\circ}$ C, with a slightly opaque texture, above which temperature a clear, colorless liquid can be observed. The water content was estimated to be 1.2 wt% in a sample stored in a closed bottle at room temperature. The white salt-precipitate formed during the metathesis was examined by means of SEM-EDX which confirmed the formation of NaCl. The compound is easily soluble, at least, in acetone, acetonitrile and ethyl alcohol, to mention a few. The density of the compound is slightly below that of water, although the exact value is not available due to the high melting point and viscosity (*e.g.* Anton Paar DMA512P densitometer, could not be used).

The ionic liquid was not controlled for residual chlorine since relatively extensive washing with H₂O was carried out (although one thus risked some break-down of PF₆ and HF formation). Moreover, a slight excess of NaPF₆ over Aliquat 336[®] was used. Indeed, indirect evidence was obtained that chlorine residues were not present in the ionic liquid, since no

**Fig. 4** FTIR spectrum for the [A336][PF₆] ionic liquid.

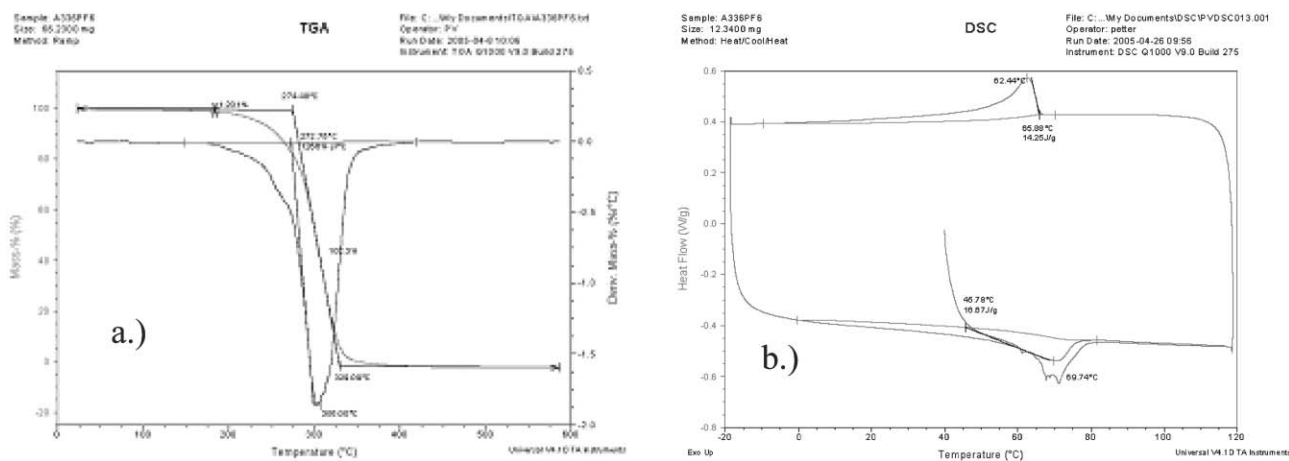


Fig. 5 TGA (a) and DSC (b) graphs for the [A336][PF₆] ionic liquid.

acetal formation from citral could be detected during the hydrogenation experiments: in the paper of Aumo *et al.*,²³ prominent acetal formation was observed when the reaction was carried out over a conventional Pd on active carbon catalyst prepared from a chloride precursor. In XPS measurements of the catalyst, chloride traces (0.2%) were observed. By contrast, when nitrate precursor was applied, no acetalization could be observed. A more thorough IL characterization will be published and presented later elsewhere.²⁵

Catalyst properties and characterization

The active carbon cloth had a fibre diameter of $\varnothing = 9.2 \mu\text{m}$. SEM images revealed the morphology of the active carbon cloth catalyst (Fig. 2). Nitrogen physisorption was performed and BET surface areas as well as specific Dubinin micro-pore volumes and BET pore volumes can be found in our earlier publication.²⁶

After drying off acetone, the active carbon mats were seemingly dry pieces of textile, easy to handle. The final amount of catalytic metal, Pd, was only 1.4×10^{-2} – 1.5×10^{-2} g or 1.3×10^{-3} – 1.4×10^{-3} mol. The palladium metal loading as well as the ionic liquid loading were in the range of 1 wt% and 10 wt% of the active carbon support (Table 2), based on the weight increase of the catalyst carrier (ACC). The Kynol[®] active carbon cloth (ACC) specific surface area and pore volume were measured: as the ACC is a microporous (72%) support, the specific surface areas and pore volumes have been calculated by using the method of Dubinin. The

Dubinin specific surface area was found to be $1348 \text{ m}^2 \text{ g}^{-1}$ and the micropore volume $0.48 \text{ cm}^3 \text{ g}^{-1}$. Thus, taking into account that the IL loading of [bmim][PF₆] and [bmim][BF₄] were approximately 0.15 g and that of [A336][PF₆] 0.17 g on ACC as well as that the densities (25 °C) were in the range of 1.4,^{27,28} 1.1–1.2^{28,29} and 0.9 g cm^{-3} (at ambient temperature), respectively, the ionic liquid loading was around $0.1 \times 10^{-3} \text{ g m}^{-2}$. On the other hand, one can estimate that roughly 20–25 vol% of the pore volumes were filled with an ionic liquid layer of [bmim][PF₆], [bmim][BF₄] and [A336][PF₆].

According to the ESCA-XPS results, the reduction state of Pd varied, depending on the ionic liquid. Somewhat surprising, in fresh (non-reduced) samples with dissolved Pd acetylacetonate with the dissolved transition metal species the Pd reduction state was Pd⁴⁺ after dissolution, suggesting immediate reaction of the Pd acetylacetonate with the ionic liquid. However, in the case of reduced samples, palladium reduction state was found to be Pd⁰ in the case of [bmim][BF₄], indicating decomposition of the transition metal complex and formation of nano-particles. For [bmim][PF₆] and [A336][PF₆], by contrast, the results indicated a reduction state of Pd⁺ suggesting formation of complexes with the ionic liquids (Table 3).

It could be observed that the active metal in fresh catalysts is in a highly oxidized state. The noble metal is then reduced in the activity test treatment towards the metallic state. In the case of [bmim][PF₆] and [A336][PF₆], fluorine exhibited a higher binding energy in the spent catalyst.

Table 3 XPS analysis of the samples

Sample	C 1s/eV	O 1s/eV	Pd 3d _{5/2} /eV	Metal state (est.)	F 1s/eV	Pd/F
[bmim][BF ₄] Pd(acac) Kynol	285.0	532.5	338.8	Pd ⁴⁺	686.0	0.044
[bmim][BF ₄] Pd(acac) Kynol spent (after hydrogenation batches)	285.1	532.6	335.2	Pd ⁰	686.1	0.041
[bmim][PF ₆] Pd(acac) Kynol	284.9	532.5	338.3	Pd ⁴⁺	686.0	—
[bmim][PF ₆] Pd(acac) Kynol spent (after hydrogenation batches)	285.2	533.5	335.7	Pd ⁺	686.8	0.20
[A336][PF ₆] Pd(acac) Kynol	284.9	532.0	338.5	Pd ⁴⁺	686.1	0.33
[A336][PF ₆] Pd(acac) Kynol spent (after hydrogenation batches)	284.9	532.9	335.9	Pd ⁺	687.2	1.0

Table 4 Data on the experimental conditions and hydrogenation performance on the batches performed

Pd/IL/ACC type (ionic liquid)	[Bmim][PF ₆]	[Bmim][BF ₄]	[A336][PF ₆]
Batch I	(batch nr. refers to the order of consecutive batch)		
Experimental conditions, <i>T</i> /°C, <i>P</i> /bar	100/10	100/10	100/10
Conversion (%) / batch time/min	95/163	97/270	100/225
Citral feed/g	3.35	3.01	3.05
Citral-to-metal (Pd) ratio/mol mol ⁻¹	156	150	142
TOFs for citral hydrogenation/mol mol ⁻¹ h ⁻¹	55	32	38
Batch II			
Experimental conditions, <i>T</i> /°C, <i>P</i> /bar	100/2	90/10	80/10
Conversion (%) / batch time/min	39/230	66/234	95/288
Citral feed/g	3.03	3.01	3.17
Citral-to-metal (Pd) ratio/mol mol ⁻¹	141	150	148
TOFs for citral hydrogenation/mol mol ⁻¹ h ⁻¹	14	25	29
Batch III			
Experimental conditions, <i>T</i> /°C, <i>P</i> /bar	120/10	100/20	80/2
Conversion (%) / batch time/min	80/122	82/240	68/393
Citral feed/g	3.06	3.18	3.24
Citral-to-metal (Pd) ratio/mol mol ⁻¹	143	159	151
TOFs for citral hydrogenation/mol mol ⁻¹ h ⁻¹	56	33	16
Batch IV			
Experimental conditions, <i>T</i> /°C, <i>P</i> /bar	100/5	100/10	100/2
Conversion (%) / batch time/min	46/146	91/210	61/282
Citral feed/g	3.05	3.07	3.11
Citral-to-metal (Pd) ratio/mol mol ⁻¹	142	153	145
TOFs for citral hydrogenation/mol mol ⁻¹ h ⁻¹	27	40	19
Batch V			
Experimental conditions, <i>T</i> /°C, <i>P</i> /bar	100/10	120/20	—
Conversion (%) / batch time/min	75/244	99/380	—
Citral feed/g	2.95	2.93	—
Citral-to-metal (Pd) ratio/mol mol ⁻¹	138	146	—
TOFs for citral hydrogenation/mol mol ⁻¹ h ⁻¹	24	23	—
Batch VI			
Experimental conditions, <i>T</i> /°C, <i>P</i> /bar	100/10 ^a	150/30	—
Conversion (%) / batch time/min	92/300	100/90	—
Citral feed/g	3.0	3.0	—
Citral-to-metal (Pd) ratio/mol mol ⁻¹	140	150	—
TOFs for citral hydrogenation/mol mol ⁻¹ h ⁻¹	26	100	—

^a Batch after catalyst rejuvenation experiment.

Hydrogenation experiments

Citral-to-metal ratios (mol mol⁻¹) for Pd/IL/ACC catalysts are reported in Table 4, along with TOFs (turnover frequencies) of citral hydrogenation. For each type of catalyst, several consecutive batchwise experiments were carried out at different experimental conditions according to the scheme introduced in Table 3. The catalyst with the [bmim][PF₆] ionic liquid favoured the formation of citronellal over dihydrocitronellal (the primary products), at the experimental temperature and pressure range (Fig. 6), whereas the [bmim][BF₄] favoured dihydrocitronellal (Fig. 7). Moreover, higher temperatures and hydrogen pressures clearly increased the yield of dihydrocitronellal. Another important feature of the latter kind of catalyst seems to be its very prominent durability against deactivation, since the 4th batch under similar conditions as the 1st one performed at least equally well. The selectivity profile for the catalyst with the novel [A336][PF₆] ionic liquid was yet slightly different: upon standard conditions the formation of dihydrocitronellal was even more prominent than in the case of the catalyst with [bmim][BF₄], whereas low hydrogen pressure shifted the

product distribution towards citronellal (Fig. 8). However, low hydrogen pressures such as in this last series were not tried in previous ones. All three types of catalyst usually favoured geraniol and citronellol, also valuable fragrances, as the third and fourth major hydrogenation product species. For the [bmim][BF₄] containing catalyst, tetrahydrogeraniol could be obtained, at appropriate reaction conditions, in significant yields (Fig. 7). In addition, minor amounts of several other species were detected (molar fractions generally less than 0.05), such as nerol, isopulegol, pulegols, mentols and terpenes. The tendency of a particular catalyst for further hydrogenated products, *i.e.* dihydrocitronellal instead of citronellal, can perhaps be explained by the better hydrogen solubility of the ionic liquid, since it is known that *e.g.* [bmim][BF₄] and [bmim][PF₆] have significant differences in their ability to dissolve hydrogen: the latter one has a magnitude of order lower hydrogen solubility than the former one.³⁰ This was the case when comparing [bmim][PF₆] and [bmim][BF₄]. However, it seems that also the cation might have a significant effect on the hydrogen solubility, since the [A336][PF₆] ionic liquid also favours the formation of dihydrocitronellal, provided that

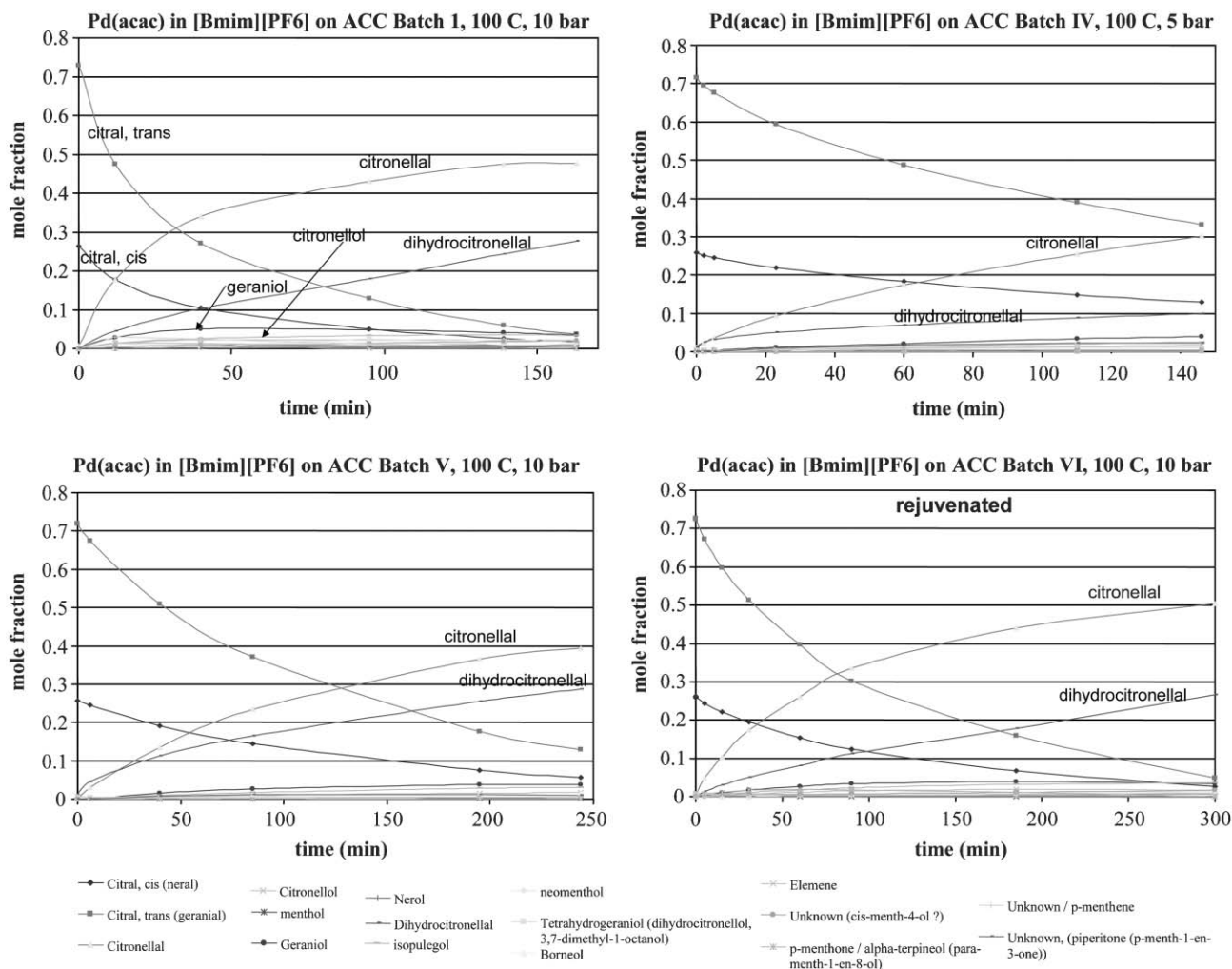


Fig. 6 Sample kinetic experiments with the Pd(acac) [bmim][PF₆] catalyst.

enough hydrogen is available (which was not the case in the experiments with lower hydrogen pressure).

Generally, no ionic liquids or their residues were detected, in GC-MS, thus, indicating that the ionic liquids remained immobilized on the support. However, with HPLC very minor ionic liquid contamination was found in the samples taken from the first batch (1.6 mg, indicating 0.3 wt% of the IL mass), whereas in the batches that followed no IL traces were found in the bulk solvent. Ionic liquid standards were first made and analysed with HPLC. Calibration curves were drawn according to these results. Samples were analysed after that. The amount of ionic liquid was determined by using the linear part of calibration curves. The analysis for the control of possible leaching of Pd metal into the bulk solvent is in progress. However, this does not seem likely since the catalytic activity was retained so well in spite of low Pd amounts in the catalysts. For the sake of reasoning, one should, though, remember that [PF₆⁻] in particular might not be a very good ion to utilize due to the risk of possible HF formation under experimental conditions.

The deactivation of all catalysts proved to be reasonably low, displayed by the repetition of the control experiment, the standard experiment, 100 °C and 10 bar (Table 3), although

the ionic liquid loadings and Pd-metal contents were very low. The last batch was carried out after a simple reactivation procedure: the catalyst was removed from the reactor and exposed to 10 mbar vacuum for one hour, followed by a re-reduction as described earlier. The goal with the vacuum treatment was to remove potential accumulated degradation and by-products as well as accumulated impurities originating from the standard that might occupy the Pd metal sites. The treatment resulted in improved catalytic performance which can be seen upon comparison of the concentration evolutions in batch V and VI (Fig. 6), respectively. The reader should be reminded that this procedure was by and large not optimized (time, conditions), thus only providing a conceptual route for a possible reactivation method of this kind of system with transition metal species supported in an ionic liquid.

Baiker and co-workers³¹ studied the hydrogenation of citral over Pd/alumina catalyst in a continuous fixed bed reactor and a batch autoclave and observed that Pd was highly selective to the saturation of the C=C bonds. Upon study of the deactivation, it was revealed that citral and 3,7-dimethyl-2-octenal block the Pd surface resulting in strongly adsorbed CO and C_xH_y-type hydrocarbon fragments. The observations

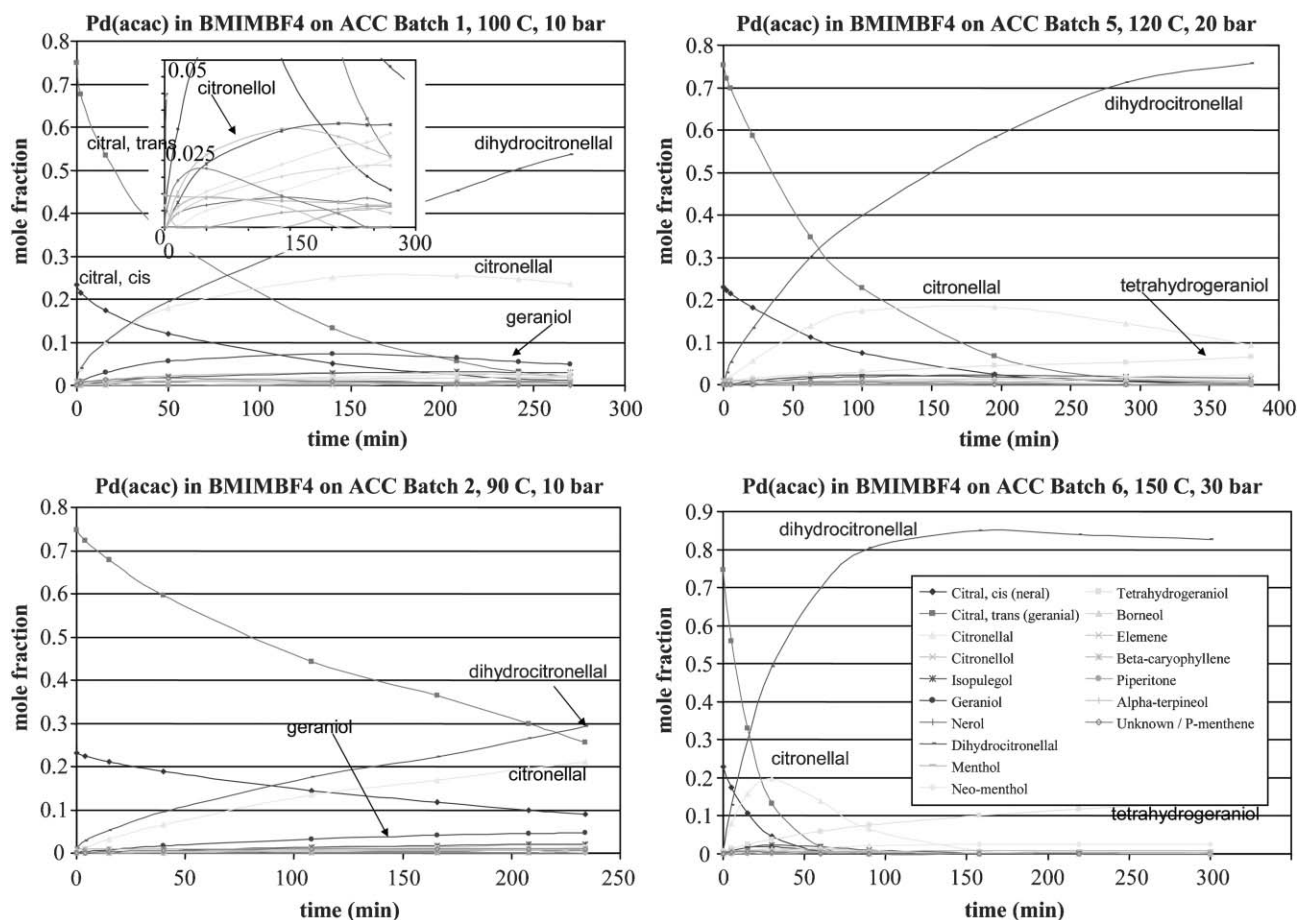


Fig. 7 Sample kinetic experiments with the Pd(acac) [bmim][BF₄] catalyst. The small insert illustrates a representative concentration evolution of the minor components.

indicated that the irreversible deactivation of Pd/Al₂O₃ cannot be traced to CO poisoning. In accordance to their findings, we propose that site blocking caused by heavier oligomeric surface products might be the major reason for the observed catalyst deactivation, together with possible agglomeration of the nanoparticles into larger ones that presumably are formed in the ionic liquid layer.

Conclusions

Three different ionic liquids, [bmim][PF₆], [bmim][BF₄] and a novel one [A336][PF₆], with the same transition metal species, Pd(acac), were immobilized on a structurally active carbon cloth (ACC) carrier. Pd(acac) was reduced to various oxidation states, Pd⁰–Pd⁺. A series of hydrogenation experiments, at various temperatures and pressures, were carried out and the performance of the different catalysts discussed. It became evident that the selectivity profiles of citral hydrogenation can be elegantly influenced not only by varying the transition metal species in line with classical catalysis and the experimental conditions (temperature, pressure), but also by the choice of the ionic liquid in which the transition metal species is dissolved. Selectivity vs. conversion plots might provide the best illustration of the facts and will be introduced in future. The amounts of both ionic liquids as well as the transition metal species involved in the preparation of catalysts

were very low and the preparation procedure very easy, thus displaying very good performance from an economic point of view. Furthermore, it is probable that almost any ionic liquid seems to be able to stabilize the active Pd species, since the catalytic activity was very well maintained from batch-to-batch, even without cumbersome and expensive use of specially dried solvents and reactants. Very minor loss of ionic liquids into the bulk solvent, n-hexane, was detected in the first batches of the series. It is possible that a small portion of ILS residing on the outer most surface of the ACC was washed away into the bulk solvent due to the intense mixing and centrifugal forces in the reactor.

Nevertheless, the concept shows prominent potential for industrial operations. Further studies following the same concept are in progress.

Acknowledgements

The authors are grateful to colleagues from Åbo Akademi University for their assistance: Clifford Ekholm (SEM), Markku Reunanen (GC-MS) and R. Sjöholm (consultancy). Financial support from the Academy of Finland is gratefully acknowledged (Decisions nr. 209391 and 211463). This work is part of the activities at the Åbo Akademi Process Chemistry Centre (PCC) within the Finnish Centre of Excellence Programme (2000 – 2005) by the Academy of Finland.

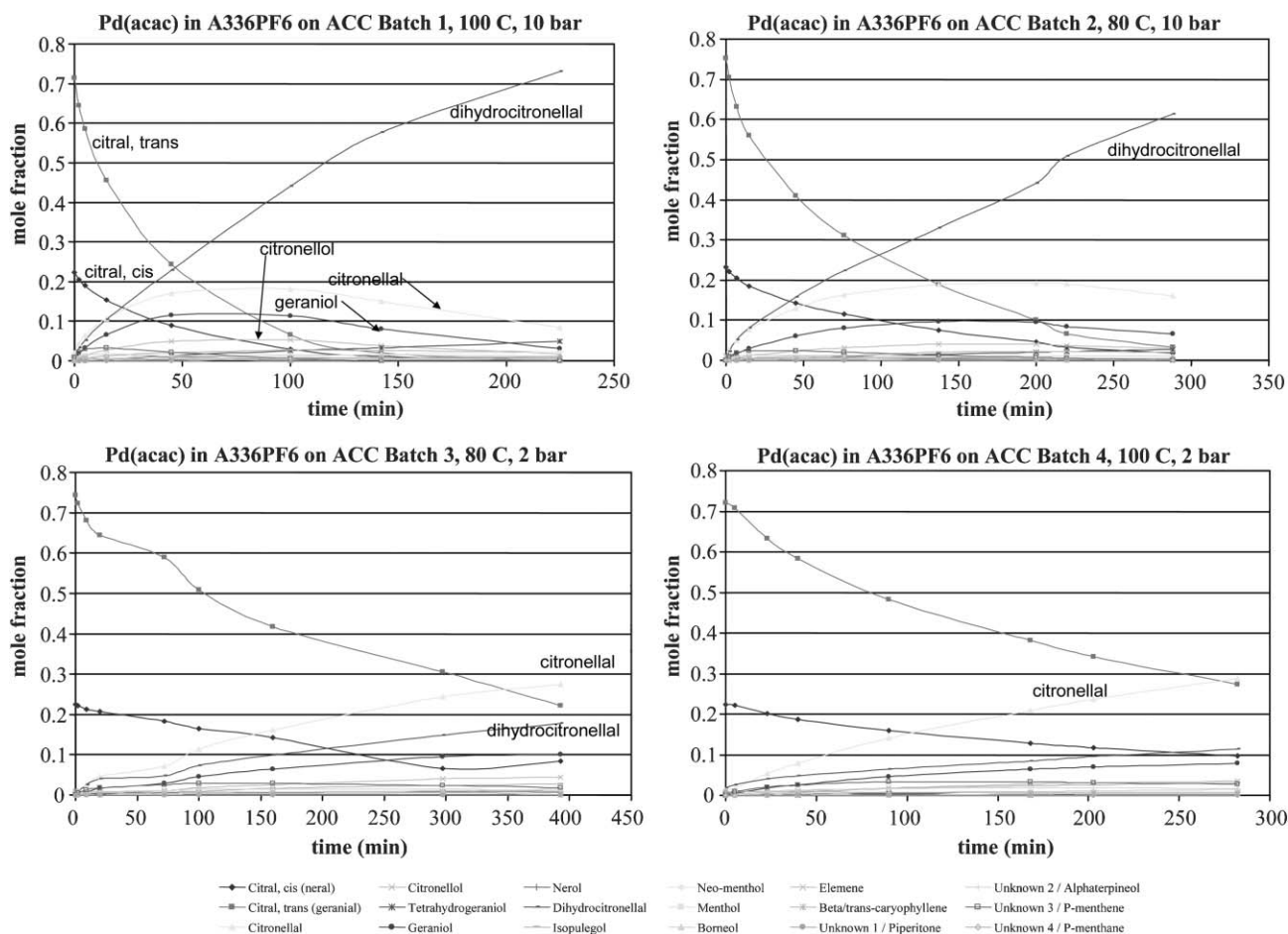


Fig. 8 Sample kinetic experiments with the Pd(acac) [A336][PF₆] catalyst.

References

- P. J. Dyson, *Transition Met. Chem.*, 2002, **27**, 353–358.
- H. Ohno and M. Yoshizawa, *Solid State Ionics*, 2002, **154–155**, 303–309.
- M. J. Earle and K. R. Seddon, *Pure Appl. Chem.*, 2000, **72**, 1391–1398.
- J. D. Holbrey and K. R. Seddon, *Clean Prod. Process.*, 1999, **1**, 223–236.
- A. Riisager, P. Wasserscheid, R. van Hal and R. Fehrmann, *J. Catal.*, 2003, **219**, 452–455.
- J. Dupont, G. S. Fonseca, A. P. Umpierre, P. F. P. Fichtner and S. R. Teixeira, *J. Am. Chem. Soc.*, 2002, **124**, 4228–4229.
- C. W. Scheeren, G. Machado, J. Dupont, P. F. P. Fichtner and S. R. Teixeira, *Inorg. Chem.*, 2003, **42**, No.15, 4738–4742.
- Y. Zhou and M. Antonietti, *Chem. Mater.*, 2004, **16**, 544–550.
- M. H. Valkenberg, C. deCastro and W. F. Hölderich, *Green Chem.*, 2002, **4**, 88–93.
- B. Gadenne, P. Hessemann and J. J. E. Moreau, *Chem. Commun.*, 2004, **15**, 1768–1769.
- D. W. Kim and D. Y. Chi, *Angew. Chem., Int. Ed.*, 2004, **43**, 483–485.
- C. P. Mehnert, *Chem. Eur. J.*, 2005, **11**, 50–56.
- Yu. Matatov-Meytal and M. Sheintuch, *Appl. Catal., A*, 2002, **231**, 1.
- M. H. Valkenberg, C. deCastro and W. F. Hölderich, *Green Chem.*, 2002, **4**, 88.
- R. T. Carlin and J. Fuller, *Chem. Commun.*, 1997, 1345.
- K. Anderson, P. Goodrich, C. Hardacre and D. W. Rooney, *Green Chem.*, 2003, **5**, 448.
- P. Mäki-Arvela, L.-P. Tiainen, A. N. Kalantar, R. Sjöholm, T.-K. Rantakylä, E. Laine, T. Salmi and D. Yu. Murzin, *Appl. Catal., A*, 2002, **237**, 181–200.
- J.-P. Mikkola, T. Salmi, P. Mäki-Arvela, J. Aumo and J. Kuusisto, *Catal. Org. React.*, 2000, **89**, 91.
- J. Aumo, S. Oksanen, J.-P. Mikkola, T. Salmi and D. Yu. Murzin, *Ind. Eng. Chem. Res.*, 2005, **44**, 14, 5285–5290.
- G. R. Cairns, R. J. Cross and D. Stirling, *J. Catal.*, 1997, **166**, 89.
- G. Neri, L. Mercadante, A. Donato, A. Visco and S. Galvano, *Catal. Lett.*, 1994, **29**, 379.
- U. K. Singh and M. A. Vannice, *J. Catal.*, 2001, **199**, 73.
- M. Rönholm, T. Salmi, D. Yu. Murzin, J. Aumo, J. M. Bernechea Rojas, J. Wärnä and J.-P. Mikkola, Proc. of 13th Int. Congress on Catalysis, Paris, France, July 11–16, 2004.
- J. F. Moulder, W. F. Stickle, P. E. Sobol and K. D. Bomben, *Handbook of X-ray Photoelectron Spectroscopy*, Perkin-Elmer Corp., Palo Alto, CA, USA, 1992.
- J.-P. Mikkola, presented at the 1st International Congress on Ionic Liquids, Salzburg, Austria, June 19–22, 2005.
- J. Aumo, S. Oksanen, J.-P. Mikkola, T. Salmi and D. Yu. Murzin, *Catal. Today*, 2005, **102–103**, 128–132.
- M. Koel, *Proc. Est. Acad. Sci., Chem.*, 2000, **49**, 145–155.
- J. G. Huddleston, A. E. Visser, W. M. Reichert, H. D. Willauer, G. A. Broker and R. D. Rogers, *Green Chem.*, 2001, **3**, 156–164.
- 26.05.2005: www.nanotechlabs.biz/prodPipe/ionicLubricants.
- A. Berger, R. F. de Souza, M. R. Delgado and J. Dupont, *Tetrahedron: Asymmetry*, 2001, **12**, 1825–1828.
- M. Burgener, R. Wirz, T. Mallat and A. Baiker, *J. Catal.*, 2004, **228**, 152–161.

Biodegradable toughened polymers from renewable resources: blends of polyhydroxybutyrate with epoxidized natural rubber and maleated polybutadiene

Yashodhan Parulekar and Amar K. Mohanty*

Received 10th June 2005, Accepted 6th December 2005

First published as an Advance Article on the web 19th December 2005

DOI: 10.1039/b508213g

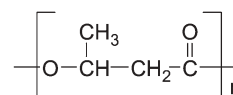
Polyhydroxybutyrate (PHB) is a biodegradable bacterial polyester emerging as a viable substitute for semi-crystalline synthetic non-biodegradable polymers. Novel toughened polyhydroxybutyrate (PHB) based *green* materials were successfully developed through reactive extrusion of PHB and functionalized natural rubber followed by injection molding. Natural rubber and epoxidized natural rubber were investigated as impact modifiers. Significant differences in the melt viscosity of PHB and the rubber phase established the need for a compatibilizer to improve the toughness. Theoretical modeling of the blend behavior by Takayanagi models also ascertained the positive effect of a compatibilizer. Maleated polybutadiene with high grafting and low molecular weight was determined to be an efficient compatibilizer for the PHB–rubber blend system thereby improving the toughness of PHB by 440%. The toughened PHB materials were characterized through thermo-mechanical analysis and differential scanning calorimetry showing the influence of the elastomer in reducing the PHB crystallinity. Morphological analysis through polarized optical microscopy, environmental scanning electron microscopy and atomic force microscopy also confirmed the ability of the compatibilizer to successfully reduce the rubber particle size and to create interphase bonding. The resultant toughened PHB exhibited impact strength (124 J m^{-1}) superior to a specific grade of thermoplastic polyolefin (TPO) and a high-impact polystyrene (HIPS).

Introduction

Plant/crop-based renewable resources are a strategic option to meet the growing need for sustainable materials for the next century.¹ The exponential growth of the use of polymeric materials in everyday life has led to the accumulation of huge amounts of non-degradable waste materials across our planet. This growing threat to the environment has led many countries to promote special programs directed towards the replacement of non-degradable, commonly used materials by biodegradable alternatives.² These initiatives led to widespread research in biodegradable materials especially focusing on modifications to make their properties comparable to conventional polymers. Biodegradable polymers can be obtained from renewable resources and can also be made from petroleum resources.³ Biodegradable polymers from renewable resources are attracting much attention because of their biomass origin, in contrast to fully petroleum-based biodegradable polymers, and their ability to maintain carbon dioxide balance after their biodegradation. Polyhydroxy-alkanoates (PHAs) are a class of such renewable resource-based biodegradable polymers. PHAs are known as bacterial polyesters and are synthesized by bacteria as intracellular carbon and energy storage compounds.^{4–6} PHAs were discovered at the Pasteur Institute with the first PHA identified

as polyhydroxybutyrate (PHB).⁴ PHB is an enantiomerically pure polymer with a methyl substituent present regularly along the backbone adjacent to the methylene group (Scheme 1). This structure is comparable with isotactic polypropylene (PP) and hence it has many similar properties to those of PP.⁷ The isotacticity combined with the linear nature of the chain results in formation of large spherulites during crystallization. These large spherulites lead to a highly crystalline and consequently brittle material.

Such semi-crystalline thermoplastics show brittle nature under severe conditions of deformation, such as low temperature and impact loading. These brittle polymers can undergo a sharp ductile-to-brittle transition and any inherent defect or crack can grow rapidly and lead to sample rupture.⁸ The crack growth is inhibited by adjoining lamella in the case of materials with small spherulites, whereas a crack can propagate along the lamella boundaries without opposition and can accelerate and fracture the sample in the case of materials with large spherulites such as PHB.⁸ Because of this poor fracture resistance there has been considerable commercial and scientific interest in the toughening of semi-crystalline thermoplastics.



Scheme 1 Chemical structure of polyhydroxybutyrate.

School of Packaging, 130, Packaging Building, Michigan State University, East Lansing, MI 48824, USA. E-mail: mohantya@msu.edu; Fax: +1 (517) 353-8999; Tel: +1 (517) 355-3603

The incorporation of dispersed rubber particles into a brittle thermoplastic matrix is known to improve the impact properties and the toughness of the polymer, at the cost of modulus. Under proper conditions and using appropriate compatibilizers, synergistic effects arise to create high impact toughened blends.⁹ The effectiveness of this toughening mechanism highly depends on the mechanical properties of the matrix, the elastomeric modifier, the dispersion of the modifier, and the interfacial adhesion among the different phases.¹⁰ Another critical factor is the particle diameter of the elastomeric phase. Modification to an optimum diameter improves the impact strength.¹¹ Rubber toughening mechanisms developed on conventional thermoplastics have been successfully applied to biopolymers. One such study on polylactic acid (PLA) toughened using rubber prepared from trimethyl carbonate reported 250% improvement in impact properties.¹²

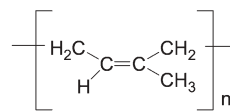
The toughness of such plastic–elastomer blends can be successfully increased if crazing and crack propagation can be minimized.¹³ Reducing the rubber particle size to around 1 μm and dispersing it efficiently into the matrix can achieve this. The blend system can be considered to be a simple binary immiscible blend of a brittle polymer and an elastic polymer. The dominant properties of such blends are dictated by the continuous phase and properties of the continuous phase. The plastic and the elastomeric phases are vastly different in their rheological properties. Hence for the elastomeric phase to be continuous the elastomer either has to be added in large amounts or a compatibilizer needs to be introduced to increase interfacial adhesion. The compatibilizer also reduces the interfacial tension that is responsible for phase separation.¹⁴ Studies on blends of scrap rubber and linear low-density polyethylene (LLDPE) reported the use of maleated LLDPE and epoxidized natural rubber (ENR) as dual compatibilizer which vastly improved the interfacial adhesion.¹⁵ Incompatible binary blend of polylactic acid and starch has been reported to be successfully compatibilized by maleic anhydride thus justifying the use of a maleated compatibilizer in this study.¹⁶

As part of a larger effort to create applications for biomaterials by making their properties comparable to the petroleum based material they are intended to replace, the focus of the present article is to create a sustainable alternative to commercial toughened polyolefins (TPOs). In this study, various toughening mechanisms for PHB were developed. The optimal toughness was achieved by incorporation of functionalized elastomeric components into the PHB matrix. Different compatibilizers were also investigated to improve the interfacial adhesion between the incompatible elastomer and plastic phases. The toughened PHB was characterized through thermo-mechanical, rheological and morphological analysis. The purpose of this study is to gain valuable insight into the toughening mechanisms in semi-crystalline PHB polymers, tailoring them to improve toughness.

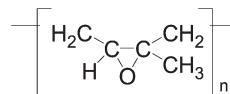
Experimental

Materials

Polyhydroxybutyrate (PHB) used in this study is a plasticized PHB (Biomer P226) (Biomer, Germany) (Scheme 1) with proprietary citrate plasticizer. The rubber used as impact



Scheme 2 Chemical structure of natural rubber.



Scheme 3 Chemical structure of epoxidized natural rubber.

modifier was a high quality, clean latex grade natural rubber (Standard Malaysian Rubber SMRCV60, Centrotech, OH) obtained as a purified product of the rubber tree (*Hevea brasiliensis*) (Scheme 2). Epoxidized natural rubber (ENR), a chemically modified form of natural rubber with epoxide rings on the chain is used as functionalized elastomer (Scheme 3). This ENR had 25% epoxidation and was obtained from the Malaysian Rubber board as research samples. Polybutadiene (PB) with maleic anhydride (MA) was used as the compatibilizer system. Two different types of maleated polybutadiene rubbers were provided by Sartomer (Sartomer Inc., PA) as Ricon series Maleated PB (RI131MA5 and RI130MA20). The RI131MA5 has high molecular weight (4700) but low grafting (2 MA groups per chain) while the RI130MA20 has lower molecular weight (3100) but higher grafting (6 MA groups per chain) as reported by the supplier.¹⁷ High impact polystyrene (HIPS Styron 421, Dow Chemical Company, MI) and thermoplastic polyolefin (TPO research grade, Basell Polyolefins, MD) were sourced for comparison purposes with the developed materials.

Instruments and methods

The virgin materials were analyzed prior to processing by thermal instruments to obtain the thermal transitions. A differential scanning calorimeter (DSC Q100, TA Instruments, DE) was used to determine the glass transition and the melting temperatures of the materials as well as the crystallinity of the PHB phase. These experiments were performed at a ramp rate of 10 $^{\circ}\text{C min}^{-1}$ from -40 $^{\circ}\text{C}$ to 200 $^{\circ}\text{C}$. Rheological properties of the materials were characterized on a parallel plate rheometer (ARES, TA Instruments, DE) at shear rates corresponding to the processing conditions.

Melt compounding of PHB with impact modifiers by twin-screw extrusion was carried out in a micro twin screw extruder with injection molder system (TS/I-02, DSM, The Netherlands). The mini-extruder is equipped with co-rotating screws having lengths of 150 mm, with L/D ratio of 18 and net capacity 15 cm^3 . An attached injection-molding unit is capable of 120 psi injection force. PHB and elastomer were weighed as per the calculated compositions and mixed together and fed to the extruder barrel. The materials were melt compounded at 175 $^{\circ}\text{C}$ and 200 rpm for 3 minutes. The compatibilizer system was introduced into the barrel exactly midway through the experimental residence time. After extrusion the melted materials were transferred through a preheated cylinder to the mini injection molder (pre-set at a mold temperature of

60 °C) to obtain the desired specimen samples for various measurements and analysis. The optimized processing conditions (speed, temperature and residence time) were determined from analysis of extensive experiments with variations in parameters. HIPS was melt compounded in the micro-compounder at 250 °C and 200 rpm for 2 minutes and TPO was processed at 185 °C and 200 rpm for 2 minutes.

Izod notched impact properties of the materials were measured on an Izod Impact Tester (TMI Model 43-02, TMI, NY) as per ASTM D256 for notched Izod impact testing with a 5 lb-ft pendulum. The samples were notched up to the prescribed depth using a mechanical notcher (TMI Model 22-05, TMI, NY) and then conditioned for 48 hours at 50% RH and 23 °C. Ten specimens were tested for each sample material. Storage modulus of the materials was measured using a Dynamic Mechanical Analyzer (2980 DMA, TA Instruments, DE). The DMA was run in the dual cantilever mode over a temperature range of -50 °C to 150 °C at a scanning rate of 5 °C per minute and using a frequency of 1 Hz.

Morphology analysis was done using Environmental Scanning Microscopy (ESEM), Polarized Light Microscopy (PLM) and Atomic Force Microscopy (AFM). For ESEM studies, samples were fractured by notched Izod impact methodology and the failure surface was observed. For crystallinity studies, PHB and modified PHB-rubber blends were compression molded into films and these films were studied using polarized optical microscopy (Olympus BH-2, Olympus, NY). The films were heated using a Mettler hot stage (Mettler FP-90, Mettler, OH) to above the melting temperature of PHB and cooled at 5 °C per minute to the crystallization temperature and held isothermally. The crystallization and spherulite growth were observed using a polarized lens. AFM studies of polished samples were done using an AFM microscope (Digital Instrument MultiMode SPM with Nanoscope IV controller, Digital Instruments, NY) in the force modulation mode.

Results and discussion

PHB-natural rubber system (incompatibility evidenced by rheology and theoretical calculations)

Natural rubber and semi-crystalline polymers similar to PHB form an immiscible blend, which has been widely reported in literature.¹⁸⁻²⁴ PHB is a linear polymer with no side-chains and hence there is minimal entanglement.⁴⁻⁶ This causes the chains to slip and move among themselves easily at elevated temperatures.²⁵ Because of this effect, PHB exhibits a drastic drop in viscosity with increasing temperature very much like a pseudoplastic material. The viscosity of rubber is a function of its purity and quality and the qualitatively best rubber has been reported to have the highest initial viscosity.²⁶ Our study used a high purity grade rubber and hence the viscosity values were 50 times higher than those of PHB. The melt viscosities of the virgin materials were determined by rheological studies. The shear rate in the micro-extruder was calculated from the processing speed (200 rpm) and from the minimum (0.1 cm) and maximum (0.35 cm) clearance between the screws and the barrel wall. These values gave the shear rate window of the microcompounder to be between 8.42 s⁻¹ to 230 s⁻¹. These

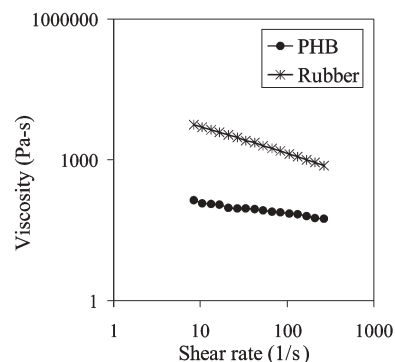


Fig. 1 Melt viscosity values of PHB and rubber for the shear rate range in the micro-extruder.

shear rate conditions were simulated in a parallel plate rheometer and the corresponding melt viscosity values were obtained for PHB and rubber (Fig. 1). Thus it was determined that rubber is 20–50 times more viscous than PHB at the processing temperature used (170 °C).

Blending physics dictates that for a binary blend, the lower viscosity phase tends to be continuous. This is quantified by eqn (1) which gives the relation between volume fraction (V) and melt viscosity (η) as:²⁷

$$X = V_{\text{PHB}}\eta_{\text{rubber}}/V_{\text{rubber}}\eta_{\text{PHB}} \quad (1)$$

The value of X determines the continuous phase. The PHB phase is continuous if $X > 1$ whereas at $X \approx 1$, phase inversion occurs and the rubber phase will become continuous. In order for the toughness of the blend to be close to the toughness of rubber, the rubber phase has to be continuous. However the high viscosity of natural rubber in comparison with PHB makes it almost impossible for this to happen. Hence phase inversion can occur only by using either large quantities of rubber in relation to PHB or by using a low molecular weight rubber, which will give lower viscosity. The above methods are not feasible for obvious reasons, and hence a compatibilizer was selected to improve the blend properties by increasing the interaction between the components.

The incompatibility of PHB and rubber in the absence of compatibilizer was also established by using the Takayanagi model that predicts the blend moduli of phase separated systems.²⁸ These models give a lower bound and upper bound estimate of the modulus of a binary blend system based on the morphology of the blend components. In all the models E is the elastic modulus and the quantities λ and ϕ or their products are the volume fractions of rubber phase. For example in eqn (4) and (5) the volume fraction of the rubber phase is given by the product $\lambda\phi$.

The upper bound value of the modulus of the blend is given by eqn (2) which represents an iso-strain system with both rubber and PHB phases continuous (Fig. 2A).

$$E_{\text{max}} = (1 - \lambda)E_{\text{PHB}} + \lambda E_{\text{rubber}} \quad (2)$$

The lower bound value of the modulus is given by eqn (3) which is for a blend system wherein neither the PHB nor the

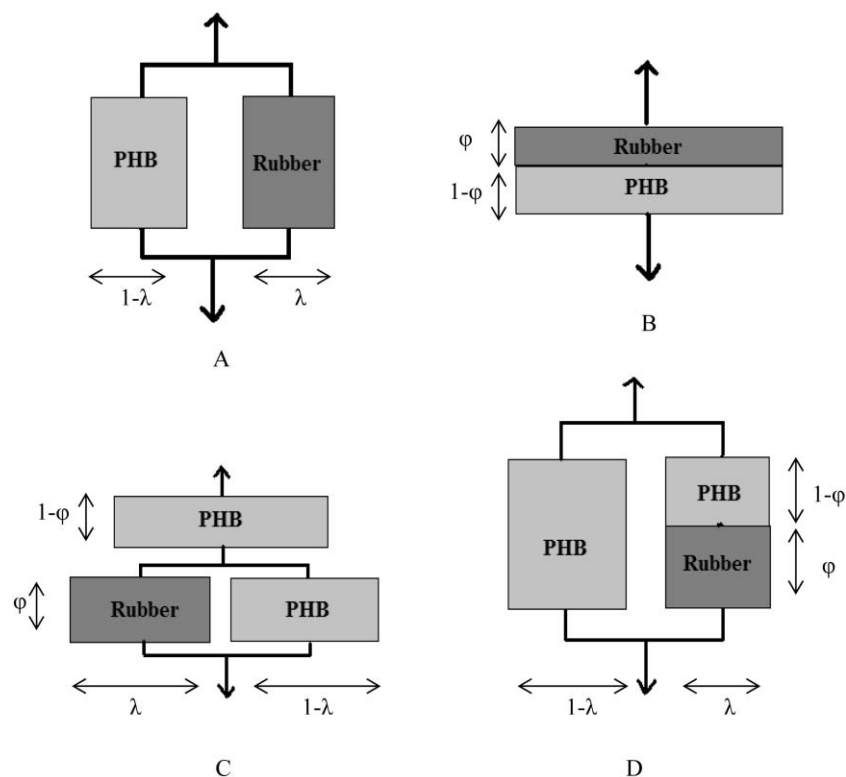


Fig. 2 Takayanagi model systems for the different possibilities for the PHB–rubber blend. A) Both phases continuous, B) both non-continuous, C) PHB continuous in series with discontinuous rubber, D) PHB continuous in parallel with discontinuous rubber.

rubber phases are continuous and the modulus of the blend is nearer to that of the phase that will fail first *i.e.* the rubber phase (Fig. 2B).

$$E_{\min} = [(\varphi/E_{\text{rubber}}) + (1 - \varphi/E_{\text{PHB}})]^{-1} \quad (3)$$

The storage modulus of PHB was measured as 1600 MPa and the storage modulus of rubber as 1.70 MPa (measured in DMA). The storage modulus measured by DMA relates to the elastic component of the material. These values were equivalent to tensile modulus values measured earlier for the same materials and hence the DMA modulus values are used in calculations. The volume fraction of rubber in all the systems is 0.25. Substituting these values gave the upper bound value as 1200 MPa and the lower bound value as 6.78 MPa.

The intermediate values are for a continuous PHB phase with a discontinuous rubber phase and are dependent on the morphologies of the blends and are given by eqns (4) and (5). Eqn (4) has a continuous phase (PHB) in series with a parallel connection of the discontinuous rubber phase and another PHB phase (Fig. 2C):

$$E = \{[\varphi/(\lambda E_{\text{rubber}} + (1 - \lambda)E_{\text{PHB}})] + [(1 - \varphi)/E_{\text{PHB}}]\}^{-1} \quad (4)$$

Eqn (5) assumes the continuous phase (PHB) is in parallel with a series connection of the discontinuous rubber phase and another PHB phase (Fig. 2D):

$$E = \lambda[(\varphi/E_{\text{rubber}}) + ((1 - \varphi)/E_{\text{PHB}})]^{-1} + (1 - \lambda)E_{\text{PHB}} \quad (5)$$

The volume fraction of the rubber phase is $\varphi\lambda = 0.25$ and so $\varphi = \lambda = 0.5$. Eqn (4) predicts the modulus value to be 1067 MPa and this will be possible if the rubber phase is encapsulated by the plastic and also these phases are significantly compatible. Eqn (5) predicts the modulus value to be 801 MPa and will be possible if again the rubber phase is encapsulated by PHB and these form a dispersed yet uncompatibilized blend that gives the lower bound value. The actual value of the PHB–rubber blend modulus was 600 MPa and this is lower than the lower predicted value of the modulus for a blend with a dispersed rubber phase (eqn (5)) thus establishing the need for a compatibilizer.

Comparison of DSC thermal transition profiles of PHB and the PHB–natural rubber blend showed that the blend gave two melting peaks (Fig. 3). Since natural rubber is completely amorphous, the only explanation of this behavior is that some PHB crystallites were affected by the rubber to form a different type of crystal due to some interaction between them.²⁹ When there are two types of crystals, it is possible for them to have different melting points. The DSC curves were also used to obtain the melting enthalpies of the PHB phases in the virgin polymer and the blend. For PHB, the melting enthalpy is dependent on the spherulite size and the blend morphology.^{30,31} Hence the rubber and the compatibilizers are expected to significantly affect the melting enthalpy.

The melting enthalpies ΔH for PHB and for the PHB phase in the PHB–natural rubber blends are given in Table 1 along with their corresponding specific melting enthalpies. These specific melting enthalpies of the PHB phases in all the systems remain relatively unchanged, thus implying that the natural

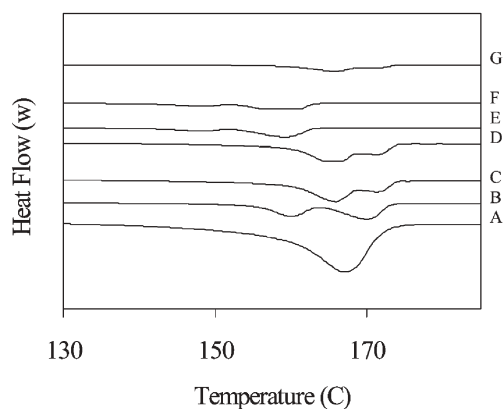


Fig. 3 DSC curves denoting melting peaks: (A) PHB, (B) PHB + 40% NR, (C) PHB + 10% MR1 + 30% NR, (D) PHB + 10% MR2 + 30% NR, (E) PHB + 40% ENR, (F) PHB + 30% ENR + 10% MR1 and (G) PHB + 30% ENR + 10% MR2. Note: PHB: Polyhydroxybutyrate, NR: Natural Rubber, MR1: RI131MA5, ENR: Epoxidized Natural Rubber and MR2: RI130MA20.

Table 1 Melting enthalpies and corresponding specific melting enthalpies of PHB and the PHB phase in the toughened blends

No.	Composition	W_{PHB}^a	$\Delta H/J \text{ g}^{-1}$	$\Delta H/W_{\text{PHB}}$
1	PHB	0.9	81.37	90.41
2	PHB + 40% NR	0.54	49.83	92.27
3	PHB + 30% NR + 10% MR1	0.54	48.24	89.33
4	PHB + 30% NR + 10% MR2	0.54	48.21	89.27
5	PHB + 40% ENR	0.54	48.25	89.35
6	PHB + 30% ENR + 10% MR1	0.54	47.65	88.24
7	PHB + 30% ENR + 10% MR2	0.54	42.96	79.55

^a The PHB in this study has 10% proprietary plasticizer mixed in it as supplied and hence the weight fraction of PHB is 0.9 in the case of virgin polymer and correspondingly 0.9 of the PHB content in the blends. PHB: Polyhydroxybutyrate, NR: Natural Rubber, MR1: RI131MA5, ENR: Epoxidized Natural Rubber and MR2: RI130MA20.

rubber is not interacting with the PHB, nor is it compatible. The polarized light micrographs of PHB (Fig. 4A) and the PHB–natural rubber blends (Fig. 4B) also do not exhibit any change in the size of the spherulites. If the rubber phase were compatible with the PHB, it would interfere with the PHB crystallites and reduce the spherulite size.

The large spherulites of PHB cause it to be brittle under severe conditions of deformation such as low temperature or high strain rates and it can undergo a sharp ductile-to-brittle

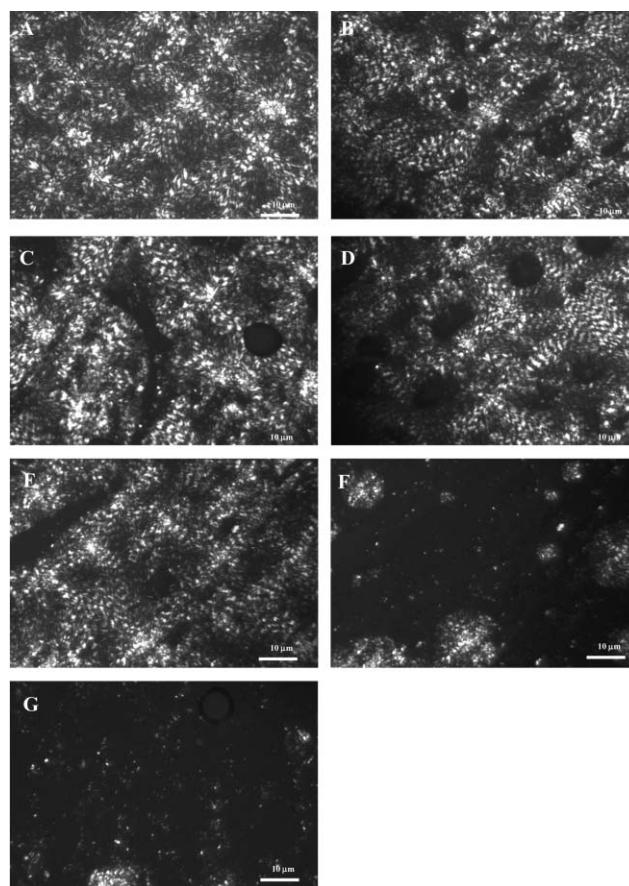


Fig. 4 Polarized light micrographs denoting spherulites. (A) PHB, (B) PHB + 40% NR, (C) PHB + 10% MR1 + 30% NR, (D) PHB + 10% MR2 + 30% NR, (E) PHB + 40% ENR, (F) PHB + 30% ENR + 10% MR1 and (G) PHB + 30% ENR + 10% MR2. (Scale bars on all images are 10 μm .) Note: PHB: Polyhydroxybutyrate, NR: Natural Rubber, MR1: RI131MA5, ENR: Epoxidized Natural Rubber and MR2: RI130MA20.

transition. These large spherulites are capable of initiating cracks. A crack can also propagate with little resistance in the brittle regime. The notched Izod impact strength of PHB was measured to be 23 J m^{-1} . This value was unaffected by the rubber phase in the PHB–rubber blend (Table 2). The modulus of PHB was reduced from 1.6 GPa to 0.6 GPa by addition of the rubber as expected (Table 2). The fracture surface from the impact tests was observed in ESEM to determine the mode of

Table 2 Notched Izod impact strength, modulus and approximate rubber particle sizes

No.	Composition	Impact strength/ J m^{-1}	Storage modulus/GPa at 23 °C	Rubber particle size/ μm
1	PHB	23 ± 1.53	1.6 ± 0.03	—
2	PHB + 40% NR	24 ± 1.53	0.6 ± 0.02	25–30
3	PHB + 30% NR + 10% MR1	22 ± 1.61	0.8 ± 0.01	15–25
4	PHB + 30% NR + 10% MR2	28 ± 1.57	0.8 ± 0.01	15–25
5	PHB + 40% ENR	25 ± 2.32	0.5 ± 0.02	20–25
6	PHB + 30% ENR + 10% MR1	62 ± 0.92	0.6 ± 0.01	15–25
7	PHB + 30% ENR + 10% MR2	124 ± 4.64	0.8 ± 0.03	1–5
8	Thermoplastic olefin (TPO)	84 ± 1.17	1 ± 0.08	—
9	High impact polystyrene (HIPS)	70 ± 4.98	2.4 ± 0.08	—

PHB: Polyhydroxybutyrate, NR: Natural Rubber, MR1: RI131MA5, ENR: Epoxidized Natural Rubber, MR2: RI130MA20, HIPS: Dow Styron 421, TPO: Basell Research grade TPO.

failure and to investigate the morphology. PHB exhibits a clean fracture surface devoid of any tendrils or fibrils due to its high crystallite size (Fig. 5A). The surface of the PHB–natural rubber sample (Fig. 5B) shows that the unbonded rubber phase, as indicated with an arrow, has separated from PHB in the blend. All these above observations validated the

prediction of the theoretical model and indicated the need for a compatibilizer.

PHB–natural rubber system with maleated polybutadiene (MR1: RI131MA5) as compatibilizer

Polybutadiene adducted with maleic anhydride (2 MA groups per chain) was used as a compatibilizer so as to increase interfacial adhesion. This system was not successful in increasing the impact strength of PHB (Table 2) and this was attributed to the lack of sufficient reactive groups both on the maleated rubber and the natural rubber. This estimation was supported by the ESEM micrographs which showed no bonding and a clean fracture surface (Fig. 5C). The polarized light micrographs (Fig. 4C) did not show evidence of any spherulite size reduction and the amorphous rubber phase was seen distinct from the PHB spherulites.

PHB–natural rubber system with maleated polybutadiene (MR2: RI130MA20) as compatibilizer

The high molecular weight of the MR1 compatibilizer was determined to be hindering the penetration of the compatibilizer into the interfacial regions. Researchers have reported that the extent of MA grafting and the molecular weight of the compatibilizer determine the efficiency of the additive.³² Hence low molecular weight polybutadiene adducted with a higher amount of maleic anhydride (6 MA groups per chain) was used as a compatibilizer. The lower molecular weight of this compatibilizer (MR2) compared to the molecular weight of the maleated rubber used earlier (MR1) meant that it would penetrate and disperse more easily into the blend and hence create a thin film between the phases.

This system too was not successful in increasing the impact strength of PHB (Table 2) and was backed by the ESEM micrographs which again showed a clean fracture surface (Fig. 5D). The polarized light micrographs (Fig. 4D) also did not show evidence of any spherulite size reduction and from these observations it was determined that the lack of reactive groups on natural rubber was hindering the compatibilization mechanism.

PHB–epoxidized natural rubber system

Epoxidized natural rubber (ENR) is a chemically modified form of natural rubber, with epoxide rings on the main chain. This epoxy linkage is expected to be a reactive site for bonding between the PHB and the rubber chains.²⁴

The impact strength of PHB was not affected by ENR (Table 2) and also the ESEM micrographs (Fig. 5E) showed the lack of interfacial adhesion between the ENR and the PHB phases. The enthalpy values (Table 1) also were not affected and the ENR phase did not show any distinct interference with spherulite growth (Fig. 4E). Hence it was concluded that again a compatibilizer was necessary to obtain better properties.

PHB–epoxidized natural rubber system with maleated rubber compatibilizer (MR1: RI131MA5)

The MR1 compatibilizer did not significantly improve the mechanical properties of the blend (Table 2) as was expected

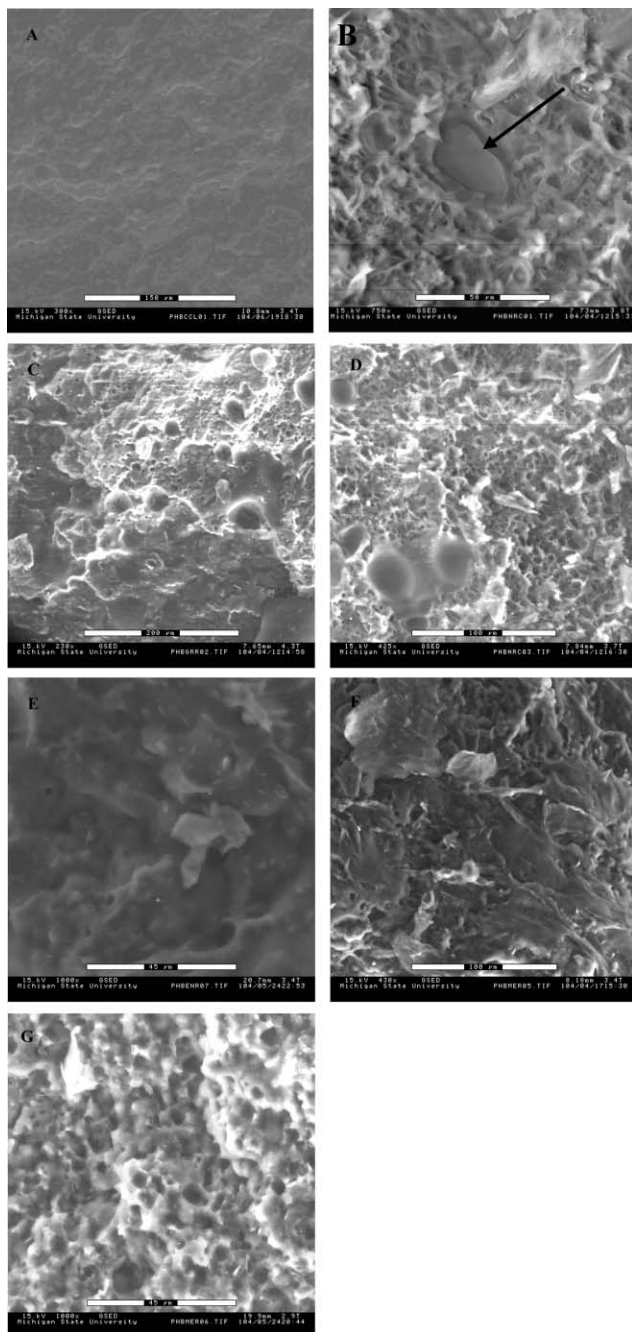


Fig. 5 ESEM micrographs of fracture surfaces of pure PHB and its toughened blends. (A) PHB (scale bar: 150 μm), (B) PHB + 40% NR (scale bar: 50 μm), (C) PHB + 30% NR + 10% MR1 (scale bar: 200 μm), (D) PHB + 30% NR + 10% MR2 (scale bar: 100 μm), (E) PHB + 40% ENR (scale bar: 45 μm), (F) PHB + 30% ENR + 10% MR1 (scale bar: 100 μm) and (G) PHB + 30% ENR + 10% MR2 (scale bar: 45 μm). Note: PHB: Polyhydroxybutyrate, NR: Natural Rubber, MR1: RI131MA5, ENR: Epoxidized Natural Rubber and MR2: RI130MA20.

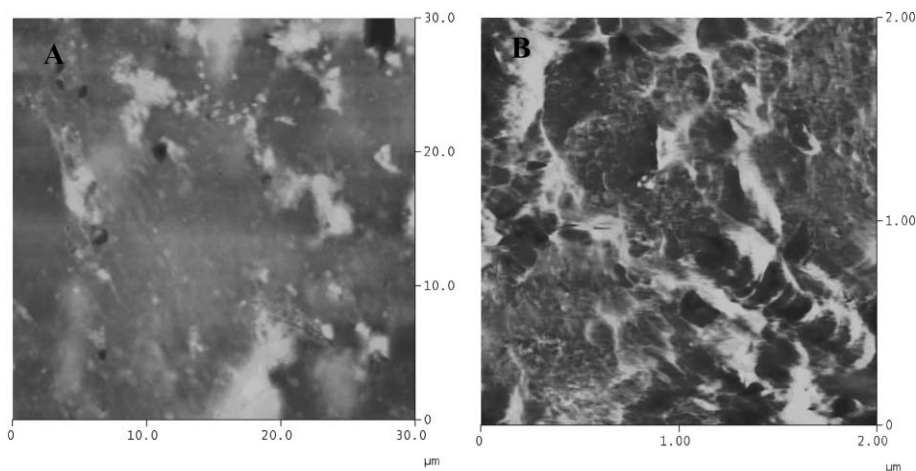


Fig. 6 AFM micrographs of polished sample surfaces in force modulation mode: (A) PHB + 40% ENR (scale bar: 30 μm), (B) PHB + 30% ENR + 10% MR2 (scale bar: 2.00 μm). Note: PHB: Polyhydroxybutyrate, ENR: Epoxidized Natural Rubber and MR2: RI130MA20.

due to the high molecular weight of the compatibilizer which hinders its penetration and dispersion. The fracture surface (Fig. 5F) did not show sufficient dispersion and some large MR1 molecules were evident. The PLM micrographs (Fig. 4F) also did not show significant reduction in the spherulite size and thus the need for a low molecular weight compatibilizer with higher grafting was established.

PHB–epoxidized natural rubber system with maleated rubber compatibilizer (MR2: RI130MA20)

The MR2 compatibilizer system significantly improves the toughness of the PHB–ENR as evidenced by the 440% increase in notched Izod impact strength (Table 2). This impact strength (124 J m^{-1}) is superior to comparable grades of commercial toughened semi-crystalline polymers like high-impact polystyrene (HIPS) (70 J m^{-1}) and thermoplastic polyolefin (TPO) (84 J m^{-1}). The modulus of PHB reduced by 63% by addition of ENR but only by 50% when MR2 and ENR were added together thus showing the positive effect of the compatibilizer (Table 2). This modulus value of 800 MPa agreed with the Takayanagi model prediction of 801 MPa for a well-dispersed compatibilized system.

Morphology analysis of the blends validated these observations and the ESEM micrographs (Fig. 5G) of the compatibilized system showed good dispersion. The evident droplet morphology and a rough fracture surface also confirmed strong bonding. The compatibilizer successfully reduced the rubber particle size to about 1 μm thus creating a well dispersed particulate morphology ideal for toughening. The PLM micrographs showed a distinct increase in the amorphous content and a reduction in spherulites (Fig. 4G). AFM analysis in the force modulation mode was also used to study morphology of the toughened blends. In this mode, the variation in the moduli of the blend components can be observed: the softer rubber phase appears lighter under AFM and the stiffer PHB phase appears darker.³³

In the case of the PHB–ENR two-phase system, distinct dark regions and light regions were observed (Fig. 6A) denoting a two-phase uncompatibilized system with no

intermediate regions. But in the case of the PHB–ENR–MR2 system (Fig. 6B), besides the dark PHB and light rubber regions, intermediate regions of medium darkness can also be seen denoting formation of interphases and bonding. These interfacial adhesions led to dramatic improvement in impact strength yet with acceptable loss in modulus. The moduli of PHB, the uncompatibilized PHB–ENR blend and of the PHB–ENR with MR2 compatibilized blend were studied as a function of temperature (Fig. 7) in the DMA apparatus. At $-50 \text{ }^\circ\text{C}$, the modulus of PHB reduced by 63% by addition of ENR but only by 50% when maleated rubber and ENR were added together and similar behavior was seen at room temperature ($30 \text{ }^\circ\text{C}$) and at $120 \text{ }^\circ\text{C}$. As seen from Fig. 7, the loss in storage modulus with increasing temperature was less drastic for the blends than PHB, denoting the reduction in brittleness at sub-ambient temperatures. The compatibilized blend gave an intermediate value; low enough to indicate toughness yet high enough to maintain the structural integrity of the material.

Conclusions

Bacterial polyhydroxybutyrate (PHB) was successfully toughened by reactive extrusion with epoxidized natural

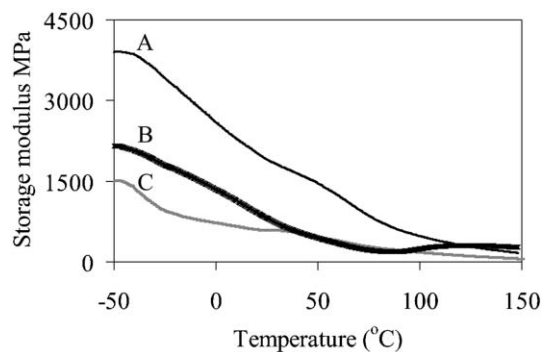


Fig. 7 Variation of modulus with temperature for (A) PHB, (B) PHB–ENR–MR2 and (C) PHB–ENR. Note: PHB: Polyhydroxybutyrate, ENR: Epoxidized Natural Rubber and MR2: RI130MA20.

rubber and using maleated rubber as the compatibilizer. Maleated rubber having a high amount of maleic anhydride (MA) grafting and low molecular weight was found to be an effective compatibilizer whereas the maleated rubber having low MA grafting and high molecular weight did not show any significant effect in improving the impact strength of the virgin PHB–rubber blend. Rheological, morphological and mechanical characterization substantiated these results. The experimental results matched Takayanagi model predictions of the blend moduli well. The toughened and compatibilized blends were found to have 440% better impact resistance and only 50% loss in modulus when compared to virgin PHB. The impact strength of the toughened PHB is superior to a specific grade of thermoplastic polyolefin (TPO) and high-impact polystyrene (HIPS). One of our on-going research activity targets is to improve the stiffness of developed toughened PHB through nano-reinforcement.

Acknowledgements

The authors thank the US Environmental Protection Agency (EPA) for supporting this research under the Science to Achieve Results (STAR) program through grant number RD 830904. We are thankful to Professor L. T. Drzal for encouragements. We are also thankful to Dr M. Misra, Mr Mike Rich, Mr Brian Rook, Dr Per Askeland, Dr Xuemei Liang, Dr H. Miyagawa, Dr Q. Wu, Mr Dinesh Aithani and Mr Rahul Bhardwaj.

References

- R. A. Gross and B. Karla, *Science*, 2002, **297**, 803–807.
- M. Duncan, *J. Ind. Ecol.*, 2003, **7**, 3–4, 193–202.
- A. K. Mohanty, M. Misra and L. T. Drzal, *J. Polym. Environ.*, 2002, **10**, 1/2, 19–26.
- R. W. Lenz and R. H. Marchessault, *Biomacromolecules*, 2005, **6**, 1, 1–8.
- H. Brandl, R. A. Gross, R. W. Lenz and R. C. Fuller, *Adv. Biochem. Eng. Biotechnol.*, 1990, **41**, 77–93.
- J. Luengo, A. Garcia, A. Sandoval, G. Naharro and E. Olivera, *Curr. Opin. Microbiol.*, 2003, **6**, 251–260.
- S. Y. Lee, J. Choi and S. H. Lee, *Macromol. Symp.*, 2000, **159**, 259–266.
- A. Peterlin, *Annu. Rev. Mater. Sci.*, 1972, **2**, 349–380.
- Z. Bartczak, A. S. Argon, R. E. Cohen and M. Weinberg, *Polymer*, 1999, **40**, 2331–2346.
- A. van der Wal, J. J. Mulder, J. Oederkerk and R. J. Gaymans, *Polymer*, 1998, **39**, 26, 6781–6787.
- M. Mehrabzadeh and K. Hossein Nia, *J. Appl. Polym. Sci.*, 1999, **72**, 1257–1265.
- D. W. Grijpma, R. D. A. Van Hofslot, H. Supèr, A. J. Nijenhuis and A. J. Pennings, *Polym. Eng. Sci.*, 1994, **34**, 22, 1674–1684.
- D. R. Paul and C. B. Bucknall, in *Polymer Blends*, ed. D. R. Paul and C. B. Bucknall, John Wiley and Sons, NY, 2000, vol. 2, pp. 177–224.
- R. B. Thompson and M. W. Matsen, *J. Chem. Phys.*, 2000, **112**, 15, 6863–6872.
- B. Guo, Y. Cao, D. Jia and Q. Qiu, *Macromol. Mater. Eng.*, 2004, **289**, 360–367.
- J. Zhang and X. Sun, *Biomacromolecules*, 2004, **5**, 4, 1446–1451.
- Maleinized Polybutadiene Product Literature (<http://sartomer.com/prodsubgroup.asp?plid=8&sgid=47>), Sartomer Corporation, Exton, PA, 2004.
- A. van der Wal, R. Nijhof and R. J. Gaymans, *Polymer*, 1999, **40**, 22, 6031–6044.
- A. van der Wal and R. J. Gaymans, *Polymer*, 1999, **40**, 22, 6045–6055.
- A. van der Wal, A. J. J. Verheul and R. J. Gaymans, *Polymer*, 1999, **40**, 22, 6057–6065.
- Y. Wang, Z. Cai and J. Sheng, *J. Macromol. Sci. Phys.*, 2004, **43**, 5, 1075–1093.
- I. Aravind, P. Albert, C. Ranganathaiah, J. V. Kurian and S. Thomas, *Polymer*, 2004, **45**, 14, 4925–4937.
- W. M. Hess, C. R. Herd and P. C. Vegvari, *Rubber Chem. Technol.*, 1993, **66**, 3, 329–346.
- H. K. Lee, J. Ismail, H. W. Kammer and M. A. Bakar, *J. Appl. Polym. Sci.*, 2005, **95**, 1, 113–129.
- H. Cartier and G. Hu, *Polymer*, 2001, **42**, 21, 8807–8816.
- N. Levin, *Natuurrubber*, 1996, **5**, 9–11.
- D. R. Paul and J. W. Barlow, *J. Macromol. Sci., Rev. Macromol. Chem.*, 1980, **C18**, 109.
- M. Takayanagi, *Mem. Fac. Eng. Kyushu Univ.*, 1963, **23**, 41.
- X. Shuai, Y. He, Y. Na and Y. Inoue, *J. Appl. Polym. Sci.*, 2001, **80**, 2600–2608.
- S. Bloembergen, D. A. Holden, G. K. Hamer, T. L. Bluhm and R. Marchessault, *Macromolecules*, 1986, **19**, 2865–2871.
- H. Mitomo, P. J. Barham and A. Keller, *Polym. Commun.*, 1988, **29**, 4, 112–115.
- A. Sanadi, D. Caulfield, R. Jacobson and R. Rowell, *Ind. Eng. Chem. Res.*, 1995, **34**, 1889–1896.
- A. A. Galuska, R. R. Poulter and K. O. McElrath, *Surf. Interface Anal.*, 1997, **25**, 418–429.

Catalytic dehydration of glycerol in sub- and supercritical water: a new chemical process for acrolein production

L. Ott, M. Bicker and H. Vogel*

Received 5th May 2005, Accepted 14th November 2005

First published as an Advance Article on the web 5th December 2005

DOI: 10.1039/b506285c

Investigations on using renewables as alternative raw materials for intermediates are becoming more and more important as the crude oil and natural gas resources will be exhausted in a few decades. Acrolein is an important and versatile intermediate for the chemical industry, *e.g.* for the production of acrylic acid esters, superabsorber polymers or detergents. Up to now, the production route is the gas phase oxidation of propylene with a Bi/Mo-mixed oxide catalyst. As an alternative, acrolein can be produced by the dehydration of glycerol, which appears as a basic component of natural fats and is accumulated to a great extent as a by-product during fat saponification and biodiesel production. Here, the usage of sub- and supercritical water as the reaction media has shown a certain potential for the dehydration of glycerol, although the conversion and acrolein selectivities which have been achieved so far, are not satisfying for an economical process. Only the addition of mineral acid leads to sufficient acrolein yields. To evade the disadvantage of intensifying corrosion, the influence of the addition of electrolytes such as zinc sulfate on this reaction has been investigated. Experiments were conducted in a high pressure plug flow reactor from 300–390 °C, 25–34 MPa, 10–60 s residence time and varying amounts of zinc sulfate. It was shown that in the near subcritical temperature, increasing the amount of salt enhances the glycerol conversion. The maximum acrolein selectivity is 75 mol% at 360 °C, 25 MPa, 470 ppm (g g^{-1}) zinc sulfate and a conversion of 50%. The activation volume was determined to be $-(274 \pm 65) \text{ cm}^3 \text{ mol}^{-1}$ (at 360 °C, 25–34 MPa and 790 ppm (g g^{-1}) zinc sulfate) and it turned out that the addition of zinc sulfate causes a decrease of the activation energy from 150 kJ mol^{-1} to $(140 \pm 12) \text{ kJ mol}^{-1}$.

1 Introduction

The world climate has been exposed to huge changes in the past. The time-constants of these changes were, in contrast to the evolutionary time-constant, long enough so that the ecosystems did have sufficient time for alignment. Since the world's population almost exclusively covers its increasing energy and raw material demand with fossil basic materials (crude oil, natural gas, coal), the CO_2 -gradient has increased so much that the world climate is changing dramatically in a short time period.

If hydrocarbons from fossil sources are running short and the atmosphere cannot tolerate any more CO_2 without suffering irreversible damage, the only possibility is to use biomass as the carbon source for the synthesis of fuels. Because other energy forms like electricity and heat can be made available through other (non-material) ways (*e.g.* photovoltaics, wind, water, nuclear power), biomass has to be acquired exclusively for transportation. In 1999, Germany had a fuel demand of 62 million tons for transportation, which corresponds to 200 million tons of CO_2 , whereas the overall CO_2 -emission in Germany in that year was 860 million tons.¹

This means that traffic is one of the major CO_2 -sources and a great leverage effect for CO_2 -reduction can be achieved by changing over the fuel basis from fossil to renewable sources. Enhancing the cultivation of renewable raw materials will not suffice for establishing renewables for fuel production. For their use in economically relevant chemical synthesis new processes have to be developed so that crude oil can be substituted.²

One possible substitution might be the production of biodiesel where rape-oil is converted with methanol. As a fuel, the resulting rape-oil methyl ester already contributes an important part towards climate protection. Fig. 1 shows the

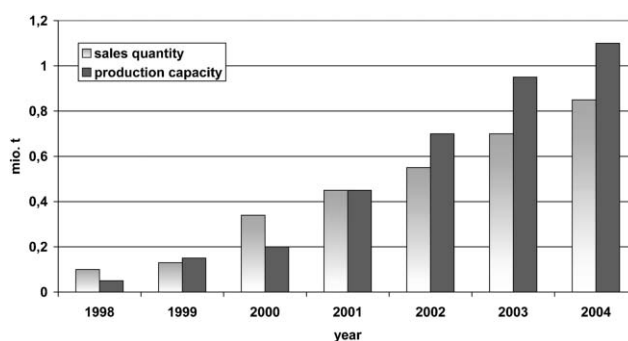


Fig. 1 Comparison of biodiesel production capacity and sales quantity in Germany.³

Department of Technical Chemistry and Macromolecular Science, Darmstadt University of Technology, Petersenstraße 20, D-64287 Darmstadt, Germany. E-mail: vogel@ct.chemie.tu-darmstadt.de; Fax: +49 6151 163465; Tel: +49 6151 164795

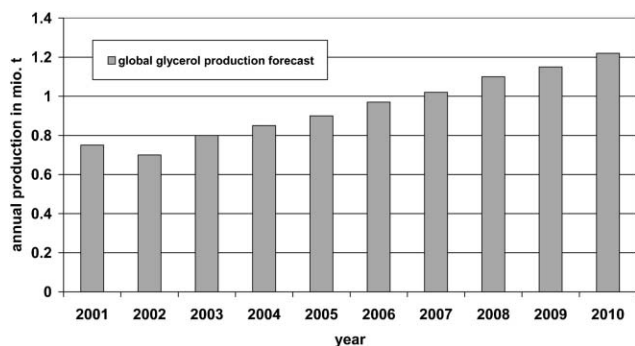


Fig. 2 Projection of the global glycerol production [source: Procter & Gamble].

comparison of biodiesel production capacity and sales quantity in Germany.

One problem accompanying the biodiesel production increase is the production of glycerol as a by-product. Therefore the increase of biodiesel production results in the accumulation of glycerol, which leads to a price decline. The effect is that the sale of glycerol is becoming the bottleneck of biodiesel production enhancement. Fig. 2 shows a forecast for the development of the global glycerol production. In order to expand biodiesel production an economical follow-up chemistry of the by-product glycerol has to be developed.

One possibility is to perform an acid-induced dehydration of glycerol (1) to acrolein (2) as can be seen in Scheme 1.

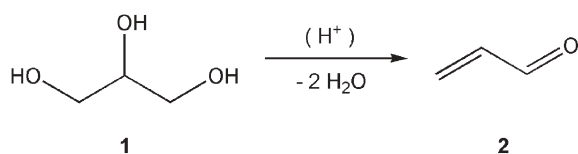
Acrolein is an important chemical intermediate so the task is to develop a sustainable and cost-effective production route *via* glycerol from biodiesel, which offers an alternative for the presently dominating petrochemical process based on propylene. The economic incentives are:

- a cheap renewable raw material which is unsusceptible to risk
- independence from both crude oil and steam cracker
- low specific investment costs and small decentralised plants.

This paper presents the results of the catalytic dehydration of glycerol to acrolein in sub- and supercritical water with zinc sulfate. A proposition for an industrial process will be introduced.

2 State of the art

There are only a few works concerning the dehydration of glycerol in sub- and supercritical water (*SCW*). Bühler *et al.*⁴ found only low glycerol conversions and low acrolein selectivities ($S_{\max} = 37$ mol%, $X_{\max} = 31\%$) in pure water at a temperature range from 300–474 °C, pressure from 25–45 MPa and residence time from 16–100 s. The initial glycerol concentration varied from 0.19–0.57 M.



Scheme 1 Acid-induced dehydration of glycerol to acrolein.

Ramayya *et al.*⁵ previously reported that the addition of sulfuric acid dramatically enhances the acrolein yield. They conducted experiments at 300–350 °C, 34.5 MPa and 16–39 s residence time. The glycerol concentration was 0.5 M and the sulfuric acid content 0.005 M.

Antal *et al.*⁶ showed that a high reaction temperature is needed for glycerol dehydration in water because glycerol conversion was only 1% and acrolein was not detected at 250 °C, 34.5 MPa, 0.1 M glycerol and 0.01 M sulfuric acid content.

Other reaction methods to gain acrolein from glycerol are also known, but they are less promising than the approach *via SCW*. In 1950, Waldmann and Frantisek⁷ obtained 13.5 g acrolein, which was distilled from a reaction mixture of 50 g glycerol, 100 g phthalic anhydride and 3 g benzenesulfonic acid.

There are two patents concerning the gas phase dehydration of glycerol: in 1933 Scheering-Kahlbaum AG⁸ reported an acrolein yield up to 80 mol% during conversion of glycerol vapour with phosphates of Cu or Li at a temperature from 300–600 °C. The second one actually aims at the preparation of 1,2- and 1,3-propanediol out of glycerol so that instead of isolating the resulting acrolein, it is hydrated *in situ* to the propanediols. This patent is claimed by Degussa AG⁹ and the reaction is conducted at 240–350 °C with an acid catalyst. No data on the acrolein yield is given.

So far the use of *SCW* is only promising if acid is added. But as water itself under these conditions induces corrosion, the acid content intensifies the corrosive effect. Therefore expensive corrosion-resistant materials (*e.g.* iniconel) are needed for the apparatus, which results in higher specific investment costs for the construction of an industrial plant. It is known from literature that salts might be able to enhance dehydration reactions in *SCW*.^{10,11} Dai *et al.*¹² found that zinc chloride is a promising addition for the dehydration of 1,2-propanediol in *SCW*. As halides have the same corrosion potential in *SCW* as mineral acids,^{13,14} another less corrosive anion that is more stable under these reaction conditions should be taken into consideration. This leads almost automatically to sulfates reported by Kruse and Dinjus.¹⁵ Therefore we conducted experiments on glycerol dehydration with the addition of zinc sulfate in *SCW*.

3 Experimental

3.1 High pressure tube reactor

The experiments were conducted in a high pressure tube reactor made of stainless steel (specification 1.4401, with 3.175 mm e.d., 2.0 mm i.d. and a length of 500 mm). The resulting reactor volume V_R is 1.6 cm³. The tube helically proceeds around an aluminium cylinder which is heated *via* a 500 W electrical heating cartridge, controlled by a temperature regulator with two thermo elements. A pipe-in-pipe heat exchanger (operated at 200 °C with a liquid heat transfer fluid) is used for pre-heating. In preliminary experiments it was ensured that no reaction occurs at this temperature. The reactor discharge is cooled down in a pipe-in-pipe heat-exchanger (water at 15 °C) before pressure is completely released by a spill valve. A second heat exchanger (ethylene

glycol–water at 2 °C) is used to cool down further the reactor solution and the sample vessel. This prevents volatile substances from evaporating. The homogeneous feed solution is delivered by a two-piston HPLC pump (10 mL pump head) into the reactor. Fig. 3 describes the high pressure tube reactor schematically.

The appropriate flow rate of the pump is calculated with eqn (1). The change in water density caused by glycerol and salt is neglected.

$$\tau = \frac{V_R \cdot \rho_{\text{water,reactor}}}{\dot{V} \cdot \rho_{\text{water,STP}}} \quad (1)$$

τ = residence time/s

V_R = reactor volume/cm³

$\rho_{\text{water,reactor}}$ = water density at process temperature and pressure/g cm⁻³

$\rho_{\text{water,STP}}$ = water density at standard temperature and pressure/g cm⁻³

\dot{V} = volume flow/cm³ s⁻¹

3.2 Analytic

A quantitative analysis of the glycerol content of the reactor samples was done by HPLC. Each sample was diluted with deionised water and stirred over an acidic cation exchanger (Amberlite IR-120H, Fluka Company) for 20 min. It was confirmed that this procedure has no effect on the sample's

composition. The column was held at 50 °C, the RI-Detector's temperature was set at 40 °C. The eluent was 2 mM sulfuric acid.

The content of acrolein and other liquid by-products was determined *via* GC-FID (DANI Model 3800, column: ZB-WAX, Zebron, $L = 30$ m, $d_i = 0.25$ mm, $d_f = 0.25$ μ m) with nitrogen as the carrier gas and 1-hexanol as the internal standard. The reactor sample was diluted with 1-propanol in a 1 : 1 (g g⁻¹) ratio because the GC's injection system was not able to homogeneously evaporate pure aqueous samples. It was confirmed that the dilution neither had an effect on the sample's content nor led to an overlay of possible by-product peaks.

Qualitative analysis was performed by GC-MS on a GCQ Finningan MAT apparatus using a F&W DB5 FSAP 50 m column, split injection at 275 °C and helium as carrier gas.

4 Results

The dehydration of 1% (g g⁻¹) glycerol in SCW with zinc sulfate as the catalyst was investigated by varying the following process parameters:

- temperature
- pressure
- zinc sulfate concentration
- glycerol concentration
- residence time.

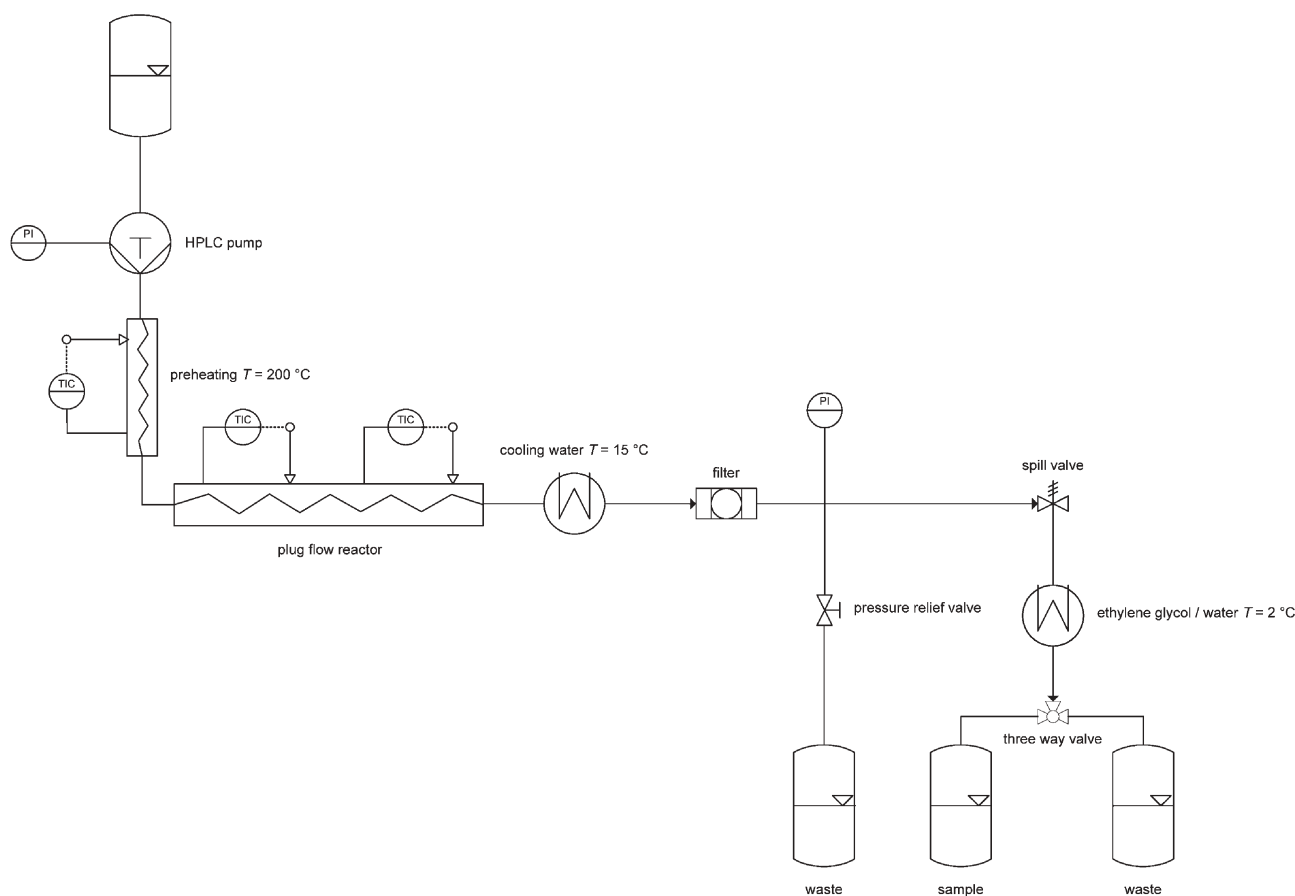


Fig. 3 Schematic flow sheet of the high pressure micro plant.

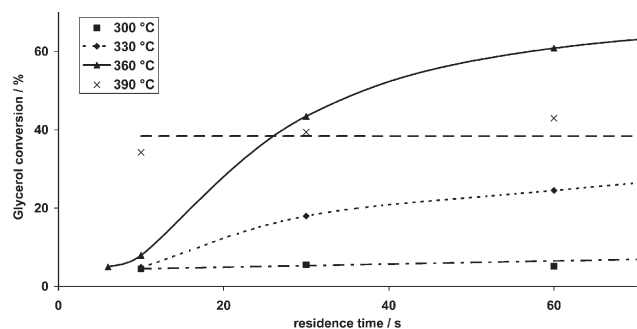


Fig. 4 Dependency of the glycerol conversion on temperature in the range 300–390 °C at 25 MPa and 790 ppm (g g^{-1}) zinc sulfate concentration.

As concentrations under reaction conditions are relevant for kinetic analysis a corrected concentration c_{corr} is introduced. The corrected concentration c_{corr} can be obtained by using eqn (2):

$$c_{\text{corr}}(i) = c_{\text{STP}}(i) \frac{\rho_{\text{water,reactor}}}{\rho_{\text{water,STP}}} \quad (2)$$

$c_{\text{corr}}(i)$ = corrected concentration of compound i /mmol L^{-1}
 $c_{\text{STP}}(i)$ = concentration of compound i at standard temperature and pressure/mmol L^{-1}

4.1 Influence of the temperature

Fig. 4 shows the influence of the temperature with respect to the conversion of glycerol. The zinc sulfate concentration was kept constant at 790 ppm (g g^{-1}), the pressure was 25 MPa. As long as the temperature stays below the critical temperature of water, increasing glycerol conversion can be obtained at higher temperatures. At temperatures above the critical point the conversion is lower than in the subcritical region and seems to be independent of the experimental residence time, which might be an indication for a switch in the reaction mechanism.

The influence of the temperature in a range from 300–390 °C on the acrolein selectivity at 25 MPa and 790 ppm (g g^{-1}) zinc sulfate concentration can be seen in Fig. 5. Similar to the glycerol conversion, the acrolein selectivity increases in the subcritical region with increasing temperature. In the supercritical region the selectivity declines probably due to consecutive reactions of acrolein.

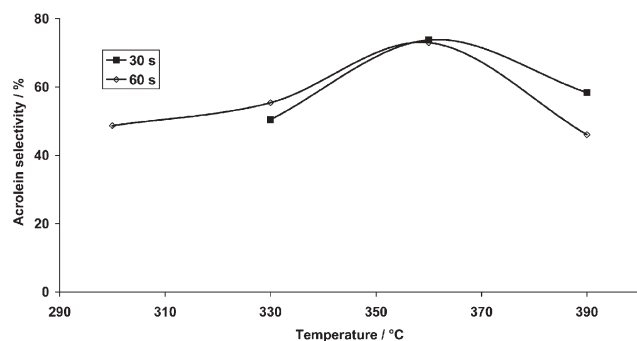


Fig. 5 Influence of the temperature range 300–390 °C and residence time at 25 MPa and 790 ppm (g g^{-1}) zinc sulfate concentration in terms of acrolein selectivity.

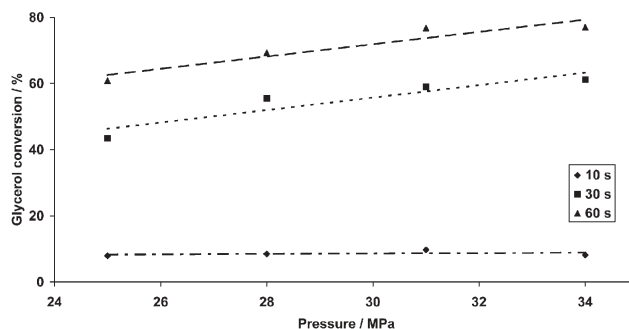


Fig. 6 Pressure influence on the glycerol conversion at 360 °C and 790 ppm (g g^{-1}) zinc sulfate concentration.

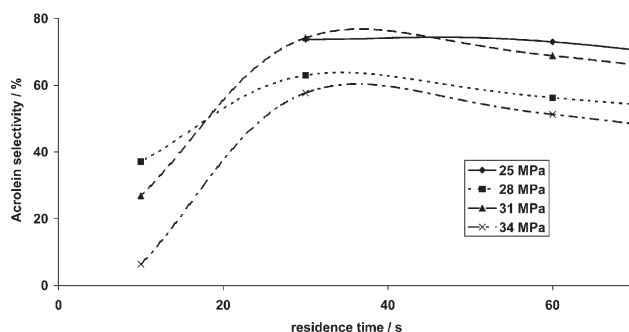


Fig. 7 Pressure influence on the acrolein selectivity at 360 °C and 790 ppm (g g^{-1}) zinc sulfate concentration.

4.2 Influence of the pressure

Fig. 6 shows the glycerol conversion and Fig. 7 the acrolein selectivity under various pressures. The conversion slightly enhances with increasing pressure. In contrast, the acrolein selectivity declines with increasing pressure from 25 to 34 MPa.

4.3 Influence of the catalyst concentration

The influence of the zinc sulfate concentration with respect to the glycerol conversion is shown in Fig. 8. The conversion rises with increasing zinc sulfate content up to 80% at 60 s and 790 ppm (g g^{-1}) zinc sulfate.

As can be seen from Fig. 8, the glycerol conversion is not proportional to the zinc sulfate concentration. The reason for this behaviour is that proportionality is only given if the

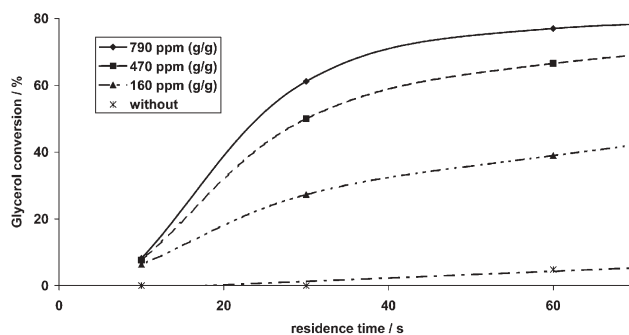


Fig. 8 Influence of the zinc sulfate concentration on the glycerol conversion at 360 °C and 25 MPa.

reaction rates are considered. For example, the reaction rates r_i for two different catalyst concentrations $c_{i,\text{cat}}^n$ with n as the reaction order concerning the catalyst are given by eqn (3) and eqn (4):

$$r_1 = kc_{1,\text{cat}}^n \quad (3)$$

$$r_2 = kc_{2,\text{cat}}^n \quad (4)$$

The ratio of the reaction rates in the logarithmic form defines the reaction order n or rather the proportionality, as shown by eqn (5):

$$\ln \frac{r_1}{r_2} = n \ln \frac{c_{1,\text{cat}}}{c_{2,\text{cat}}} \quad (5)$$

So this is the explanation why the glycerol conversion is not proportional to the zinc sulfate concentration.

The dependency of the acrolein yield at 25 MPa on the zinc sulfate concentration can be seen in Fig. 9. The addition of zinc sulfate clearly causes an increase in the acrolein yield from 3 mol% without salt to 45 mol% with 470 ppm (g g^{-1}) zinc sulfate. Further zinc sulfate enhancement leads to a decline of the yield to 40 mol%. In the experimental residence time range, a zinc sulfate concentration above 160 ppm (g g^{-1}) also accelerates consecutive reactions of acrolein, which can be seen in the decline of the yield.

4.4 Influence of the glycerol concentration

The dehydration of a 5% (g g^{-1}) aqueous glycerol solution in SCW with 470 ppm (g g^{-1}) zinc sulfate has the same conversion as a 1% (g g^{-1}) solution. The maximum acrolein selectivity of the more concentrated feed is 72 mol% at 30 s and therefore a little lower than the diluted feed with 75 mol% at the same residence time. The selectivity drop of a 5% (g g^{-1}) aqueous glycerol solution with increasing residence time is faster in contrast to the 1% (g g^{-1}) solution, which might be an indication that a high glycerol content enhances the consecutive reactions of acrolein. Fig. 10 shows the experimental results.

4.5 Kinetic analysis

The kinetic analysis was performed according to Bühler *et al.*'s⁴ reported reaction order of one and the account of an ideal plug flow reactor. The temperature and pressure dependency of the

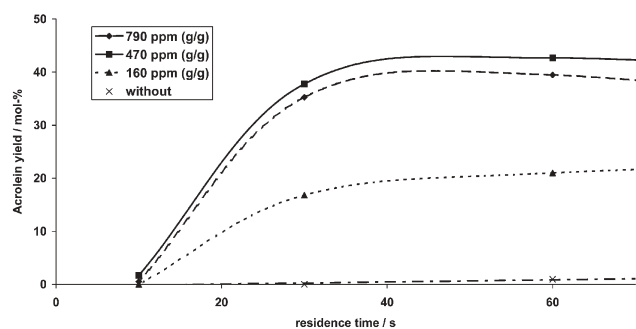


Fig. 9 Influence of the zinc sulfate concentration on the acrolein yield at 360 °C and 25 MPa.

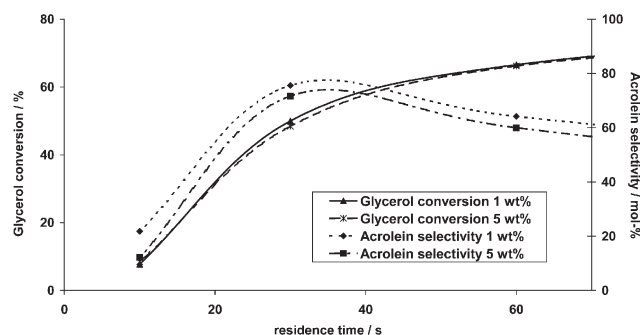


Fig. 10 Influence of the initial glycerol concentration at 360 °C, 34 MPa and 470 ppm (g g^{-1}) zinc sulfate concentration on the conversion and the acrolein selectivity.

kinetic constants were obtained *via* $\ln(1 - X)$ vs. τ plots. With these constants the activation energy and the activation volume were determined. Results for the kinetic constants are listed in Table 1.

The resulting activation energy from 300–360 °C, 25 MPa and 790 ppm (g g^{-1}) zinc sulfate is $(140 \pm 12) \text{ kJ mol}^{-1}$ and therefore lower than the non-catalysed reaction with 150 kJ mol^{-1} .⁴ The according frequency factor is $1.3 \times 10^8 \text{ s}^{-1}$. The activation volume has a value of $-(274 \pm 65) \text{ cm}^3 \text{ mol}^{-1}$, which means that pressure enhancement leads to an increased glycerol conversion (see Fig. 6).

4.6 By-products and total carbon balance

Acrolein stability. The stability of the main product acrolein under reaction conditions was clarified in preliminary investigations. The experiments for an 1% (g g^{-1}) aqueous acrolein solution at 34 MPa, 360 °C and $\tau = 120 \text{ s}$ gave the following results:

- 40% conversion without any addition
- 62% conversion with 790 ppm (g g^{-1}) zinc sulfate.

This means that zinc sulfate also promotes the consecutive reactions (*e.g.* decarbonylation, polymerisation) of acrolein. Evidence for this account is the strong gas production, which could be observed during sampling (no gas analysis was performed due to very low mass flows) and the occasional plugging of the micro plant. Liquid by-products could not be detected. Thus the reverse reaction of acrolein to glycerol does not take place.

By-products and total carbon balance. The average carbon recovery of the chemical analysis was 86%. The missing 14%

Table 1 Kinetic constants for the dehydration of glycerol in SCW with 790 ppm (g g^{-1}) zinc sulfate

Pressure/MPa	Temperature/°C	k/s^{-1}	R^2
25	300	0.0010 ± 0.0002	0.92
25	330	0.0053 ± 0.0005	0.90
25	360	0.0161 ± 0.0011	0.97
28	360	0.0208 ± 0.0020	0.97
31	360	0.0249 ± 0.0019	0.98
34	360	0.0255 ± 0.0027	0.97

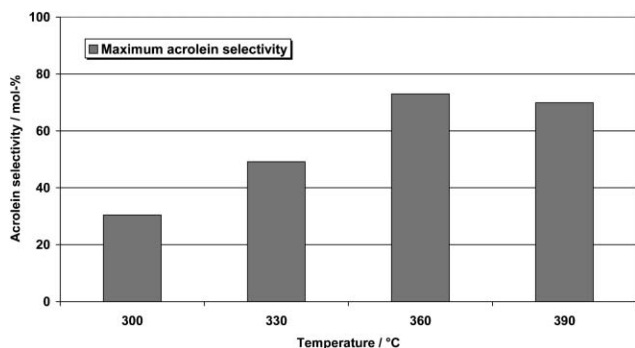


Fig. 11 Maximum acrolein selectivity (various residence times) at 25 MPa and 790 ppm (g g^{-1}) zinc sulfate and dependency on temperature.

mainly have to be gaseous products (e.g. C_2H_4 , H_2CO , CO , CO_2), which have neither been qualified nor quantified due to very low mass flows. Only traces of other possible liquid by-products such as propionaldehyde and methanol could be detected.

Heat transfer peculiarity of the reactor. As can be seen from Fig. 4, 7 and 8, the glycerol conversion seems not to pass through zero for a residence time of zero. It appears that the conversion is already zero for residence times higher than zero; of course, this cannot be true. In our case, the insufficient heat transfer management of the reactor—especially for high flow rates or rather short residence times—is the reason for this behaviour. We have done fluid dynamic simulations with FemLab 3.0[®] in order to estimate the desired reactor length for heating up the reaction solution to the reaction temperature. For high flow rates (10 mL min^{-1}), the reaction temperature of $360 \text{ }^\circ\text{C}$ is obtained only after 30% of the reactor volume. The exact calculations can be taken from ref. 17.

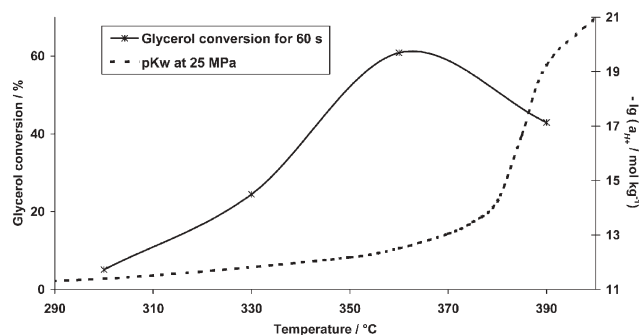


Fig. 12 Comparison of the glycerol conversion (25 MPa, 790 ppm (g g^{-1}) zinc sulfate) with the $\text{p}K_w$ value of pure water.

5 Discussion and conclusion

The use of zinc sulfate for the dehydration of 1% (g g^{-1}) glycerol in subcritical water clearly improves the acrolein yield. The attained selectivities even make the process interesting for industrial use as an alternative for petrochemical based production. Fig. 11 gives a short overview of the obtained maximum acrolein selectivity depending on temperature at 25 MPa and addition of 790 ppm (g g^{-1}) zinc sulfate.

Fig. 12 shows the comparison of the glycerol conversion from 300–390 $^\circ\text{C}$ with the $\text{p}K_w$ value of pure water at 25 MPa. A correlation of the conversion with the dissociation constant of water can be recognised. The conversion decreases in the area of the strongest $\text{p}K_w$ gradient above 370 $^\circ\text{C}$ (increase of the $\text{p}K_w$ value means decrease of the self dissociation of water) and therefore the assumption that the glycerol dehydration in the near subcritical region follows an ionic mechanism is confirmed. In the supercritical region the glycerol conversion declines and becomes independent of the experimental residence time from 10–60 s (see Fig. 4). This suggests another reaction mechanism

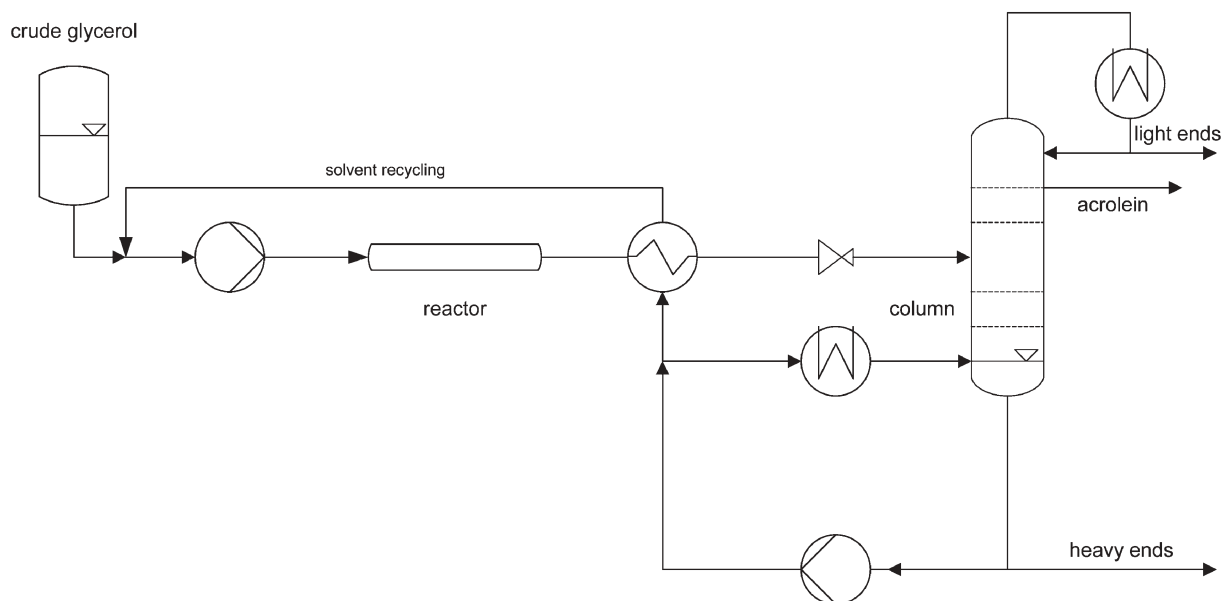


Fig. 13 Proposition for a technical process for glycerol dehydration to acrolein with zinc sulfate in SCW.

because in the supercritical region a free radical mechanism for the dehydration of glycerol is postulated.⁴

A possible flow sheet for an industrial process can be seen in Fig. 13. Together with the recycled solvent, the crude glycerol is pumped into the reactor. After heat exchange and pressure release the acrolein is stripped from the reactor effluent in a distillation column with side stream. The light and heavy ends are rejected whereas the residual solution (with zinc sulfate) is recycled. Prior to this, it has to be clarified if the crude glycerol solution has to undergo an ion exchange. In the future framework of process development the recycle stream will be tested as well as a higher glycerol concentration than 5% (g g⁻¹). But so far, no higher glycerol content could be realised because otherwise plugging (coking) occurred.

A simple raw material cost calculation with an expected glycerol price of 150 € t⁻¹ resulted in 342 € t⁻¹ acrolein. The calculation is based on the usage of 60% (g g⁻¹) crude glycerol as feedstock (which is accumulated during fat saponification, mainly during biodiesel production) and an acrolein yield of 75 mol% (due to circuitry of glycerol). The zinc sulfate content of the feed solution and the reactor discharge has been determined *via* ion chromatography. It resulted in a constant zinc sulfate concentration before and after the reactor so that the salt can probably be recycled (which has not yet been tested).

With a reasonable energy management and further optimisation of the acrolein yield as well as an increasing crude oil price, the acrolein process based on the catalytic dehydration of biomass derived glycerol in *SCW* can be an economical and ecological alternative in contrast to the crude oil based process.

Of course, the corrosion potential of zinc sulfate has to be clarified but from known literature it is expected to be low.^{13,14}

Acknowledgements

The authors thank the Fachagentur Nachwachsende Rohstoffe (FNR) for funding this project (FKZ 22007600).

References

- 1 Federal Statistical Office Germany, <http://www.destatis.de/download/e/ugr/ugrkurzengl.pdf>.
- 2 J. O. Metzger, *Nachr. Chem.*, 2003, **51**, 458–460.
- 3 Union for the Promotion of Oil and Protein Plants Germany, <http://www.ufop.de/>.
- 4 W. Bühler, E. Dinjus, H. J. Ederer, A. Kruse and C. Mas, *J. Supercrit. Fluids*, 2002, **22**, 37–53.
- 5 S. Ramayya, A. Brittain, C. DeAlmeida, W. Mok and M. J. Antal, *Fuel*, 1987, **66**, 1363–1371.
- 6 M. J. Antal Jr., W. S. L. Mok and G. N. Richards, *Carbohydr. Res.*, 1990, **199**, 111–115.
- 7 H. Waldmann and P. Frantisek, *Chem. Ber.*, 1950, **83**, 287–291.
- 8 E. Schwenk, M. Gehrke and F. Aichner (Schering-Kahlbaum AG), *US Pat.* 1 916 743, 1933.
- 9 T. Haas, A. Neher, D. Arntz, D. Klenk and W. Girke (Degussa AG), *Eur. Pat.* 598 228 A1, 1994.
- 10 C. T. Lira and P. J. McCrackin, *Ind. Eng. Chem. Res.*, 1993, **32**, 2608–2613.
- 11 M. S. Tam, R. Craciun, D. J. Miller and J. E. Jackson, *Ind. Eng. Chem. Res.*, 1998, **37**, 2360–2366.
- 12 Z. Dai, B. Hatano and H. Tagaya, *Appl. Catal., A*, 2004, **258**, 2, 189–193.
- 13 P. Kritzer, N. Boukis and E. Dinjus, *J. Supercrit. Fluids*, 1999, **15**, 205–227.
- 14 P. Kritzer, *J. Supercrit. Fluids*, 2004, **29**, 1–29.
- 15 A. Kruse and E. Dinjus, *Z. Phys. Chem. (Munich)*, 2005, **219**, 341–366.
- 16 C. Haar, J. S. Gallagher and G. S. Kell, *NBS/NRC Steam Tables*, Hemisphere Publishing, Washington, DC, 1984.
- 17 L. Ott, Doctoral thesis, Darmstadt University of Technology, 2005.

An environmentally benign process for the efficient synthesis of cyclohexanone and 2-methylfuran

H.-Y. Zheng, Y.-L. Zhu, Z.-Q. Bai, L. Huang, H.-W. Xiang and Y.-W. Li

Green Chem., 2006, **8**, 107–109 (DOI: 10.1039/b513584b)

On p. 108, the equilibrium constant for the dehydrogenation of CHL to CHN [eqn (4)] is incorrect and should be:

$$K^0 = K_p K_\phi (P^0)^{-1} = \left(\frac{\chi_{\text{CHN}} \chi_{\text{H}_2}}{\chi_{\text{CHL}}} \right)_{\text{eq}} \left(\frac{\phi_{\text{CHN}} \phi_{\text{H}_2}}{\phi_{\text{CHL}}} \right)_{\text{eq}} \left(\frac{P^0}{P} \right)^{-1} \quad (4)$$

The Royal Society of Chemistry apologises for these errors and any consequent inconvenience to authors and readers.

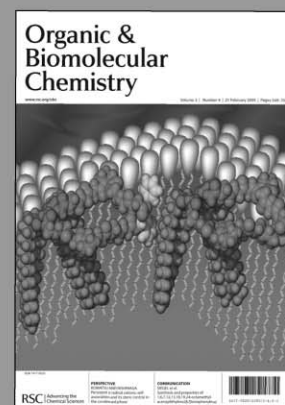
Additions and corrections can be viewed online by accessing the original article to which they apply.

Organic & Biomolecular Chemistry

A major peer-reviewed international, high quality journal covering the full breadth of synthetic, physical and biomolecular organic chemistry.

Publish your review, article, or communication in OBC and benefit from:

- The fastest times to publication (80 days for full papers, 40 days for communications)
- High visibility (OBC is indexed in MEDLINE)
- Free colour (where scientifically justified)
- Electronic submission and manuscript tracking via ReSource (www.rsc.org/ReSource)
- A first class professional service
- No page charges



Submit today!

RSC Publishing

www.rsc.org/obc

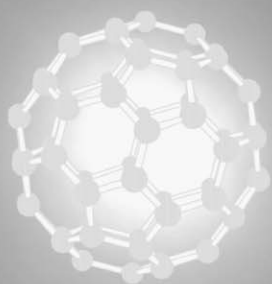


Image reproduced by permission of Jean-Francois Niergarten, *New J. Chem.*, 2004, 10

Downloaded on 07 November 2010
Published on 02 February 2006 on <http://pubs.rsc.org> | doi:10.1039/B600993J

21030532

NJC

New Journal of Chemistry

A prime source of international, cutting-edge research,
encompassing all areas of the chemical sciences

- Impact factor: 2.735
- Fast times to publication
- Multidisciplinary with broad appeal

Read it today!

RSC Publishing

www.rsc.org/njc



SEPTEMBER 10–15, 2006 • DRESDEN, GERMANY

IUPAC ICGC-1

1st International IUPAC Conference on Green-Sustainable Chemistry

Gefördert vom



Bundesministerium
für Umwelt, Naturschutz
und Reaktorsicherheit



www.gdch.de/vas/tagungen/tg/5559.htm

ReSource

Lighting your way
through the publication
process

A website designed to
provide user-friendly,
rapid access to an
extensive range of online
services for **authors** and
referees

Search it today!

www.rsc.org/resource

RSCPublishing



ChemComm

08060512

The leading international journal for the publication of communications on important new developments in the chemical sciences.

- Weekly publication
- Impact factor: 3.997
- Rapid publication – typically 60 days
- 3 page communications – providing authors with the flexibility to develop their results and discussion
- 40 years publishing excellent research
- High visibility – indexed in MEDLINE
- Host of the RSC's new journal, *Molecular BioSystems*



RSC Publishing

www.rsc.org/chemcomm